Field evaluation of ventilation wetting and drying of rainscreen walls in coastal British Columbia

Ying Simpson

A Thesis

in

The Department

of

Building, Civil and Environmental Engineering

Presented in Partial Fulfillment of the Requirements
For the Degree of Master of Applied Science (Building Engineering)
Concordia University
Montreal, Quebec, Canada

April 2010

Your file Votre référence
ISBN: 978-0-494-67259-4
Our file Notre référence
ISBN: 978-0-494-67259-4

Abstract

Field evaluation of ventilation wetting and drying of rainscreen walls in coastal British Columbia

Ying Simpson

The climate in southern coastal British Columbia (BC) is characterized by a long rainy winter. Building envelope failures that have occurred in recent years in this region promoted the adoption of the rainscreen principle in both rehabilitation and new construction and are now mandatory in the wet regions of BC. In addition to the functions of a capillary break and drainage, drying in an air cavity behind the cladding of the rainscreen wall system may occur through cavity ventilation. Current practice varies in terms of cavity depth and vent heights for rainscreen walls clad with panel systems, especially with respect to the top slot vents. The awareness of potential drying provided by cavity ventilation initiated the idea of providing top vents on brick veneer walls recently in the BC construction industry. However, there exist different views on the drying provided by cavity ventilation based on existing research. Whether cavity ventilation would be beneficial for this climate remained open for discussion.

To answer this question, a comprehensive research program was designed by Dr. Hua Ge with the candidate using a two-storey building envelope test facility at British Columbia Institute of Technology (BCIT) which Dr. Hua Ge developed. The candidate investigated twelve wall specimens, six clad with brick veneer and six clad with fibre cement panels, installed on the southeast façade, which faced the prevailing wind-driven rain direction.

The test variables include cladding type, air cavity depth and height, vent configurations and initial moisture load in plywood sheathing to evaluate the impact of cavity ventilation on the drying and wetting of test walls. The hygrothermal conditions across the wall assemblies were monitored for moisture content (both resistive and gravimetric), temperature, relative humidity, air speed in the cavity and pressure differentials between top and bottom of each cavity. The on-site weather conditions were measured including wind speed, wind direction, solar radiation, horizontal rainfall, and wind-driven rain. Indoor conditions were controlled at 22±1°C and 55±5% RH

In this study, the drying and wetting rates of plywood sheathing in the test walls during the winter and spring seasons were quantified, under-cooling effects on the temperature of cavity-surfaces of claddings and plywood sheathing were analyzed and the daily hours of condensation on the cavity-surface of claddings for all test walls were calculated. Simulation and measurements of MC in plywood sheathing for two brick veneer walls and two fibre cement walls were compared.

Acknowledgements

Undertaking this Master thesis project, I was not fully aware of its complexity, scope, time and energy it would require. Despite hindrances, I kept on going and carried it out to the completion. However, without the help of many extraordinary individuals and organizations who have assisted with their knowledge and experience, understanding, or financial support, the success and completion of thesis would not have been possible.

To my family; I would like to thank my parents who have been taking care of me and supporting my curiosity, ambition, and decisions through my life which allowed me to challenge myself by entering the graduate engineering program with my urban planning background. Special gratefulness to my dear husband Brian John Simpson for encouragement, understanding, full support and extreme patience through these wonderful five years. In this Masters project, he was my loyal partner from fabrication of wall panels and pre-made gravimetric samples, experimental set-up, gravimetric data collection, discussion of data analysis to the thesis editing.

To my supervisors, Dr. Paul Fazio and Dr. Hua Ge; thank you for expecting the best from me and providing me with extraordinary experiences. I would like to thank Dr. Paul Fazio for giving me the opportunity to pursue my Master's degree. His practical teaching and experience are reflected in my approach to building science. I would also like to thank Dr. Hua Ge particularly for her dedicated support and guidance in this endeavour over the past four years. She devoted her efforts and applied her knowledge of building science and physics to guide my research in detail. Having worked together with her, I

have learnt from her not only how to do research, but also how to keep on moving forward with great details and various aspects to achieve goals. I am also grateful to Hua's husband, Ye Zheng, for helping me to pre-drill plywood sample holes.

To BCIT which provided an environment for me to do this research work, I appreciate that I had the privilege to design and execute such a comprehensive experiment at BCIT's new field Building Envelope Test Facility. I would like to thank instructors and staff at the School of Construction and the Environment: Rene Guerin who helped me to fabricate the tracer gas manifolds and constantly gave me support; Dennis Yablonski who contributed his experience of construction and building material properties to the project and discussed about new BC Building Code with me; Yves Blaison and Don Shortt and their students who helped me to pre-cut studs and plywood and to drill the sample-holes in wood members; Dr. Mehrzad Tabatabaian, Dr. Fitsum Tariku, and Ronald Krpan who discussed and answer the questions in the project to me.

To my colleagues in Building Science Centre of Excellence (BSCE) at BCIT; I would like to acknowledge Doug Horn who provided technical support and did a huge amount of work for the mock-up wall built-up, sensor calibrations, experiment and acquisition system set-up, gravimetric sample collections. Also to Steve Tucker who helped me to fabricate and install all the test wall panels and greatly shared his ideas for the installation of experiments; Maria Fedorov, Andrew Larose, Christaine Secrieru and Stephen Roy, the technicians at BSCE for their help along the way, the great people with whom to work and share ideas and experience.

Many other experts have contributed to the success of this research study. I would like to express my gratitude to Terry Aellog in Tek Roofing Company, a great roofing expert, for providing metal flashing and had being done an excellent job to install flashings for the test walls; Bill McEwen and J.P. LeBerg in Masonry Institute of BC with discussion and input for brick veneer walls in the experiment and contributions of test materials and labour from local masonry industries; particularly to Graham Finch in RDH Building Engineering, an expert of WUFI use, who provided improved opinions to my modeling and discussed the experiment; Christine Ho who helped me to write a Macro and saved my significant time for data analysis; all my other friends and BCIT' students who helped me in this project.

Last but not least, I would also like to acknowledge the financial support of NSERC from Dr. Fazio and Dr. Hua Ge's grants, BCIT, BC Housing and Concordia University.

Table of Contents

List of Figures

List of Tables

Chapter 1: Introduction

1.1 Background

The 2006 British Columbia Building Code (BCBC, 2006) calls for rainscreen wall construction in the coastal and high moisture index regions in British Columbia which climate is characterized by a long rainy winter (less than 3400 degree days and the moisture index is greater than 0.9, or 3400 degree days or more and the moisture index is greater than 1.0). The primary functions of the air cavity behind the cladding are to provide a capillary break and drainage for accidentally entered rain water or condensation. The ventilated air cavity also provides drying for wet materials enclosed in the cavity, i.e. wetted cladding or wetted sheathing panels. As a result of building envelope failures that occurred in the coastal British Columbia (BC), the rainscreen principle has been widely adopted in both retrofit and new construction. The current BCBC requirement in this region is to design a rainscreen wall with a minimum air cavity depth of 10 mm. The City of Vancouver Building By-law (1999) requires an air cavity of at least 19 mm depth unless that the cladding is not a rigid pane such as vinyl, cement, or wood siding. Although rainscreen design is already a common practice in this region, questions regarding the drying capacity provided by the cavity ventilation still remain. For example, how much drying can cavity ventilation provide under damp winter conditions in this region? There is also the question regarding the potential of wetting when ventilation introduces moist air into the cavity.

Thus, for panel cladding such as fibre cement panel and stucco, there is no consensus regarding the size of top vent height. Some practitioners prescribe the same opening size for both bottom and top vents while others prefer much smaller top vents to minimize rain penetration and ventilation wetting. Field examination has shown a variation of construction, some with clear openings at the top while others are without top openings or with top vents partially blocked. Brick veneer wall construction traditionally incorporates weep holes only at the bottom to allow drainage. In recent years, the awareness of drying potential provided by cavity ventilation has initiated the idea of providing top vents. However, there is a concern in the industry regarding the provision of top vents for brick veneer walls. This concern relates to rain penetration from the vent openings into the air cavity causing wetting of back wood-frame walls and corrosion of brick ties.

Extensive research has been done evaluating the airflow rate in the air cavity and the moisture removal by cavity ventilation through laboratory testing and field measurements. The general conclusions are that ventilation drying is beneficial for wet panel cladding and for solar-driven inward vapour diffusion in summer. The drying provided in winter is minimal (Rousseau and Dalgliesh, 2004; Shi and Burnett, 2006). There exist different views on the drying provided by cavity ventilation for brick veneer walls. Hens and Fatin (1995) found that the provision of top vents did not have significant impact because of the small airflow rate and the high moisture storage capacity of bricks, while Straube (2004) concluded that brick veneer walls with open top vents provided higher drying potential. European researchers found that the opening of brick head joints did not

increase the amount of rain penetration, while a CMHC study found increased levels of moisture by opening the top vents (Laviolette and Keller, 2000).

In spite of existing research, there has been no field data reported in the coastal climate (which has long, rainy winter) of BC to clarify the above questions. A comprehensive research program is designed to evaluate the influence of cavity configurations on the ventilation drying and wetting in rainscreen walls using both field measurements and computer simulations (Ge and Ye, 2007). This is the first study carried out in a unique two-storey building envelope field test facility on the BCIT campus which was developed by Dr Hua Ge with funding from her CFI New Opportunities Fund and BCIT. Dr Ge consulted other world experts in the building science field Dr. Paul Fazio and Dr. Hugo Hens. Mr. Ronald Krpan participated in the development and design of the facility.

1.2 Objectives

The objective of this study is to evaluate ventilation drying and wetting of rainscreen walls having different claddings, cavity depths, vent types and sizes, and initial moisture load in plywood sheathing for the coastal climate of BC through full-scale field measurements.

More specifically, this study will:

- Compare the hygrothermal performance of wall assemblies with different vent configurations by monitoring drying and wetting of plywood sheathing having different initial moisture loads.

- Determine the influence of vent configurations i.e. vent type, size, cavity height, and weather conditions on the cavity ventilation rate by comparing the predicted cavity ventilation rates based on the combined buoyancy and wind-induced pressure differentials.
- Evaluate the wetting potential due to ventilation, i.e. moist air and clear sky radiation effect induced condensation (under-cooling condensation).
- Evaluate the reliability of a commercially available computer simulation program on predicting the hygrothermal performance of ventilated rainscreen walls by comparing the simulation results to the measured moisture contents in plywood sheathing.

1.3 Approach

The approach employed in this thesis consists of, measurements of hygrothermal responses of full scale test panels installed on a two-storey field test facility, and comparison of MC in plywood sheathing between measurements and simulations. It also includes computer simulation analysis. The hygrothermal responses will be correlated to the real-time field environmental conditions with constant indoor conditions. The methodology developed for the field experiment is built upon previous laboratory and field research. The moisture content variation of plywood sheathing is used as an indicator to investigate the impact of ventilation on the wetting and drying of rainscreen walls. Two levels of moisture were introduced in the plywood sheathing. Four fibre

cement walls and two brick walls were pre-wetted to a high initial moisture content (MC) of 38 - 41% while the other six walls started with a low initial MC of 7%.

1.4 Outline of the thesis

The background, objectives and approach for this research work have been stated in the previous section of Chapter 1. Chapter 2 reviews previous laboratory and field experiments and modeling work related to the objectives of the present project including the development of rainscreen wall systems, practical design issues in the construction industry in BC, functions of an air cavity, major driving forces for cavity ventilation, airflow rate in the cavity as well as the effect of cavity ventilation on building envelope performance. Chapter 3 presents the experimental design and set-up on the building envelope test facility. Chapter 4 consists of analyses of experimental results and discussions including on-site weather observation, moisture performance of test wall assemblies, drying and wetting rate of plywood sheathing, and vapour pressure differentials between air cavity and ambient air. Chapter 5 consists of experimental analysis on thermal performance of test wall assemblies, temperature differences between air cavity and ambient air and condensation caused by clear-sky effect. Chapter 6 includes analysis of wind and buoyancy-induced pressure differentials and the predictions of ventilation rate. Chapter 6 compares the MC of plywood between measurements and simulation using WUFI computer software and the sensitivity analysis of input parameters used in the simulation. Chapter 7 presents general conclusions, contributions of this study, and recommendations for future work.

The experimental work focuses on the hygrothermal performance of wood-framed back wall assembly clad with fibre cement panel or brick veneer cladding systems above ground. Rainwater penetration and air leakage analysis is beyond the scope of this thesis.

Chapter 2: Literature Review (State of knowledge)

2.1 Introduction

The principles of rainscreen wall systems have been demonstrated, in theory and industry practice, to prevent most rain penetration through rainscreen wall. Designers and researchers have understood well three of the 4 D principles (Hazleden,1999) of rainscreen wall systems; drainage, deflection, and durability, but the drying capacity and air cavity ventilation functions are still an uncertainty (CMHC, 2001) even though there has been a lot of research done on cavity ventilation and drying.

In this chapter, literature regarding the rainscreen wall system design in term of 4 D's principles is reviewed. Major driving forces for cavity ventilation and measurements of ventilation rate carried out in previous research are reviewed. This literature review also includes modeling, laboratory and field experiments of ventilation drying and wetting influenced by building envelope designs, boundary conditions, and moisture loads in the wall components. The state of knowledge of cavity ventilation drying is summarized.

2.2 Rainscreen wall systems

Moisture problems become the biggest threat for the durability of building envelopes, the separator between outdoor environment and a comfortable indoor space. Damage caused by moisture is up to 80% of total damage in the building envelope according to surveys

in Canada (Bomberg, M.T. and Brown, W.C., 1993). In general, the deterioration of building envelopes includes material shrinkage, wood decay, paint and membrane blisters, metal corrosion, masonry efflorescence, concrete and mortar leaching, freezing destruction and aesthetics deterioration (Latta, K, 1962). The deterioration caused by moisture problems also decreases the thermal resistance of insulation materials (Kerr, 2004), promotes mould and mildew growth on the interior surface which may cause health problems (Rousseau, J. 1983). Consequently, the damage caused by moisture can reduce structural strength, affect the safety of occupants and shorten building life.

In the early to mid 1990's, the problems of moisture damaged buildings were realized in coastal BC and are still an issue to this date. A large percentage of condominium buildings were affected initially and the total rehabilitation cost was over $2-billion (BCdex 2006). Among the causes of moisture problems, water penetration is a dominant factor. Therefore, rainscreen wall systems have become a legal requirement of residential building design for both new and retrofit construction in wet zones in BC (BCBC 2006). City of Vancouver by-laws have required using rainscreen walls since 1999 (City of Vancouver, 1999).

2.2.1 Moisture problems of building envelopes

In the 1980's, the Canadian Mortgage Housing Corporation (CMHC) sponsored a series of moisture problem investigations. The moisture-induced problems are grouped into five types (Rousseau, 1983):

1. mould and mildew;

2. window condensation and water penetration
3. attic and roof condensation
4. condensation in wall cavities
5. exterior siding damage

The moisture problems in the building envelope continue to happen. The major area of moisture problems in wall assemblies are window-surrounds, saddle flashings, balconies and walkway membranes caused by rain penetration (Morrison Hershfield 1998, RDH, 2003). The estimate of rehabilitation due to premature failure is $225 to $375 million / year in Canada (Marshall, 2001).

The main causes of moisture-induced problems include (CMHC, 1989; Lawton, M.D. 1999; Rousseau, 1984; and Finch 2007,):

- Rain penetration with high risk elements such as balconies, walkways and eliminating eves and overhang of a building envelope.
- Air leakage - no continuity of air barrier with penetration holes, high attic and interior humidity with lack of ventilation.
- Prolonged heating season with high RH and minimum sunshine in coastal regions such as BC.
- Use of high R-value insulation with low permeable cladding and strong wind washing (create mould and mildew in the interior finishing).
- "Built-in" MC in the wood materials during construction which is above 19% and even over 30% MC, beyond the fibre saturation point.

2.2.2 Rain penetration protection

Among various moisture sources, rain penetration is the major source causing moisture related problems in building envelopes. The researchers and practitioners are seeking a suitable building envelope design to keep walls dry through "4-Ds" strategies (Hazleden, 1999; Kerr, D. 2004):

- **Deflection:** using overhangs and flashing at eaves and window sill to limit exposure of the walls to rain – water source control, the most important strategy.
- **Drainage:** providing an air cavity to drain water that does penetrate the cladding back to outside – the second important strategy
- **Drying:** creating some features of the walls such as vents on the cladding to dry materials which get wet – not as reliable as first and second strategies since drying is very slow either by ventilation or vapour pressure diffusion.
- **Durability:** using materials which have more tolerance to moisture – redundancy strategy incorporating detail design.

For water penetration to occur, three conditions are required: water source on the surface, opening through the wall, and driving forces. The climate of coastal BC has a long period of rain from late fall to early spring. The strong wind during this rainy period drives numerous rain droplets and impinges them on the cladding. Roof overhangs can effectively reduce rain exposure on the exterior surface of the walls in low and multi-floor buildings. The forces such as kinetic energy, capillarity and surface tension, gravity and pressure differentials can drive rainwater on the exterior face through the opening into the walls. These forces can be minimized by incorporating appropriate design details

such as drip flashings, outward slopes, capillary break, and moderating pressure differential across the cladding. However, openings in the cladding are difficult to eliminate, for example cracks in stucco due to the porous nature of the materials, movement under thermal and moisture loads, workmanship, etc. The face-seal approach is to eliminate the openings which require intensive maintenance work, but it often fails due to the unavoidability of cracks. The more forgiving approach is to employ the rainscreen principle, which allows water that incidentally enters the wall to move back out (Lawton, 1999).

The rainscreen wall system developed from drained cavity walls, open or simple rainscreen walls to pressure modified rainscreen walls to minimize the dominant force of pressure differential for rain penetration (Kerr, A. 2001).

1. Drained cavity walls

A drained cavity wall; uses the cladding as the first defence to shed water on its exterior surface and it has a drain opening at the bottom. This acts as an air cavity or free-draining channel behind the cladding preventing water penetration through the cladding by capillarity or gravity into the back wall horizontally. The cavity and the free-draining material can also direct penetrated water to the back of cladding, where it runs down and drains out of the cavity or onto flashing. A second defence on the exterior of the back wall – a water resistant material (moisture barrier) sheds water which incidentally has penetrated the first defence line, down to the base of the wall where it drains out of the cavity.

2. Open or simple rainscreen walls

The three basic components of a drained cavity wall are not changed in open or simple rainscreen walls. The difference is that the cladding is designed into the rainscreen in order to control rainwater entry at the first defence line. The back wall is much more airtight than the cladding so that the air barrier at the back wall carries most of the pressure differential. The rainscreen intentionally has openings i.e. vents to minimize pressure differential.

This approach partially controls the pressure differential between the first and second defence line but offers no control on the lateral pressure differential in the air cavity since the wind pressure across rainscreen is not evenly distributed on all of the exterior surfaces of a building, especially at the roofline and the corners.

Traditionally, the overlapping siding, shingles and shakes with wood-fame back walls are simple rainscreen walls with small air spaces fixed between lapped single and back board. The simple rainscreen wall is commonly used in the brick and stone veneer walls vinyl siding on wood or steel frame walls.

3. Modified rainscreen walls

The additional features are introduced in the design of the cavity such as compartmentalization and air tightness at the interface joints to improve the performance of an open or simple rainscreen wall system in terms of preventing the lateral air flow in the air cavity. The walls with vertical furring or strapping in the air cavity can achieve the pressure modified rainscreen wall approach incorporating interface details. In

addition, pressure modified rainscreen wall principle also applies to a curtain wall system with spandrel panels.

2.2.3 Building code requirements

After determining the dominant cause of leaky condos, the City of Vancouver effectively enhanced some important design changes and mandated the use of the rainscreen principle in the wall system when the city building bylaw was introduced in 1999 (City of Vancouver, 1999). The law required that all future stucco wall systems for multi-floor residential building must be designed and constructed with a drainage cavity with a 19 mm vertical strapping, or some other relevant method to create a cavity. The bylaw also required that the drainage cavity must be at each floor level with specific details and various elements such as flashing. The bylaw requirement of rainscreen wall principle had a significant influence on the design in the BC's coastal area.

The adoption of rainscreen principles by the construction industry and professional designers has demonstrated that the design is an effective envelope resolution to external moisture penetrating through the wall (CMHC 2001). Hence, in 2006 the BC building code mandated precipitation protection using the rainscreen wall principle in wood-frame walls of residential buildings, including single family houses. According to the BC building code, exterior walls exposed to precipitation should have two planes of protection (cladding and sheathing membrane on the back wall) incorporating a capillary break in regions with high exterior moisture loads (BCBC, 9.27.2. 2006). The capillary break is "a drained and vented air space not less than 10mm deep behind cladding". The

brick veneer with a thickness of not less than 75mm over the full height and width with wood-frame walls shall have "not less than a 25 mm air space behind the veneer". Cavity ventilation is not mandatory in the code and bylaw.

2.2.4 Functions of the air cavity in rainscreen walls

To keep the wall dry, an air cavity is used to separate a cladding (rainscreen) and a back wall, the cavity should be designed to be within an optimum degree of pressure equalization. The air cavity functions as a capillary break, as a drainage path for liquid form water to drain out and as a ventilation passage for vapour form moisture to dry out.

1. Pressure Equalization

Pressure equalization of the air cavity can reduce water source passing through the cladding by eliminating (ideal) or reducing (moderation) air pressure differential of outer and inter surfaces of cladding. The pressure equalization can be affected by many factors such as vent opening area and layout, cavity volume, airtightness of air barrier, stiffness of air cavity boundaries of both rainscreen and back-up wall, sealing quality of cavity perimeter, and static and dynamic air pressure (Morrison Hershfield Limited, 1990).

Many experimental measurements and field monitoring have been carried out to investigate the processes and variations of pressure equalization in air cavities (Inculet and Davenport 1994; Rousseau, 1998). They concluded that the net mean pressure differentials across the cladding diminish with the decrease of compartment sizes or the increase of venting area. Therefore, at locations near edges of a façade where greater exterior pressure gradients normally exist, smaller compartments are required to decrease

pressure differences (Mao, et. al. 2004). Straube (2001) investigated a group of test panels in a field test hut and found that the moderation of wind gusts induced-pressure is difficult to measure due to the fluctuation and unpredictability of wind pressures. Kontopidis (1992) and Kontopidis, Fazio and Mallidi (1993) proposed a pressurized cavity principle to improve rainscreen principle by replacing vent holes with valves. The test result showed that the pressurized cavity wall with valves had good performance to prevent rain penetration and air leakage.

2. Capillary break

Capillarity is a major mechanism that leads to rainwater ingress through cracks and joints of cladding. When liquid water such as rainwater driven onto the surface of a porous cladding, the cladding will absorb water through cracks and pores of material until free water saturation is achieved (Künzel, 1995). The moisture exchange will occur by absorption when the cladding is in contact with inner wall components until both materials reach an equilibrium level.

The suction pressure, moisture potential, and relative humidity (RH) are functions of the pores, cracks, or joint's radius or width (Künzel, 1995). The smaller radius or width has larger suction stress and surface tension. To break the surface tension, the cavity depth should be at least 5 mm deep (Brown, et al 1999). However, considering the variation of construction, the minimum depth in the practice should be not less than 10mm for the panel type cladding while the cavity depth should be 25mm for the brick veneer to ensure the cavity has clear path compensating for intrusion of mortar (Chown, 1997).

However, the air cavity cannot provide a clear break completely due to intentioned furring, strapping or brick ties and unintended materials such mortar droppings or insulation displacement. Through these bridges, water still can transfer into the wall components from the cladding if there are openings and driving forces.

3. Drainage

Drainage is the most recognized and effective control mechanism as one of the air cavity's functions in a rainscreen wall to reduce moisture damage. The air cavity between the cladding and the back wall provides a path for free water to drain. Water that has incidentally penetrated the rainscreen can run down by gravity force and then drain out through the base flashing and weep holes or bottom slot vents. It is important that drainage in some form of narrow air space or drainage space provided between the cladding system and the drainage plane can have sufficient capacity to dissipate free water very quickly (Lawton and Meklin, 1999; Straube.2006). Straube (2006) monitored the drainage between building components and found that water drained surprisingly well between two layers of building paper. To understand how easily water can be drained and how much water is retained in the drainage space a specific drainage test was set up as shown in Figure 2-2-1. The procedure was to pour 1.5L of water at the top of the test panel in approximately 60 seconds and then measure the time to store the water and the amount of water retained. The result shows that most of the water drained out within a short time period through a clear path as small as 1mm (Straube.2006). However, there is always an amount of water within 300-500 ml either retained on the surfaces of the cavity as droplets or absorbed into the material. Moreover, drainage can not start until the water deposition rate surpasses the absorption rate, i.e. capillary saturation, of the

cladding made of hygroscopic porous materials such as wood, stucco, fire cement and brick.

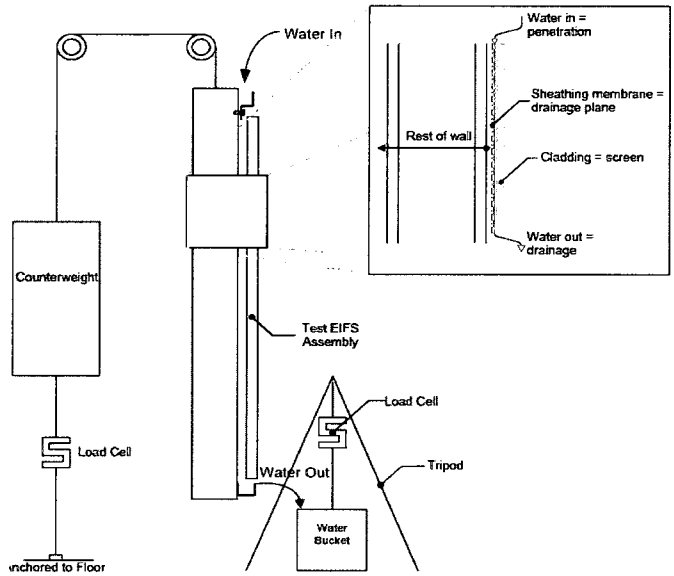

Figure 2-2-1: The specific drainage test setup in the test hut of University of Waterloo (from Straube, 2006).

Straube and Burnett (1998a, b) pointed out that drainage would not be the largest contributor for moisture removal. There were only a few occasions in which water draining behind the claddings was measured in a two-year testing. Most of the time moisture stored in the cladding or building materials in vapour form and needs other mechanisms such as ventilation or vapour diffusion to dry out.

4. Ventilation

Ventilation can increase the drying potential in assemblies that either store significant amounts of water or have cladding with a high vapour resistance. The intentional airflow moving through the cavity can bypass vapour resistance of the cladding, allow fast drying, and reduce inward vapour diffusion. Ventilation has more drying effect when the cladding is vapour tight. Even tiny air gaps allow ventilation to occur (Straube, 2007).

Field monitoring has proven that water may not be completely prevented despite the air gaps and water drainage. Some water may still penetrate by wind driven-rain or condensation may still occur by air leakage. Drainage by gravity cannot function until moisture is in the free liquid form. Water in the vapour form can be removed from a rainscreen wall with a wood-frame back wall by two other basic ways: evaporation from the surfaces of each wall component either to the indoor or to the outdoor, and moisture transport by diffusion or ventilation.

2.3 Ventilation in an air cavity

In order to control the tolerance of wood components against mould growth and ensure building enclosure durability, many researchers have looked into the drying potential of rainscreen wall systems provided by air cavity ventilation (Straube and Burnett, 1998).

2.3.1 Category of air cavity design related to vent openings

2.3.1.1 Existing category in literature

Of all literature reviewed, in terms of air cavity ventilation and drying research, there are two research papers that clearly describe the categories of venting design or strategy.

First, Bassett and McNeil (2005) in New Zealand categorized the rainscreen wall systems in terms of the cavity function as:

1. **Drained and ventilated cavity** – openings on the cladding, i.e. vents, designed at top and bottom, common for brick veneer walls
2. **Open rainscreen wall** – similar to a drained and ventilated cavity wall but without intentional top vent. Leakage openings are left at the top of the cavity and results in a cavity with a small top vents. This construction is common for panel type such as stucco cladding
3. **Drainage plane** – a narrow cavity with fibrous drainage mat or grooves behind the cladding designed only for drainage function i.e. only having a bottom vent.

Second, in North America, Karagiozis, Burnett and Straube (2005) categorized the rainscreen walls in terms of cavity strategies as:

1. **Ventilated cavity** – vents designed at top and bottom in the forms of open joint or slot to allow ventilation to occur effectively.
2. **Vented cavity** – vents provided at bottom of the cavity only.
3. **Non-vented (or unvented) cavity** – no intentional openings (vents) designed on the cladding but the cladding system is self-ventilated such as siding.

Many other papers, which study cavity ventilation effect, have no clear definition between ventilated and vented cavity. The rainscreen walls with venting in the literature in general referred only to **vented** or **drained** walls. Often the term is used for either cases in which the cavity had vents at both bottom and top or the cavity had vents only at bottom.

In this thesis, the definitions of cavity in terms of vent configurations follow the category of Karagiozis, Burnett and Straube (2005) through each section.

2.3.1.2 Practical design and construction of air cavity

In Europe, a traditional and very popular simple open screen wall is called "back ventilation cavity" wall, as shown in Figure 2-3-1 (Kerr, A. 2001). The vents in the outer rainscreen are quite large and located at both the top and bottom. The vent configuration takes advantage of wind pressure differentials and solar-induced thermal stack effect to create cavity air ventilation and dry out any moisture that penetrates the wall. The unique feature of this wall is that the top vent is protected by a cover to shed wind-driven rain away.

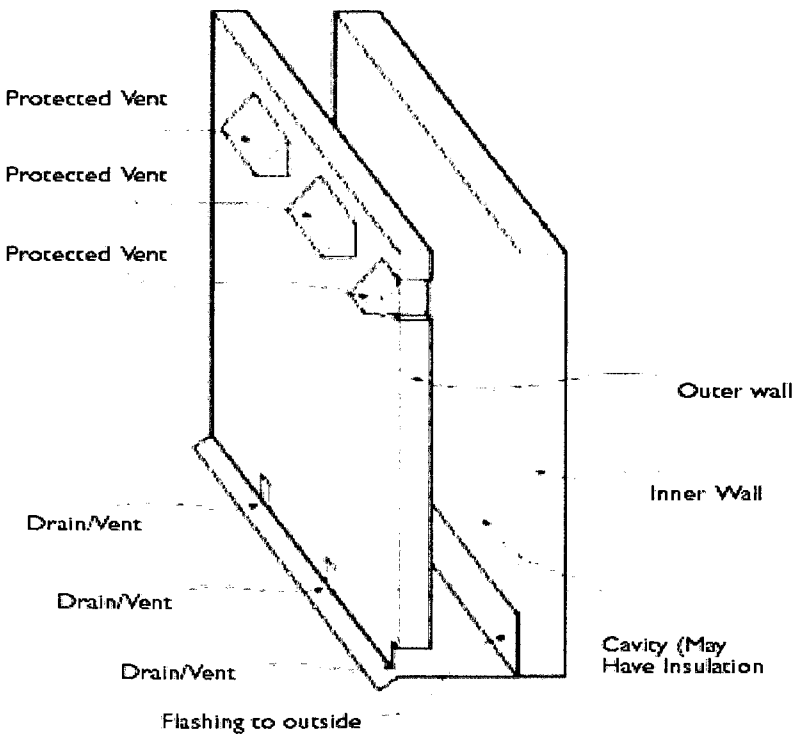

Figure 2-3-1: Back ventilated cavity wall in Europe (from Kerr, A. 2001).

Double wythe cavity walls are common in Europe, particularly in the high wind-driven rain areas (Straube and Burnett, 1997). The cavity is filled with insulation, a practice started following the 1970's oil crisis. These walls are able to drain water, allow air flow

and provide thermal resistance. Research has demonstrated that these kinds of filled-cavity masonry walls perform well.

In Canada, rainscreen with wood-back walls are very common. However, the effect of cavity ventilation is still uncertain, especially in the coastal climate of BC, and results in both ventilated and vented cavity designs and construction practices in the field. First of all the reasons, the existing research results are not consistent in term of the ventilation drying effects (Lawton, M. 1999; Don Hazleton 2001; and Straube, J. and Bennett, E. 1995). Secondly, CMHC's best guide for the wood-frame in the coastal climate of British Columbia is also not conclusive as to the function of cavity ventilation. It states that the construction details provided are "not vented at the tops of walls". It explains that venting at the top of cavity, particularly at the top of a building, may have negative pressure in the cavity under some circumstances and may draw water into the cavity (CMHC, 2001). Third, building codes and bylaws do not require top vents at the top of the cavity (BCBC, 2006, City of Vancouver, 1999).

The author reviewed some construction drawings designed by several building engineering companies for BC housing projects (BC housing, 2006). It is found that all the detail drawings have very clear dimensions for the bottom vent heights for panel type claddings while some of the top vents or gaps between cladding and flashings have no dimension, indicating the detail designs of the air cavity of a rainscreen wall system are more focused on the drainage than on ventilation.

Site observations of the vent configurations for panel type cladding have been done recently by the author. As shown in Figures 2-3-2, the bottom vents were to be about

19mm high; and the insect screen was in place. The vent was very clear and clean. However, the top of stucco cladding reaches the bottom of flashing and no gap could be seen.

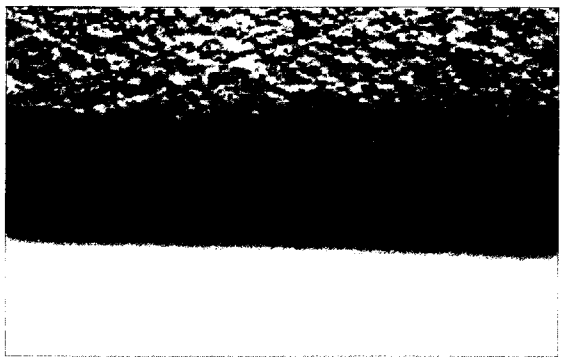

a) Clear and clean bottom slot vent on stucco cladding

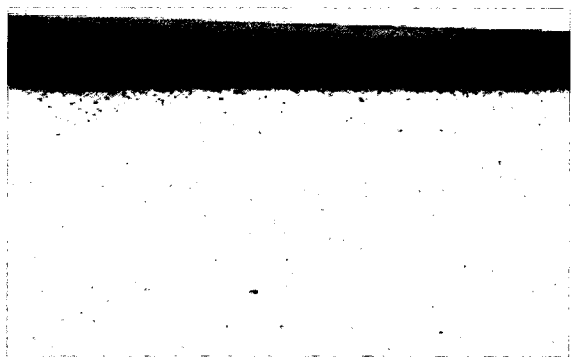

b) Close line between top of stucco and flashing

Figure 2-3-2: Clear bottom vent but not intended top vent of a stucco cladding of a rainscreen wall in Vancouver.

The workmanship of stucco installation seems very good and the connection line with flashing is clear and clean, showing there is no intended open top vent. Another building appeared to have a ventilated cavity design with slot vents at bottom and top. The bottom vents can be clearly observed while the top vents varied in width: at some places they were blocked but at some other locations they were wide open as shown in Figure 2-3-3.

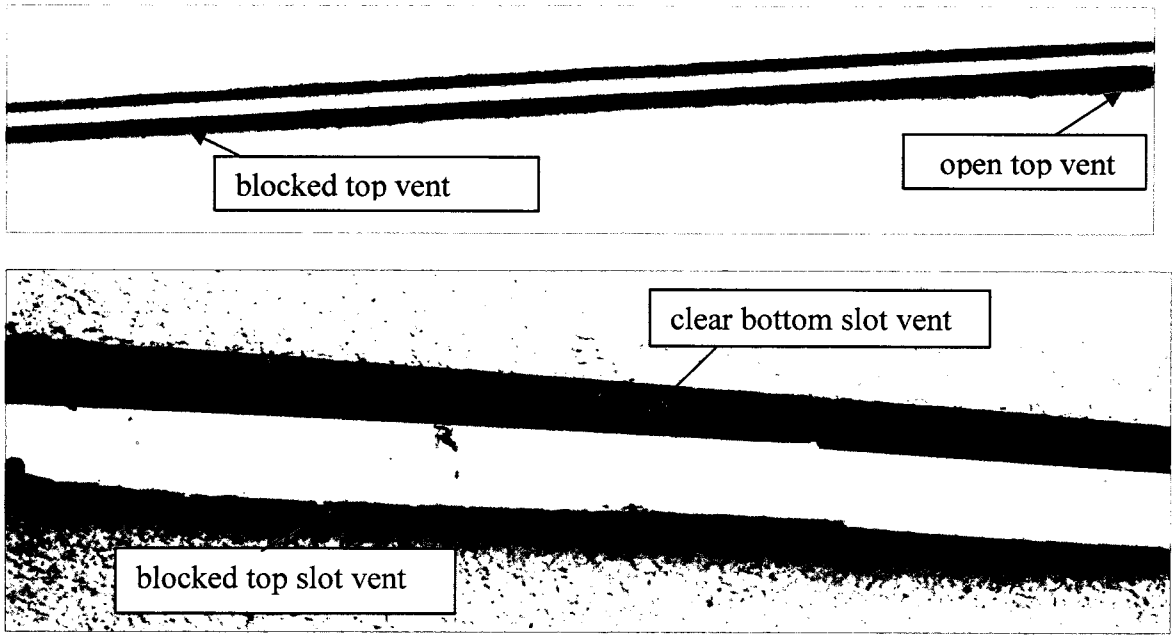

Figure 2-3-3: A rainscreen stucco wall with blocked top slot vent and clear bottom vent.

For the rainscreen wall systems with brick veneer which were built with 90mm thick solid brick in BC, most vents are designed with open head joints on the top and open joint between bricks as weep holes at the bottom on the brick veneer wall. Different points of view on ventilation drying effect influence the local construction practices. It is found that on the same street in Vancouver, brick veneer buildings were designed with vented cavity (without top vents) on one side of the street while the other brick veneer buildings were designed with ventilated cavity (with top vents) on the other side. Various vent configurations are observed on some buildings. Figure 2-3-4 shows that the buildings with vented cavities have bottom weep holes at different spacing.

a) weep holes between each brick

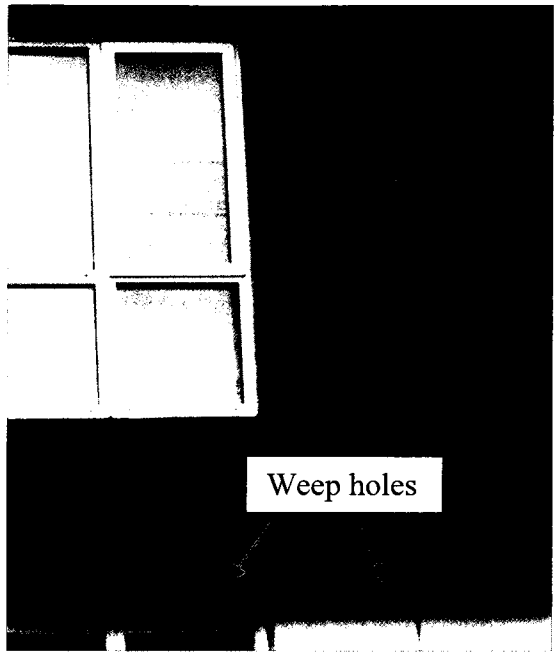

b) weep holes between every third brick

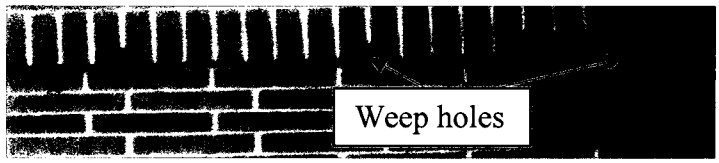

c) weep holes in the soldier-brick course (two brick spacing)

Figure 2-3-4: Vented cavities with different bottom vent openings of some buildings found in BC's construction practice.

For the buildings with ventilated cavities, the vent configurations are varied in spacing, arrangements of open joints, and height between top and bottom vents, as shown in Figure 2-3-5. The use of insect screen also varies. It is inserted into the vents to keep the insects away and is also intended to reduce the wind-driven rain or run off rainwater passing through the vent. However, insect screen also reduce the vent areas and blocks the airflow entering and exiting the cavity (Straube and Burnett 1998a). Some of the cavities have insect screens on the top vent but fully open bottom vents, as shown in Figure 2-3-6.

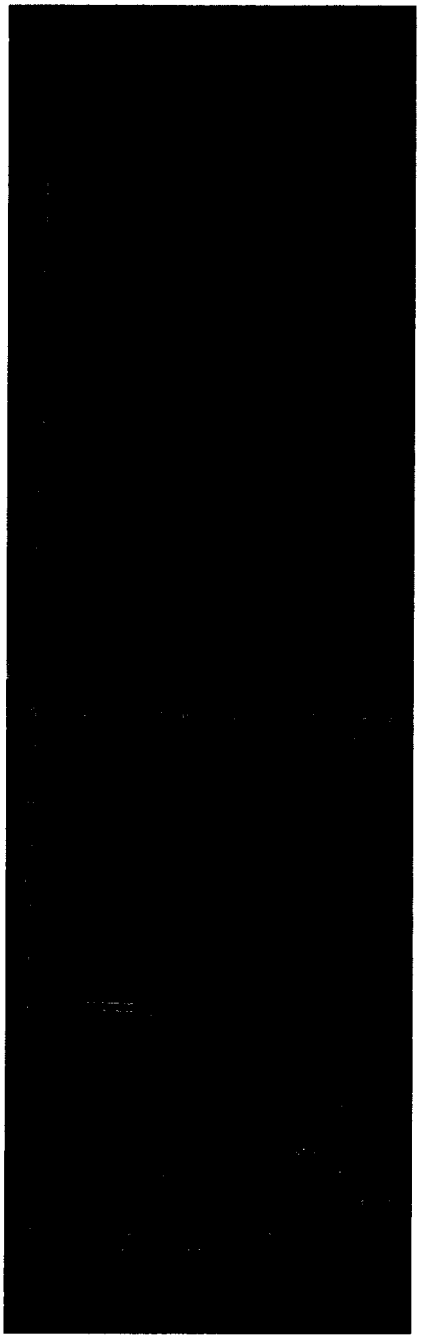

a) One-floor high ventilated cavity with various vent configurations

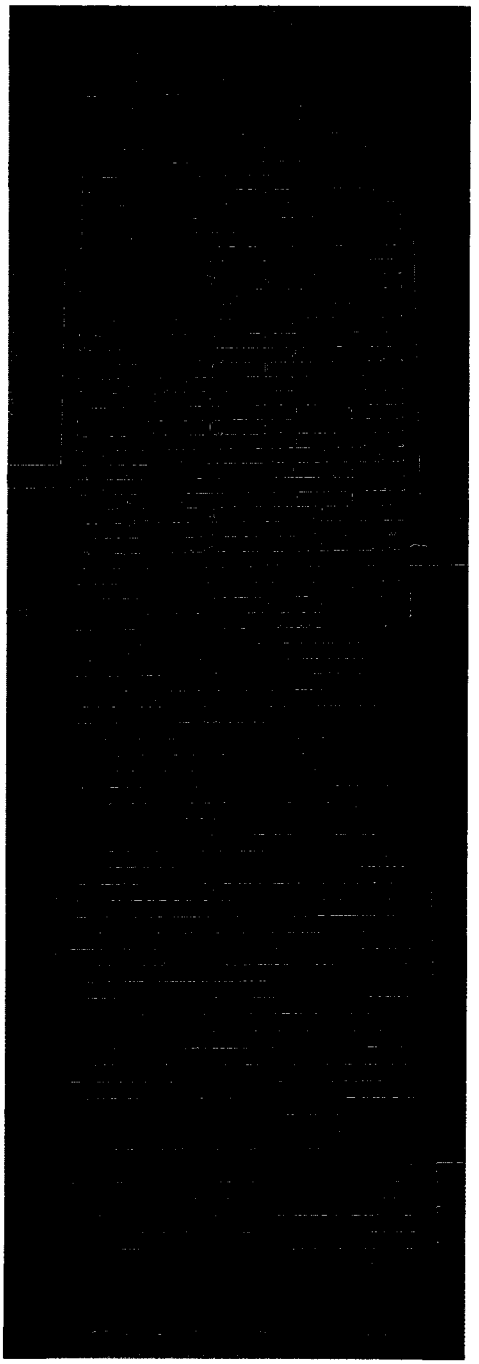

b) Two-floor high ventilated cavity

Figure 2-3-5: Ventilated cavities with various vent configurations and cavity heights.

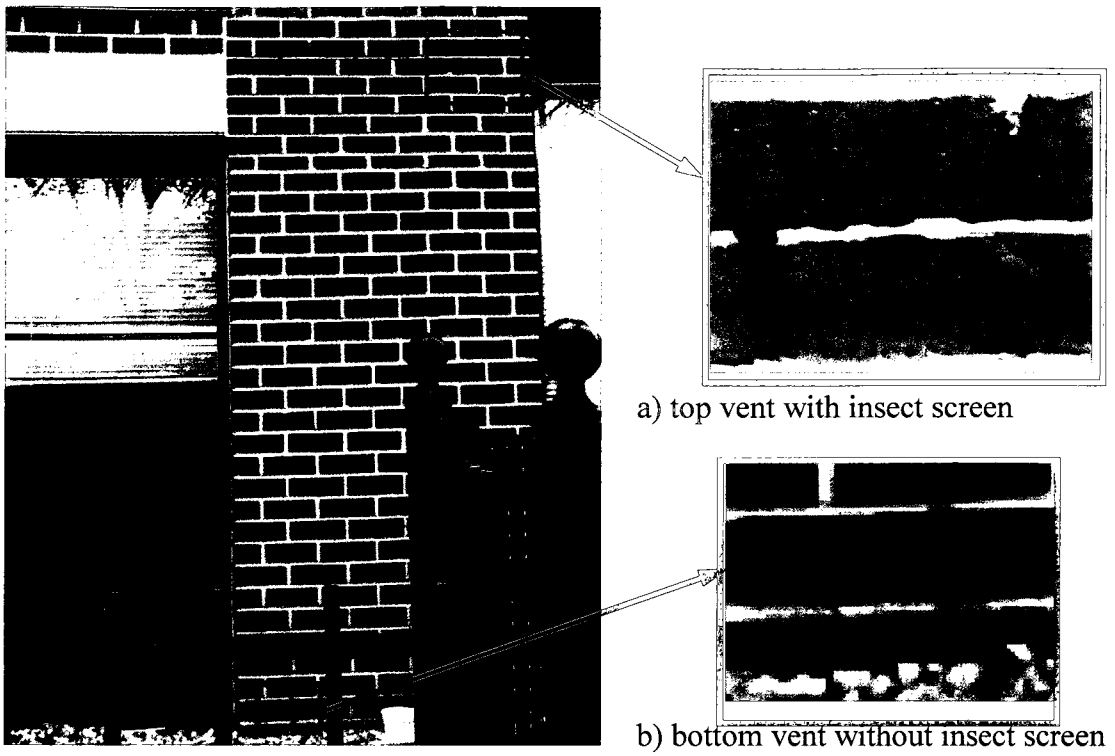

Figure 2-3-6: Ventilated cavity with fully open bottom vent and top vents with insect screens.

2.3.2 Major driving forces for cavity ventilation

Burnett & Straube (1995) in their CMHC research report summarized that ventilation is driven by the following forces:

- Wind pressure
- Thermal-induced buoyancy (Stack effect)
- Moisture-induced buoyancy.

The first two forces are the primary forces driving the cavity ventilation. Thermal buoyancy is caused by different densities between the exterior and cavity air and resulted in pressure difference, whereas wind pressure differentials are due to the vertical gradient

of wind speed, i.e. wind velocity increases with wall height (Mayer and Küenzel 1983, Burnett & Straube 1995).

The moisture-induced buoyancy is the secondary force to drive ventilation flow. As moist air has a lower density than dry air, the difference in MC between the cavity and outside air creates moisture buoyancy which drives air flow in the same manner as thermal buoyancy.

Sandin, K. (1991) found that cavity air change rates were higher when cladding temperature was higher than the ambient air temperature compared to the situation when the cladding temperature was the same as the ambient air temperature in his field study(quoted by Straube, et. al. 2005).

Straube and Burnett (1998) found in their field measurements that wind pressure driving force can be expected at an average of 1 Pascal (Pa) with a broad range between 0.1 to 10 Pa on façades of low-rise buildings. The average buoyancy pressure differential induced by temperature and moisture difference between bottom and top vents is about 1 Pa.

In a summary of an ASHRAE project on field experiment of ventilation drying, Burnett, Sraube and Karagiozis (2004) concluded that buoyancy effect is a common and stable driving force for the cladding system that facilitates vertical airflow through air cavity. For contact-applied horizontal siding such as vinyl siding, wind may be the governing force except for the siding on vertical strapping. Buoyancy-induced force alone could drive consistent and relatively low ventilation rates which could remove moisture significantly. Wind pressure differentials can either complement or act against the thermal buoyancy effect. Wind-induced force is instantaneous and varies at the different

locations of a building; hence, it is difficult to evaluate the wind effect and the combination of wind and buoyancy effect. Further research is required.

For the roof attic, Forest and Walker (1993) found that wind speed is a dominant factor affecting the ventilation rate through the attic. The ventilation air change rate expressed as air changes per hour (ACH) could vary by more than 10 ACH when the wind speed is in the range of 2 – 5 m/s, as shown in Figure 2-3-7. They also conclude that the buoyancy effect had much less influence on the attic ventilation rate, only a maximum of 2 ACH contributed by the stack effect alone over a two-year test period.

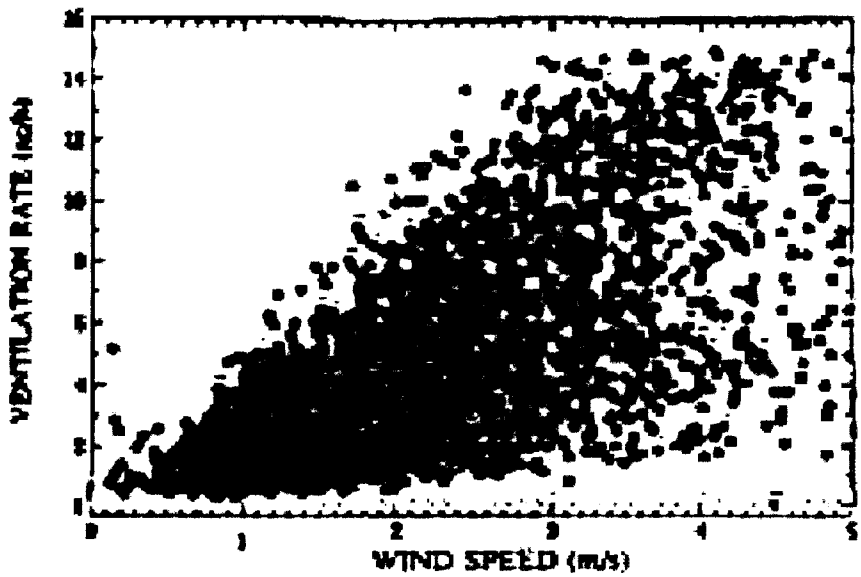

Figure 2-3-7: Ventilation rate measurement in an attic vs. wind speed (adopted from Forest and Walker, 1993)

2.3.2.1 Wind pressure differential measurement and prediction

The factors affecting the wind pressure differentials are the geometry and size of the building, locations and distance between vents, wind speed and wind directions (Straube and Burnett, 1995). Low-rise buildings may often be shielded by adjacent buildings and

their position close to the ground while mid-and high-rise building will frequently be completely exposed to the wind.

In theory, to quantify the wind pressure on the exterior surface of a rainscreen wall Bernoulli's equation can be used (ASHRAE, 2005):

$$P_w = \frac{1}{2} \cdot C_d \cdot \rho \cdot V^2 \tag{2-1}$$

where P_w is wind pressure on the surface, Cd is wind pressure coefficient from reference point to measuring points, ρ is air density and V is wind speed measurement at the reference point that should be outside the influence of the building and surroundings. The wind pressure coefficient is used to determine ventilation and / or air infiltration rates and can be obtained from wind tunnel model testing for the single, unshielded rectangular building (ASHRAE 2005) or from field measurements for the specific locations and buildings (Straube and Burnett, 1995; Gudum, 2004). The pressure coefficient is derived from the wind pressure on the surface at a specific location and stagnation pressure at the reference point such as at the weather station nearby. The average hourly pressure coefficients are often used since the wind pressures change frequently with time:

$$\overline{C_d} = \frac{\overline{P_w}}{\overline{P_{ref}}} \tag{2-2}$$

where, $\overline{C_d}$ is average hourly pressure coefficient, $\overline{P_w}$ is average hourly wind pressure on the surface, $\overline{P_{ref}}$ is the stagnation pressure at the reference point.

Then the wind-induced pressure differential can be calculated using the coefficient C_d as:

$$\overline{P}_{w(vent,in-vent,out)} = (\overline{C}_{d(vent,in)} - C_{d(vent,out)}) \cdot \overline{P_{ref}} \qquad (2\text{-}3)$$

where $\overline{C_{d\ (vent,in)}}$ is wind pressure coefficient between entrance vent and reference point, $\overline{C_{d\ (vent,out)}}$ is wind pressure coefficient between exit vent and reference point.

Measurements of pressure differentials between vents at top and bottom have also been taken in previous studies. VanStraaten, R. (2003) measured the pressure differential between the top and bottom vents under a constant airflow rate to determine the local discharge coefficient of vents, as shown in Figure 2-3-8. The discharge coefficients measured were used for the prediction of cavity airflow rate in the field experiment. He found that the local discharge coefficient is 0.8 and larger than the theoretic value of 0.6 recommended by ASHRAE (2005) and Straube and Burnett (1995).

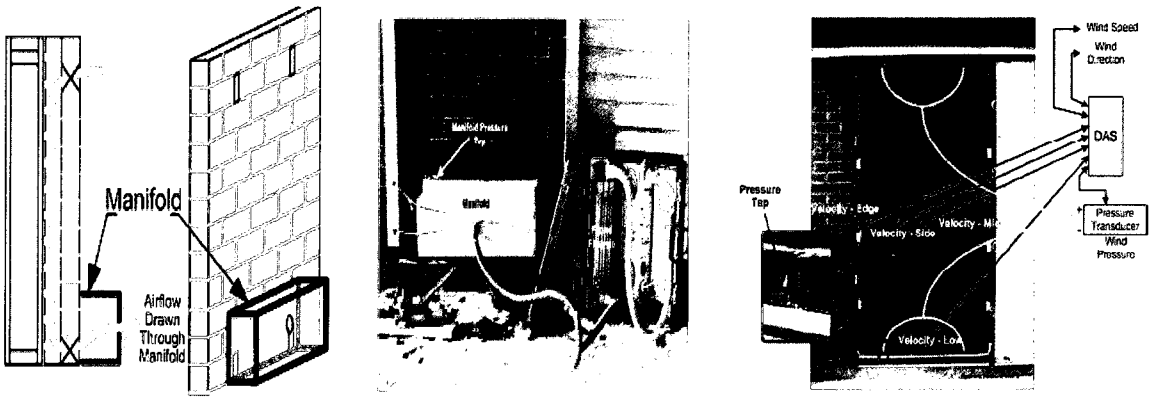

Figure 2-2: Forced Air Flow Path through Ventilation Cavity Figure 2-3: Photograph of Setup for Induced Flow Measurements Figure 2-4: Experimental Setup for Natural Flow Measurements

Figure 2-3-8: Steady ventilation rate manifold and pressure differential measurement set-up (from Vanstraaten, R. 2003).

The wind pressure differentials in most research are predicted using wind speed and wind pressure coefficient from the existing literature or measured coefficient. The pressure differences between a reference point above the roof and a point outside and inside of

each vent were measured to calculate the pressure coefficients in Gudum's experiment carried out to study the cavity convective moisture transfer (Gudum, 2003), as shown in Figure 2-3-9.. However, Gudum measured wind pressure differential directly between P1 and P2, which is outside the air cavity near the top and bottom vents, and between P3 and P4, which is inside the air cavity near the top and bottom vents. She also measured the reference wind pressure above the test house at the Technical University of Denmark in Lyngby. She used measurement of pressure differential between P1 and P2 and wind pressure at reference point to compare the measured pressure differential coefficient with theoretic wind pressure differential coefficient. She found that the difference between measured and theoretic wind pressure coefficients is high when wind speed is low.

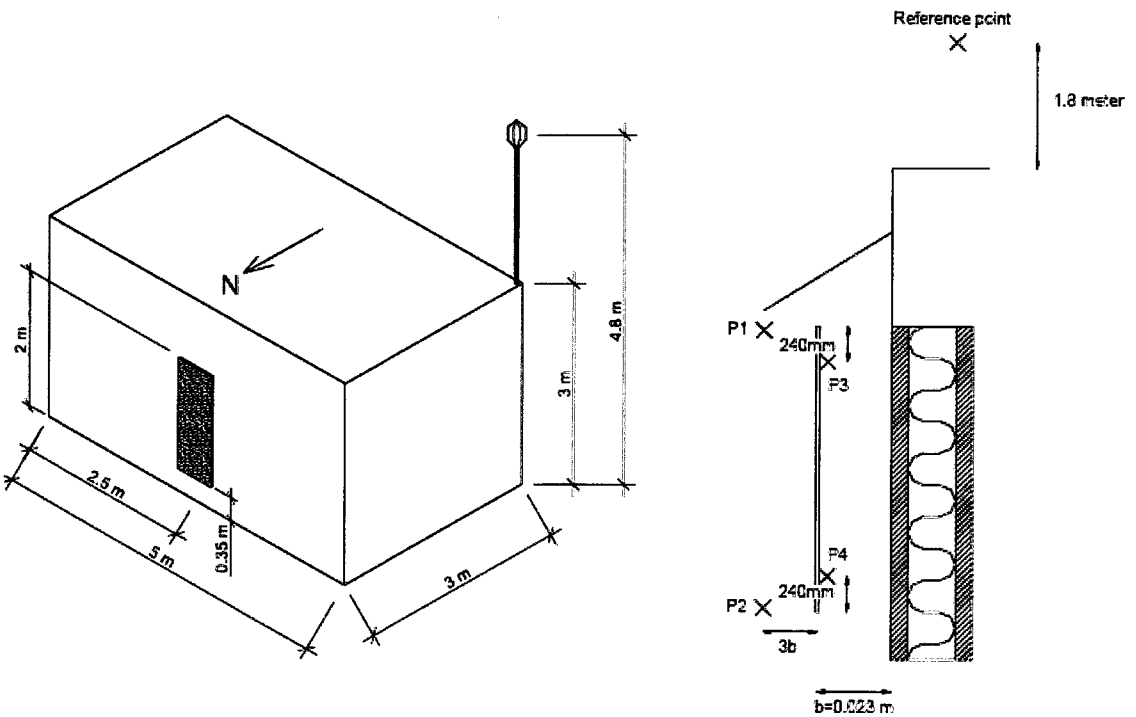

a) reference point of wind pressure measurement above the test house in Denmark

b) wind pressure difference measured between P1 and P2, P3 and P4 with the reference point

Figure 2-3-9: Wind pressure measuring point of the test wall and reference point above test building (from Gudum, 2003).

2.3.2.2 Buoyancy pressure differentials

The factors affecting buoyancy pressure differentials between air cavities of test walls and outdoor air are:

- Temperature differences between the cavities and outdoor air cause air density difference. Hence it creates thermal buoyancy pressure differential to induce air movement in and out of air cavity
- Moisture differences in the air between cavities and ambient air also cause air density change since the density of water vapour is smaller than that of dry air. More vapour in the air, the lower mixed density the air has. It creates moisture buoyancy pressure differential to drive airflow in and out of air cavity.

This phenomenon produces pressurization in the upper space between cavity and outside environment to induce the cavity air moving out through top vents in a cladding. At the same time the bottom of the cavity is depressurized and the ambient air enters the air cavity from the bottom vents by the reverse pressure differential. If the cavity air is colder than the outdoors, it would be reversed (ASHRAE 2005).

With the aid of Figure 2-3-10, variation of the absolute air pressure with height between air cavity and outside with different vent configurations can be described. Figure 2-3-10a indicates a cavity with bottom vents only and the cavity temperature is greater than ambient air temperature. The air pressure in the cavity is equivalent to the ambient pressure at the bottom opening. The air pressure decreases with height. The decline of outdoor pressure is faster than cavity pressure as the density of the ambient air is higher than the cavity air (Wilson, A.G. and Tamura, G.T. 1968). Hence, the cavity pressure

above the openings is greater than the ambient air. The horizontal distance between the lines, which represent pressure inside and outside of cavity, defines thermal buoyancy pressure differential. It is also called buoyancy effect or stack effect. In this case, the maximum magnitude which occurs at the top is the buoyancy effect for the total height (H) of the cavity. The air movement would be restricted and may only have circulation and air exfiltration through the cladding if the cladding material is air permeable but no ventilation would occur since there is no top vent.

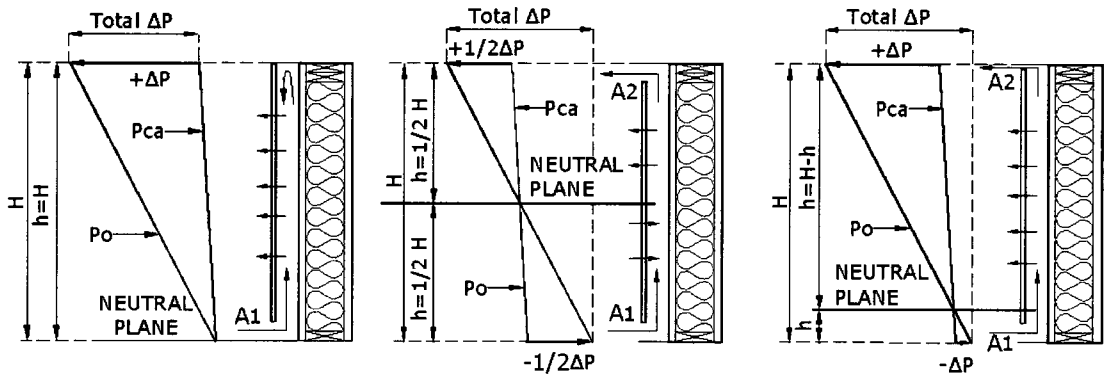

a) Only bottom vent A1

b) Equal sizes of bottom vent A1 and top vent A2

c) Large bottom vent A1 and small top vent A2

Figure 2-3-10: Different cases of thermal buoyancy effect in air cavity (modified from Wilson, and Tamura, 1968).

Figure 2-3-10b describes a cavity with equal sizes of top and bottom vents on the cladding. The air in the cavity is warmer so that it is lighter than the ambient air. The cavity air tends to rise and escape through the top openings while the colder ambient air enters through the bottom vents to replace outgoing air. The pressure differentials at the bottom and the top would be equal since the top and bottom vents are dual size (Wilson, A.G. and Tamura, G.T. 1968). The level at which the pressure differential change is from positive to negative as shown in Figure 2-3-10b is called neutral plane and represents no pressure differential between air cavity and ambient air at this level. In this case, the neutral plane is at the middle of the cavity.

The vents in a cladding are not always identical, but the in-flows are always equivalent to the out-flows. When the top vents are smaller than the bottom vents, the resistance to the airflow at the bottom vents becomes smaller. The pressure differential through the bottom vent therefore will be less than that across the top vent. The neutral plane moves down to a lower level depending on the area ratio of top vent A2 and bottom vent A1 as shown in Figure 2-3-10c.

The thermal buoyancy pressure differential above the neutral plane can be calculated from the equation (2-4) (ASHRAE 2005), considering the outdoor dry air density with temperature variation between inside and outside of cavity (ASHRAE 2005):

$$\Delta P_s = \rho_{outdoor} \left(\frac{T_{outdoor} - T_{cavity}}{T_{cavity}}\right) \cdot g \cdot (H - h_{npl}) \qquad (2\text{-}4)$$

where ΔP_s is thermal buoyancy pressure differential, Pa, $\rho_{outdoor}$ is ambient air density, kg/m^3, $T_{outdoor}$ is ambient air temperature, K°, and T_{cavity} is cavity air temperature, K°

2.3.3 Airflow rate in the cavity

Airflow in a cavity is complex in terms of its path, conditions of the cavity and surrounding environment, building geometry and vent configuration setting. The major factors affecting the airflow rate in the cavity are driving forces, resistance factors through the cavity and vents, and physical conditions of cavity such as cavity depth and vent size, type and layout.

Techniques for cavity airflow speed and airflow rate measurements used in previous studies are thermal anemometer and tracer gas. A smoke pencil detector can also be used

for a single point measurement in a short time to verify the measurements using other methods (VanStraaten and Straube, 2004). According to Gudum, (2003), both thermal anemometer and tracer gas technique are suitable for the measurement of average ventilation airflow rate.

The advantage of hot-sphere thermal anemometer is its short response time. It is suitable for point measurement of real-time air speed and can capture the change of air movement and turbulence intensity. If using the thermal anemometer technique to estimate cavity airflow rate, multi-point measurements are needed to evaluate the air speed distribution in the air cavity in order to obtain a reasonably accurate average cavity air speed.

Tracer gas technique has a reasonably long time constant of around 10 minutes and is suitable for measuring average airflow rate over a relatively long time intervals (Bassett and McNeil, 2005). It can also be used to determine the direction of airflow movement according to the change of gas concentration from the sampling points in the air cavity.

Gudum (2003) measured the air change rate in a cavity in the field using both tracer gas and thermal anemometer to identify whether both techniques are suitable to measure air velocity in the cavity under real weather conditions. Six thermal anemometers were placed in the mid-depth of the cavity and symmetrically along the vertical centre line and below the mid-height in the cavity. Two more probes were placed near the vents (Figure 2-3-11). According to Andersen (2000) the average velocity across the cavity depth is approximately 2/3 of the maximum velocity measured at the centre of the depth for laminar flow. Thus, the average velocity through the ventilated cavity was determined from 2/3 of the average value of six probes measurements. However, it was noticed from

the measurements that airflow is not laminar in the cavity with large air speed fluctuations across the cavity width.

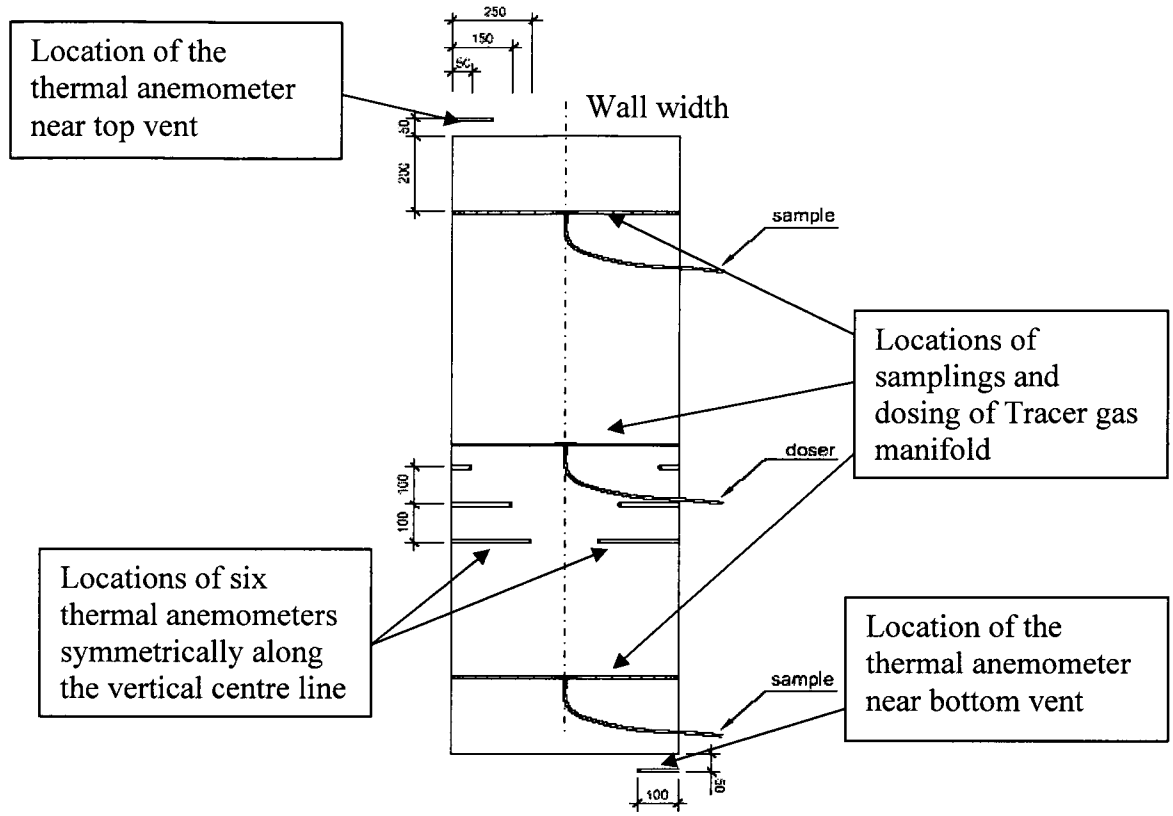

Figure2-3-11: Thermal anemometer probe layout and tracer gas dosing and sampling manifold in the cavity (from Gudum, 2003).

In the meantime, the air velocity, and direction of airflow were obtained from the tracer gas measurement. Dinitrogenoxide (N_2O) was used as a tracer gas in this work because its density is close to the atmospheric air. The tracer gas was uniformly distributed across the width of the cavity through a tube with 9 drilled holes. Using a gas analyser based on the photo-acoustic infrared detection method and sampling gas concentrations at upper and lower parts of cavity, the tracer gas technique can identify the recirculation, velocity, and direction of cavity airflow. The gas analyser also can be used to measure the convective moisture transfer between cavity and ambient air at the same time. The results from both measurements of thermal anemometer and tracer gas in Gudum's

experiment showed that the average air speed in the cavity is within the range of 0.12 – 0.22 m/s by thermo anemometer while within a range of 0.08 – 0.32 m/s by tracer gas measurements. At the same time, the mean wind is within a range of 0.7 – 2.1m/s with the mean wind direction from 260°(west) or 150°(south-east).

Bassett and McNeil.(2005b) also used tracer gas method to measure seven 1.2 m by 2.4 m walls installed on a test hut in New Zealand, three were open rainscreen walls which were without intended top vents but there were tiny continuous gaps with height of 0.2mm exist and four were ventilated walls. All of the cement claddings were painted and considered as non-absorption materials. Carbon dioxide was used as a tracer gas. The measurements were continued over 5 to 20 days with the constant injection of tracer gas. The average ventilation rate was determined from averaged tracer gas concentration measurement from four sampling points in the cavity at 15 minute intervals.

They conclude that the tracer gas method has a reasonably long time constant but cannot be used to measure the changes of ventilation rate within a short time period. The results show that the ventilation rates in the cavity of open rainscreen walls between theoretical calculations and measurements show a good agreement, The daily mean ventilation rates has better agreement rates than the hourly ventilation rates. The average ventilation rate of 0.4 L/ s·m was measured, indicating that even a very tiny and non-intentional leakage at the top of the rainscreen wall can result in a significant amount of cavity ventilation (M.R. and McNeil, S.2005a, b). An average ventilation rate of 1.4 L/ m·s was measured in another four ventilated walls and the airflow rate is higher than those in the cavity of open rainscreen walls. VanStraaten and Straube (2004) measured natural ventilation velocity in a cavity (equal top and bottom vents) of brick veneer wall in the field

condition using thermal anemometers. The conclusion made from the test is that the continuity equation (Q=V*A) cannot be used for single point air speed measurements due to the complexity of flow behaviour. The airflow at the centre of the cavity is much higher than the edge of the cavity (including the end of width and edge of depth). The correlation between prediction and the measurement of average ventilation air speed in the BEG test is established from three mid-height air speed measurements located at centre, the point between centre and the end of width, and the end of width in the air cavity (VanStraaten and Straube, 2004):

$$BEG\_correlation = 2.3 \cdot \left(\frac{BEG\_V\_mid + BEG\_V\_edge + BEG\_V\_side}{3} \right)$$

where, all the measured points are at the mid-height of the air cavity; V is the air speed, mid refers to the centre of cavity, edge refers to 100mm from the edge of air cavity in width, and side refers to 230mm from the edge of air cavity in width (see Figure 2-3-8).

The air speeds measured in the field tests by VanStraaten and Straube are shown in figure 2-3-12. The air speed measured at the mid-width is much higher than the air speeds at the edge of the cavity in width.

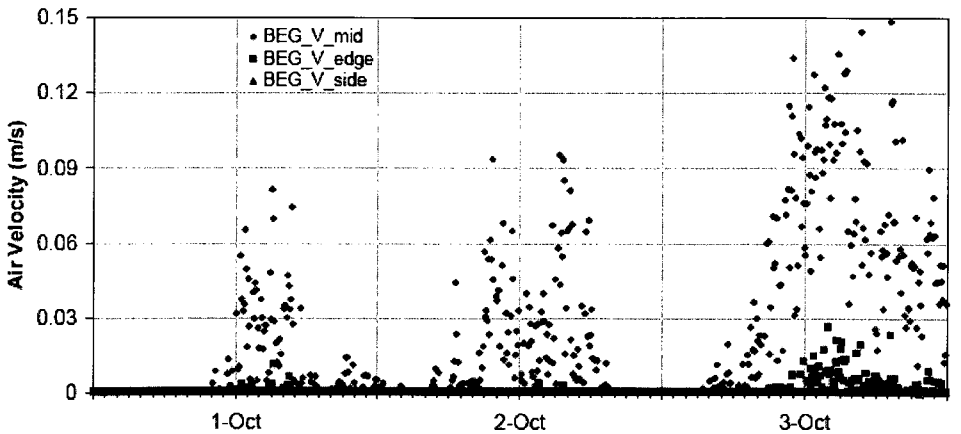

Figure 2-3-12: Air speed measurements in the cavity of brick wall by natural forces under the field condition on BSGHUT at University of Waterloo (from VanStraaten, 2003).

The natural ventilation air speed was also measured by using smoke pencil to confirm and validate the ventilation rate calculated based on air speed measurements. Smoke was drawn into the bottom vent of the 2.4m high wall and the time it took for the smoke to exit the top vent was recorded. A 0.03 m/s smoke flow speed was measured, which is similar to the measurements by thermal anemometer and correlates to a ventilation rate of 0.3 l/s.m according to VanStraaten and Straube (2003).

Straube, et. al. (2004) conducted an extensive review of previous research on cavity ventilation effect including laboratory and field experiments and simulations. A summary of the previous research reviewed in his report is included here as follows:

Schwarz (1973) measured the cavity air velocity in an 18-floor apartment building with a 1.25m x 1.35m open-jointed panel cladding system in Hamburg, Germany. They found that the cavity air velocities were in the range of 0.2 – 0.6 m/s under 0 – 8 m/s of wind speed range. They also found no direct relationship between building height and cavity air velocity and ventilation velocities were stable at 0.2 m/s in the leeward side but lower than in the windward side of the building.

The Institute for Brick Research in Germany (German Institur Für Ziegelforschung) has set up a field experiment of ventilation effect on the drying of the brick veneer walls in a test building in Essen, Germany (Jung, 1985). The cavity was 40mm deep with a 30 mm open joint under the eaves and at the bottom at 250 mm spacing. The average cavity ventilation velocity was measured at about 0.1 m/s under an average wind speed of 2.6 m/s resulting in an average of 100 air change rate per hour (ACH).

Sandin (1991) in Sweden studied different types of brick-veneer with wood-frame walls under field conditions and measured cavity air change rate using tracer gas technique. He found the cavity air change rate was 0.3 – 8 ACH in a cavity with a depth of 20 – 50mm. However, when the vent opening was changed from the open joint to removing an entire brick at 1200mm spacing, the air change rates increased significantly to 3 – 25 ACH.

The ventilation rates and velocities with correlated parameters and outdoor wind speed reported in the literatures above are summarized in Table 2-3-1. The assembly of measured results from various sources shows that:

- The larger the vent size, the higher the cavity ventilation rate.
- Ventilation rates in walls with panel-type claddings are higher than those in brick walls with discrete vents (open joints).
- Ventilation rates do not change much when the air cavity depth is changed from 20 to 50 mm.

Table 2-3-1: Ventilation rate or velocity measured in field tests

Reference	Bassett & McNeil, 2005			VenStraaten, & Straube, 2004	Gudum, 2003		Sandin, 1991		Jung, 1985	Schwarz, 1973
Location	New Zealand			Waterloo, Canada	Denmark		Sweden		Germany	Hamburg, Germany
Cladding	Brick	Fibre cement		Brick	Plexiglas panel		Brick		Brick	Panel
Air cavity depth, mm	40	20	20	20 or 50	25		20 -50		40	
Air cavity width, mm	1200	550	550	1200	559		1200	1200		1250
Top vent	1200 - 1650 mm^2	100 mm^2	560 mm^2	800 mm^2	50 mm		Open joints between bricks	A whole brick space	30 mm	open joint
Bottom vent	1970 - 3150 mm^2	560 mm^2	560 mm^2	800 mm^2	50 mm				30 mm	
Wind velocity, m/s	2.1 – 2.9	2.0 – 4.8	2.4 – 3.8	1 - 4	0.69- 2.12				2.6	0 – 8
Air speed in cavity, m/s				0 – 0.06	0.12 – 0.22	0.08 – 0.32			0.1	0.2 – 0.6
Ventilation rate, L/s. m	0.75 - 1.32 l	0.22 - 0.52	1.38– 1.90	0 - 0.5			0.3 – 8 ACH	3 – 25 ACH	100 ACH	
Instruments used	Tracer gas			Anemometer	Ane-mometer	Tracer gas	tracer gas			

2.4 Effect of cavity ventilation on building envelope performance

This section firstly provides a general review of the ventilation drying concept, the requirements of ventilation drying of building enclosure, and previous research done on the effect of ventilated roofs and wall cavities. Secondly, the review focuses on research on ventilation effect in the air cavity of rainscreen wall system including effects of parameters affecting the ventilation drying and drying process of rainscreen wall systems. The parameters related to ventilated air cavities include cladding, cavity depth, vent size and location, and airflow rate. The environmental parameters such as outdoor and indoor conditions, solar radiation, and rain penetration and building envelope hygrothermal control parameters such as weather resistive barrier, air and vapour barrier system will also be discussed.

2.4.1 Concept of ventilation drying

Ventilation is an exchange of outdoor air with the air in a building or in an air space within building envelope and usually refers to an intentional air exchange from outside into a building or in a building envelope system (ASHRAE 2005). Regarding the drying function provided to the building envelope, natural ventilation is the process of airflow driven by natural forces through open attics, crawl spaces, air cavity of a wall or any other planned building envelope penetrations, which is intended to be used to dry the components of building envelope.

2.4.2 Basic requirements of ventilation drying

For effective ventilation drying in an air space of a building envelope, at least two requirements must be met: drier air flowing into the air space and a sufficient amount of airflow.

1. Drier air with warmer air temperature in an air space

Outside drier ambient air flowing through the air space has the capacity of holding more moisture; thus, entering air can move out the moisture from the building materials (Straube, et. al. 2004). When heated by the sun, the increased air temperature in the air space has lower RH and can hold more moisture so that the entering air can remove more moisture (Roodvoets, 2001).

2. Effective ventilation

Air movement must exist in the air space when the ventilation drying occurs. The pressure differential in the space due to wind pressure or stack effect is the major convective force to drive ventilation. If there is no pressure differential, on the other hand, ventilation does not occur even through there are top and bottom vents. In theory, ventilation will be more effective when balanced ventilation can be achieved with equal vent areas at top and bottom (Roodvoets, 2001). Therefore, the National Building Code of Canada (NBC, 1995) and British Columbia Building Code (BCBC, 2006) require the top and bottom venting areas are equal in the roof attic ventilation and uniform distribution of vent areas are on the opposite sides of crawl space if there is nature ventilation.

2.4.3 Effect of ventilation on attic roofs and cathedral ceilings

Attic ventilation that diminishes condensation on roof sheathing in the cold weather was first reported by Rowley, et. al. (1939). The current requirement by BCBC (2006) of 1: 300 vent area ratio for roof attic ventilation was probably established based on this report (Rose, & TenWolde, 2002). Attic ventilation becomes an important part of residential roof design. Both American and Canadian National building codes require attic ventilation to minimize condensation on the underside of roof sheathing and ice dams on the roof eave in the winter and to provide cooling attic air and reduce cooling load in the summer (ASHRAE 2005). The ASHRAE fundamental handbook has recommended attic and cathedral ventilation to control moisture for decades (Rose, & TenWolde, 2002).

Rose and TenWold (2002) summarized the earlier studies on attic and cathedral ceiling ventilation and found that ventilation of attic and cathedral ceiling is not always practical and desirable. Many studies showed that condensation in the attic occurred with high humidity in the living space. Vapour retarder is not a reliable moisture control because the major condensation source was air infiltration through the ceiling into the attic. In humid and cold climates, a main moisture source in the attic is the moisture laden outside ambient air carried into the attic by ventilation. Forest and Walker (1993) simulated the moisture performance of ventilated attics in several climates of Canada using a model that was verified by field measurements in Alberta. This first attic simulation program modeled ventilation, thermal and moisture in attics. They concluded that either too much or too little attic ventilation would cause MC increase in wood components. The ventilation related-moisture problems were mainly induced by a high ventilation rate

when the sheathing temperature of airtight attic was cooled at night. The higher wind speeds at night caused the worst moisture problem if the relative humidity (RH) of outdoor air was high. Specifically, in wet coastal climates of Canada, higher attic ventilation rates caused higher roof sheathing MC than the lower ventilation rates (Forest and Walker, 1993).

Houvenaghel, el. at. (2004) studied two design parameters in insulated pitched roofs through field testing: (1) vapour-permeable versus vapour-impermeable underlay at the warm side of the insulation; and (2) ventilated versus non-ventilated on roof rafters between the underlay and insulation.

Because the attics were included in the living space, the insulation was installed in roof pitch instead of the horizontal ceilings. All the roof slopes were 45° and roof pitches had low air permeance. The testing took place at the test hut in Belgium over two winters. The average outdoor temperature was 4.3°C and 7.5°C, the RH was 82% and 85%, and solar radiation was 329 W/m² and 219 W/m² in the first winter and the second winter, respectively. The interior conditions were 23°C with an average vapour pressure difference between inside and outside of 423 Pa. The test results showed all the roofs worked properly without major condensation problems and rain penetration. Overall, both roofs with and without ventilation had similar thermal performance. Ventilated roofs have slightly lower RH than the roof without ventilation.

2.4.4 Effect of air cavity ventilation on rainscreen wall systems

In recent years, a number of studies have been done to evaluate the effect of air cavity ventilation on the hygrothermal performance of rainscreen wall systems in North America. The research topics included cavity ventilation rates, impact of environmental conditions and moisture loading, and impact of wall configurations such as cladding selection, permeance of sheathing membrane, and vapour barrier systems.

One such study, the ASHRAE 1091 project (Schumacher, et. al. 2004; Shi, et. al, 2004; Straube, & VanStraaten, 2004; Karagiozis, 2004a and b; Burette, et. al. 2004), completed a series of modeling, and laboratory and field testing to evaluate the effect of air cavity ventilation drying in screen-type wall systems. The field testing in this project was monitoring the drying effect of cavity ventilation by introducing wetting events onto fibreboard sheathing in different seasons with different vent configurations, claddings and depth of air cavity. The Seattle hygrothermal performance project assessed the moisture performance of rainscreen walls and traditional face sealed stucco walls under simulated and field conditions (Karagiozis, 2002).

The Moisture Management for Exterior Wall Systems (MEWS) Project at the National Research Council (NRC) also reviewed typical construction practices and evaluated wall performance under the climatic moisture loads to be found at different North American locations. This research was through laboratory testing and simulation to predict moisture balances within the wall assemblies at selected North American cities (Rousseau, & Dalgliesh, 2004).

Canadian Mortgage and Housing Corporation (CMHC) earlier conducted several modeling, field and laboratory tests on stucco wall drying performance (Nehdi, 2001; Hazleden, 2001, Lawton, 1999). A field monitoring of hygrothermal performance of rainscreen walls under in-service conditions in Vancouver was recently completed (RDH, 2005; Finch, et. al. 2005; Hubbs & Finch 2006).

The ongoing Vancouver Field Exposure Testing was started in 2005 to evaluate the moisture performance and drying potential of absorptive cladding in face sealed and rainscreen walls and the ventilation effect in attic and cathedral roofs (Straube, 2006). One of the objectives in this project was to investigate whether polyethylene is a suitable vapour barrier for the west coastal climate (Lazaruk, 2006).

In Europe, simulation, field and laboratory tests have been carried out to evaluate the air cavity ventilation drying effect as well as ventilation airflow rate and vapour control strategies (Hansen, 2001; Gudum, 2003; Vinha, et. al. 2004; Simonson, 2005; and Bassett, et. al 2005).

A summary of findings and conclusions is presented below:

1. Influence of wall components

a. Cladding

The properties of exterior claddings have a significant influence on the ventilation drying. Walls with wood siding, vinyl siding, stucco, metal panels, plexiglas panels and brick veneer have all been tested and modeled for their drying capacities. Metal and plexiglas are impermeable materials and vinyl belongs to non-absorptive materials. All of the

other claddings mentioned above are absorptive or storage materials. The following points summarize the salient results of these tests:

- The wall panel with wood siding dried faster than the wall panel with stucco without solar radiation while the results was reversed with solar effect in the laboratory testing (Hazleden, 2001).
- Comparing metal cladding panels with vinyl siding panels, the climatic chamber experiments showed that the fibreboard sheathing behind metal panels dried slightly faster than that in the vinyl clad panel in the winter due to the high thermal conductivity of metal and continuous slot vents at the bottom and top while vinyl siding does not have intended vent opening. As a result, a large volume of warmer air heated up by solar radiation in the cavity of the wall clad with metal panel enhances drying. However, the vinyl siding wall dried significantly faster than the metal clad-panel in the summer since the ventilation path between the vinyl sidings is much shorter than the metal panel (Shi, et. al. 2004). The ventilation paths in the cavity through vinyl sidings run horizontally through loosely assembled joints and edges between two pieces of vinyl sidings (each individual piece is 8" - 12") and vertically through the air cavity (Straube, et. al. 2004), as shown in Figure 2-4-1. Whereas the ventilation path behind the metal panel runs vertically through the height of air cavity (2.4 m).

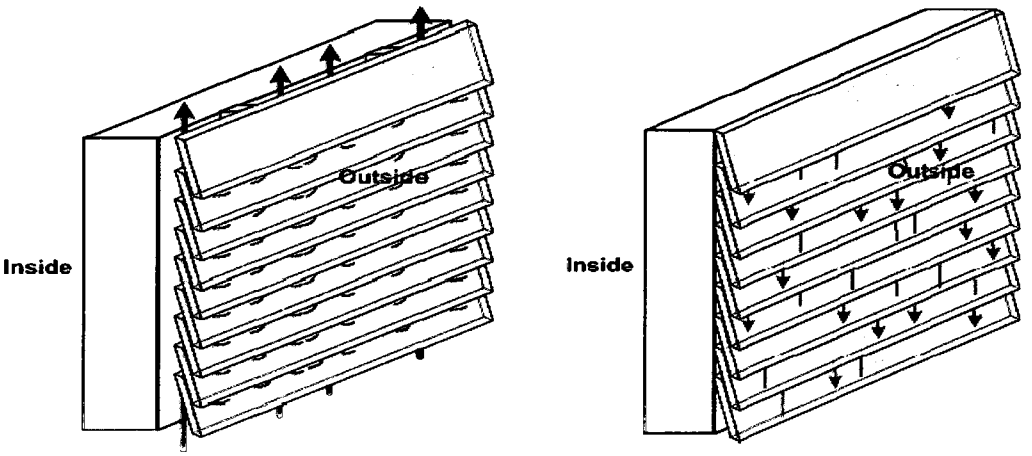

a) With vertical strapping b) Without vertical strapping

Figure 2-4-1: Airflow paths around vinyl siding with and without vertical strapping (adapted from Straube, et. al. 2004).

- In the field testing, the drying rate of the wet sheathing (by injecting water seasonally) in vinyl-clad walls was lower in the winter and spring but similar to those of brick clad-walls in the summer and fall (Straube and VanStraaten, 2004).
- Karagiozis (2002) concluded that major climate regions in the U.S.A. likely benefit from the use of ventilation behind the absorptive cladding. Non-absorptive wall system such as vinyl siding can also benefit from ventilation due to the leaky nature of material, but much lesser than the absorptive cladding.

b. Permeance of exterior sheathing membrane

The three types of exterior sheathing membrane that are most commonly used in the construction industry include 30- and 60-minute building paper (BP), #15 asphalt-impregnated felt paper (#15 felt paper), and spun bonded polyolefin (SBP). Permeance of the exterior sheathing membranes may have an influence on the drying rate of rainscreen wall systems. The properties of these materials are listed in Table 2-4-1 below.

Table 2-4-1: Vapour permeance of exterior sheathing membrane

Membrane material	Vapour permeance ng/s.m².Pa		Source
	Under 50%	Above 50%	Shi, 2004
SBP	3400		
#15 felt paper	300	3000	Karagiozis, 2004
HAL-TEX 30 min BP	420		HAL Industries Inc. 2006
HAL-TEX 60 min BP	320		
HAL-TEX double 30 min BP	260 - 300		
HAL-TEX double 60 min BP	N/A		

The climatic chamber testing under a simulated cold climate for Minneapolis (-15 - -5°C and 70% RH with a maximum daily solar radiation of 600 W/m²) and constant indoor conditions (21°C and 50% RH) and field testing at the test hut of University of Waterloo confirmed that the test walls with SBP had significantly drier conditions in the stud space than the walls with #15 filter paper (Shi, 2004, Straube & VanStraaten, 2004). The drying rates, a measure evaluated by the time required for the first 10% MC dropped in wood fibreboard sheathing after wetting, in walls with SBP sheathing membrane were at least three times faster than those with #15 filter paper (Shi, 2004).

In the simulation of moisture performances of stucco clad walls for Seattle climate Karagiozis (2002) found that the wall with two-layer 60-minute BP had lower MC in oriented strand board (OSB) sheathing than the walls with one-layer 60 minute BP or with15# felt paper. The two-layer BP is relative impermeable at low RH condition but become quite permeable at high RH, i.e. 80% RH. In addition, two-layer BP can accelerate drying if there is water penetration due to its better drainage performance. The Seattle simulation results indicated that the weather resistive membrane had less influence over drying performance when used in the ventilated cavity.

Other modeling and testing showed no significant difference in the drying rates of wet wood members with different sheathing membrane (Hazleden, 2001; Rousseau, & Dalgliesh. 2004).

c. Sheathing materials

The sheathing materials used in the testing and modeling are wood fiberboard, OSB and plywood. In the construction industry, plywood and OSB are typically used as exterior sheathing materials. Fibreboard might be used in cold and dry climates in North America, but the use in the west coastal climate was restricted due to its high vapour permeance under cold and wet winter conditions. The high vapour permeance of fibreboard would accumulate much more moisture in the wet climate and cause deformation i.e. swelling and strength decrease. Fibreboard is not allowed for the attachment of cladding (BCBC 2006). The properties of these three sheathing materials used as exterior sheathing are shown in Table 2-4-2:

Table 2-4-2: Moisture properties of sheathing materials

Materials	Test conditions	Thickness mm	Dry density Kg/m^3	Vapour permeability ng/m.s.Pa	Source
4-ply Plywood (Canada)	22 °C & below 70% RH	12.8	394.9	0.8 - 3.7	Ojanen & Ahonen, 2005
	22 °C & above 70% RH	12.8	394.9	3.5 - 8.9	
OSB (Canada)	22 °C & RH from 25% - 70%	11.6	579.3	0.6 – 1.7	
	22 °C & RH from70% - 85%	11.6	579.3	1.7 - 5	
Wood fiberboard	10 – 100% RH	12	440	12.4 - 19	Kumaran, et. al. 2002

From Table 2-4-3, it can be seen that the wood fiberboard has the highest water vapour permeability followed by plywood and OSB has the lowest vapour permeability. It should be noted that these values may vary depending on the species of wood and manufacturing processes.

In the ASHRAE project 1091, both laboratory and field testing showed that the fiberboard sheathing dried quickly by solar radiation due to its higher vapour permeability (Shi, et. al. 2004; Straube & VanStraaten, 2004). Hazleden found in the laboratory experiment that the test walls with plywood sheathing dried faster than the panels with OSB due to its high initial MC as a result of greater storage capacity (Hazleden, 2002).

Using hygIRC hygrothermal numerical model, Rousseau and Dalgliesh (2004) demonstrated that all masonry walls with a clear cavity and higher air and vapour permeance sheathings had a remarkable increase in drying potential of walls for a wide climate range. Salonvaara, et. al. (1998) concluded that a high enough vapour permeable exterior sheathing is required in order to improve the drying capacity of a wall based on the comparison made between the laboratory testing results and the simulations. Cavity ventilation could not increase the drying in the insulation layer if the exterior sheathing has low vapour permeance (Salonvaara, et. al. 1998). However, using MOISTURE EXPERT (Karagiozis, 2001), Karagiozis concluded in modeling that sheathing materials in the non-cavity walls significantly influenced the moisture performance of stucco-clad walls when the interior open-vapour strategy is used. But, if a ventilation cavity or interior vapour tight strategy is employed, the overall effects of exterior sheathings are similar and the material selection is negligible (Karagiozis, 2002).

2. Influence of air cavity configuration

a. Air cavity depth

The laboratory testing showed that panels with cavities dried faster than comparable panels without cavities and the walls with a 19mm cavity dried faster than panels with a 10mm cavity (Hazleden, 2001). The climatic chamber testing showed that drying rates were the same behind strapped and contact – applied vinyl siding, indicating air flow along contact-applied vinyl siding to be sufficient to promote drying. Field testing produced the same result indicating that adding strapping behind vinyl did not have a noticeable increase in drying rate (Shi, et. al. 2004; Straube and VanStraaten, 2004) Changing the cavity depth from 20mm to 50mm in the brick veneer wall produced no noticeable difference of drying capacity, either (Straube and VanStraaten, 2004) .

b. ventilated and vented air cavity

It is clear that the walls with an air cavity have more tolerance for rain penetration. Generally, having ventilated air cavity improves the drying capacity of walls in a large range of climate regions (Karagiozis, 2004; Rousseau, & Dalgliesh, 2004). The difference of drying rates between ventilated cavities or unvented panels can be as much as 3 to 4 times, i.e. ventilated walls dried 33% faster than in unvented walls in a Vancouver laboratory experiment (Hazleden, 2001). The same result was found in the Seattle modeling (Karagiozis, 2004). The evaluation made by MOIST 3.0 (MOIST, 1997) in a simulated Vancouver study confirmed that even a factor of 5 could be achieved if expanded polystyrene was used (Nehdi, 2001).

One very interesting study that produces different results is a modeling and field testing project done in Denmark (Hansen, et. al. 2002). This study was based on the concept that "ventilation with dry air will remove moisture from the construction whereas ventilating with humid air might add moisture to the construction" (TenWolde, A. et. al. 1995). This research evaluated the effect of cavity ventilation on the drying potential of timber frame walls. Simulation results using MATCH (MATCH, 2003), a one-dimensional HAM program, showed that a ventilated cavity behind the cladding would increase the MC in exterior sheathing. A field experiment was conducted as well during 1999 to 2002 on an 11.5 m by 7.9 m test house at the Danish Building and Urban Research. All the timber frame test walls were identical with varied parameters of ventilated or non-ventilated cavity or no cavity behind the cladding. Panels were installed on the north and south façades of the test house under real weather with temperature of 17 - 22 °C and 65 - 80% RH in the summers and temperature of -5 - 8 °C and 80 - 98% RH in the winters. Indoor conditions were maintained at 20 °C and 60% RH.

No conclusions were made after two and a half year-measurements in term of proving non-ventilated cavities performed better than ventilated cavities. On the other hand, there were no conclusive evidence demonstrated that a ventilated cavity is to be preferred. In some of the vented cavity walls, the top and bottom of the cladding was not perfectly airtight. These walls dried faster or at least similar as the walls with ventilated cavity (Hansen, et. al. 2002). That might have contributed to the very little difference between ventilated and non-ventilated test walls.

Bassett & McNeil (2005) also found in the field testing of stucco rainscreen walls that, even though the air gap at the top of their panel was merely a 0.2mm opening, the

resulting air flow rate enhanced ventilation (far greater than merely air leakage). The measurement of airflow rate in the cavity was 4 times larger than the expected air leakage rate (0.011 – 0.1 L/s.m^2) in the cavity. They concluded that this kind of design and construction of a stucco clad system was suitable in New Zealand even though the ventilation rate is 4 times smaller than that in ventilation walls which had equal area of designed vents.

After the highest effective permeance of 1663ng/pa.s.m^2 was found in a wall with a 19mm cavity and bottom vents only in a laboratory experiment, Hazleden recommended that ventilated air cavity construction should be encouraged but that the top vent should be very small and shielded to prevent water ingress (Hazleden, 2001). The drying of bottom vented walls was similar to that of the ventilated wall (with equal top and bottom vents) since the bottom vented walls were not perfectly air sealed at the top. It was possible that a small amount of air flow out from the top of the cavity and this small amount of air through the cavity was adequate to vent the wall panel. The modeling with WALLDRY also predicted that the panels with bottom venting (with very tiny top gap) would perform similarly to those with top and bottom vents, indicating the large area of top venting could be eliminated because sufficient air flow in the air cavity can be achieved with a small top opening (Hazleden, 2001).

In summary, cavity ventilation has a positive effect for drying. Ventilation in the air cavity fosters more drying of ventilated walls than that in a vented cavity, i.e. no top vent completely. Whether a fully ventilated (equal areas of top and bottom vents) or partially ventilated cavity (a smaller top vent) is needed in rainscreen walls may depend on the climate and indoor humidity conditions.

On the other hand, the diurnal change of drying at daytime and wetting at nighttime observed in the laboratory experiment and field testing indicated that ventilation brings moisture into the cavity and wets sheathings in under-cooling conditions (Shi, et. al. 2004; and Gudum, 2003).

The preliminary observation of the ongoing project at the Vancouver Field Exposure Testing showed that wetting from outside through the cladding to the wall assemblies occurred due to the wind-driven rain and under-cooling effect but did not result in a serious increase of MC for all the test walls including both face-sealed and rainscreen walls. This conclusion relied on good construction of test wall assemblies without defects or deficiencies and was restricted to a suburban location (Straube 2006).

c. Correlations of ventilation airflow rate and drying rate

Laboratory testing and simulations showed that ventilation drying potential was affected by the ventilation flow rate (Shi et al. 2004; Piñion, et. al. 2004; Finch, 2007). The theoretical drying potential of convection can be determined according to the ventilation air flow rate and its RH and temperature. A mass transfer coefficient (equivalent permeance) can be calculated to provide an equivalent measure of drying capability of air cavity ventilation (Schumacher, et. al. 2004). Shi et al. (2004) showed that for the wall with vinyl siding at 1.6 L/s airflow rate, the initial drying rates (first 10% MC dropped from 20% of wood fibreboard sheathing) was 2 times faster than that at 0.4 and 0.8 L/s airflow rates and about 3 times faster than without ventilation flow (vents were sealed). Very little drying took place without ventilation air flow. The greater the ventilation flow rate, the faster the drying rate and ventilation airflow can remove significant amounts of moisture (Burnett, et. al. 2004, Finch, 2007). However, Burnett, et. al. (2004) found that

the theoretical potential drying by ventilation was always much higher than that measured results in the test of ASHRAE project 1901.

3. Moisture load on the sheathings or stud space

Rousseau & Dalgliesh (2004) concluded in MEWS project that a cladding of a rainscreen wall assembly provided sufficient water resistance in a wide range of climate moisture loading if no direct water leaks into the stud cavity to wet the exterior sheathing. However, if water penetrated into the stud space, the prolonged wetting of wall assembly resulted in lower drying potential by evaporating and ventilation. The level of deterioration risk for the wood components would be linked to the severity of the climatic moisture loads and the amount of water ingress into the stud cavity. The more humid the indoor and outdoor conditions, the less evaporation drying of the wetted stud cavity. The ventilation drying capacity of the wall can only cope with a small amount of water penetrated into the stud space.

Karagiozis (2004) simulated the MC in OSB sheathing of brick veneer walls and vinyl walls for five different North American climates during two years period. He found that when the initial MC of OSB was as high as 32% (twice of the equilibrium level of OSB in October), all the ventilated and vented brick walls could not dry within an acceptable period (4-6 weeks) to the equilibrium MC level of RH 80%. When the initial MC of OSB was 16%, drying in all the walls was sufficient for all vinyl claddings and for all ventilated brick walls in all climate regions. The vented brick wall have problems drying within an acceptable time in the Seattle climate, indicating the limitation of drying capacity under high moisture loads of exterior climate. The conclusions were made that ventilated air cavity enhanced the overall drying for absorptive cladding wall system.

The non-absorptive wall system benefited from ventilation due to inherent air leaky structure of the vinyl siding (Karagiozis, 2004, karagiozis, et. al. 2005). Table 2-4-3 summarizes the wetting load, initial MC and time required to dry in existing testing and modeling.

Karagiozis (2004) also evaluated the drying of sheathing under 1% rain penetration load for the five climate regions using simulations. Only two cities, Charlotte and Seattle, were selected for the analysis of drying factor of ventilated walls in comparison to unvented walls. The major difference between the ventilated and unvented brick clad-wall cases were observed and listed in Table 2-4-4. The amount of 1% rain water penetration is very small. For instance, 1% of horizontal rainfall in Seattle equals to a total amount of 3.2mm water penetrated onto the surface of the sheathing membrane over the entire year (Karagiozis, 2004b). The simulation results demonstrated that ventilation benefited when the wetting load is small. Seattle is the worst region for the ventilation drying performance due to its cold and wet climate.

Table 2-4-3: Drying time required for sheathing or wood frame with built-in moisture in rainscreen walls

Authors	Method	Wetting Locations	Wetting load	Initial MC of sheathing	MC changes and time to dry
Lawton, 1999	Lab testing	whole wall assembly	4000 ml		150 days
Hazleden, 2001	Lab testing	wood frame	7800ml - 7400ml	Without solar radiation OSB: 20 - 28% Plywood: 26-35%	For the wall panels without solar radiation at the first stage: In total weight, 1500ml water reduced in 63days with solar radiation after the first stage 2100ml water reduced in 83 days
				With solar radiation (120 W/m²) OSB: Average 23% Plywood: 37%	For the sheathings without solar radiation in 63 days: OSB: 1 – 3% MC drop Plywood: no change or increase 8% MC with solar radiation in 83 days after the first stage: OSB: 11% MC increase Plywood: 6-10% MC drop
Straube and Vanstraaten, 2004	Field testing	sheathing	1350ml – 1800ml	Fiberboard: 25%	The first 10% MC drop in 6-10 days in summer 20-80 days in winter
Shi, et. al. 2004	Climate chamber	sheathing	1800ml	fiberboard: 25%	The first 10% MC drop on about 6 days in summer 40 days in winter
Karagiozis, 2004	Modeling for Five climate regions: Charlotte Houston Miami Minneapolis Seattle	sheathing		OSB: 32%	No walls drop to16% MC in 4 – 6 weeks.
				OSB: 16%	Below 16% MC within three month from Oct to the end of the year. In the Seattle climate vented walls difficult to dry.

Table 2-4-4: Drying potential of ventilated walls under 1% rain penetration load in five different cities.

Location	MC difference of OSB in ventilated and vented walls within acceptable time (4 weeks)	The drying factor of ventilated to unvented
Charlotte	25% lower than unvented Only ventilated walls can dry to below16% MC of OSB within acceptable time	10
Houston	16% lower than unvented	
Seattle	8% lower than unvented	3 to 4
Miami	Ventilated wall has the highest drying potential	
Minneapolis	ventilated walls perform satisfactorily	

4. Climate conditions

a. Drying effect in different seasons

Seasonal effects on the drying potential of wet walls were found in both climatic chamber and field testing. All the walls in the field testing were dried to the equilibrium level in 4 days in the summer and in 3 months in the winter (Straube and VanStraaten, 2004). Walls dried much slower in the cold weather than hot weather. Compared to the non-ventilated wall, the sheathing of ventilated walls dried at the same rate in the hot weather but faster in the cold weather

In the climatic chamber testing, the initial drying rates (10% MC drop from 25% for wood fibreboard sheathing) for all the walls with metal cladding were about two times faster in summer than in winter. The initial drying rates for the walls with vinyl siding were about five times faster in summer than in the fall and 8 times than in winter (Shi, et. al. 2004).

In the hot weather, a strong inward diffusion was observed. The fiberboard sheathing dried quickly mainly by redistributing the moisture inwards to the stud space due to strong solar radiation. Condensation accumulated on the bottom plate, stud, and the stud

facing surface of vapour control paint, indicating inward diffusive drying is important for the interior and built-in moisture control (Shi, et. al 2004,). In the walls with ventilation, the air cavity exhibited less condensation than that in vented walls, showing ventilation can reduce solar-driven inward vapour condensation (Straube & VanStraaten, 2004).

b. Effect of different climate region in North America

Effect of climate on drying rate of rainscreen walls can be observed in simulations by Karagiozis (2004b). Five major climate zones were evaluated using MOISTURE EXPERT program (Karagiozis, 2001) including:

- Humid-hot and cool winter climate – Houston, TX; the month with most rain fall is May.
- Cold-summer humid region - Minneapolis, MN; the month with most rain fall is June.
- Cool and wet region – Seattle, WA; the month with most rain fall is November.
- Mild humid region – Charlotte; NC, the month with most rain fall is July.
- Hot and humid region – Miami; the month with most rain fall is June.

The simulation results found that in Minneapolis and Miami, a ventilated cavity performed similar to the vented cavity, but in Seattle and Charlotte, vented cavity performed between the unvented and ventilated systems at mid level. In Houston, there was a difference between the vented and ventilated air cavity during the winter but a smaller difference during all other seasons (Karagiozis, 2004). These simulations were done with OSB sheathing only. Conclusions may be different for walls with other sheathing as they have different vapour permeance.

The Ontario wall Drying Project – Phase 2 (Burnett, et. al. 2001) concluded that, in Ontario's climate, drying before warm weather was a crucial factor affecting the MC levels of the test walls and found warm weather could increase wood MC by 2 to 3% or more. The drying process can not only slow down, it can reverse.

2.5 Summary

The purpose of including ventilation in building enclosures such as roofs, crawl spaces, and walls is to allow drier outdoor air to pass through the building envelope to dry the structure and building envelope components within an acceptable period of time if wetting occurs.

A considerable amount of research on the effect of cavity ventilation in a rainscreen wall has been conducted. The impact varies from region to region based on climatic conditions. In summary, cavity ventilation has positive effects for a building envelope design, such as encouraging drying, reducing inward diffusion by solar radiation, and preventing condensation in roof attics. These benefits, however, are limited when the initial MC of wood components exceeds certain levels. Exterior sheathing materials and sheathing membrane have insignificant influence on walls with a ventilation cavity. Whether walls with ventilated cavity benefit more in term of drying than walls with vented cavity depends mainly on climates and seasons. In cold and wet regions such as Seattle and Vancouver, walls with vented cavity have demonstrated a problem drying when the moisture load is high in the sheathing or stud space. Ventilated cavities demonstrated better performance.

On the other hand, in such cold and wet areas, exterior moist air is the main moisture source to enter the air cavity and to potentially wet the sheathing due to elevated RH during long periods of rainfall in winter. It might be beneficial to prevent such moisture from entering wall cavities. It is also possible that wind driven rain can enter the cavity even when flashing is in place. This would be greatly restricted in a vented cavity. Thereby reducing water penetration and moisture wetting of the exterior sheathing and stud space may be more essential than ventilation.

Smaller opening but sufficient ventilation in the cavity and adequate drainage may be the better design of rainscreen walls in the cold and wet climates. In practice, these two designs (fully ventilated or partially ventilated cavities) are both used; however, they may or may not exhibit different performance in term of drying or wetting the walls. There may be an optimum range of ventilation rates that promotes effective drying. Whether an air cavity needs to be fully ventilated or partially ventilated in a rainscreen wall in the west coastal climate of North America has yet to be resolved. To answer these questions, a field study together with analytical analysis and computer simulations will be carried out and presented in following chapters.

Chapter 3: Experimental Design and Setup

The design and instrumentation of various test walls and their installation at a Building Envelope Test Facility (BETF) with field exposure at the British Columbia Institute of Technology (BCIT) are described in this chapter. Twelve full scale test walls, six clad with brick veneer and six clad with fibre cement panel were installed on the southeast facade of BETF. These walls were fully instrumented to monitor their hygrothermal responses under field conditions. The details on the configurations of the test walls and instrumentation and monitoring are presented in the following sections.

3.1 Building Envelope Test Facility (BETF)

BETF is located at a relatively exposed area at the southeast end of the Burnaby campus of BCIT, as shown in Figure 3-1-1. One of its long-sides faces the prevailing wind-driven rain direction, i.e. southeast. BETF is a unique two-storey structure designed to investigate the hygrothermal performance of building envelopes, and the interaction between the building envelope and its indoor environment (Ge, et al., 2008). This facility measures 13.6m long by 8.6m wide and 5.7m high. A broad range of building envelope wall assemblies and junctions can be tested, from wood frame construction to steel, concrete, and masonry assemblies—including window walls and curtain walls. Test panels can be of various sizes, from 1.2 m wide by 2.4m high to 2.4 m wide by 4.8 m

high to a maximum size covering the full length and height of the facility. The roof geometry and size of roof overhang can be adjusted.

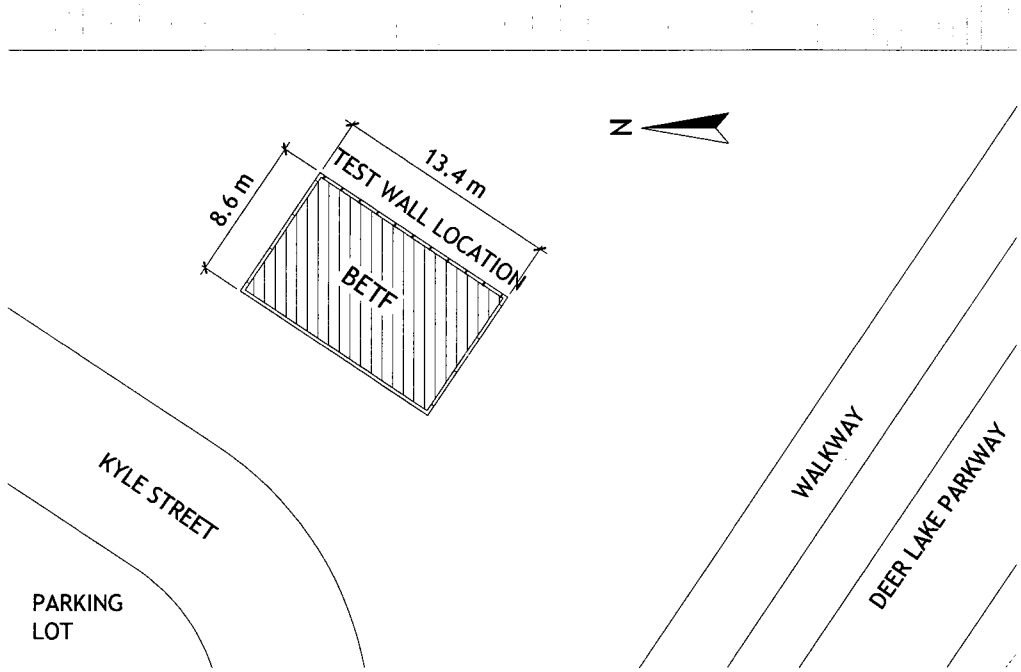

Figure 3-1-1: Site plan of the Building Envelope Test Facility (BETF) at the Burnaby campus of BCIT.

Two mechanical systems are fitted within the facility allowing the separation of interior spaces into two conditioned horizontal zones in the future, and each system has the capability to maintain indoor temperature within a range of 18-26°C with a precision of ±2°C and RH within a range of 40-80% with a precision of ±5%. The structure also allows for construction of a complete second floor over the entire floor area and allows for subdivision of the interior space into individual rooms (Figure 3-1-2).

A weather station is located at the centre of the BETF's rooftop to monitor the on-site environmental conditions including wind speed, wind direction, global solar radiation, and horizontal rainfall. In total, there are fifteen custom designed driving rain gauges installed on each façade of the facility to quantify the wind-driven rain load. The facility

is equipped with an Agilent 34980A data acquisition system with a capacity of over 500 channels allowing for the monitoring of hygrothermal conditions within wall assemblies including temperature, relative humidity, moisture content, heat flux, incidence of condensation and rain penetration. A 32 channel Campbell CR10X data logger is dedicated to collect the on-site microclimate conditions including wind speed, wind direction, global solar radiation, horizontal rainfall and driving rain on wall surfaces. Figure 3-1-3 shows a photo of the facility.

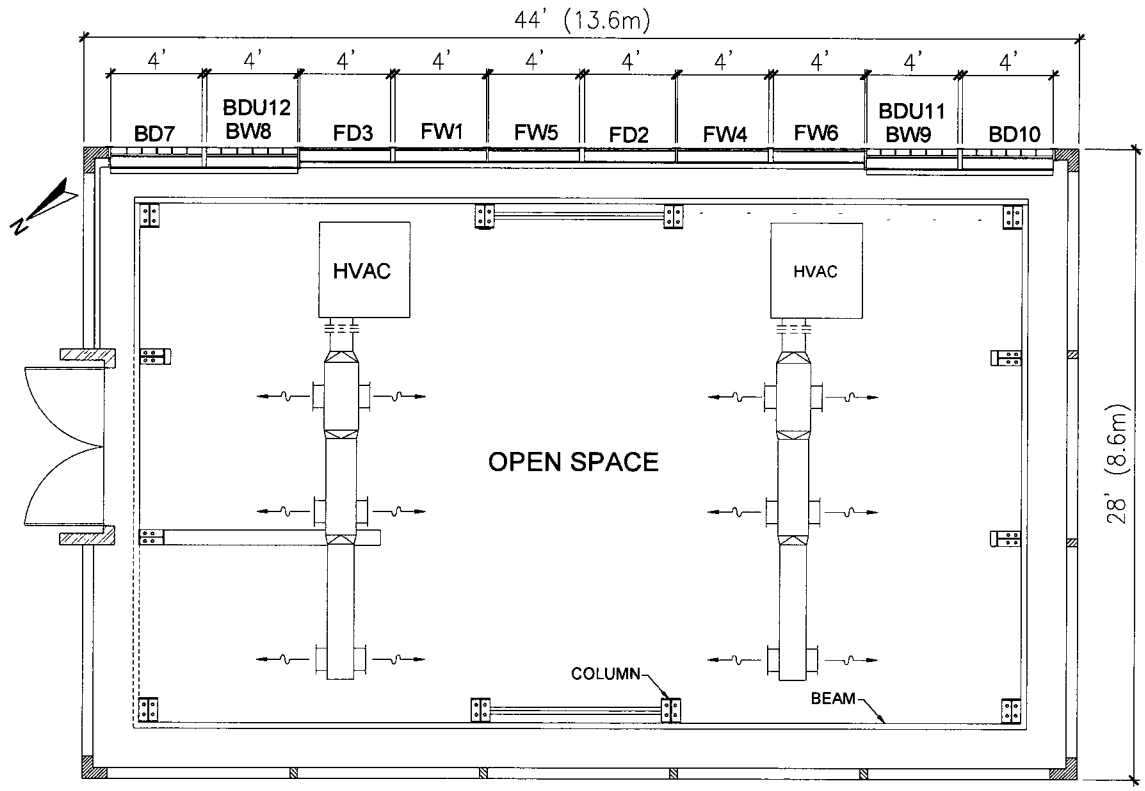

Figure 3-1-2: Plan view of the Building Envelope Test Facility at the Burnaby campus of BCIT.

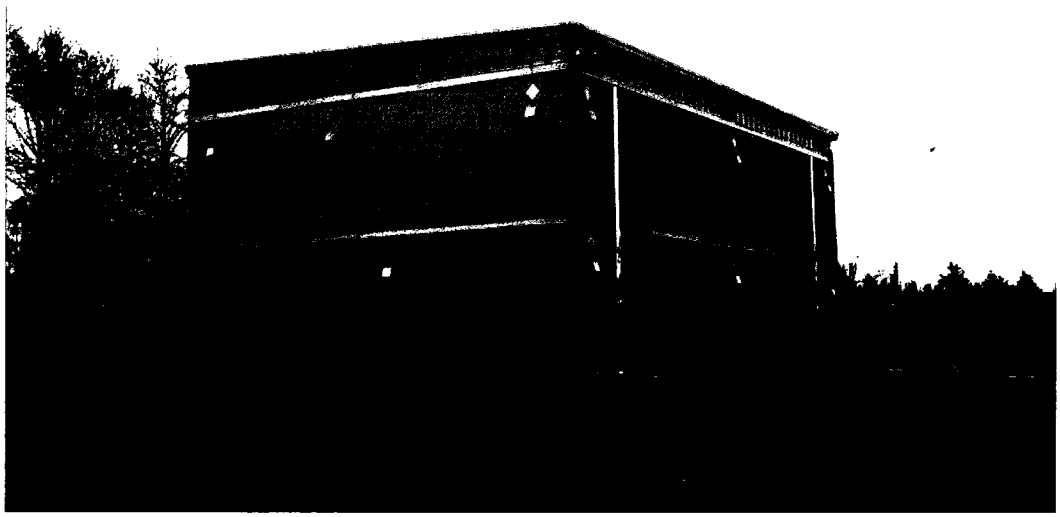

Figure 3-1-3: Photo of Building Envelope Test at the Burnaby campus of BCIT.

3.2 Configuration of test walls

Ten of twelve test walls are 1.22m by 2.44m and two test walls measure 1.22m by 4.88 m. The wood-frame back wall assembly for all the test walls are identical and built using common residential building materials and construction method. It consists of:

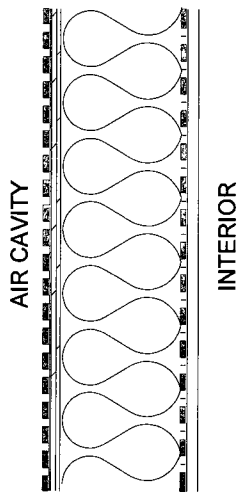

- An interior finish of 12mm (1/2") thick unpainted gypsum board with a vapour barrier of 6 mil polyethylene film,
- A 38mm x 140mm (2 x 6) wood frame with double top plates and single bottom plate, filled with R20 fibreglass batt insulation
- 12.7mm (1/2") sheets of plywood (Douglas fir) sheathing
- Spun bonded polyolefin (SBP) sheathing membrane.

There is a gap of 6mm between the two plywood sheets. The grain on the plywood surface layers are aligned horizontally.

The test variables include cladding material, height and depth of air cavity, and vent configuration. Two cladding types are studied, brick veneer and fibre cement panel. Brick was chosen because it is a unique and thick material which has mass capacities to store heat and moisture. In contrast, the fibre cement panel is thin and without much heat and moisture storage capacities. Both claddings are used extensively in residential buildings in BC's industry recently. All six brick walls have an air cavity depth of 25mm, two walls with an air cavity of 4.88m high and four walls with an air cavity of 2.44m high. The discrete vent configurations vary as indicated in Table 3-2-1. Five of the six fibre cement wall panels have a 19mm deep air cavity and one has a 10mm air cavity. The bottom vents are all 12mm high continuous slot vents with insect screen. The top slot vents also have insect screen and vary in height, i.e. 1mm, 6mm, and 12mm. The location of each test wall on the test facility is shown in Figure 3-2-1.

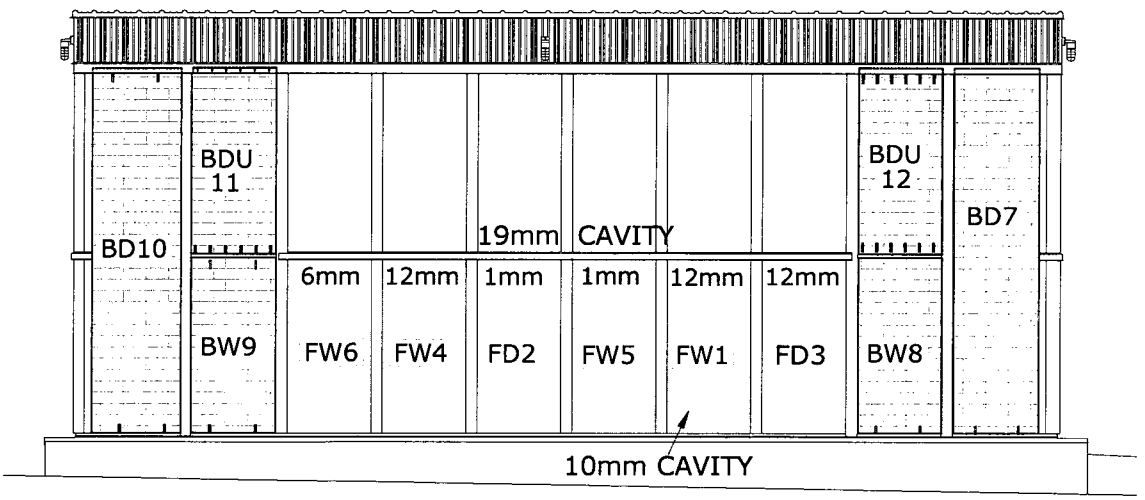

Figure 3-2-1: Location of test walls on the southeast facade of the test facility.

The significance of cavity ventilation on the drying is sensitive to the moisture loads within the test walls (Ye, et. al. 2009). To evaluate the drying and wetting provided by the cavity ventilation, two levels of moisture loads were introduced into plywood sheathing, four fibre cement walls and two brick walls were pre-wetted to a high initial MC of 38 - 41% in the BETF before installation to represent a construction situation where the plywood sheathing is wetted by rainwater during construction. The other six walls had a low initial MC of about 7 - 8%, which is the equilibrium MC level inside the test facility. The vent configurations and variables are summarized in Table 3-2-1.

Table 3-2-1: Vent configurations and test variables of all test wall specimens

Test wall label*	Cladding	Types and sizes of vents			Flashing above of top vents	Air cavity depth	Initial MC in plywood sheathing
		Vent type	Size				
			Top	Bottom			
FW1	Fibre cement panel	Continuous slot vents	12 mm	12mm	yes	10 mm	high
FD2			1 mm			19 mm	low
FD3			12 mm			19 mm	low
FW4			12 mm			19 mm	high
FW5			1 mm			19 mm	high
FW6			6 mm			19 mm	high
BD7	Brick veneer	Discrete vents	without	2-12x78mm with insect screen	no	25 mm	low
BW8			without				high
BW9			2 – 12mm x 65mm	2-12x78mm			high
BD10			2 - 12mm x 65mm				low
BSU12			6 - 12mm x 65mm	6-12x78mm	no		low
BDU13			6 - 12mm x 25mm		yes		low

*"F" refers to fibre cement walls and all walls have insect screens, "B" refers to brick walls.

3.3 Air seal strategy and methods

Since the impact of air leakage on the hygrothermal performance of rainscreen walls is not included in this study, care was taken to ensure the air-tightness of each test wall and the air tightness at the junctions between the test walls and its surrounding building envelope components. The steps employed to ensure a good air seal for the wall assembly and installation to minimize air leakage include:

- Designed and fabricated the individual wood frame back wall as an air tight and individual unit.
- Isolated each test compartment in the air cavity (in which the instruments are located), sealing the connection between vertical strapping and cladding and SBP sheathing membrane to restrict the airflow interacting between the test compartments and buffering compartments in the cavity.
- Sealed the gaps between test walls and their surrounding building envelope components horizontally and vertically as well as all the holes drilled for instrumentation after installation.

All the wood-frame back walls were fabricated inside the facility on the floor following the design of wall assembly and the layout of sensors and gravimetric samples. Holes for the gravimetric samples in plywood sheathing, studs and plates were pre-drilled. All the sensor wires were glued onto the interior surfaces of a stud at the edge of each wall, which were slightly notched just enough for the wire thickness so that the wires would not be damaged during the installation of the interior gypsum board. All the wires come

out from a slit of polyethylene film which was stabilized and sealed at a side of the wall to connect to a terminal strip.

To ensure all the individual wood-frame back walls are air tight, the air barrier of Tyvek SBP sheathing membrane wrapped over the vapour barrier of polyethylene film on the four sides of a wall. Then the edge of sheathing membrane were sealed to the polyethylene surface, forming an isolated and air tight wall unit, as shown in Figure 3-3-1. The overlapping of polyethylene sheet and SBP membrane also serve as moisture and air barrier/separator between the test wall and its surrounding building envelope components.

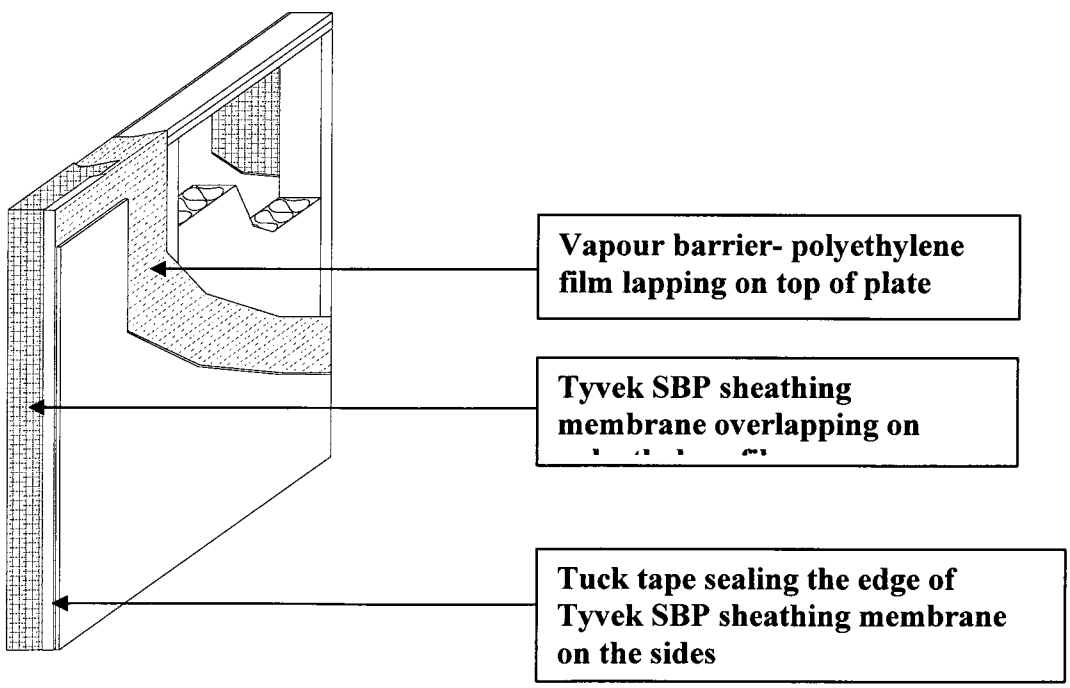

Figure 3-3-1: An isolated and sealed wood frame back wall unit.

The treated plywood strapping of each fibre cement test wall at each side of the back wall was extended to a base flashing at the bottom and to a flashing at the top to form an enclosed air cavity behind the cladding. After the cladding was installed, the edge of

fibre cement panel on both sides were sealed with construction tape before the panel trim covered up the junction of two adjacent walls, as shown in Figure 3-3-2.

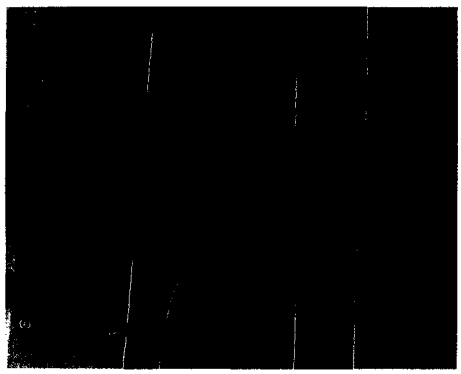

Figure 3-3-2: Sealing the edge of fibre cement panel cladding before the fibre cement trim is installed.

For the brick walls, L-shape brick or backer rods were used to enclose the edge of air cavity. The edges of air cavity between the brick walls and their surrounding building envelope components were sealed with a layer of self-adhesive membrane from Tyvek SBP sheathing membrane to a piece of rigid insulation, which was filled in the gap between two walls. The typical vertical connection details between brick wall and fibre cement wall are shown in Figure 3-3-3.

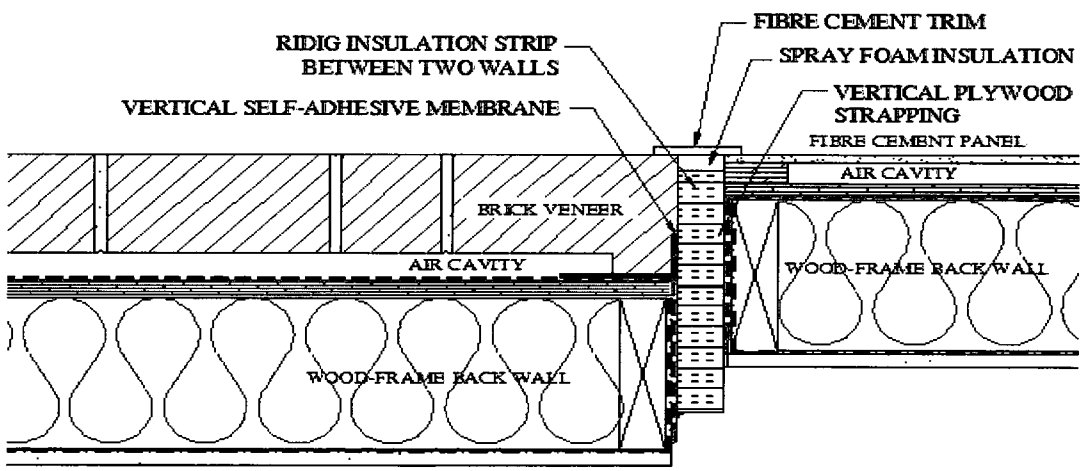

Figure 3-3-3: Typical vertical connection detail between brick wall and fibre cement wall.

3.4 Monitoring protocol and instrumentation

During testing, all the specimens were subjected to the same indoor conditions. All the walls were installed on the same façade of the test facility and the outdoor loadings in term of temperature, solar radiation, and RH are similar. Wind-driven rain loads and wind pressure may vary slightly depending on the location of the wall specimens. Exterior loading conditions recorded during the tests will be used for the interpretation of results.

The hygrothermal conditions of wall specimens are used to evaluate their performance. To compare the drying/wetting potential provided by the cavity ventilation, a set of wet walls has plywood sheathing with high initial MC of approximate 38-42%. The other set of dry walls has an initial low MC in plywood of approximate 7-8%. The indoor conditions are maintained at 22±1°C and 55±5% RH throughout the test duration.

Each wall specimen is made up of three 38mm by 140mm (2x6) studs at 406mm spacing. The central bay of the wall is instrumented, and the other two 406mm side bays are used as guarded bays, as shown in Figure 3-4-1.

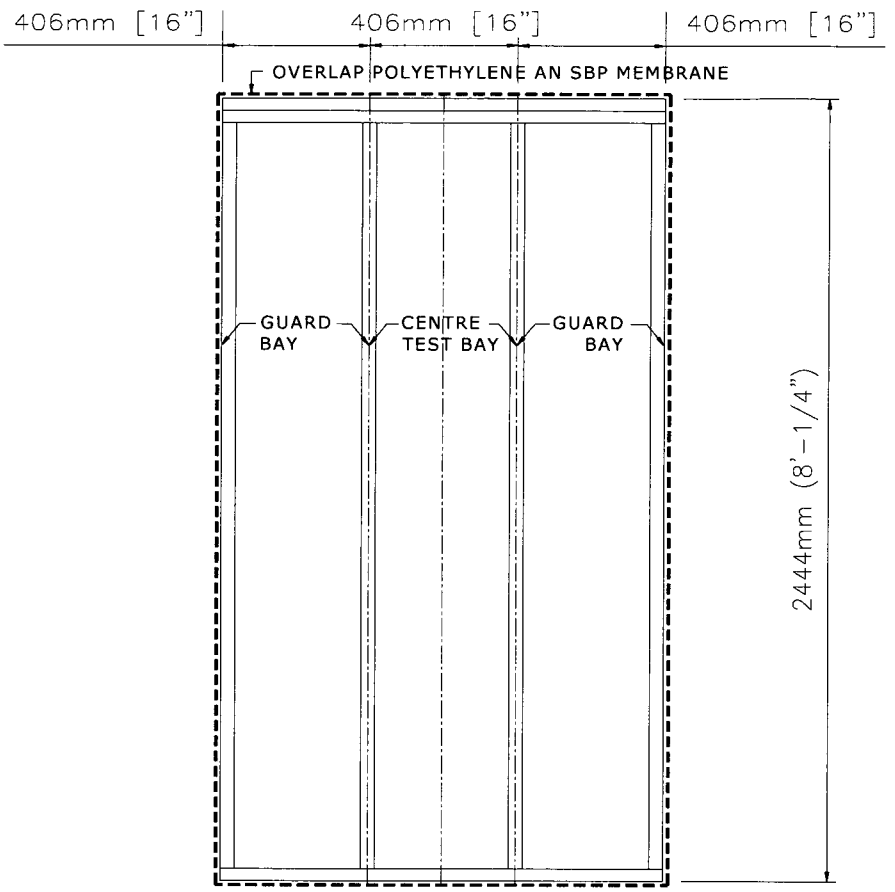

Figure 3-4-1: Typical test bay and guard bays of a test wall specimen.

3.4.1 Initial moisture loading conditions

Monitoring of moisture performance of the wall specimens includes the measurement of moisture content of wood components, RH and temperature in the air cavity and insulation space.

A sheet of sheathing is the most vulnerable wood component compared to other wall layers in terms of the moisture performance due to its location nearest to the air cavity and at the cold side of insulation. Condensation may occur on the surfaces of sheathing if the vapour pressure is higher than its saturation level due to overload of moisture brought

from outside moist air or from high humidity of indoor air. Thus, the MC of plywood sheathing is used as an indicator to evaluate the ventilation drying and wetting potential in the experiment. Both gravimetric samples and resistive moisture-pins are used to measure MC in plywood sheathing. To monitor moisture distribution within the wood-frame, MC of the stud and the bottom plate is also measured using both resistive moisture-pins and gravimetric samples.

1. Initial moisture content of wood components

The initial MC of plywood sheathing, wood studs and plates, and pre-treated plywood strapping were at the equilibrium level under the BETF's indoor conditions of about 20 °C and 50% RH and the EMC is listed in Table 3-4-1.

Table 3-4-1: initial MC of wood components at their equilibrium level under indoor conditions

Wood components	Initial MC (%)	Note
Plywood sheathing	7.5 %	Gravimetric measurement
Stud and plates	10.0 %	Gravimetric measurement

During fabrication of the wood frame, the MC of studs and plates stayed at their equilibrium level. The initial MC of plywood sheathing of test wall was set at different levels.

The initial MC of plywood was at its equilibrium level under the indoor conditions to simulate a situation that all wall components are well stored. Two fibre cement and four brick walls had plywood sheathing with low initial MC, named dry walls in this study.

Economy and construction booming creates high demands of residential building in the market, which requires construction to be sped up, so residential buildings are often to be built during rainy period in the winter. Materials used for construction are often covered

up when they are still wet and sometimes are left unprotected and exposed to rain for days. To simulate this situation, the plywood sheathing was pre-wetted to 38 - 40% MC. Moisture in plywood was redistributed to the wood frame and insulation during and after the fabrication of wood-frame back walls. Four fibre cement and two brick walls have plywood sheathing with high initial MC, named wet walls in this study.

2. Selection of plywood sheathing, studs, and plates

In selecting plywood sheathing for the test, care was taken to ensure that all the panels had similar density, species and qualities, no cracks in the test bay. As a result, all the plywood sheathing panels were chosen from two bundles and they were all made of Douglas fir for both interior and exterior surface-layers (12.7mm thick plywood sheathing which has 4 layers of thin wood glued together). They were all checked and weighted individually in the lumber yard.

One piece of plywood sheet was used to produce all plywood gravimetric samples and to cut out three 305mm by 305mm (1' x 1') plywood square planks from the centre part of this plywood sheet. All gravimetric samples and the planks were oven dried at 103 °C to obtain the oven-dry weight of and plywood gravimetric samples and plywood sheathing installed in the test walls. The procedure prescribed is in ASTM D 4442-92 "Standard Test Methods for Direct Moisture Content Measurement of Wood and Wood-base Materials" (ASTM, 1992).

In the selection of wood for studs and bottom plates, care was taken to ensure that all the wood pieces were all straight, similar qualities and no cracks in the test bay. Each

gravimetric sample on the stud and bottom plate was made from the same piece of wood stud for each wall.

3. Wetting method of plywood sheathing and gravimetric samples

To simulate the actual construction practice, the 1.22m by 2.44m (4' by 8') plywood sheathing was cut into two pieces of 1.22m by 1.22m panels and a 6mm gap is left in between when they are assembled in the test walls. To pre-wet plywood sheathing, the plywood panels were immersed into water completely for about 40 hours, as shown in Figure 3-4-2. To ensure all the plywood sheets to be evenly soaked, a 12mm-gap between each sheet was created using small wood cubes placed at four corners of each plywood panel. After the plywood was taken out of the water, its surface water was removed using a damp towel and its weight was measured. The initial MC level of plywood was determined by weights compared with the average oven-dry weight of three 1' by 1' plywood planks. The soaking time required to reach about 40% MC was tested before using a mock-up panel in the laboratory in the summer of 2007. The wet plywood panels were weighed again before fabrication. The designated MC of 38 – 41% was achieved as expected. The uniformity of wetting was confirmed by measuring the MC at different depths using insulated moisture pins before and during the tests. The procedure of immersing plywood gravimetric samples for the wet walls was similar to wetting the plywood sheathing. It took about 6 hours to soak the samples to reach 40% MC. Some of the samples were over-wetted and they were left on the desk inside BETF to dry to the designated MC level. All the samples were kept in the individual plastic bags to maintain the same MC level before being inserted into the plywood sheathing. Figure 3-4-3 shows the plywood gravimetric samples being soaking in water. Figure 3-4-4 shows the

procedure of wiping the surface water using damp paper towel before weighing the sample.

Figure 3-4-2-: plywood panels immersed into a water pool completely.

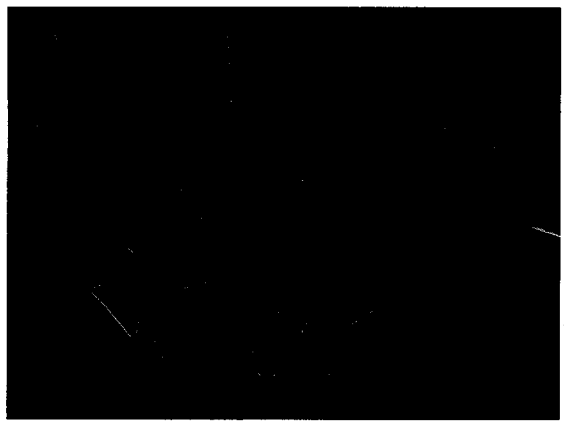

Figure 3-4-3: Plywood samples being soaked in water.

Figure 3-4-4: Wiping surface water on plywood sample before weighing.

3.4.2 Instruments in test walls

The hygrothermal state of the wall assemblies monitored includes MC, temperature, and RH. The MC of plywood, stud and bottom plate is monitored by both gravimetric

samples and resistive moisture pins. The number and type of sensors installed for each test wall is listed in Table 3-4-2.

Table 3-4-2: Number of sensors and gravimetric samples in a typical test panel

wall component	MC gravimetric samples	sensors type & No.			
		Thermocouple	RH-T	Moisture pin	
				Wet wall	Dry wall
cladding		2			
air cavity			1 or 2		
plywood sheathing	8	7		11	7
studs	2	1		1	1
bottom plate	2	1		1	1
insulation space		2	1		
gypsum board		1			

In total, there are 120 gravimetric samples and 140 pairs of moisture-pins in plywood, studs and bottom plates; 192 thermocouples, 140 along with the moisture-pins and 52 on wall components, 28 relative humidity and temperature (RH-T) sensors in the insulation and air cavities. The accuracies, specifications and calibrations for all the instruments used in the experiment can be found in Appendix 4 "Specifications and Calibrations of Instrumentations".

The overall layout of electronic sensors and gravimetric samples is shown in Figure 3-4-5 for a typical fibre cement wall specimen and shown in Figure 3-4-6 for brick wall specimens.

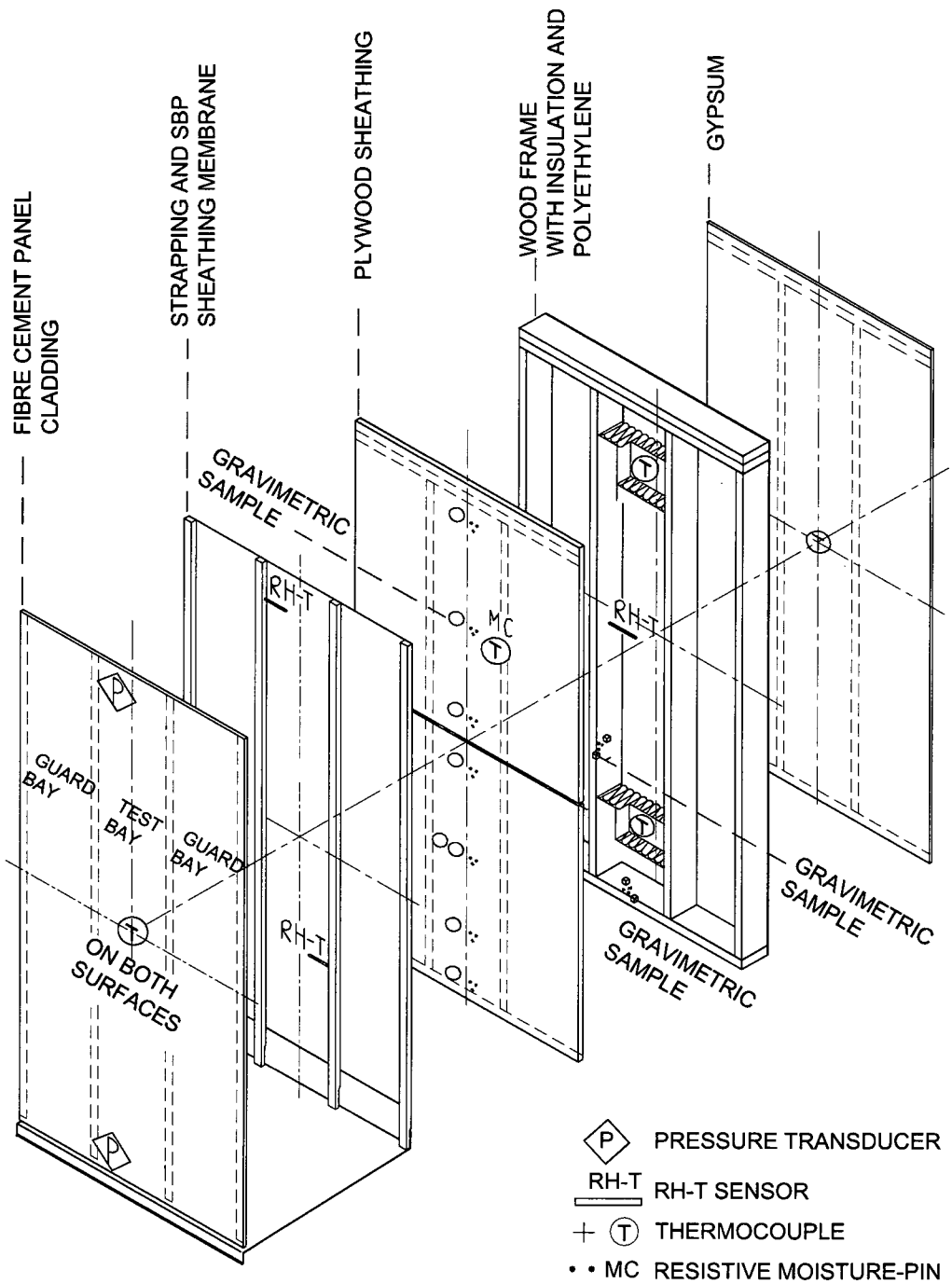

Figure 3-4-5: Layout of gravimetric samples and electronic sensors in a typical fibre cement wall specimen.

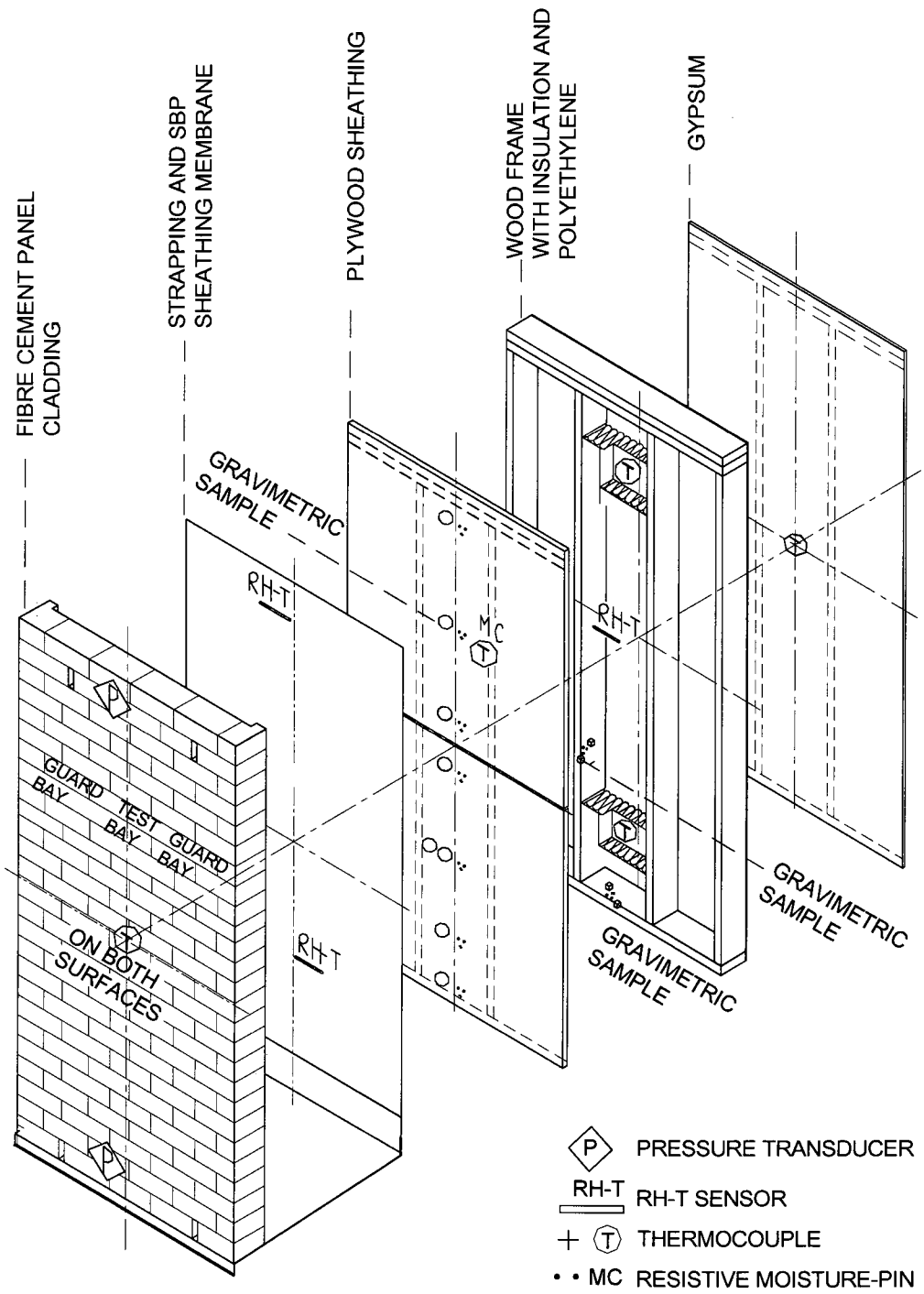

Figure 3-4-6: Layout of gravimetric samples and electronic sensors in a typical brick wall specimen.

3.3.2.1 Moisture content in wood components

1. Gravimetric samples

The gravimetric method is direct and accurate as it determines the MC by dividing the mass of moisture in a wood sample by the mass of the oven-dry sample as:

%MC = ((Gross Mass – Dry Mass) / Dry Mass)* 100

where, gross weight is total weight of moist sample, dry weight is the oven-dry weight obtained according to ASTM D 4442-92 standard (ASTM. 1992). The gravimetric measurement is the average moisture content of the whole sample and can be used for a wide range of MC.

A total of one hundred and twenty gravimetric samples were taken out from the test walls and weighed from inside of BETF weekly. A wood screw was fastened to each sample to be used as the handle for easy sample collection. Each of these wood samples was sealed in a plastic bag when it was taken out from the wall specimen and weighed using a scale precise to 0.001 mg. Every individual wood screw and plastic bag were weighed and recorded prior to being used for the sample collection. All the samples were oven-dried before they were inserted in the wood components of wall specimens or pre-wetting.

The MC of plywood sheathing is measured using resistive moisture-pins on one side of the central line while manually collected gravimetric samples are used to measure the MC on the opposite side at the symmetrical location. The layout of gravimetric and resistive MC pins installed on the plywood sheathing is shown in Figure 3-4-7.

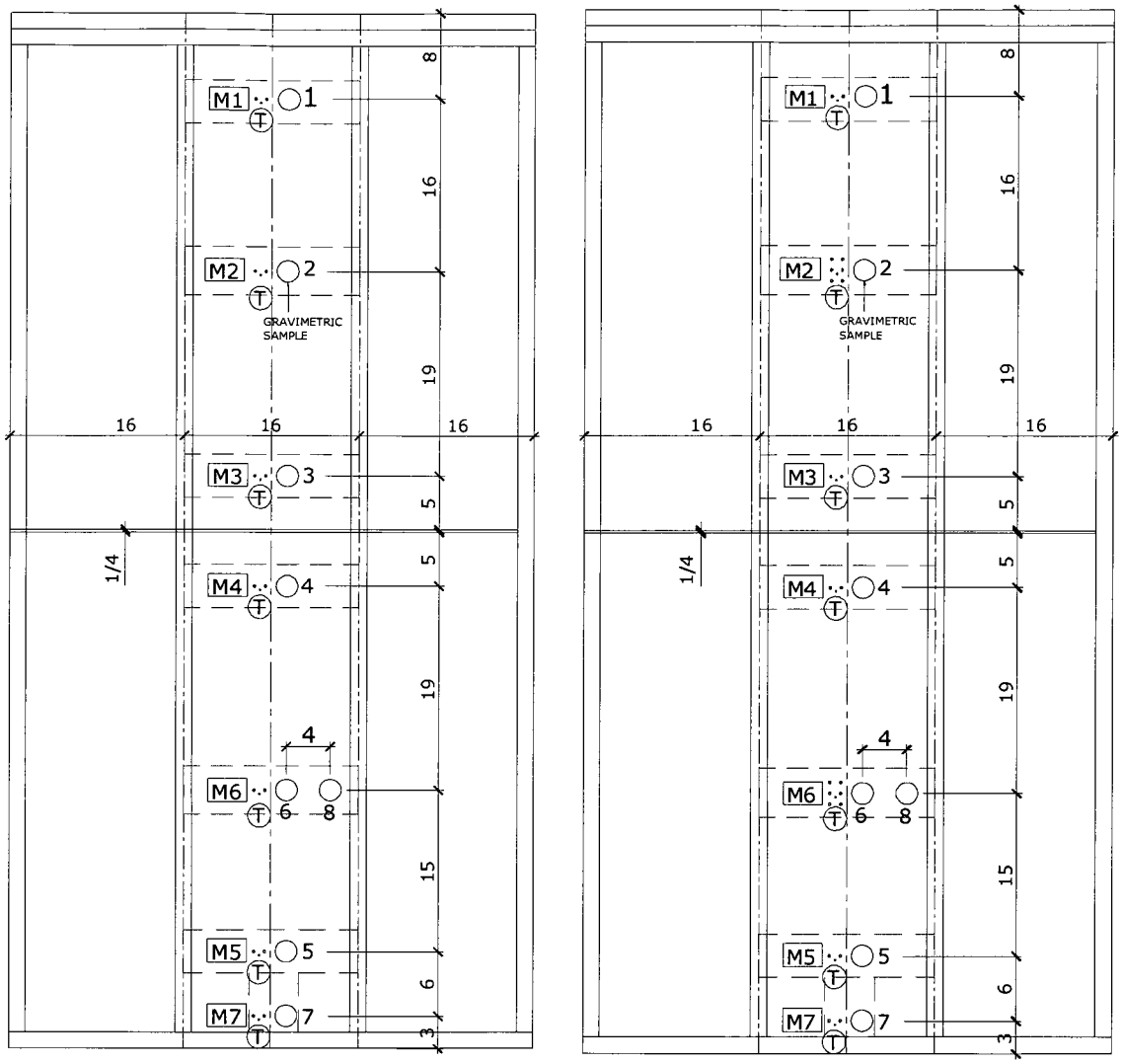

a) Typical layout of a dry wall

b) Typical layout of a wet wall

Figure 3-4-7: Typical layout of resistive moisture-pins and gravimetric samples in plywood sheathing; a) a dry wall, b) wet wall.

where:

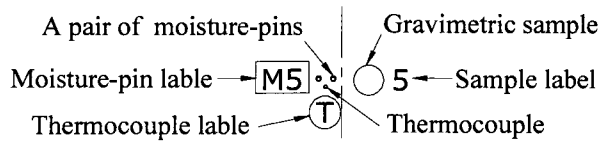

A total of five pairs of resistive MC sensors was installed in the plywood of upper brick walls without gravimetric samples, as shown in Figure 3-4-8.

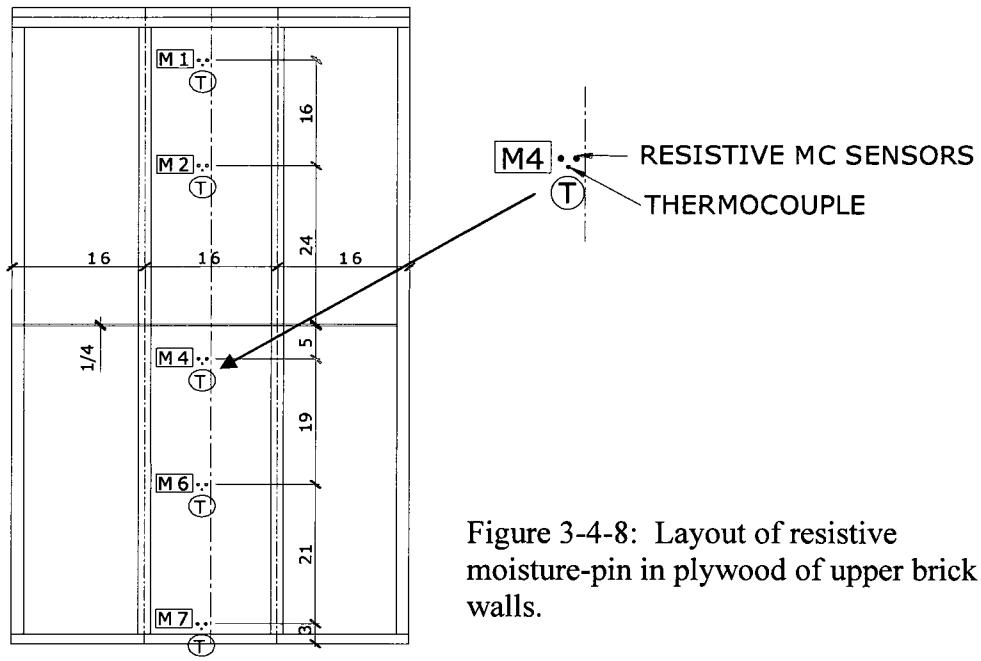

Figure 3-4-8: Layout of resistive moisture-pin in plywood of upper brick walls.

Eighty gravimetric samples were cut from plywood as disks of 50.8mm (2") in diameter. The perimeters of these samples were sealed with tape to allow only one dimensional moisture transfer from the surfaces of sample and minimize moisture transfer through sample edges. Nevertheless, the perimeters of the gravimetric sample holes were not sealed since it is difficult to seal without damage. Figure 3-4-9 shows the plywood gravimetric samples and the holes in the test walls.

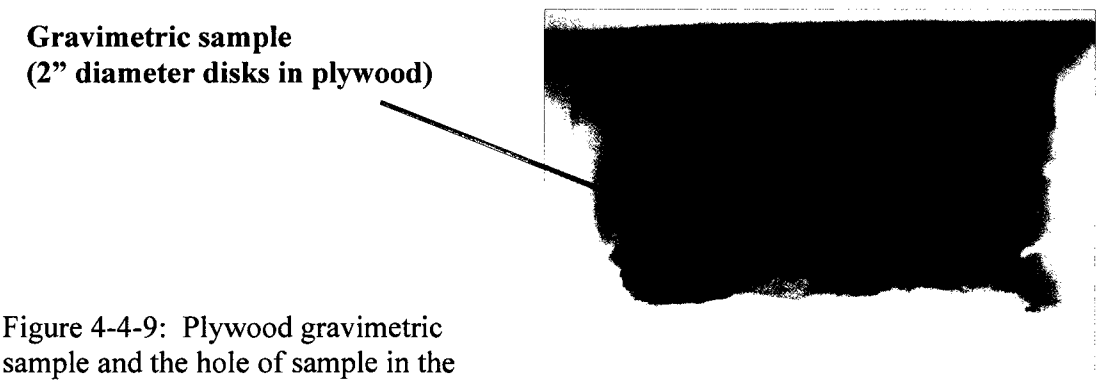

Figure 4-4-9: Plywood gravimetric sample and the hole of sample in the wall.

Forty gravimetric samples in the stud and bottom plates were cut as cubes of 19mm (3/4") in length. The purpose to have samples in stud and bottom plates is to monitor the moisture redistribution from wet plywood and the influence of weather conditions. One cube wood gravimetric sample was inserted at the exterior edge of a stud and bottom plate near plywood sheathing while another cube sample was installed in the middle of the stud and the bottom plate. The locations of samples in stud and bottom plate show as Figure 3-4-10.

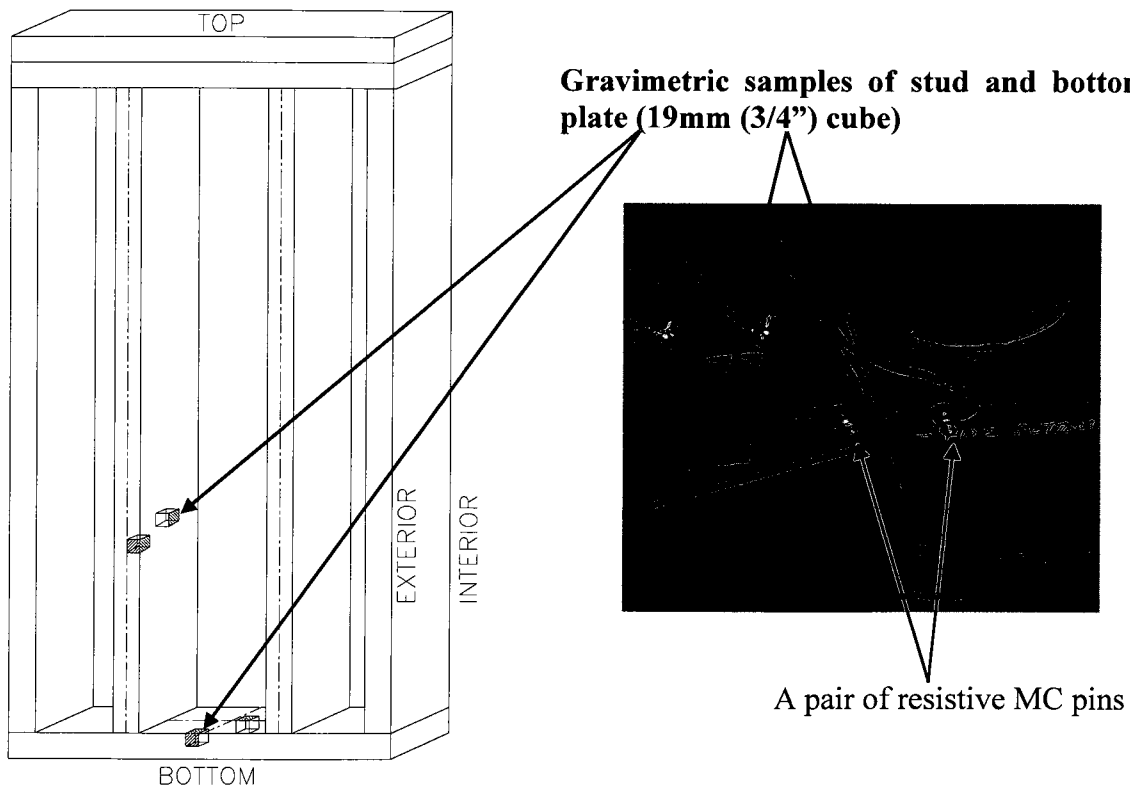

Figure 3-4-10: Locations of samples in stud and bottom plate.

To access the gravimetric samples of plywood, stud and bottom plate, six windows for each wall specimen from the interior gypsum board through polyethylene and fibreglass batt insulation were carefully sealed during and after the samples weighting to minimize

the potential disturbance such as air leakage. Figure 3-4-11 shows the access windows cut on the gypsum board.

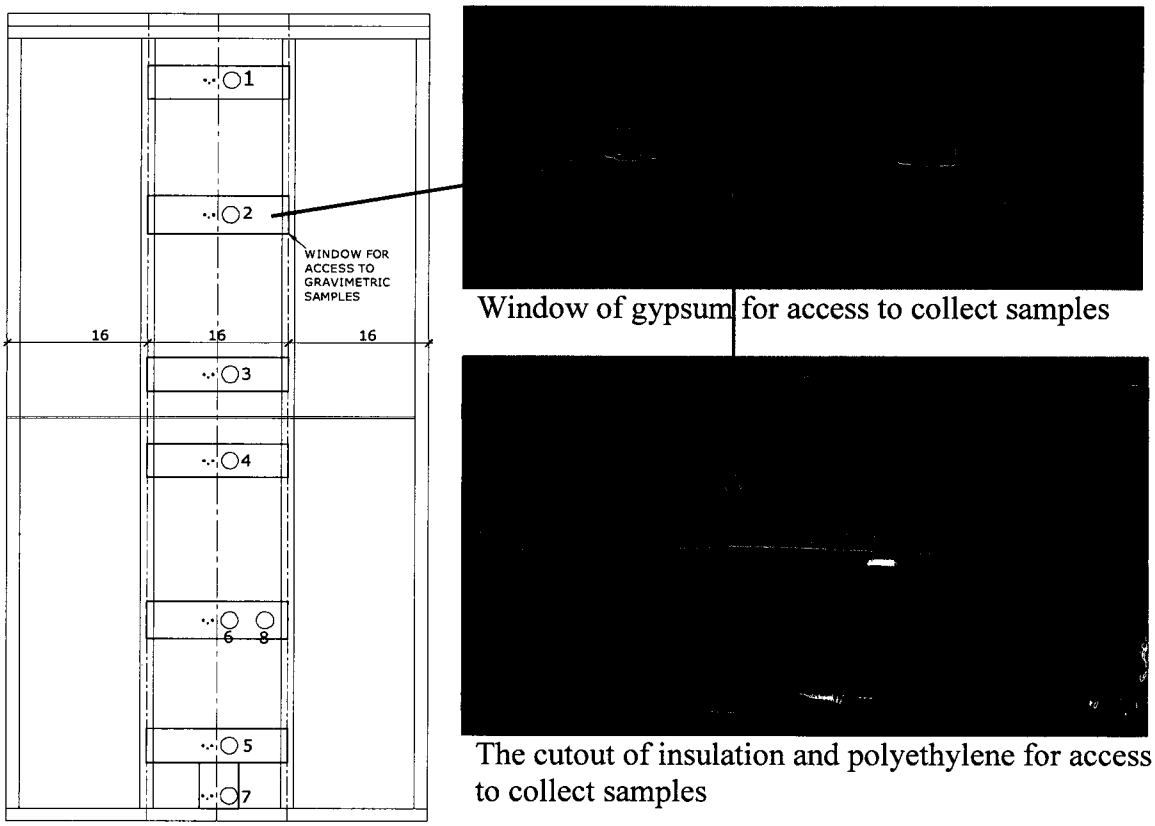

Figure 3-4-11: Window to access to samples.

In addition, the procedure of sample weighing was completed quickly, one wall at a time so that the potential disturbance can be ignored. To ensure the samples tightly fit in the holes with little gap around, the hole diameters of dry walls and wet walls were slightly different. The diameter of holes in wet walls is 1.5mm bigger than that in dry walls to accommodate the expansion of wet plywood after being immersed in water. In contrast, the diameter of plywood gravimetric sample in the dry walls increased with the increase of its MC during the wetting period, therefore, regular sanding of the holes was needed using a sanding drum to ensure the samples can fit tightly into the holes but not too tight to damage the samples when taking them out.

2. Resistive moisture-pins

Resistive moisture-pin measurement is a more convenient method compared to gravimetric measurement. No opening is required and it is less labour intensive. Measurements of resistive moisture-pins can be acquired automatically through the data acquisition system at any desired sampling rate, which can provide continuous readings to capture the responses of the walls to various weather events. The disadvantage, however, is that readings are only accurate within a certain range.

A total one hundred and forty pairs of resistive moisture-pins were installed in plywood sheathing, studs and bottom plates of the test walls. Most pairs of the moisture-pins were un-insulated stainless steel screws. There were in total twenty pairs of insulated moisture-pins installed to measure the MC at a certain thickness of plywood to obtain the moisture gradient across the sheathing. The measurements of moisture-pins were automatically taken by a data acquisition system at a five-minute interval.

A pair of resistive moisture-pins, using stainless steel screws, was installed to about 10mm (3/8") thickness of plywood from its interior surface and was located symmetrically to each gravimetric sample along the centre axis of plywood sheathing. To measure the MC distribution of plywood, three pairs of moisture-pins, using stainless screws and insulated pins, were installed at three different depths (3mm, 6mm and 9mm from inside surface) of the wet plywood sheathing at the symmetrical locations of gravimetric samples #2 and #6. Figure 3-4-12 depicts the layout and depths of three pairs of moisture-pins in plywood sheathing.

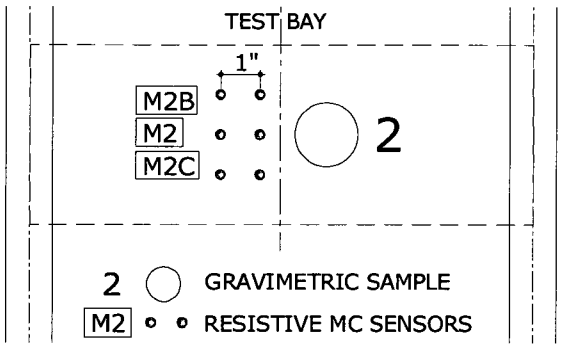

a) layout of three pairs of moisture pins at the same position

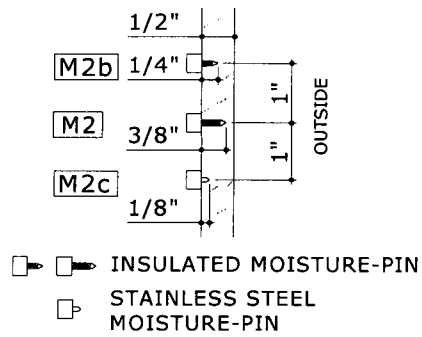

b) The depths of three pains of moisture pines into plywood

Figure 3-4-12: Layout of three pairs of moisture-pins at the same location but at different depths of plywood.

To monitor the moisture re-distribution from wet plywood sheathing and moisture response to weather conditions, a pair of stainless screws was installed at the locations of the gravimetric samples in stud and bottom plate near the plywood sheathing, as shown in Figure 3-4-10. The insert points of screws were parallel with the edge of studs and bottom plate and about10mm (3/8") away from the plywood sheathing since this was the closest fastening point possible to the edge of stud and bottom plate without creating cracks on the wood components.

3.3.2.2 Temperature and relative humidity (RH)

In order to evaluate the hygrothermal performance of the wall specimens in relation to their boundary conditions and cavity ventilation, temperature monitoring is an important part of the experiment. First of all, measurements of temperature gradients through a wall assembly give a general picture of the thermal performance of test walls. Secondly, vapour pressure gradient can be determined from temperatures with RH measurements from indoor, outdoor, insulation space and air cavities to determine the direction of vapour flow and evaluate the cavity ventilation effectiveness. Finally, temperature

readings are required for deriving MC readings of resistive moisture-pins from resistance or voltage readings.

A total of one hundred and ninety two thermocouples were installed in the wall components, including in the insulation space and air cavity. They were sealed with glue after attaching on the surface of wall component and inserted in wood members to avoid any error caused by surrounding air. A total of thirty RH-T sensors were installed in the insulation space and air cavity of test walls and inside BETF. The measurements were sampled at five-minute intervals.

1. Temperature on surface of cladding and drywall

To monitor the temperature gradient though wall components, for each typical wall specimen, thermocouples were attached to the centre of both surfaces of cladding and exterior face of gypsum board for each test wall. The detail locations of thermocouples are shown in Figure 3-4-5 and 3-4-6, as described previously in this section.

2. Temperature in plywood, stud, and bottom plate

Each pair of moisture-pins requires their local temperature as one correction factor to convert the reading to moisture content. Thus, one thermocouple was installed near every location of resistive moisture-pins in plywood, studs and bottom plates of all the test walls. The thermocouples were inserted into the wood components from the interior surface at 10mm (3/8") depth as shown in Figure 3-4-13.

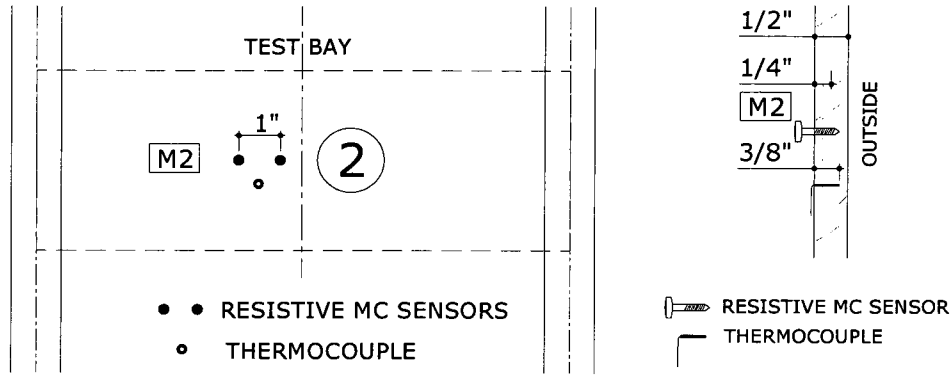

Figure 3-4-13: Thermocouple in the location and depth of plywood sheathing.

3. Temperature and RH in wall cavities and inside BETF

To monitor temperature and vapour pressure gradient through indoor to outdoor including the wall cavities; twenty two thermocouples and ten RH-T sensors were installed in the insulation spaces and eighteen RH-T sensors were installed in the air cavities. Two RHT sensors were installed inside BETF to measure indoor conditions. The outdoor RH and temperature were obtained from the on-site roof weather station. The vapour pressure is calculated using temperature and RH from the measurements of RH-T sensors.

In the insulation space, two thermocouples were mounted in middle of insulation located at lower and upper part of insulation space in each wall on the lower level. The upper level walls had only one thermocouple in the centre of insulation space. One RH-T sensors were placed in the middle of insulation space in the ten walls on the lower level of façade. No RH-T sensors were in the insulation space of upper brick walls.

For the air cavity, one RH-T sensor was suspended in the middle level of air cavity in each one-floor high dry wall to monitor the vapour pressure in the cavity. Two RH-T sensors were suspended in both lower and upper parts of the air cavity in each wet wall

and each two-floor high dry wall to monitor the change of RH and temperature so that the vapour pressure differential can be obtained as a result of ventilation wetting or drying. The RH-T sensors in the air cavity are also used to monitor the air temperature in order to evaluate the thermal buoyancy effect in the air cavity.

3.4.3 Test conditions

The test walls are exposed to natural outdoor weather and controlled indoor conditions. Both outdoor environmental conditions and indoor conditions are monitored.

3.4.3.1 Environmental parameters

Environmental parameters monitored include temperature, RH, wind speed and wind directions, global solar radiation, and horizontal rainfall by a weather station installed on top of the BETF roof and wind pressure differential on SE façade, using pressure transducers. The wind-driven rain is also measured using customized driving rain gauges mounted on the exterior surface of all the four façades of BETF.

1. On-site weather conditions

The weather station is located in the centre of BETF's roof, 10 m above grade, as shown in Figure 3-4-14. All the parameters are measured at one-minute intervals. Wind speed is measured using a propeller type anemometer. The on-site ambient air temperature and RH are measured by a Vasiala RHT sensor and the horizontal rainfall is measured using a tipping bucket rain gauge. Global solar radiation is measured using a SPLITE pyranometer located at the roof weather station.

2. Wind-driven Rain (WDR)

The amount of rain that impinges on the exterior surface of the walls is measured by customized driving rain gauges mounted on all four sides of BETF. The rain gauge includes a tipping bucket and a collector with a diamond shape and is made of 14 gauge electro-plated stainless steel. On the southeast side, six rain gauges were mounted on both edges and at the centre. Three were at the upper part of façade while another three were on the top of lower walls. Each tip of rainwater collected on the tipping bucket is 2g, which is equivalent to 0.038 mm/tip for a collection area of 522.6 cm² (Ge, 2009).

3.4.3.2 Wind-induced pressure differential

A total of six pressure transducers was installed to measure the pressure differential across the bottom and top vents of five wall specimens at both edges and centre of the southeast (SE) facade of BETF, as shown in Figure 3-4-14.

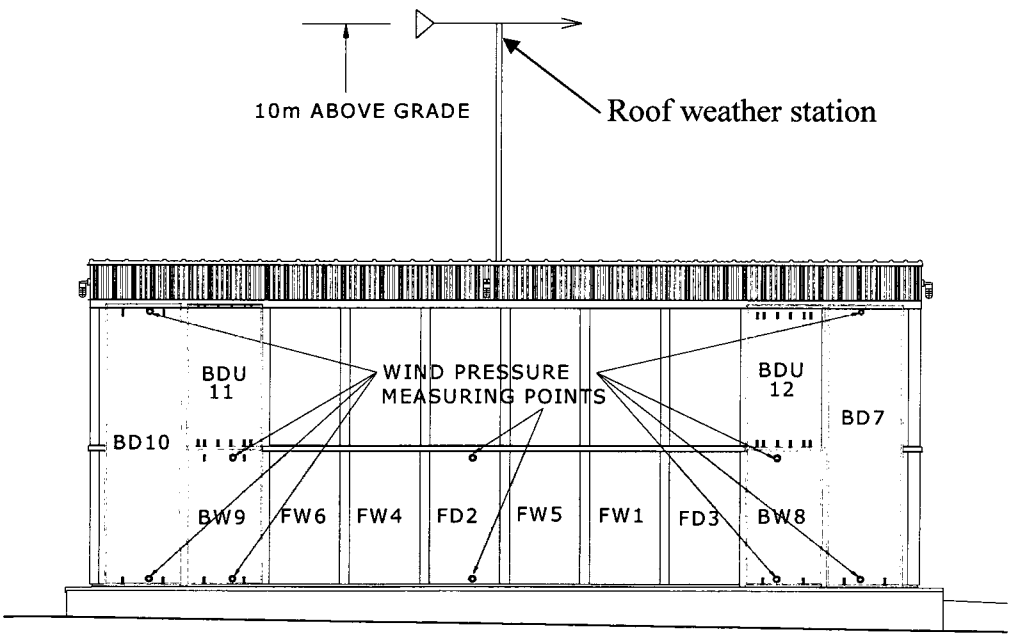

Figure 3-4-14: Locations of wind-induced pressure differential measurement points on test walls at the SE facade of the test facility.

Omega PX series pressure transducers are employed with the range of -125 to +125 Pa. Two 6mm-diameter tubes were inserted through the wall assembly from internal of gypsum board to external surface of cladding close to both bottom and top vents. These tubes are connected to a high and a low pressure output of one pressure transducer to directly measure the pressure differential for all the locations except for BD7. Two pressure transducers were installed on BD7; one measured pressure at the top and the other measured pressure at the bottom position. The pressure differential of this wall obtained is the difference of these two pressure measurements. The wind pressure differential measurements were sampled at 10Hz and averaged over one-minute (Ge, et al. 2009).

3.4.3.3 Indoor conditions

To ensure all the wall specimens experience the same indoor conditions and limit the variable during the test, the conditions inside of BETF remains constant. The parameters monitored inside BETF are temperature and RH. The air conditioning systems with electric heating element and 2 humidifiers are used to control and maintain constant indoor conditions to 22±1°C and 55±5% RH throughout the test duration. The measurements of indoor temperature and RH are obtained using two types of sensors: HOBO temperature / RH data loggers at the beginning from November 23, 2007 to January 18, 2008 and RHT-sensors from starting from January 4 to the end of June, 2008.

The indoor conditions were measured using HOBO temperature / RH data loggers at the beginning of experiment before RH-T sensors installed. The data logger was attached on a steel column near the middle of the northwest wall inside the BETF. The accuracy of

data logger for temperature measurement is ± 0.4°C within the range of 0 – 40°C and ± 5% RH in the range of 25 – 95% RH when the temperature is 5 – 55°C.

Two RH-T sensors are hung inside BETF; one at 2.4m above the ground and 0.8m away the test walls while another is hung in the middle of BETF and 3.5m above the ground.

3.4.4 Test duration

1. Criteria for selecting test commence time

The climate in the southern BC region is characterized by a long period of rain and moist air with moderate temperatures in winter and early spring, which limits drying for walls. Mould and fugal growth and wood decay may occur if moisture sensitive materials, i.e. wood stay wet for too long. Generally it is dry from the later spring to early fall. The drying capacity and wetting potential for wall assemblies from winter to spring is more of a concern than in summer and fall seasons.

According to the data collected from the Vancouver international airport weather station by Environment Canada, the month with highest rainfall based on the thirty year -average from 1971 to 2000 is in November, as shown in Table 3-4-3 and Figure 3-4-15 (Environment Canada. 2009). The wet and cold season is from November to March. During this period the average daily temperature is within 3.3 - 6.6 °C and the average monthly rainfall is within 112 to 179 mm.

Table 3-4-3: Average temperature and rainfall in 30 years from 1971 to 2000 (Environment Canada. 2009)

Average temperature and rainfall in 30 years from 1971 to 2000												
Months	Jan	Feb	Mar	Apr	May	Jun	Jul	Aug	Sep	Oct	Nov	Dec
temperature, °C	3.3	4.8	6.6	9.2	12.5	15.2	17.5	17.6	14.6	10.1	6	3.5
Rainfall, mm	139	114	112	84	68	55	40	40	54	113	179	161

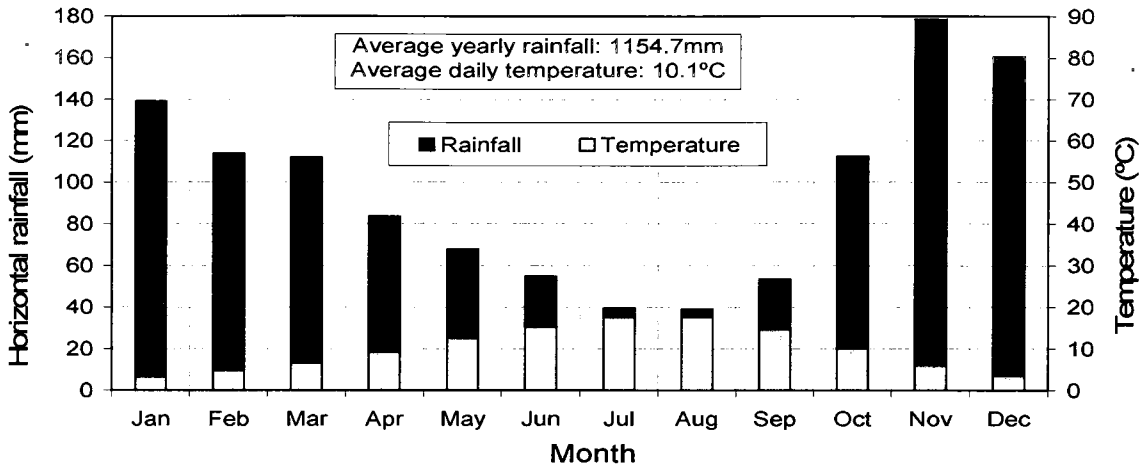

Figure 3-4-15: Average temperature and rainfall recorded at Vancouver International airport weather station in 30 years from 1971 to 2000 (Environment Canada. 2009)

Therefore, construction of the wall specimens began in November, 2007. The gravimetric measurements in the wood component were taken after fabrication and continued. The weather station had been setup in September, 2007 before the walls were assembled and started collecting weather data in November.

It was not until the end of December, 2007 that the on-site weather station and the data acquisition system were running properly and started recording all data of electronic sensors including MC, temperature, RH, wind-induced pressure differential, and cavity air speed for the test walls and the on-site environmental conditions including wind speed, wind direction, air temperature, RH, global solar radiation, horizontal rainfall. The rain gauges were installed at different times and were completed in January.

2. Test duration

This thesis presents analysis of data collected from December, 2007 to June, 2008 to evaluate the drying and wetting potential in plywood affected by cavity ventilation in wet and cold winter and spring seasons.

Chapter 4: Moisture Performance of Test Walls

A total of twelve wall specimens have been tested for more than six months from December, 2007 to June, 2008. During the testing period, these walls were a part of BETF's envelope experiencing exterior weather changes and responding to the thermal and vapour pressure differential between indoor and outdoor. The effect of air cavity ventilation on the drying and wetting of wood-based wall components was evaluated by analyzing the hygrothermal response of each individual test wall specimen.

Since all the wall specimens were well constructed and were individually airtight, it is assumed that there was negligible air leakage and rain penetration through the wall assemblies during the testing period. Only vapour diffusion through the wall assemblies is considered in the experiment. This chapter presents the moisture performance of test walls along with the environmental conditions observed. The discussion on thermal performance and prediction of cavity ventilation is presented in chapter 5 and chapter 6, respectively.

4.1 Observations of environmental conditions

The hygrothermal response of a wall with cavity ventilation is a complicated process. Both exterior weather and indoor conditions have a major impact on this process. Vapour diffusion through wall assemblies to or from the air cavity is determined by the vapour pressure gradient between indoor and outdoor. One of the main moisture sources

in the brick veneer and fibre cement panel comes from the wind-driven rain (WDR), which is the amount of rainwater impinged on the exterior surface of wall specimens under the influence of wind speed and direction.

Another moisture source wetting the sheathing and cladding surface in the cavity is caused by outdoor air when its vapour pressure is higher than that in the air cavity. The moisture carried by outdoor air is transferred to the surfaces of the air cavity by vapour convection-diffusion, an absorption process. If the outdoor dew-point temperature is higher than the cavity-surface temperature, the cavity-surfaces may experience condensation. This phenomenon often happens during clear sky nights, so called "clear sky effect" or "under-cooling" or "overcooling" (Hens, 2005 and WUFI, 2007).

Solar radiation is an important factor affecting the hygrothermal performance of wall specimens. It provides the energy required to dry water out of walls by evaporation. However, when solar radiation is high enough and a cladding is wet, the temperature of cladding increases so high that the vapour pressure in the cladding is much higher than that in the air cavity and inside the wood-frame back wall assemblies. In this situation, the water vapour is often driven into the inside of insulation space and increases the moisture content of the wood components. Therefore, solar radiation is also a powerful force to drive moisture generated by wind-driven rain and clear sky effect into the walls.

Knowing the boundary conditions during the testing period will help the interpretation of hygrothermal behaviour of wall specimens.

4.1.1 Field measurements of temperature, RH and horizontal rainfall

1. BETF's site temperature, RH and horizontal rainfall

The daily fluctuation of RH with temperature change at the BETF's site is shown in Figure 4-1-1 from December, 2007 to June, 2008. In general, the daily average RH often remained over 80 - 98% daily from December to March with low fluctuation. Then RH decreased gradually with high fluctuation after March. The range of RH varied widely from 30% to 99% in the winter and from 16% to 98% in the spring.

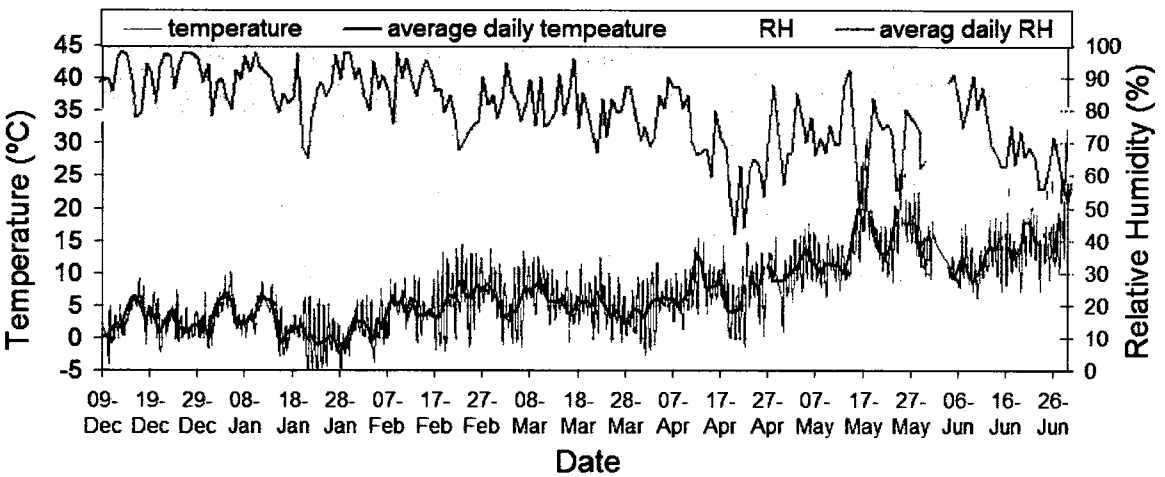

Figure 4-1-1: On-site temperature and relative humidity during the test period from Dec. 07 to June, 08.

Overall, temperature fluctuated less than RH. When the solar radiation increased with season change and even during the continuous sunny periods in January and February, the fluctuation of temperature became quite high. From the middle of January to middle of February, the daily fluctuation was within 10°C. After February, the temperature stayed approximately at the same level of 0 – 10°C until April. Then the temperature started to rise in spring.

The monthly average field temperature, RH and horizontal rainfall in the test duration are shown in Figure 4-1-2. The temperature during the test period was quite low but gradually increased with time. It was approximately 2°C in December 2007 and January 2008, around 4.5°C in February and March 2008, and 7.3°C in April. In May and June, the temperatures jumped to about 14°C. The average RH gradually decreased during the test period. From December 2007 to March 2008, RH only decreased by 10% from 91% to 81% while RH reduced rapidly in April, down to 69.8% and then stayed in the similar level in May and June.

The total amount of rainfall was 662 mm in seven months from December 6, 2007 to June 2008. In winter, except for December, the rainfall in each month (January to March) was quite even; around 104 mm to 110 mm. December had the highest rainfall of 203mm while the rainfall in April dropped dramatically to 67mm, which was only about a half of the amount in March. In May and June, the rainfall decreased to 30mm and 35mm, a half of that in April, indicating the weather in the winter was much wetter with higher RH and lower temperature than the spring.

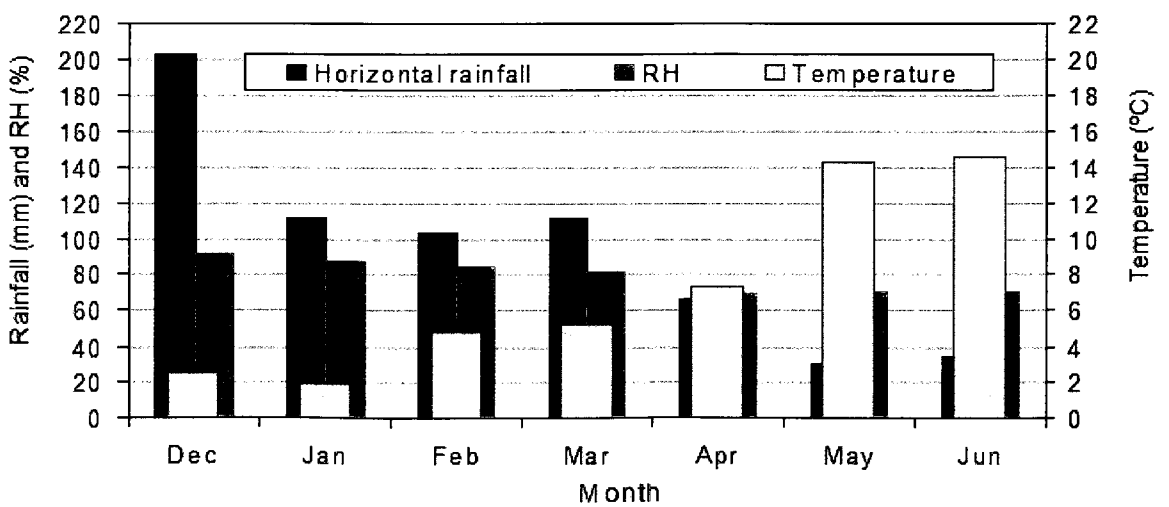

Figure 4-1-2: Average horizontal rainfall, temperature and RH recorded by the weather station on the roof of BETF from Dec. 07 to June, 08.

2. Comparison of temperature, RH and rainfall between BETF and YVR

The complexity of the local geography may affect the weather conditions in coastal BC and results in different micro-climates. Comparisons of the monthly average outdoor temperature and RH between BETF site and Vancouver airport (YVR) weather station from December, 2007 to June 2008 are shown in Figure 4-1-3. The temperature on BETF site was 0.4 – 1°C lower and the RH was 2 – 6% higher in most of months than those at YVR.

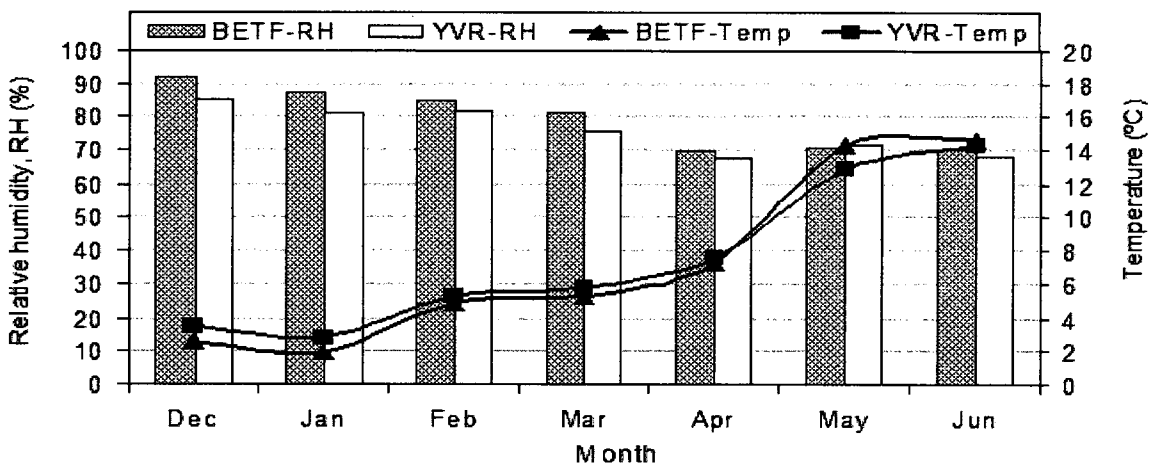

Figure 4-1-3: Comparison of average monthly temperature and RH between BETF and YVR weather stations from Dec. 07 to June, 08.

However, monthly average horizontal rainfalls between BETF site and YVR varied significantly, as shown in Figure 4-1-4. The rainfall at YVR was 22mm lower in December and about 37mm lower in February and March than those on BETF, which is about 35% difference. The rainfall in other months had 8 – 13mm difference between these two locations. The comparison results indicate that there are not many differences in temperature and RH while the local geography has significant impact on the amount of rainfall at these two locations in the same period.

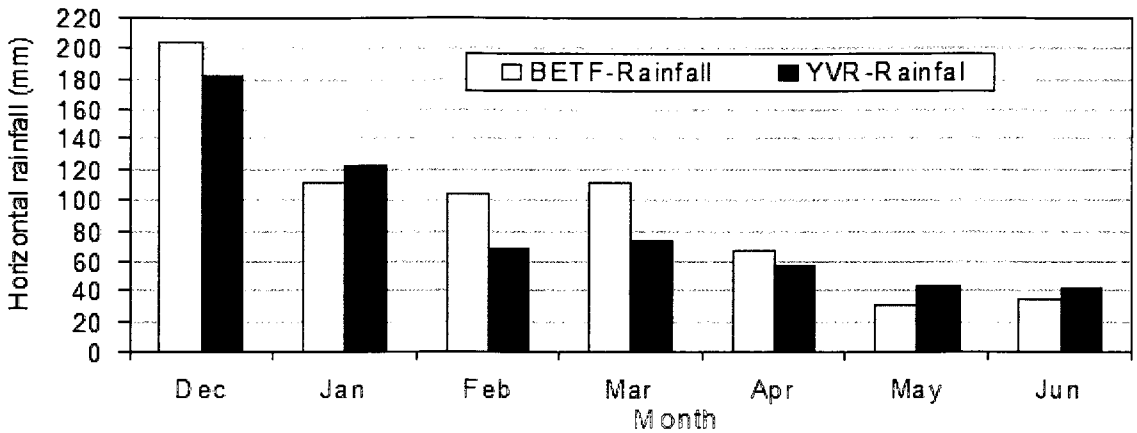

Figure 4-1-4: Average monthly horizontal rainfall between BETF and YVR weather station from Dec. 07 to June, 08.

4.1.2 Wind direction and wind speed

The analysis of the field wind direction and wind speed includes prevailing wind direction and wind speed distribution during all hours and rain hours from December, 2007 to June, 2008, excluding May. It is because that the wind direction and speed data was missing in May due to the malfunction of the data acquisition system.

1. Wind direction

During the test period, the prevailing wind direction at BETF was from the east-south-east (ESE) and the wind from the west has the second highest frequency, as presented in Figure 4-1-5. However, during the rain periods, the prevailing wind direction was from the ESE and the east, for most of the time wind blows from 67.5° to 112.5°.

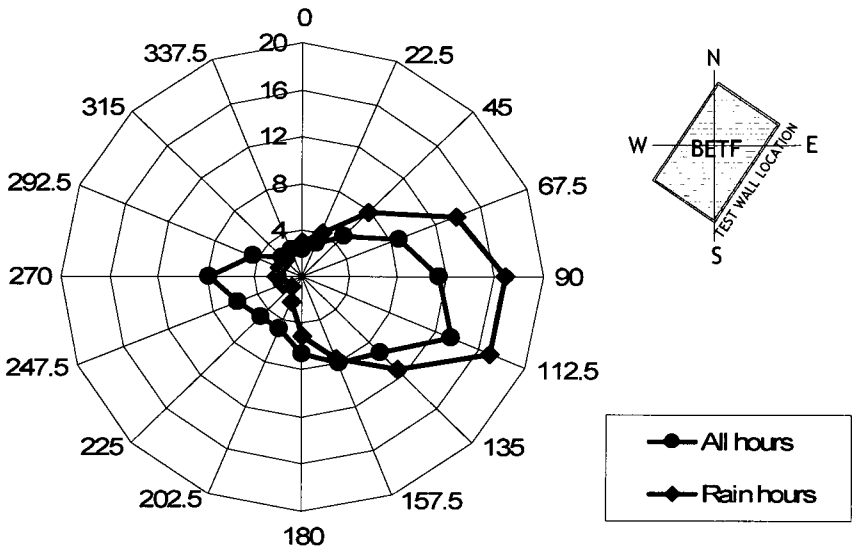

Figure 4-1-5: Wind direction rosette on the BETF site from Dec. 07 to June, 08.

The frequency distribution of wind directions for each month, in general, are similar to the wind direction rosette for all hours in the whole test period, that there were higher frequencies of wind from the west for February and April. However, each month has their individual characteristics during the rain hours, as shown in Appendix 1: "Monthly Weather Data Analysis".

2. Wind speed

Figure 4-1-6 shows the frequency of wind speed in a range of less than 0.5 m/s to above 10 m/s during the test period. The wind speed over 6 m/s had frequency of 0.1 - 0.6% only. Mostly the wind speed was within the range of 0 – 2 m/s, with a total frequency of 88% during all hours and 83% during the rain hours. The lower wind speed (such as 0.5 m/s and less) was the most frequent, which is approximately 47% during all hours and 38% during the rain hours. Then the frequency gradually reduced with the increase of wind speed. The frequency for wind speed above 1 m/s during rain hours was higher than that during all hours.

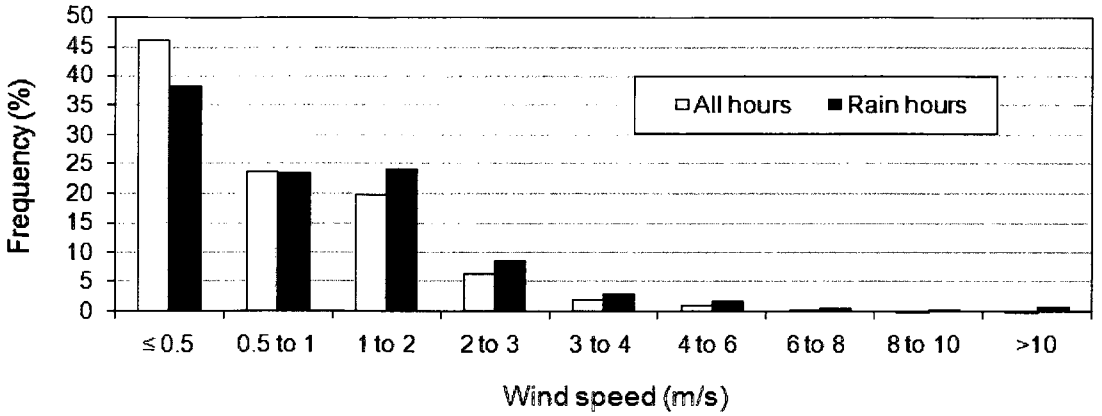

Figure 4-1-6: Wind speed during all hours and rain hours in the winter and spring test period from Dec. 07 to June, 08.

Figure 4-1-7 shows the comparison of frequency distribution of wind speed between wind from all directions and wind from ENE to SE (from 67.5° and 135°) during rain hours. The prevailing wind directions are within this range. There is a maximum of 5% higher frequency for wind from ENE to SE than wind from all directions in each range of wind speed except for wind speed less than 0.5m/s, which indicates wind speeds were higher within the prevailing wind directions when rain fell. Frequency distribution of wind speeds for each month was analyzed and is described in Appendix 1.

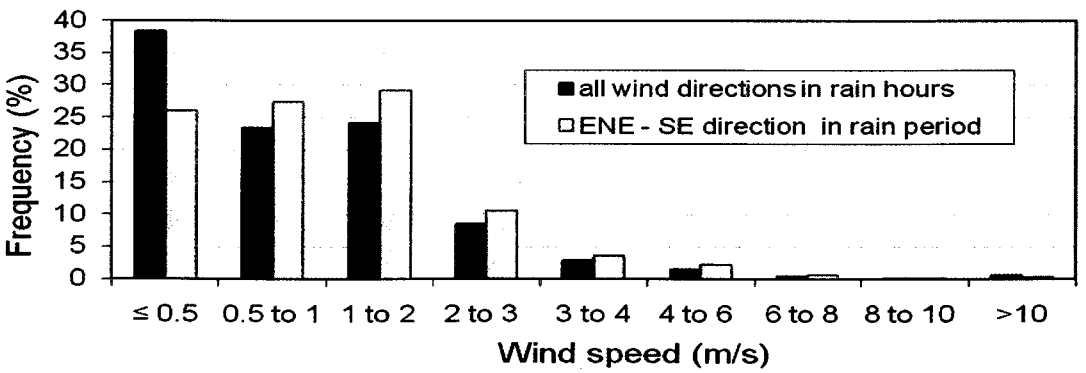

Figure 4-1-7: Comparison of wind speed distribution between wind from all directions and wind from ENE to ESE during the rain hours from Dec. 07 to June, 08.

The frequencies for all the months have the similar trends as those during all hours, rain hours and in the specific wind direction of ENE to SE (67.5° to 135°) during the rain

hours for the whole test period except in February, as shown in Appendix 1. In February, the frequency of wind speeds below 0.5m/s was the highest and decreased with the increase of wind speeds. The low frequencies in the high wind speed ranges for February, when it had relatively high rainfall, has significant influence on the reduction of wind-driven rain. The highest frequencies of wind speed in the rain hours were in the range of 1 – 2 m/s for other months, which may increase potential wind-driven rain on the SE façade of BETF.

4.1.3 Wind-driven rain

Wind-driven rain on the building facade is a major moisture load affecting its hygrothermal performance. Quantifying wind-driven rain received on the claddings will help understand its influence on the moisture performance of walls and provide the boundary conditions necessary for assessing the hygrothermal performance of walls using simulation programs.

There is a total of 15 rain gauges installed on all the façades of BETF, as shown in Figure 4-1-8. Six rain gauges were installed at the SE façade; three at the top of upper wall panels (upper rain gauges), about 4.8m above the ground and three rain gauges were installed at the top of lower wall panels (lower rain gauges), about 2.4m above the ground.

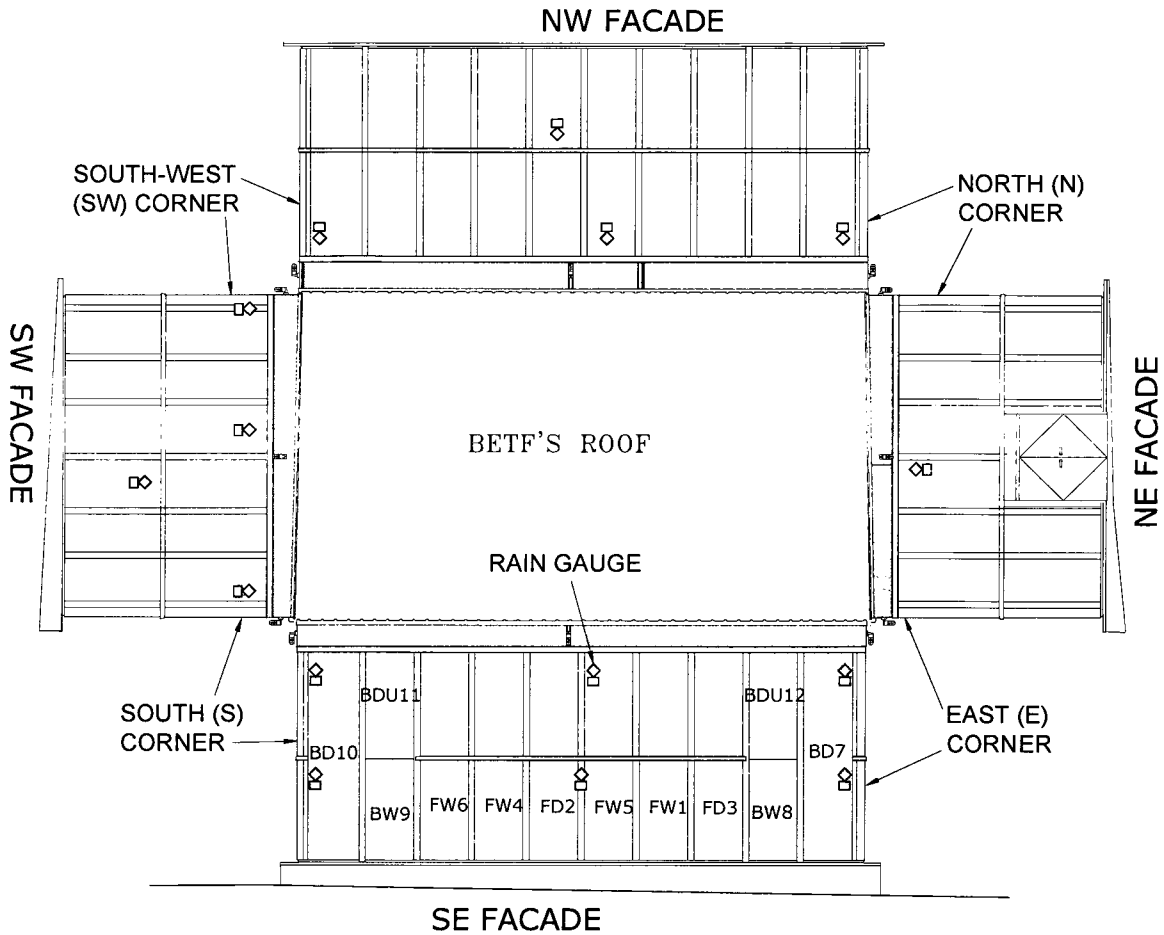

Figure 4-1-8: Locations of upper and lower rain gauges installed on all four façades of BETF.

The total amounts of wind-driven rain and catch ratio at rain gauge locations on SE façade of BETF are listed in Table 4-1-1 for the test period from January to April 2008 and June 2008. The wind-driven rain in December, 2007 and May, 2008 is excluded because the rain gauges were installed at different dates and the installations were not completed until the end of December, 2007. Data for May are missing due to the malfunctioning of the data acquisition system. The results show that the upper level received more rain than the lower level of the façade. The range of catch ratio is 0.02 - 0.04.

Table 4-1-1: Wind-driven rain and catch ratio on the SE façade of BETF from Jan. to June 08

Horizontal Rain	WDR (mm)					
(mm)	Upper rain gauges			Lower rain gauges		
	E	centre	S			
458	13.34	18.24	13.98	9.01	13.57	10.11
	catch ratio					
	0.03	0.04	0.03	0.02	0.03	0.03

The monthly WDR at rain gauge locations on SE façades of BETF is analyzed and is shown in Figure 4-1-9. The SE façade of BETF received the most rain in March because March had large amounts of rainfall with high frequency of strong winds from the ENE to ESE direction while the least amount of WDR in April since the horizontal rainfall in this month is only about half of the amount of rain in March. It is interesting to note that in February, the WDR is at least 50% less than that in January and March although there is a similar amount of horizontal rainfall and prevailing wind direction. The main reason is due to a high frequency of low wind speed in February from the ENE to ESE, the frequency of wind speed less than 1.0 m/s is 63% and 10% higher than those in January and March (Detail can be found in Appendix 1: and Ye. et. al. 2009). In addition, the frequency of wind speed within 1-2m/s in February is 20% and 13% lower than those in January and March. That means that with the same amount of rainfall and same wind direction, WDR is strongly influenced by wind speed.

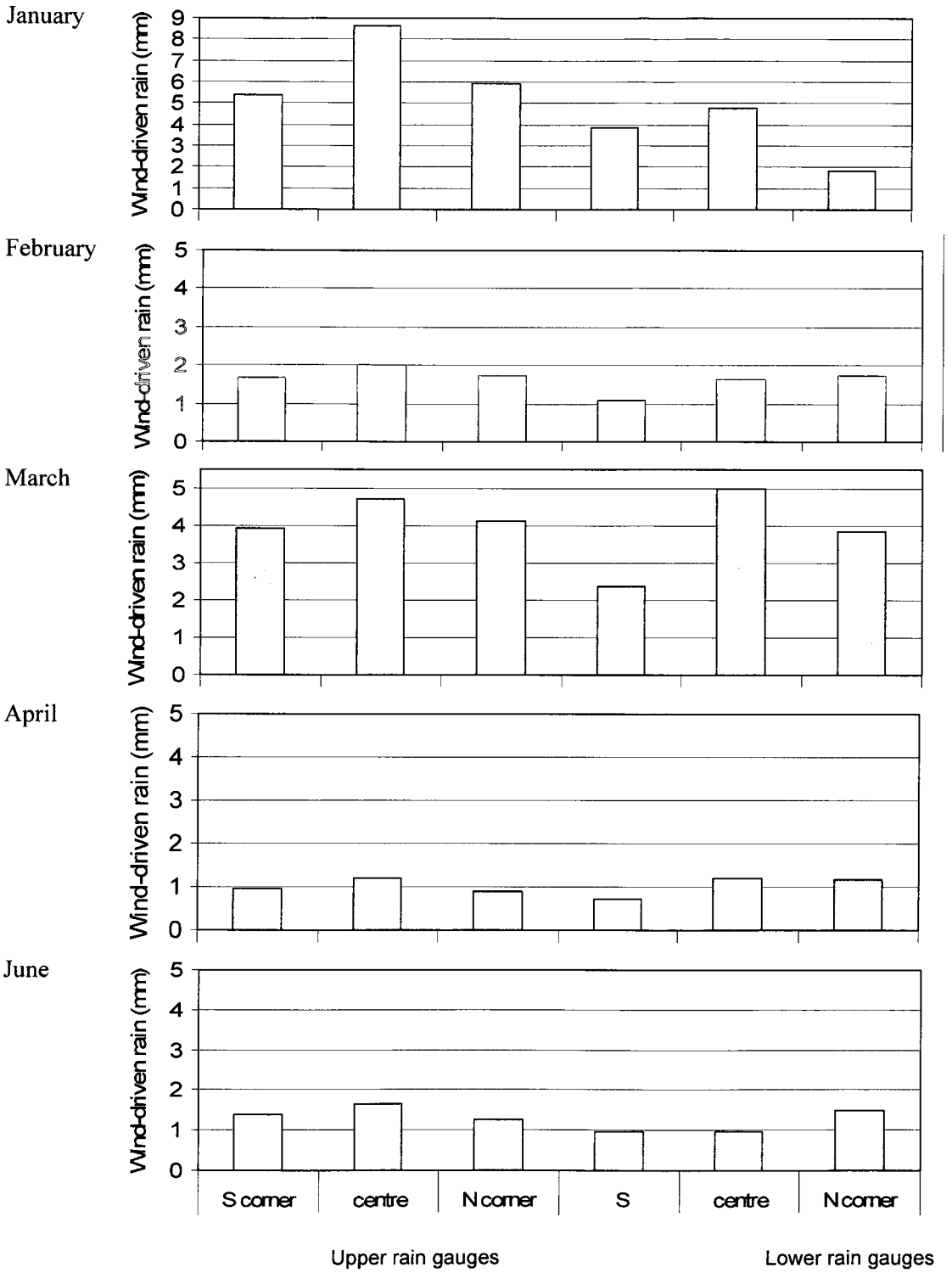

Figure 4-1-9: Total amount of wind-driven rain received by SE façade of the BETF for each individual month from Jan. to June, 08 (except for May).

4.1.4 Solar radiation

Solar radiation gradually increases from December 2007 to June 2008, as shown in Figure 4-1-10. High density of high solar radiation with flat line of rainfall represents the continuous sunny days. These continuous sunny periods are the critical times for drying the wall specimens.

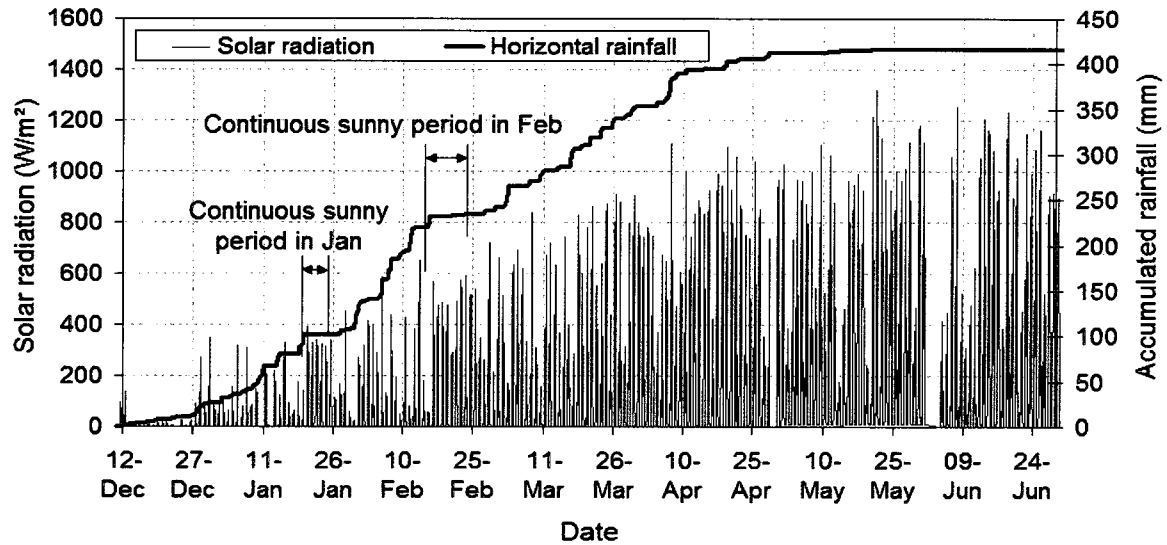

Figure 4-1-10: Solar radiation with rainfall accumulation during Dec. 12, 07 to Jun. 30, 08 on the BETF site.

It is worthwhile noting the difference between monthly average solar radiation and the maximum solar radiation recorded. As listed in Table 4-1-2, the differences between maximum and average value in the winter can be 3 – 4 times. During the continuous sunny periods of January 20 – 26 and February 17 – 25, the peak solar radiation is not only high but also stayed in a long period daily. For example in Figure 4-1-11, the frequency of solar radiation at the peak level of 400 – 550 W/m² on February 17 – 25 were 8 – 14% while the frequency of the same level of solar radiation for the whole February was only 4 – 5%.

Table 4-1-2: Monthly maximum and average solar radiation from Jan. to Jun. 08 and hourly average solar radiation during continuous sunny periods in Jan and Feb. 08 at the BETF site

	Dec	Jan	Feb	Mar	Apr	May	Jun
Maximum solar radiation in each month, W/m²	230	316	511	755	951	951	984
Monthly average solar radiation, W/m²)	51	77	139	189	278	312	302
Average solar radiation on Jan. 20-26, the first sunny period, W/m²		151					
Average solar radiation on Feb. 17-25, the second sunny period, W/m²			226				

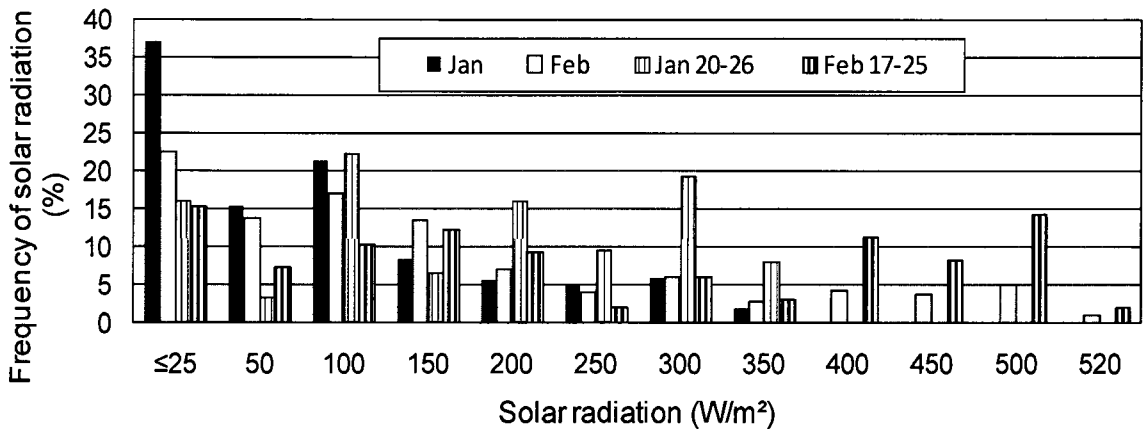

Figure 4-1-11: Accumulated hours of solar radiations in Jan. and Feb. 08, and in the sunny periods Jan. 20 – 26 and Feb. 17 – 25, 08.

The level of solar radiation has a significant impact on the drying of building envelope. For example, the "Envelope Drying Rate Experiment" conducted in a laboratory by Forintek in 1999 (Hazleden, D. 2001) obtained low drying rates using a constant simulated solar radiation of 120 W/m² for 8 hours each day. This value is slightly lower than the hourly average solar radiation recorded on BETF site in February, 2008 (139 W/m^2 as shown in Table 4-1-2). However, it is 1.6 times less than the average solar radiation in the sunny period of February 17 – 25 and 3 – 4 times less than the peak solar radiation. After 2000 hour-drying (87.5 days), the wood frame still stayed above 19% from an initial 28 – 32% moisture content level. The results were without much

difference compared with the phase 1 test without solar radiation. The simulated solar radiation was too low to heat up the walls to evaporate the built-in moisture in wood frame.

4.1.4 Indoor conditions

The indoor conditions were set at constant temperature and relative humidity. The purpose of keeping constant indoor conditions of BETF is to represent a typical room conditions for residential buildings in the coastal BC region, to reduce test variables and to simplify the control of the HVAC system in the test duration.

The control of temperature during whole test duration was quite stable and easily managed. However, the control of RH needs more attention due to the interaction between the hot steam humidifiers and air conditioning. Overall the temperature through the test period was kept at an average of 22°C with ± 1.5°C fluctuation and RH was at an average of 54% ± 5%. The measurements of two RH-T sensors are very similar; the maximum difference is only 1.3% RH and 0.2°C temperature, indicating that the indoor conditions are quite uniform, relatively stable, and constant.

4.2 Moisture performance of test wall assemblies

In this section, the moisture performance of wall assemblies is evaluated by moisture content in wood components and vapour pressure distribution in air cavities and through the wall assemblies.

4.2.1 Moisture content measurements in wood components

The change of MC in plywood sheathing is used as the indicator to evaluate the drying and wetting affected by the cavity ventilation. The moisture-pins can only measure MC up to about 23% with 2% accuracy; therefore, the MC of plywood measured by gravimetric samples is mainly used for the analysis because of the high initial MC in some test panels. The impact of vent configuration on the MC of plywood is discussed. The drying and wetting rates of plywood is quantified. The MC of plywood between gravimetric and moisture-pin measurements is briefly compared. The MC distribution in studs and bottom plates of wet panels is also described.

4.2.1.1 Gravimetric measurements

Gravimetric samples were installed in ten wall specimens at the lower level of the BETF's facade, including four brick walls and six fibre cement walls. There were in total eight gravimetric samples on the plywood sheathing. Seven were located at 38mm away from the vertical centre line on one side in the test bay. An eighth sample was near a stud, at 44mm away from the edge of the stud, as shown Figure 4-2-1a. Two samples were inserted in a stud and the bottom plate in each wall specimen. One sample was at the exterior edge of the stud and bottom plate and the other was in the middle of the stud and the bottom plate, as described in chapter 4. The gravimetric samples were weighed weekly starting from November 2, 2008 for the dry walls and November 12, 2008 for the wet walls.

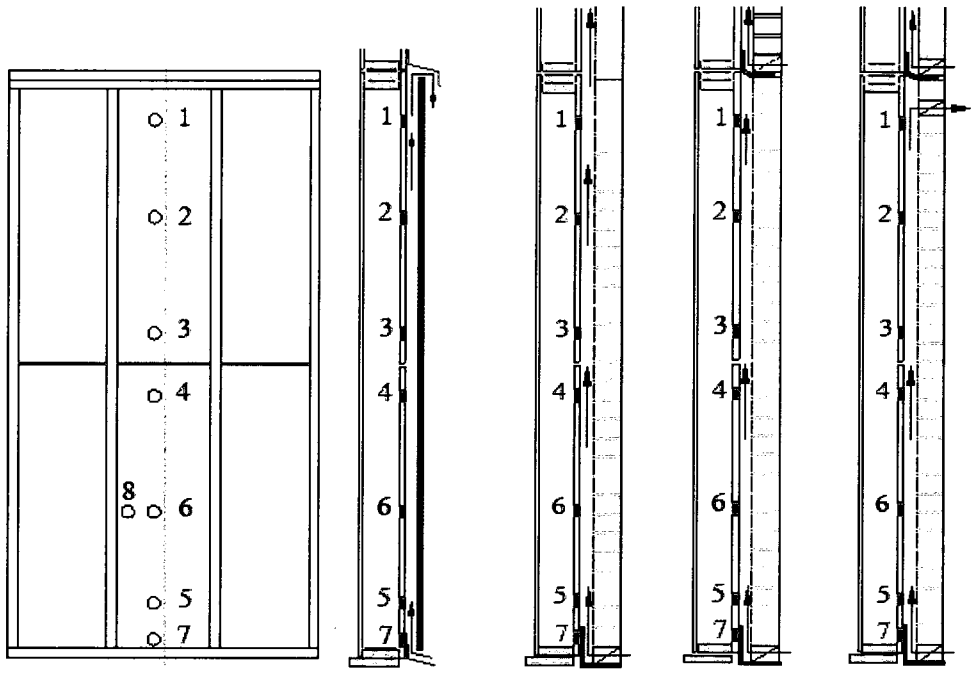

Gravimetric sample locations a) b1) b2) b3)

Figure 4-2-1a: Relationship between the location of gravimetric samples, vents and flashings in a) fibre cement wall, b1) two-floor high brick walls, b2) one-floor high brick wall with vented cavity, b3) one-floor high brick wall with ventilated cavity.

The MC of plywood near the vents and behind the airtight self-adhesive membrane varied from the MC in the middle section of plywood along the cavity, as shown in Figure 4-2-1b. Sample #7 in all the walls was located at the bottom of plywood and was totally covered by self-adhesive membrane which overlapped with a base flashing. This area of plywood had the slowest wetting during the winter and also the slowest drying in the spring, which indicates that the moisture absorption and desorption over this area is restricted by the impermeable membrane (1.6 ng/Pa.s.m^2) (BAKOR, 2009). Sample #5 was close to the bottom vents and dried faster at the entry of cavity in the winter but absorbed more moisture after the plywood reaches to its equilibrium level compared with the samples in the middle of cavity.

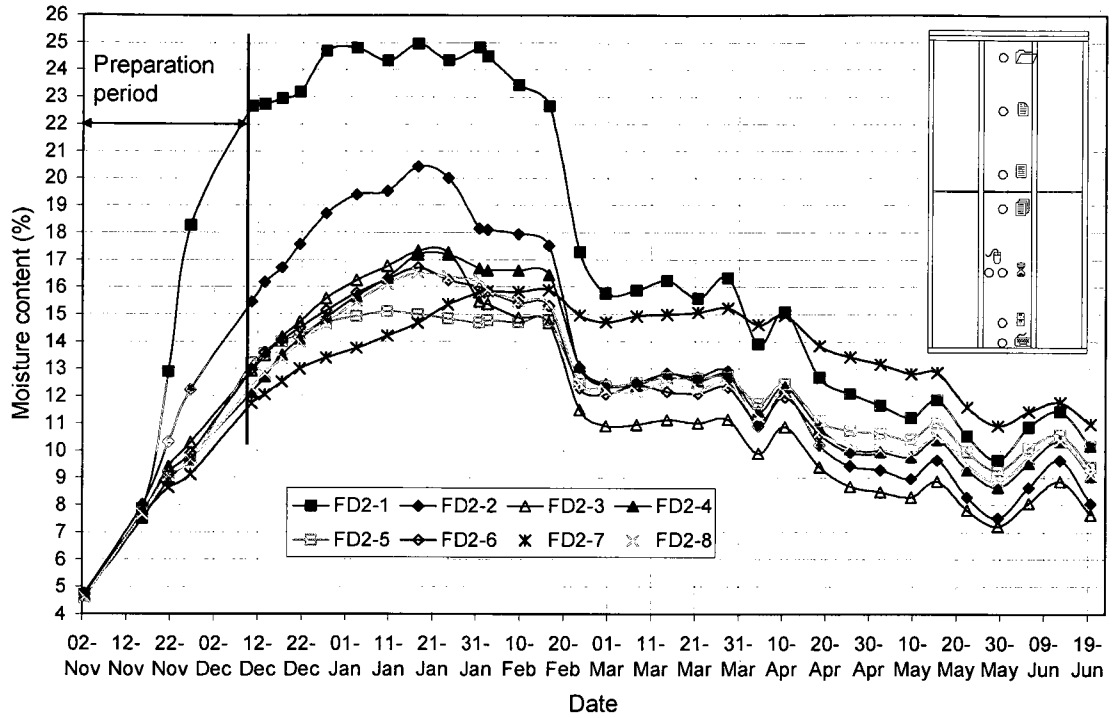

Figure 4-2-1b: MC profiles in plywood of FD2 (1mm top vent) measured with gravimetric samples From Nov. 07 to June, 08.

Sample #1 was located at the top of plywood and close to the top vents and the top plates. Condensation was observed in some of the test wall specimens at these locations, which had impact on the MC of sample #1. The upward air circulation in the insulation spaces and the air cavities, high indoor RH, and the lower surface temperature due to the thermal bridging of wood top plates may have contributed to the formation of condensation at the upper part of the plywood for some test walls. Further investigation is required to identify the actual causes.

The other four samples were located in the middle of the plywood sheathing and are influenced by the airflow through the cavity resulting from different vent configurations and weather conditions. Sample #8 is used to monitor the horizontal moisture distribution in the plywood sheathing near stud. To show the effect of ventilation, the

difference in average MC between upper and lower parts of plywood is analyzed and described in Appendix 2 "Moisture Content Measurement of plywood sheathing". The general trend in the vertical profile of MC in plywood is that the MC level increases with the increase of the height, i.e. drier at the bottom and wetter at the top in the winter. However, in the spring, the bottom is wetter than the top.

4.2.1.1.1 Average moisture content in plywood sheathing

The readings from the gravimetric samples, excluding sample #1 at the top and sample #5 and #7 at the bottom, are used for averaging to compare the influence of cavity ventilation realized with different vent configurations on the drying and wetting of four brick walls and six fibre cement walls.

At the preparation stage the walls with high initial MC in the plywood sheathing (wet walls) were temporarily wrapped with polyethylene film to prevent drying of the wet panels by vapour diffusion to the surrounding environment before the wood-frame back up walls were installed at the SE façade of BETF. The film was removed at the time of installation.

1. Brick walls

The average MC in plywood of the four brick walls is shown in Figure 4-2-2 over the preparation and test period. For the two-storey test walls, BD7 and BD10, only the first floor wood-frame back walls have gravimetric samples, therefore, the average MC is only for the plywood at the lower level.

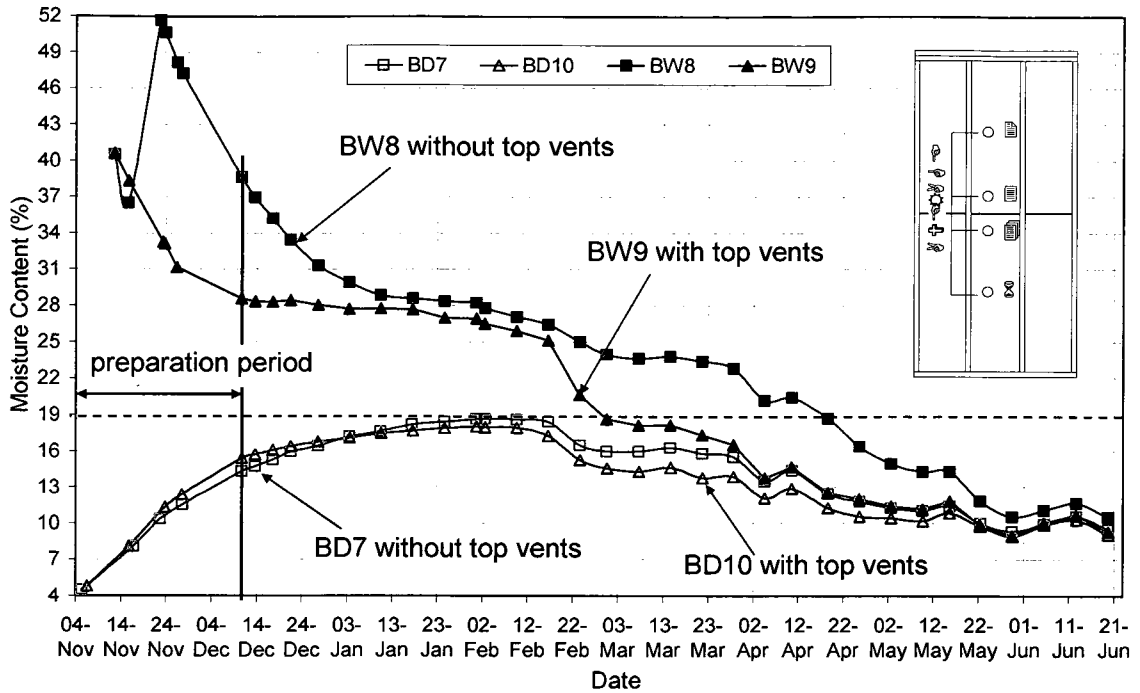

Figure 4-2-2: Comparison of average MC in plywood of four brick walls from Nov. 07 to June, 08.

During the test period (from December 10, 2007 to June 21, 2008), the gravimetric samples of BD7 and BD10 with initially low MC in plywood sheathing (dry walls) increased and reached to the maximum MC level of slightly below 19% by mid-February. The MC of plywood decreased faster during a continuous sunny period of February 17-25. In the following month, the MC level remains constant due to the wet and humid outdoor conditions. Without top vents, the MC level in BD7 was about 2% higher than that in BD10. In the spring from the end of March to June, the difference of MC in plywood between BD7 and BD10 became smaller as they dried to below 10%.

For the wet walls, BW8 and BW9 started at the similar initial MC in plywood. The spike in MC level of BW8 was due to the use of a propane torch to dry the brick and mortar during installation as the outdoor temperature dropped below zero in the morning of a sunny day. As a result, the inward vapour diffusion significantly elevated the moisture

level at some locations of the plywood. MC of BW9 decreased very slowly from the beginning of the test period until the sunny period in February when there is a sharp drop in MC by 7%. It took about 80 days to drop to below 19% MC. The MC of BW8 decreased rapidly from the high spike of 52% to 28% in mid-January and reached a similar MC level to the MC of BW9. Then the decrease of MC slowed down as the same as BW9 until the sunny period in February. However, the drying was much slower for BW8 during the sunny period. It took 129 days for the plywood of BW8 to dry to below 19% MC due to lack of cavity ventilation without top vents. BW9 reached the equilibrium MC level almost the same as dry walls at the beginning of April while it took BW8 two more months to dry to the same level as other walls. At the end of spring both walls reached a moisture level of about 10%, the same as the dry brick walls.

2. Fibre cement walls

Figure 4-2-3 and Figure 4-2-4 show the average MC in plywood over time for the six fibre cement walls. At the preparation stage, the average MC in wet plywood of walls FW1 and , FW4 to FW6 dropped by about 11% from 39 – 41% (initial MC) while the average MC level in the dry sheathing of FD2 and FD3 gained 7% from about 7% (initial MC).

During the test period from December 10, 2007 to June, 2008, the plywood sheathing in dry walls went through a wetting process followed by a drying process. January 20, the start of the first sunny period, was a turning point when the MC in dry walls reached its maximum and started decreasing and the drying of wet walls accelerated. MC of all the walls, including both dry and wet walls, reduced sharply during the continuous sunny

period in February. There was a 3.5% drop in dry walls and a 5 – 6% drop in wet walls. Then all the walls reached a MC level of 12 – 15% after the sunny period and dried to about 8% MC by the end of the spring.

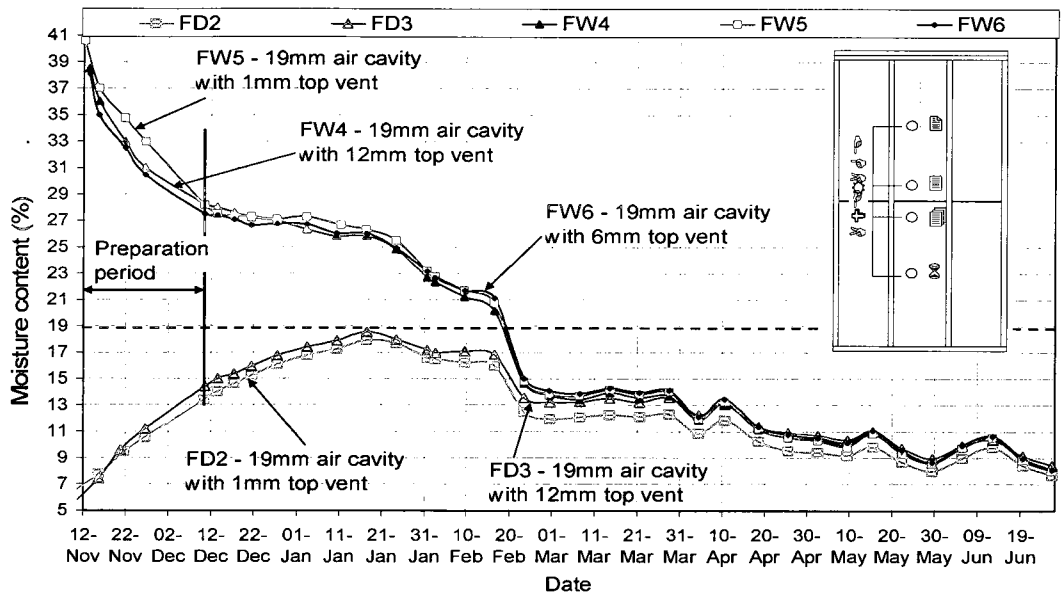

Figure 4-2-3: Average MC in plywood of five fibre cement walls with a 19mm air cavity from Nov. 07 to June, 08.

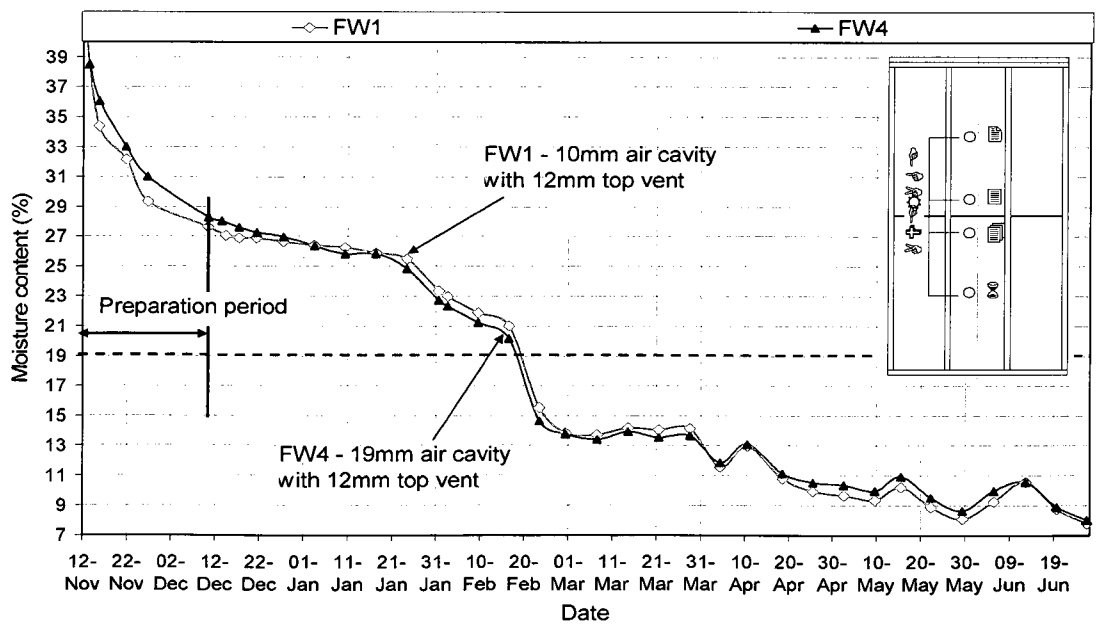

Figure 4-2-4: Comparison of average MC in plywood of fibre cement walls between FW1 with a 10mm air cavity and FW4 with a 19mm air cavity from Nov. 07 to June, 08.

For the walls with a 19mm cavity, both dry walls of FD2 and FD3 behaved similarly. The MC of both walls increased to their maximum level in 38 days, reaching to a MC level just below 19%, i.e. within a safe level considered immune to fungal growth (CMHC, 2001). The wet walls of FW4, FW5 and FW6 had very close MC value and similar trends throughout the winter and spring test duration. MC decreased from 28% to above 25 - 26% in 40 days from the beginning of the test to January and then dropped to below 19% in another 30 days. The difference among the three wet walls is negligible, indicating that the sizes of top slot vent have insignificant impact on the drying for the fibre cement walls.

For the wet wall FW1 with a 10mm air cavity, a similar trend to the wet walls with a 19mm air cavity is observed. However, MC in this wall is slightly higher in the winter but lower in the spring after reaching its equilibrium level.

4.2.1.1.2 Moisture content in stud and bottom plate

The purpose of measuring MC in stud and bottom plate is to monitor the redistribution of moisture from the wet plywood sheathing. The locations of gravimetric samples in the stud and bottom plate are shown in Figure 4-2-5. In general, the MC in the exterior edge of a stud and a bottom plate (samples #s9 and #p10) near plywood sheathing is higher than MC in the middle thickness of stud and bottom plate (#s9b and #p10b) in all the brick walls and fibre cement walls.

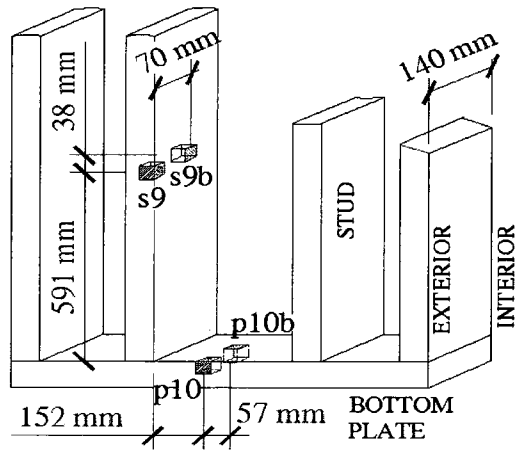

Figure 4-2-5: Locations of gravimetric samples in the stud and bottom plates for each brick and fibre cement wall panels at the first floor on the BETF.

1. Brick walls

The redistribution of moisture from the initially wet plywood in BW8 and BW9 contributed to the large MC increase in wood frames, as shown in Figure 4-2-6. MC at the edges of the bottom plates received 3 – 5% more moisture than that in studs before the brick veneer was installed on the SE facade of BETF on November 20 – 23, 2007. After the brick veneer is installed, the MC increase in both stud and bottom plate slowed down dramatically.

The samples at the edges of stud and bottom plate in BW8 remained at the similar MC levels until the end of January. The sample at the edge of bottom plate of BW9 remained at the similar MC level until the beginning of March while the MC in the sample at the edge of stud started decreasing earlier on Feb 10.

a) BW8 without top vent

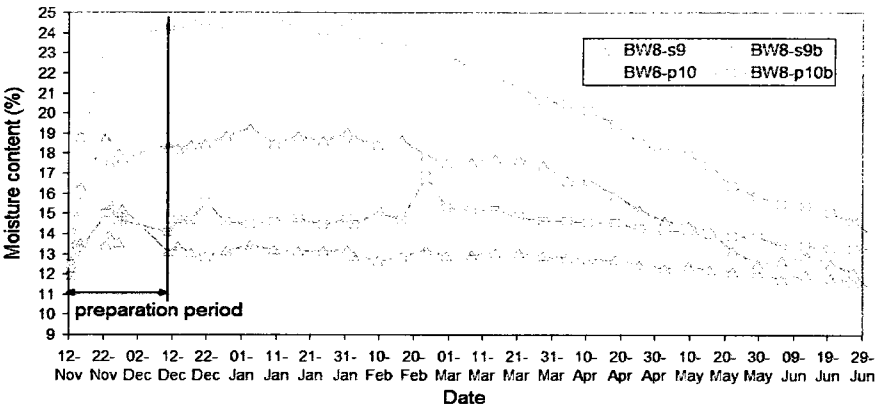

b) BW9 with top vents and insect screens

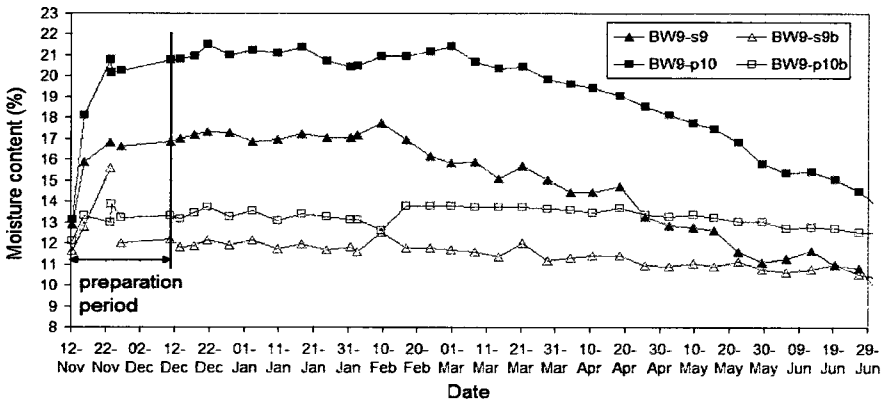

Figure 4-2-6: MC in the studs and bottom plates of a) BW8 and b) BW9 (one-floor high with initial high MC in plywood) measured by gravimetric samples from Nov. 07 to June, 08.

The samples in the middle of both studs and bottom plates for both walls were similar from the beginning of test to the end of January. From February to the mid-March, the MC of gravimetric samples in the bottom plates increased and then decreased starting from mid-March for BW8 while from mid-April for BW9. In contrast, the MC of gravimetric samples in the middle of stud started decreasing from the end of March for BW8 while from mid-February for BW9. The edges of bottom plates had higher MC than the edges of studs for both walls through the entire test duration. The maximum differences in MC between exterior edge and middle are 5 - 6% for the studs and 8 - 10% for the bottom plates. The difference in BW8 is 1 – 2% higher than those in BW9 due to the higher MC level in BW8 before and during the installations.

2. Fibre cement walls

The redistribution of moisture from wet plywood in test walls FW4, FW5 and FW6 with a 19mm air cavity significantly increased the MC at the edges of studs and bottom plates, as shown in Figure 4-2-7.

a) FW4 12mm top vent

b) FW5 1mm top vent

c) FW6 6mm top vent

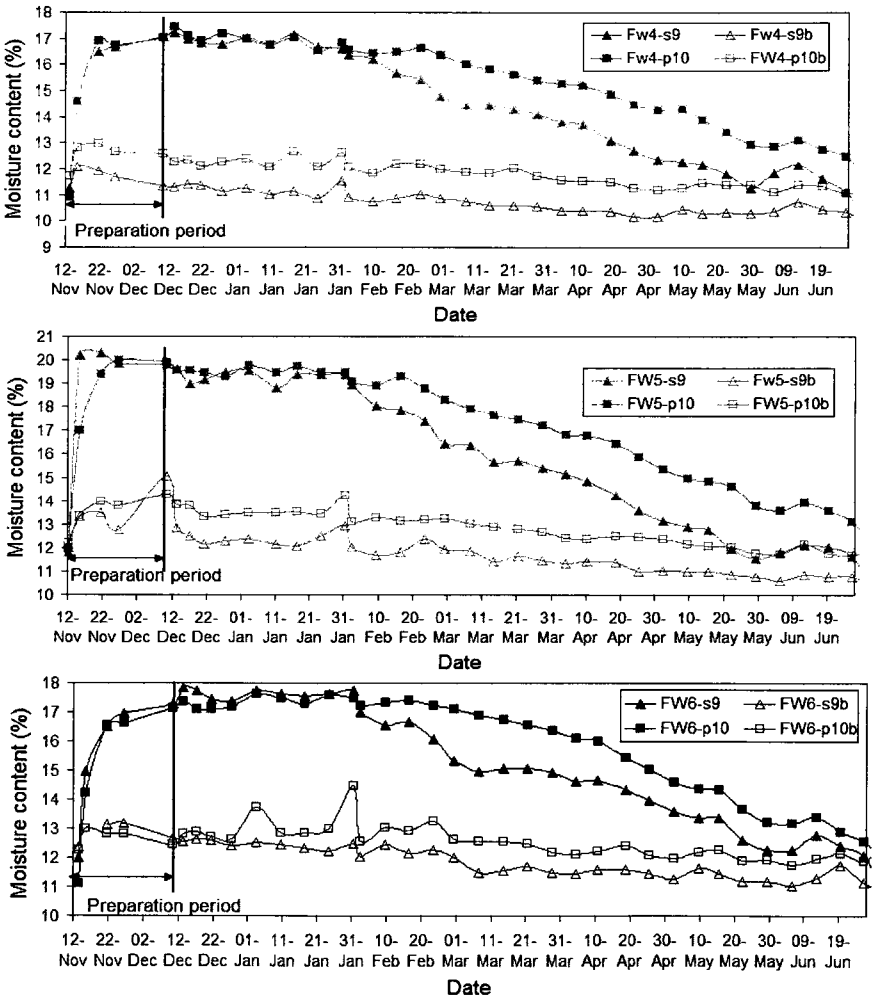

Figure 4-2-7: MC in the studs and bottom plates of a) FW4, b) FW5 and c) FW6 (initial high MC in plywood) measured by gravimetric samples from Nov. 07 to June, 08.

During the preparation period from November 12 to December 9, 2007, MC at the edge of the bottom plates and studs increased 6% for FW4 and FW6 while 7 – 8% for FW5 from initial 11 – 12% before the wood-frame back walls were covered by fibre cement claddings. In the test period, all three walls had similar trends in terms of MC changes in

the studs and bottom plates. The edges of studs dried faster than the bottom plates. The edges of stud and bottom plates incurred fast drying starting from the beginning of February while the moisture contents at the middle section of these wood frames remained almost the same until mid-March and then started drying slowly. At the end of June, the MC of all samples reached 11-13%. The maximum differences of MC between the edge and the middle point are 6 -7% for studs and 5 – 6% for bottom plates for all the wet walls with a 19mm cavity and different top vent sizes. The differences among these walls are small, within 1%.

Figure 4-2-8 shows the MC at the edge and in the middle thickness of the studs and bottom plates of FW1 compared with that of FW4. Due to the slightly higher MC increase in the stud and bottom plate of FW1 (about 2% more than that in FW4) from the initial 12-13% before the fibre cement claddings were installed, the MC at edges of stud and bottom plate dried faster than those in FW4 and eventually reached to about 12% MC, a similar level as that in FW4 by the end of spring.

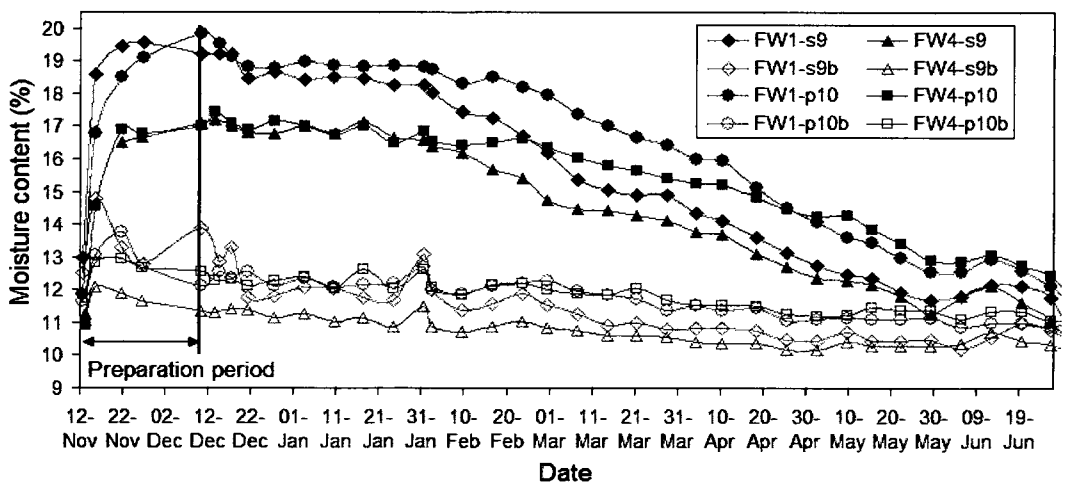

Figure 4-2-8: Comparison of MC in studs and bottom plates between FW1 (10mm air cavity) and FW4 (19mm air cavity) measured by gravimetric samples from Nov. 07 to June, 08.

The difference of MC between edge and middle of stud in FW1 is similar to FW4 while the difference in bottom plate of FW1 is around 1% smaller than that of FW4.

4.2.1.2 Drying and wetting rates of plywood sheathing

To quantify the effect of cavity ventilation, the drying and wetting rates in each test wall at the lower level of the façade is calculated and compared over the test period using gravimetric measurements. The wetting and drying of the plywood is mainly influenced by the weather conditions.

1. Brick walls

Figure 4-2-9 shows the drying and wetting rate of brick walls BD7 and BD10 with initially dry plywood. BD10 with top vents had lower average wetting rate of 0.03%/day during the initial wetting period from December 10, 2007 to February 10, 2008, a week before the sunny period. Its wetting rate is half of that in BD7 without top vent. The drying rate of BD10 was slightly higher than that in BD7 during the sunny period in February. Results indicate that the introduction of top vents helps keeping the wood component dry in the wet and cold winter. During the rainy March, the drying rates of both walls were similar while after March to the end of spring (June, 21), the drying of BD7 was slightly higher than that of BD 10.

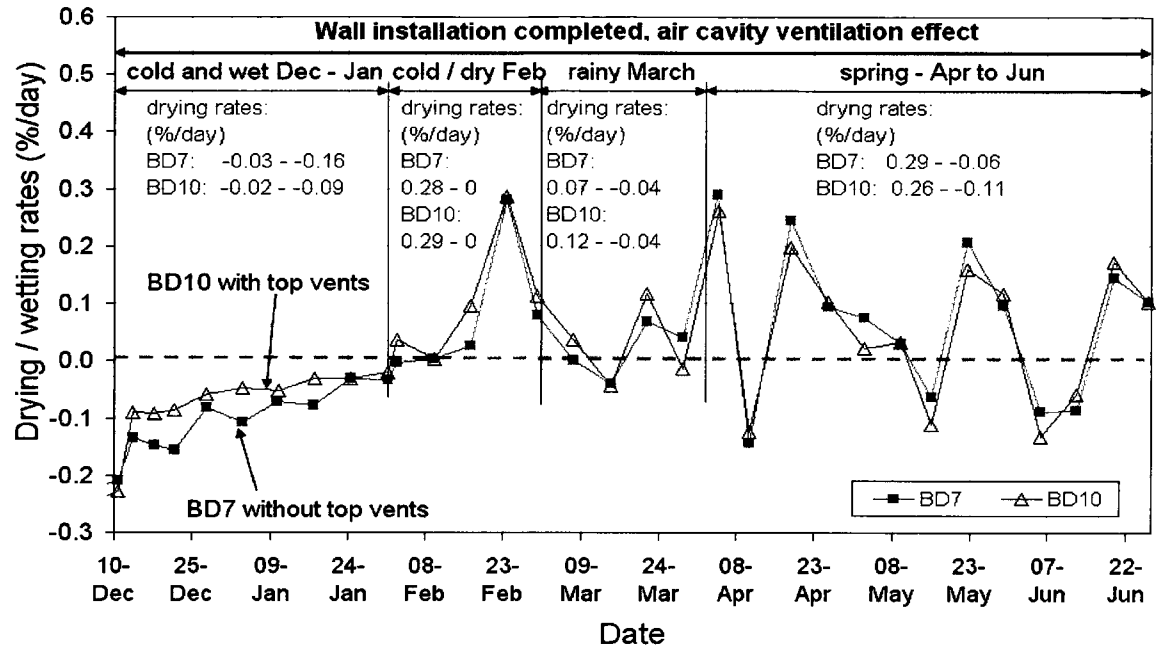

Figure 4-2-9: Average daily wetting and drying rate in plywood sheathing of BD7 and BD10 from Dec, 07 to June, 08.

Figure 4-2-10 shows the drying and wetting rates of brick walls BW8 and BW9 with initially wet plywood. BW8 had much higher drying rate than that of BW9 during the initial period to February due to the much higher initial MC level.

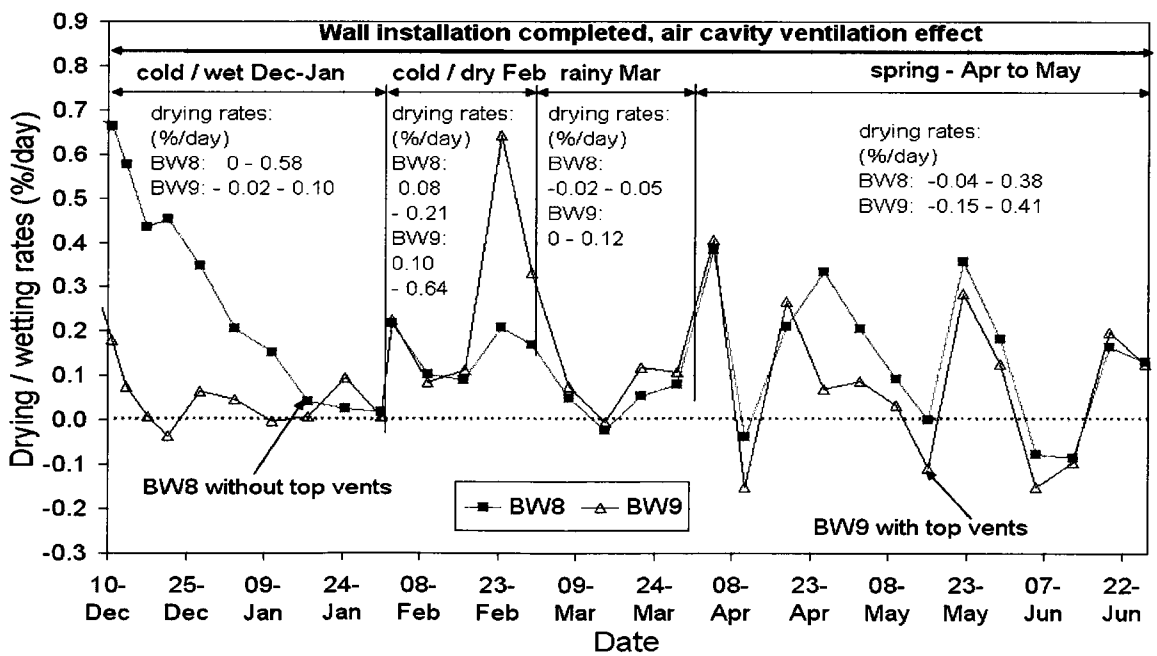

Figure 4-2-10: Average daily drying and wetting rates in plywood sheathing of BW8 and BW9 from Dec, 07 to June, 08.

Once the gravimetric samples reached comparable level of MC, the drying rate of test wall BW9 was twice of the drying rate in BW8 during the sunny period with the aid of solar radiation and top vents. The drying rate of BW9 was also higher during the rainy March period. However in April and May, the drying rate of BW8 was higher than that of BW9 due to its higher MC in plywood sheathing and the minimal air movement in the air cavity compared to that in BW9,

2. Fibre cement walls

Figure 4-2-11 shows the drying and wetting rates of the two dry fibre cement walls, FD2 and FD3. During the initial wetting period from December 10, 2007 to January 17, 2008, FD3 with a larger top vent (12mm) has the similar wetting rate to that of FD2 with a much smaller top vent (1mm), within an average wetting rate of 0.11- 0.12%/day.

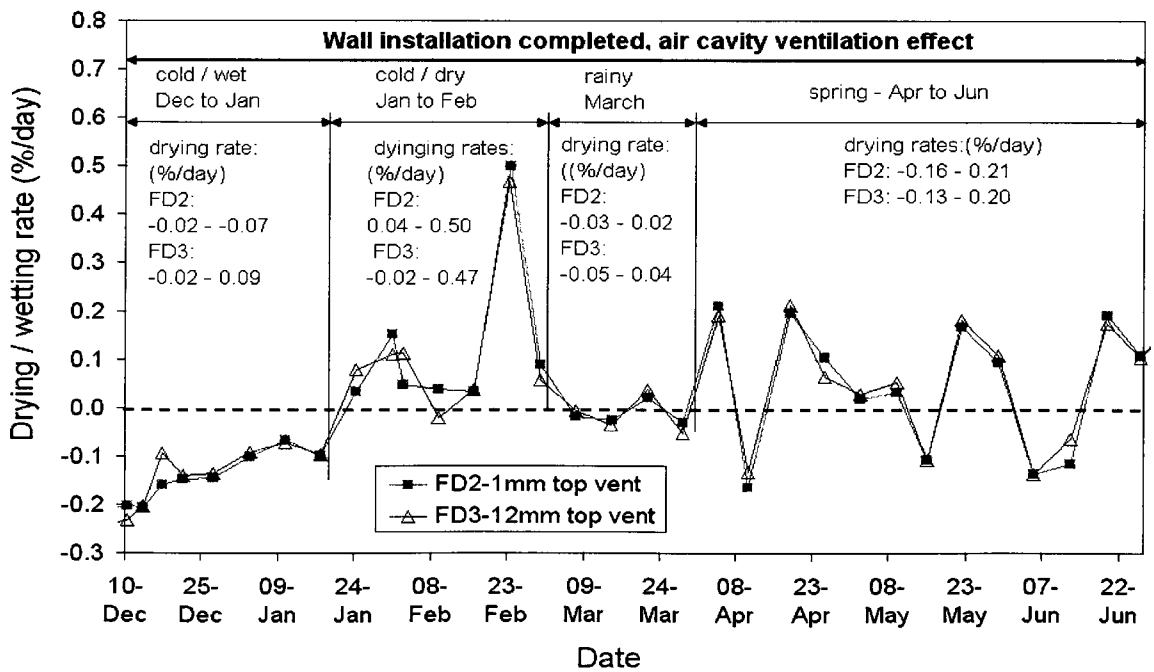

Figure 4-2-11: Average daily wetting and drying rates in plywood sheathing of FD2 and FD3 from Dec, 07 to June, 08.

When the weather gets a bit sunnier in February, FD2 has a slightly higher drying rate than FD3 by 0.03%/day. This is probably attributed to higher thermal buoyancy effect in FD2 due to higher cavity temperature in the sunny period, which allowed the removal of more moisture evaporated from cavity surfaces by enough ventilation airflow.

Figure 4-2-12 shows the drying and wetting rates of the wet walls with a 19 mm air cavity during the test period. Similarly to what has been observed from the MC shown in Figure 4-2-11, there is not much difference in terms of the drying and wetting rates among these three test walls, especially after the MC level drops to below 19% and reaches their equilibrium levels.

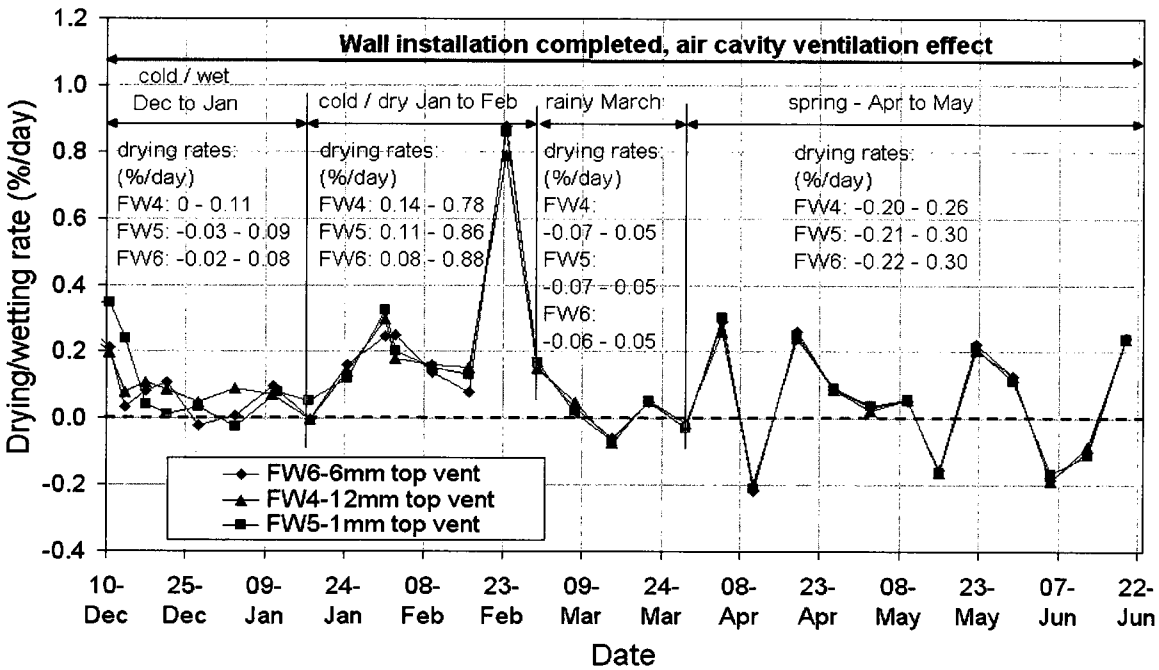

Figure 4-2-12: Average daily drying and wetting rates in plywood sheathing of FW4, FW5 and FW6 from Dec, 07 to June, 08.

During the initial drying stage from December 10, 2007 to January 17, 2008, FW4 with a 12mm top slot vent had the highest average daily drying rate of 0.06%/day and FW6 with a 6mm top vent had the lowest drying rate of 0.04%/day while FW5 with 1mm top vent

had an average drying rate of 0.05%/day. In the sunny period in February, FW5 with the smallest top vent had the largest daily average drying rate of 0.30%/day while FW4 and FW6 had the same drying rate of 0.28%/day. This can be explained with the same reason for FD2 as that FW5 with the smallest top vent has higher thermal buoyancy effect in the cavity during the sunny period compared with those in the other two walls resulting in larger moisture removal from the surfaces of plywood and fibre cement cladding.

Figure 4-2-13 shows the comparison of drying and wetting rates between FW1 (10mm air cavity) and FW4 (19mm cavity), both walls with a 12mm top vent. FW1 had a lower drying rate compared to FW4 from the beginning of the test set-up to when the MC level reached slightly below 19%, indicating that a larger cavity depth of 19mm promotes drying compared to a 10mm cavity.

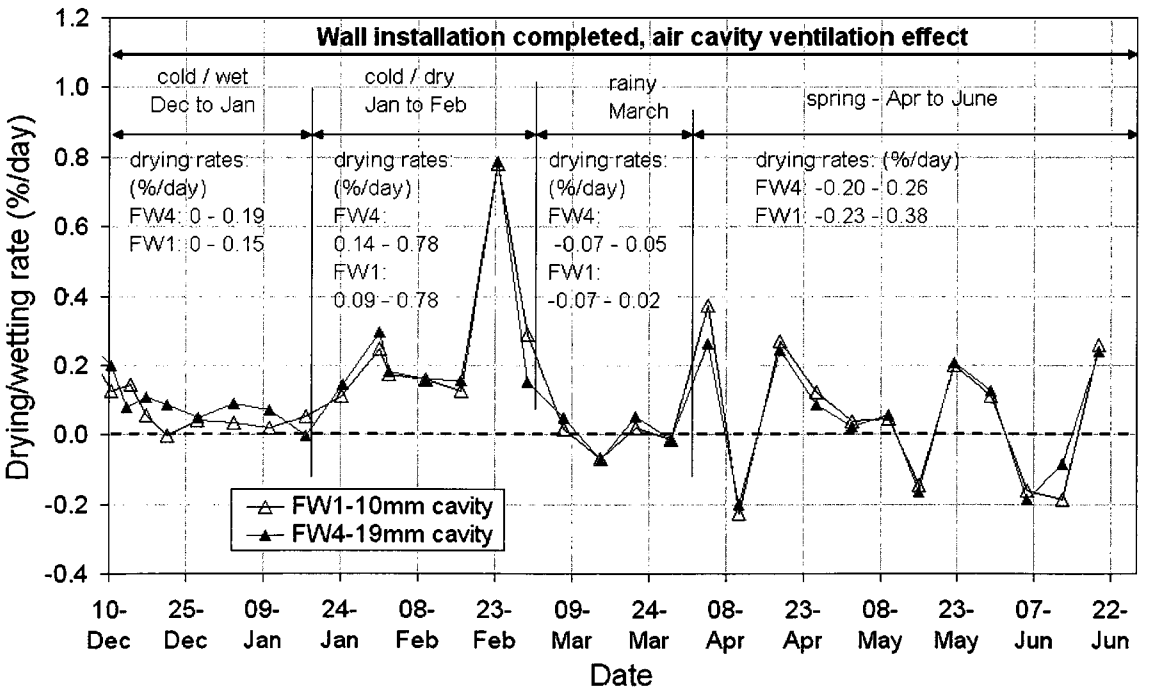

Figure 4-2-13: Average daily wetting and drying rates in plywood sheathing of FW1 and FW4 from Dec, 07 to June, 08.

Once the walls reached similar MC in their equilibrium level, the drying rate of FW1 becomes slightly higher than FW4. However, the differences of the drying rates between two walls are so small and they are insignificant.

4.2.1.3 Resistive moisture-pin measurements

There are two purposes to use moisture-pins for the measurements of plywood sheathing in this experiment. The first is to verify the accuracy of the moisture-pin measurement by comparing to gravimetric measurements. The second purpose is to evaluate moisture content in plywood for the brick walls at upper level of façade since there are no gravimetric samples in these walls due to a more difficult access for the upper level panels at the time of testing.

4.2.1.3.1 Comparison of measurements between gravimetric sample and moisture-pin

The gravimetric measurements of MC in plywood sheathing with low initial MC are compared with the moisture-pin readings, as shown in Figure 4-2-14 and 4-2-15.

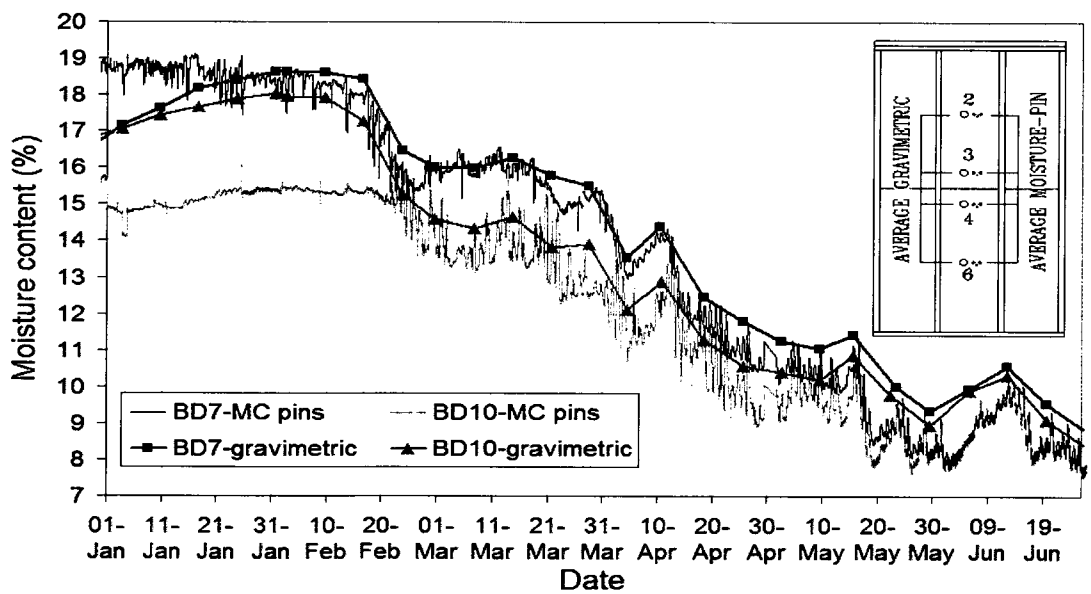

Figure4-2-14: Comparison of average MC in plywood of brick walls BD7 and BD10 with a low initial low MC between gravimetric and moisture-pin measurements.

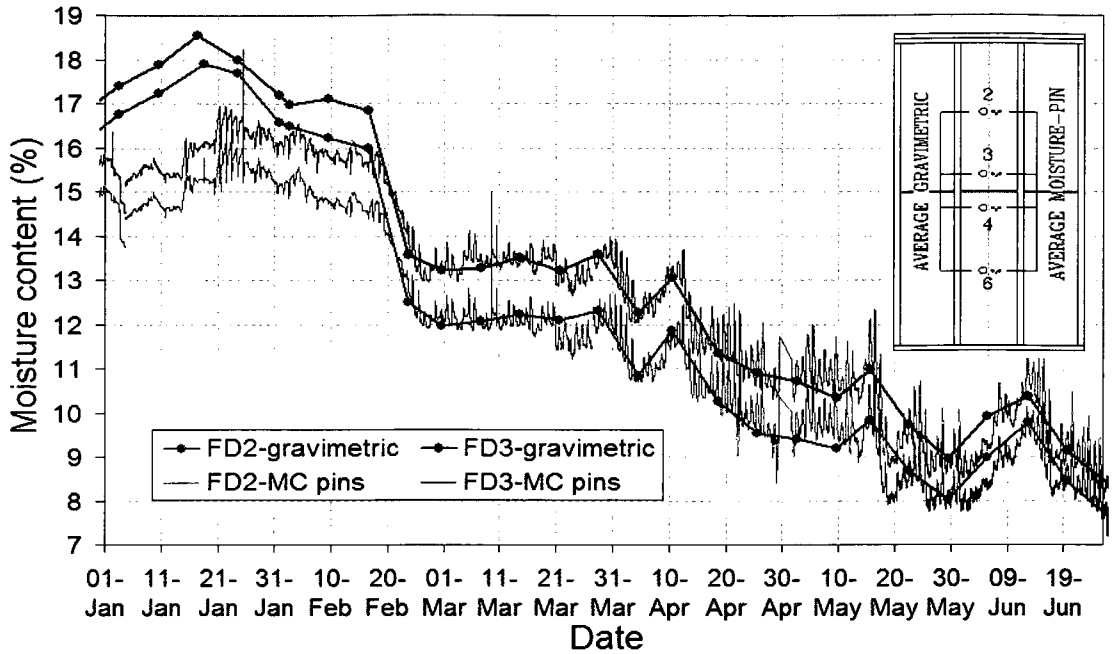

Figure4-2-15: Comparison of average MC in plywood of fibre cement walls FD2 and FD3 with a low initial MC between gravimetric and moisture-pin measurements.

The difference between gravimetric and moisture pin measurements is within 1% for most readings with a maximum difference of 2.5% at the beginning.

With initially wet plywood, the moisture-pin readings are 2-4% lower than the gravimetric measurements when the moisture content level measured by gravimetric is between 22 -18%, as shown in Figure 4-2-16 and Figure 4-2-17. The lower readings of moisture-pins in the high range of MC level indicate that the accuracy of moisture-pin measurement is limited. Laboratory calibration tests showed that the moisture-pins can measure moisture content up to 23% with accuracy of 2% and for the lower range of MC until 6% with a better accuracy of 1% (Horn, 2007). Out of this range the moisture-pin readings are not reliable. The details of the calibration procedure can be found in Appendix 5 "Calibrations and Specifications of Instrumentation".

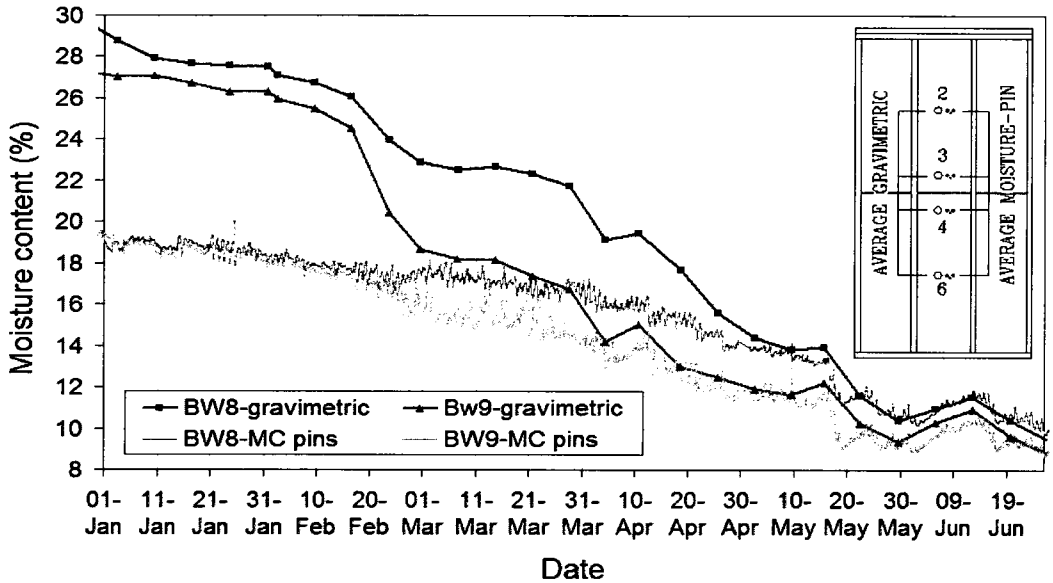

Figure 4-2-16: Comparison of average MC in plywood of brick walls BW8 and BW9 with a high initial MC between gravimetric and moisture-pin measurements.

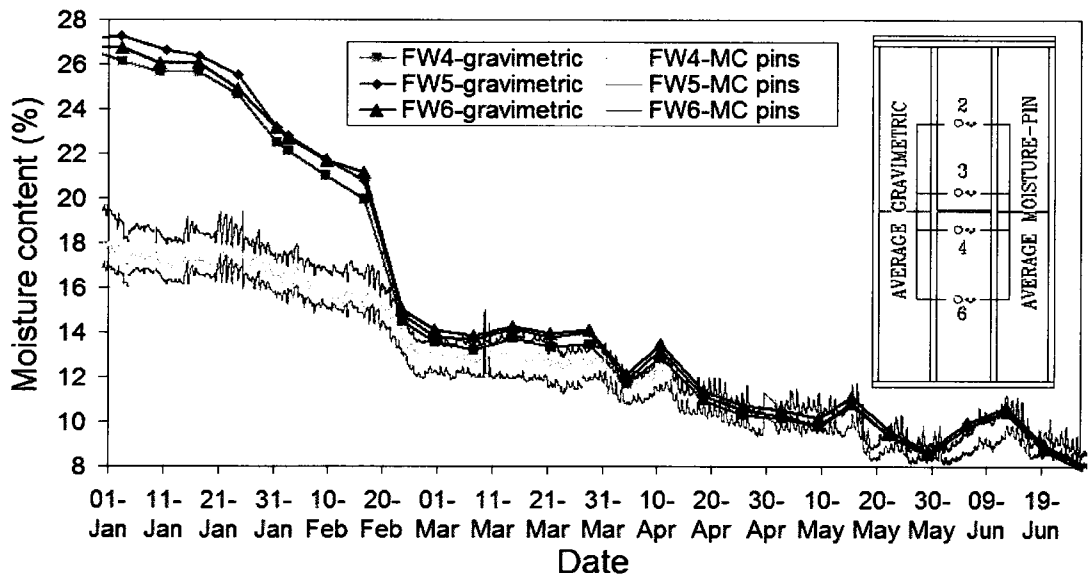

Figure 4-2-17: Comparison of average MC in plywood of fibre cement walls FW4, FW5 and FW6 with a high initial MC between gravimetric and moisture-pin measurements.

The second possible reasons for the discrepancy between moisture-pin and gravimetric readings in the MC level above 20% may include the fact that the initial MC in gravimetric samples were higher than the MC in plywood panels after the wet plywood was assembled into the test walls. The MC in both plywood and gravimetric samples

were similar before the fabrication of the wet walls. During the installation of sensors and fabrication of the wall assembly, moisture in plywood panel re-distributed to the wood fame and diffused to the indoor air of test facility even though careful planning was done to minimize the installation time. At the same time, all the gravimetric samples were sealed inside plastic bags to keep the constant high MC level. Thus, when the gravimetric samples were inserted into the plywood panel, their MC may be higher than the actual MC level of plywood sheathing.

The third possible reason is the actual drying in gravimetric sample is different from that in plywood panel where the moisture-pins were installed. The moisture-pins were installed about 25mm away from the edge of unsealed gravimetric sample holes. Such a short distance could results in two-dimensional drying, drying from wet plywood to air cavity and insulation space and drying within plywood from moisture-pin location to the edge of the gravimetric holes. The edges of gravimetric plywood samples were sealed using construction tape (tuck tape) to ensure a one-dimensional vapour flow, which eliminated the moisture transfer through the edges. This arrangement results in a higher MC in gravimetric samples than that in plywood where moisture-pins were located. To estimate the difference in drying rate between edge-sealed and un-sealed gravimetric samples, a test was set up in the laboratory with constant indoor conditions. The results shows when the moisture content level is within 42-34%, the unsealed samples dried faster on average by 4% per day than the sealed samples. When the MC dropped to within 34-20%, the unsealed samples dried faster on average by 0.49% per day than the sealed samples. The detailed test procedure and results are included in Appendix 5

The difference in drying would be smaller once the samples were installed in place because of the added vapour resistance from other component of the wall assemblies, the tight fit between the sample and the hole and the large vapour pressure differential between indoor and field conditions during the winter season. Once the MC of plywood decreases to the level of 18%, one-dimension vapour diffusion between indoor and outdoor dominates. The difference between both measurements reduces to within 1% with maximum 2% of MC, the same as that in walls with dry plywood sheathing.

4.2.1.3.2 Comparison of MC in plywood affected by vent configurations

As mentioned at the beginning of this section, the brick walls at the upper level of BETF's façade were instrumented with moisture-pins only to measure the MC of plywood. These test walls all started with dry plywood sheathing. Therefore, the readings of moisture-pins can be deemed accurate and used to evaluate the MC in plywood affected by different vent configurations.

Figure 4-2-18 shows the comparison of MC in plywood sheathing of brick walls with four different levels of cavity ventilation. BD7 and BD10 have a two-storey air cavity and BD7U and BD10U refer to the upper portion of BD7 and BD10. BDU11and BDU12 were installed at the upper level of the facility. Both walls have the same bottom vents (six 12x78mm discrete vents) but different top vent configurations, as listed in Table 1 in Chapter 3 "Experiment Design and Setup". BDU11 has six 12x25mm discrete top vents covered with roof flashing while BDU12 has six 12x65mm top vents exposed to the outdoor weather below the flashing.

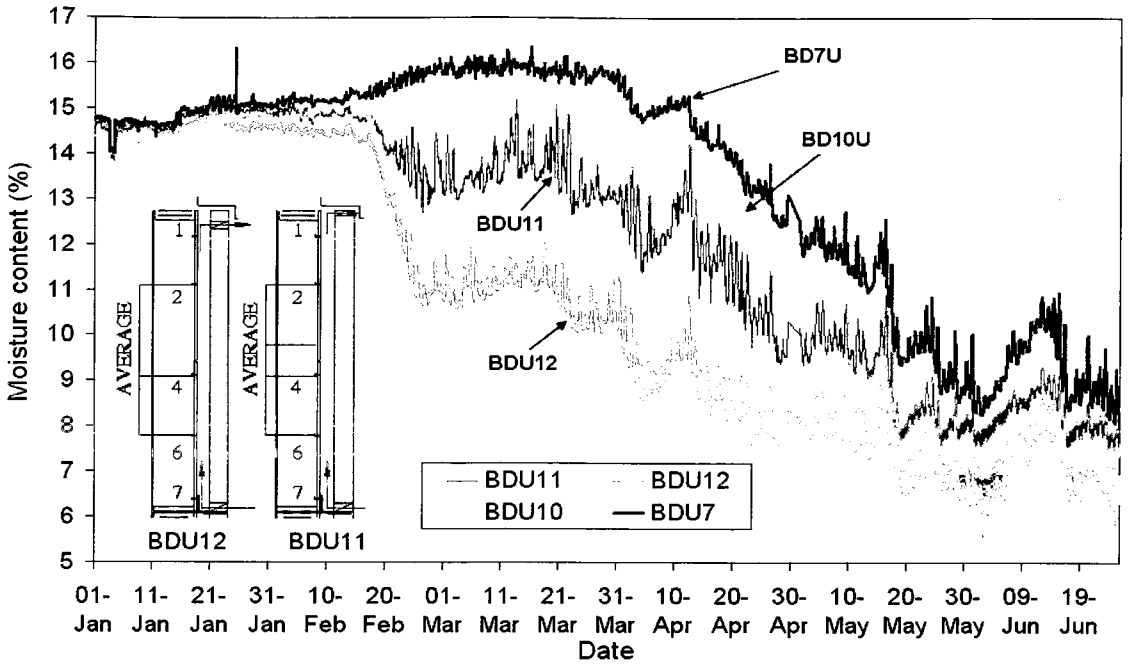

Figure4-2-18: Comparison of average MC in plywood in brick walls with different vent configurations.

All four walls started with a similar initial MC level. Over the test period from December 2007 to June 2008, BDU12 with the largest vent opening had the lowest MC level while BDU7 without top vents had the highest MC level. The maximum difference in MC level was about 5%. BDU10 (two discrete top vents with insect screens) had the second highest MC level. Drying due to cavity ventilation is obvious during the sunny period of February 17-25. The MC of BDU12 dropped by 3.5% and the MC of BDU11 dropped by 2%. It is interesting to note that the MC level in BDU7 increased while the MC level in BDU10 slightly decreased with large fluctuations during this sunny period. The solar radiation effect during this sunny period resulted in the increase of moisture level inside the air cavity. The lack of top vents or the limited size of top vents allows moisture to accumulate at the upper level due to the buoyancy effect. The more pronounced moisture redistribution in two-story air cavities is probably another contributor to their higher moisture level. The differences in MC level among these four

walls became smaller during the warm and less rainy spring and reached 7-9% at the end of June.

4.2.2 Vapour pressure through insulation space and air cavity

The moisture can be moved out of the wall components by vapour diffusion through a wall assembly. On the other hand, moisture can be drawn into the wall components if vapour is trapped in an insulation space and an air cavity. From this perspective, cavity ventilation also influences the vapour pressure distribution through the insulation space and air cavity. Hence, in this section, vapour pressure gradients through wall cavities are evaluated. Vapour pressure differentials between air cavity and outdoor air, with the corresponding MC in plywood, are discussed.

The vapour pressure through wall cavities, within the air cavities and indoor can be calculated using the RH and temperature measured by RH-T sensors. The RH-T sensors were installed in the cavities of all the test walls. Each one-floor high walls with the initial dry sheathing has one RH-T sensors installed above the middle height of air cavity (1.27m about the bottom of the walls). Two RH-T sensors were installed in the air cavity of one-floor high walls with initially wet sheathing and two-floor high dry walls. The lower level RH-T sensor was located at a quarter-height of the walls, 0.6m above the bottom. The upper level RH-T sensor for one-floor high wet walls was at 0.15m below the top. The upper level RH-T sensor for the two-floor high brick walls was placed at a quarter-height (0.6m) from the top of the wall. During the testing, some of the sensors were damaged. The available sensors are listed in Table 4-2-1.

Table 4-2-1: Location of available RH-T sensors in air cavity of test walls

Walls	Sensor positions in air cavities		
	Bottom	Top	Middle
BD7	√	√	
BW8	√	√	
FD3			√
FW1	√	√	
FW5	√		
FD2			√
FW4	√		
FW6	√		
BW9		√	
BD10	√	√	
BDU11			√
BDU12			√

4.2.2.1 Vapour pressure gradient through wall assemblies

1. Brick walls

The average vapour pressure in brick walls are listed in Table 4-2-2 during the winter and spring from January 2 to June 21, 2008. Very little difference is found for two-storey walls in terms of vapour pressures in the insulation spaces and air cavities between vented wall BD7 and ventilated wall BD10. For one-floor high walls, however, BW8 without top vents had higher vapour pressures in both insulation space and air cavity than BW9 for both seasons, probably due to the added initial moisture in plywood. In addition, the average vapour pressure was the highest inside BETF followed by insulation spaces and air cavities, and the outdoor vapour pressure is the lowest for the entire test period for all brick walls except for BW8. The vapour pressure in the air cavity of BW8 was higher than that in insulation space in the spring. Actually the average vapour pressures in both insulation and air cavity were higher than indoor vapour pressure, which indicates the frequent occurrence of inward vapour diffusion.

Table 4-2-2: Average vapour pressure gradients (Pa) through wall cavities for brick walls in the winter, spring and entire test period from Jan. 2 to Jun. 21, 08

	BD7	BD10	BW8U	BW9U	BD7	BD10	BW8U	BW9U	BD7	BD10	BW8U	BW9U
	Entire test period				Winter				Spring			
	Jan 2 to June 21				Jan 2 to Mar 21				Mar 22 to Jun 21			
Indoor	1404				1392				1414			
Insulation	1098	1087	1348	1167	1006	952	1193	1061	1180	1206	**1484**	1259
Air cavity	969	999	1363	1112	944	925	1076	1043	991	1064	**1616**	1173
Outdoor	819				691				929			
Difference between indoor and outdoor	585				701				484			

Note: "U" in the table refers RH-T sensor measurement at upper level.

For example from January 21 - 27, as shown in Figure 4-2-19, the solar radiation during this sunny period helped the evaporation of moisture from plywood and brick veneer and elevated the vapour pressures in air cavity and insulation space for both BW8 and BW9.

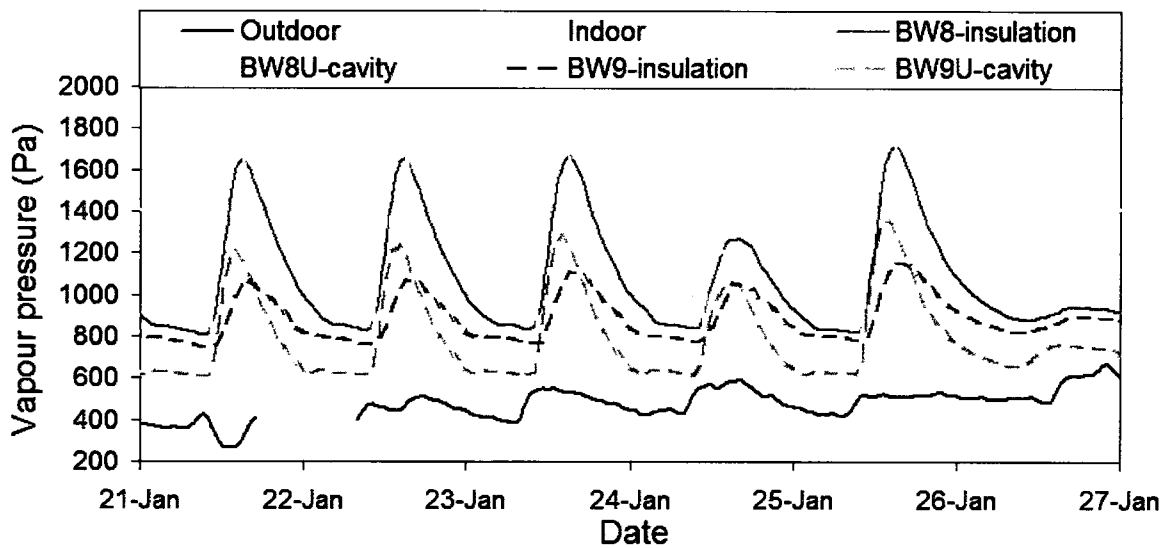

Figure 4-2-19: Comparison of vapour pressures in the air cavity and insulation space between BW8 and BW9 during a period of Jan. 21 – 27, 08.

Without the assistance of cavity ventilation provided by the top vents and with a higher initial MC in plywood, the vapour pressures in the air cavity and insulation space of BW8 elevated much higher than that in BW9, and even higher than the indoor vapour pressure.

During the sunny period in February, the average vapour pressure distribution across test walls BD7 and BD10, with low initial MC, remained the same trend as seasonal trends

i.e. high vapour pressure from inside BETF to outdoor, as shown in Table 4-2-3. However, both BW9 and BW8, with high initial MC, experienced inward vapour diffusion by solar radiation.

Table 4-2-3: Average vapour pressure (Pa) through wall assemblies for brick walls during the sunny period of Feb. 17 - 25, 08

	BD7	BD10	BW8U	BW9U
Indoor	1373			
Insulation	1286	1221	**1593**	**1373**
Cavity	1212	1192	**1583**	**1486**
Outdoor	707			
Difference between indoor and outdoor	666			

Moreover, during the peak solar radiation period all four brick walls experienced inward vapour diffusion from air cavity or probable brick veneer to indoor environment, as shown in Figure 4-2-20 and 4-2-21. It indicates that inward vapour diffusion has a significant influence on the drying of wall components with high moisture load.

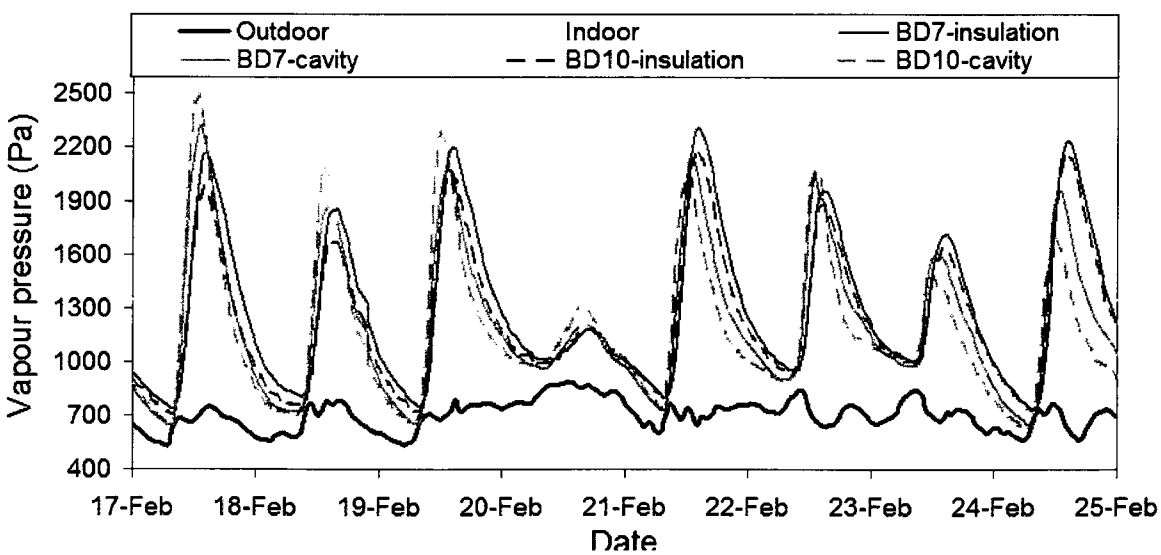

Figure 4-2-20: Vapour pressures of brick test walls, BD7 and BD10, during the sunny period of Feb. 17 – 25, 08.

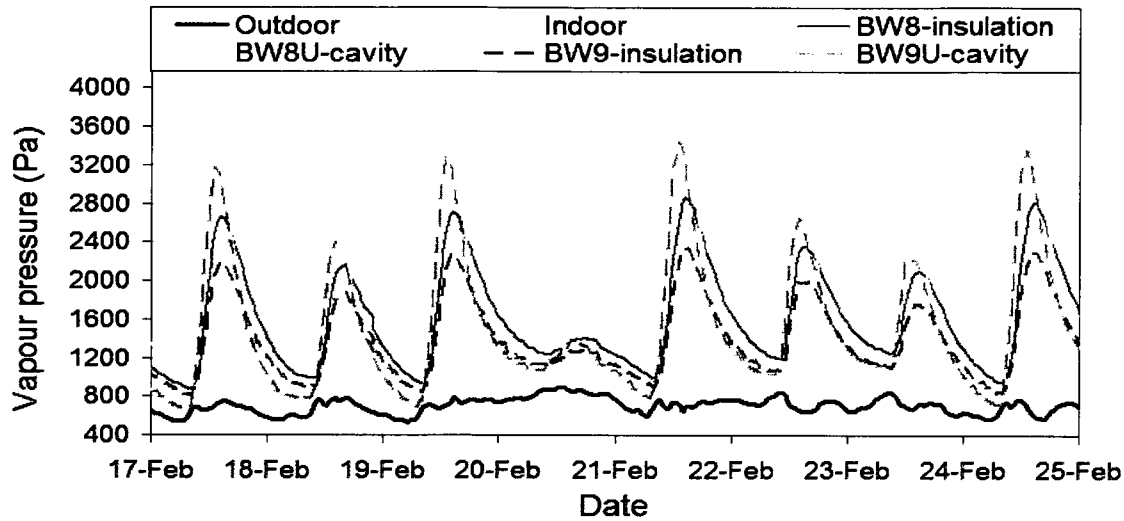

Figure 4-2-21: Vapour pressures of brick test walls, BW8 and BW9, during the sunny period of Feb. 17 – 23, 08, "U" refers at upper level of cavity.

2. Fibre cement walls

The average vapour pressures in the fibre cement walls with a 19mm air cavity are listed in Table 4-2-4 during the winter, spring from January 2 to June 21, 2008. The vapour pressure profiles across all the fibre cement walls are similar. The walls with 12mm top vent (FD3 and FW4) do not show any advantages in reducing vapour pressures in the cavity and insulation. Instead, vapour pressures in the air cavity of FD3 and FW4 are slightly higher than those in FD2 and FW5. It is probably due to the fact that higher cavity ventilation induced by larger top vents brought more moist air into the cavity.

Table 4-2-4: Average vapour pressures (Pa) through wall assemblies for fibre cement walls with 19mm air cavity in the winter, spring and the entire test periods from Jan. 2 to June 21, 08

	FD2	FD3	FW5	FW4	FD2	FD3	FW5	FW4	FD2	FD3	FW5	FW4
	Entire test period				Winter				Spring			
	Jan 2 to June 21				Jan 2 to Mar 21				Mar 22 to Jun 21			
Indoor	1404				1392				1414			
Insulation	1004	1019	1008	944	897	921	913	835	1097	1105	1090	1038
Cavity	765	793	795	809	705	709	729	731	818	867	853	878
Outdoor	819				691				929			
Difference between indoor and outdoor	585				701				484			

Table 4-2-5 shows the comparison of vapour pressures in the insulation spaces and air cavities between FW4 and FW1. Overall, the average vapour pressure in insulation space for FW1 was higher but was similar in the air cavity compared to FW4 with a 19mm air cavity and the same height of top slot vent. The average vapour pressure in the air cavity of FW4 is slightly lower than that in FW1 during the winter but slightly higher during the spring season, which indicates a slightly faster drying during the initial drying period but slightly higher wetting in the spring season due to the higher cavity ventilation rate induced by a wider cavity.

Table 4-2-5: Average vapour pressures (Pa) through wall assemblies for fibre cement walls FW1 and FW4 in the winter, spring and entire test periods from Jan. 2 to Jun. 21, 08

	FW4	FW1	FW4	FW1	FW4	FW1
	Entire test period		Winter		Spring	
	Jan 2 to June 21		Jan 2 to Mar 21		Mar 22 to Jun 21	
cavity depth	19mm	10mm	19mm	10mm	19mm	10mm
Indoor	1404		1392		1414	
Insulation	944	1028	835	947	1038	1100
Cavity	809	792	731	743	878	834
Outdoor	819		691		929	
Difference between indoor and outdoor	585		701		484	

During the sunny period in February, the average vapour gradients for all the fibre cement walls had the same trends as the seasonal average vapour gradients. Little difference is found in the walls with 19mm air cavity. The vapour pressure in the air cavity of FW1 was higher than that in the air cavity of FW4 due to the narrow cavity (Table 4-2-6). The vapour diffusion was mainly outward for all the fibre cement walls.

Table 4-2-6: Average vapour pressures (Pa) through wall assembly for fibre cement walls during the sunny period of Feb 17 - 25, 2008

	FD2	FD3	FW5	FW4	FW1
cavity depth	19mm				10mm
Indoor	1373				
Insulation	1112	1085	1121	1019	1211
Cavity	674	666	691	701	799
Outdoor	707				
Difference between indoor and outdoor	666				

Figure 4-2-22 to Figure 4-2-24 show the comparisons of the peak vapour pressures in the fibre cement walls during the sunny period. The vapour pressure in the air cavity of FD2 was 200 - 500 Pa higher than that in FD3 due to the smaller top vent. With high initial MC in plywood, the peak vapour pressures in the air cavities of FW5 was slightly higher than that of FW4 while the vapour pressure in the insulation space of FW5 was about 200 - 400 Pa higher than that in FW4, indicating ventilation in the cavity with larger top vent carries more moisture out of the wall and has less vapour inward diffusion under the sunny condition. With a narrower air cavity (10mm), the peak vapour pressure in the cavity of FW1 is about 1000 Pa higher at daytime and a maximum of 200 Pa lower at the night than those in FW4.

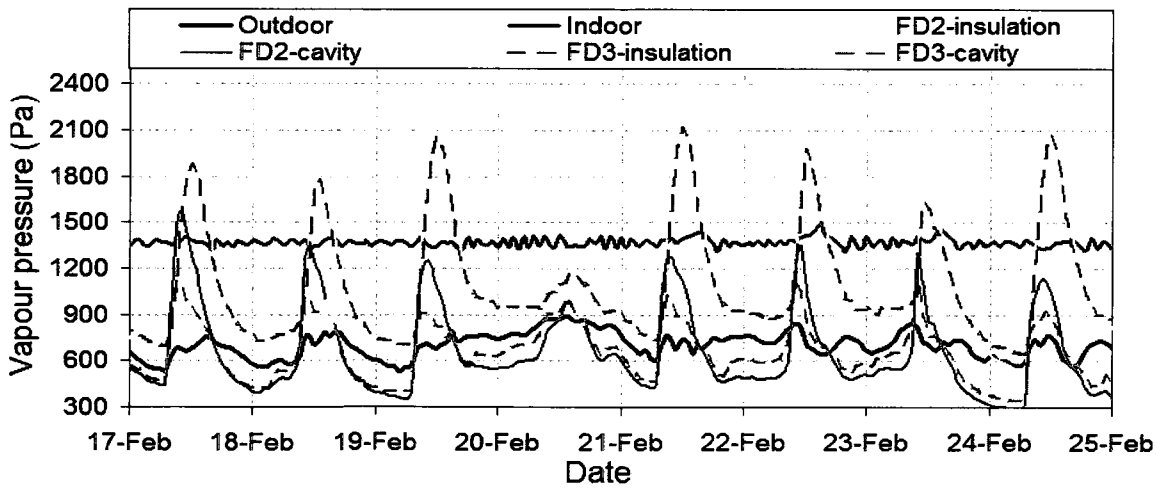

Figure 4-2-22: Vapour pressures of fibre cement walls FD2 and FD3 during the sunny period of Feb.17 – 25, 08.

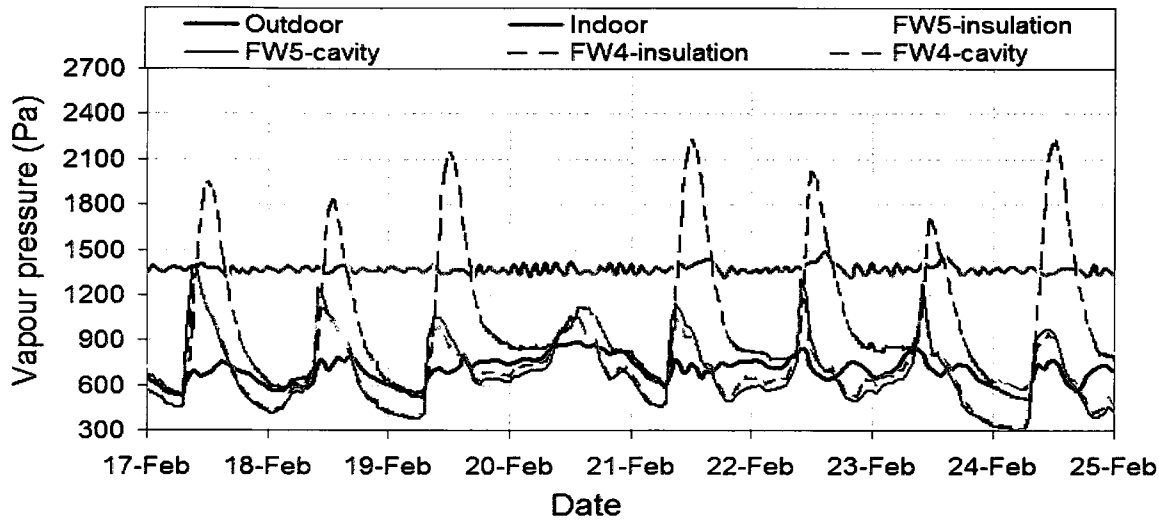

Figure 4-2-23: Vapour pressure gradients of fibre cement walls FW4 and FW5 during the sunny period of Feb. 17 – 25, 08.

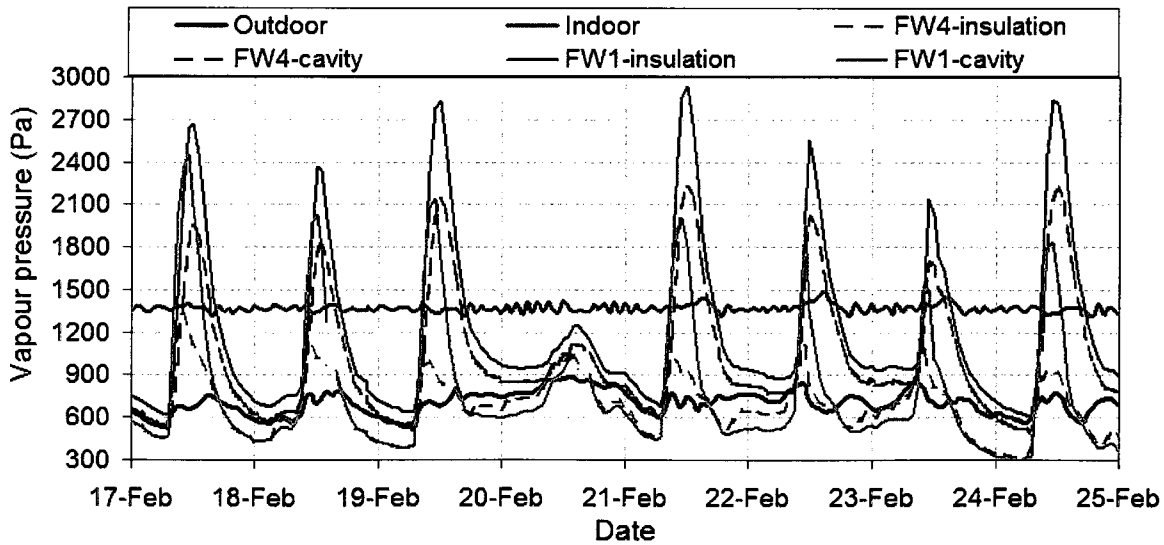

Figure 5-2-24: Vapour pressure gradients of fibre cement walls FW1 (10mm air cavity) and FW4 (19mm air cavity) during the sunny period of Feb. 17 – 23, 08.

In addition, the vapour pressure in the insulation space of FW1 is also about a maximum of 800 Pa higher than that in FW4, indicating that test wall with a narrower cavity depth carries less moisture out of the cavity and has more inward vapour diffusion under sunny conditions.

4.2.2.2 Vapour pressure differentials between outdoor air and air cavity

If vapour pressure in the air cavity is higher than the outdoor vapour pressure, i.e. outdoor air is dryer than that in the cavity, and the inflow of outdoor air will mix with the cavity air to remove moisture from the cavity. If it is reversed, the moist outdoor air will bring moisture from outside and may cause wetting on the cavity surfaces of sheathing and cladding.

Vapour pressure differential between the cavity and ambient air can clearly indicate the potential for cavity drying and wetting. In the following figures, zero means that the vapour pressure in the air cavity equals to the vapour pressure of outdoor air. A positive value denotes that the vapour pressure in the cavity is higher than that of the ambient air while a negative value denotes vapour pressure in the cavity is lower than vapour pressure of the ambient air.

The results indicate that vapour pressure differentials were mostly positive in winter for all the test walls and while varied in spring depending on the cladding types, widths of the cavities, vent configurations and initial MC of sheathing. Once the test walls reached the equilibrium MC levels, negative values were dominant, indicating that the cavity vapour pressure is lower than the outdoor vapour pressure, i.e. cavity is drier than outdoor environment.

For example during the test period of December 22, 2007 to June 21, 2008, brick walls of BD7 and BD10 with two-storey cavity and initial low MC in plywood have positive vapour pressure differential mostly between the upper part of cavity and outdoor air from the beginning of the test to the end of May, 2008 (Figure 4-2-25). Then the negative

vapour pressure differentials occur frequently in May and June after MC of the wall components reached their equilibrium levels.

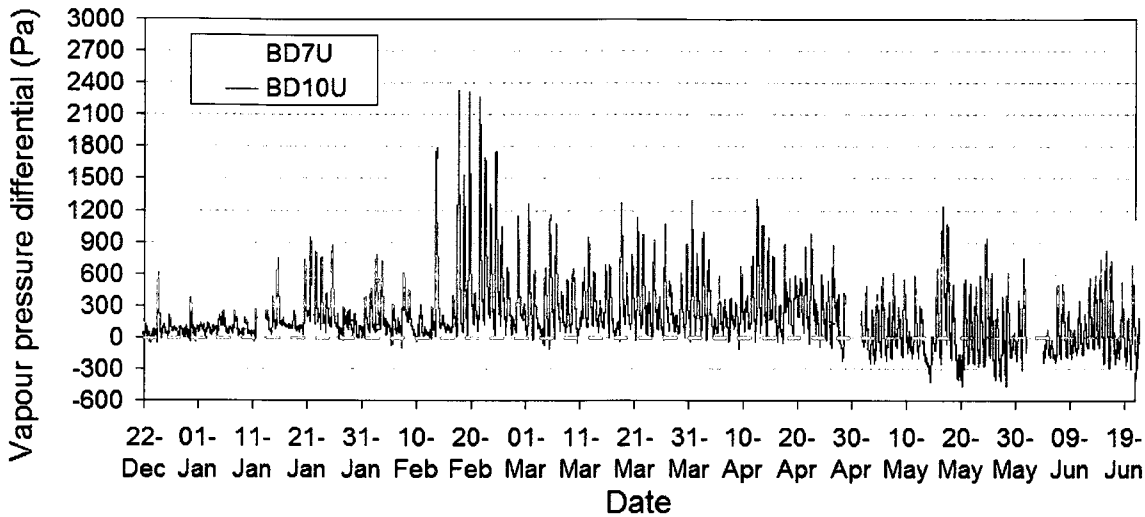

Figure 4-2-25: Vapour pressure differentials between outdoor air and the air cavity in test walls BD7 and BD10 from Dec. 22 to Jun. 21, 08 ("U" refers at the upper level of cavity).

With one-storey high cavity, the vapour pressure differentials between the upper part of cavity and outdoor air for BW9 had similar trends to those of BD7 and BD10, although the initial MC in plywood is higher, as shown in Figure 4-2-26. It is because the shorter air cavity with top vents in BW9 allows faster air change removing more moisture from the air cavity. However, for BW8 with high initial MC in plywood and without top vents, the positive vapour pressure differentials between air cavity and outdoor air remained for a longer period, until the end of May, which was one month later than that of BW9.

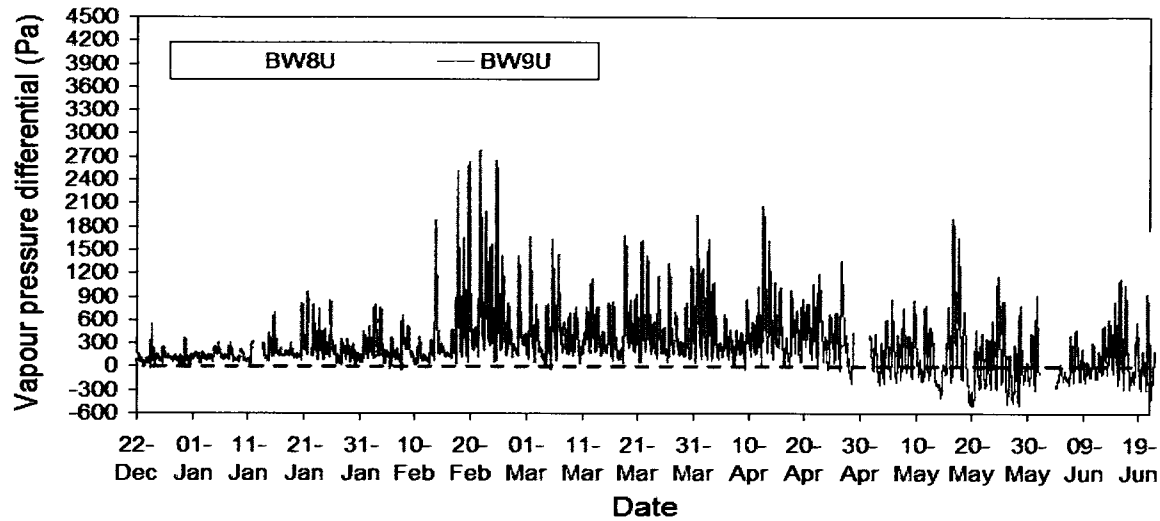

Figure 4-2-26: Vapour pressure differentials between outdoor air and the air cavity in test walls BW8 and BW9 from Dec. 22 to Jun. 21, 08 ("U" refers at the upper level of cavity).

Ventilation reduces vapour pressure in the cavity. The maximum vapour pressure differential between outdoor air and air cavity in one-floor high wall BW8 is 800 Pa higher than that in BW9 while the maximum vapour pressure differential in two-floor high cavity BD7 is 1800 Pa higher than that in BD10.

For the fibre cement walls, the negative vapour pressure differentials occurred frequently from the first continuous sunny period of January 20 -26, two months earlier than the brick walls due to larger vent areas at both top and bottom and a much smaller moisture storage capacity in fibre cement cladding. For example, Figure 4-2-27 shows the vapour pressure differentials at the lower part of cavity in FW5 and FW4 with a 19mm air cavity and high initial MC load in plywood. Figure 4-2-28 shows the vapour pressure differentials in FW1 and FW4 with different cavity depths. During and after the second sunny period in February, the negative vapour pressure differential values were getting more frequent and larger with time, indicating the cavities were getting drier than the outdoor environment.

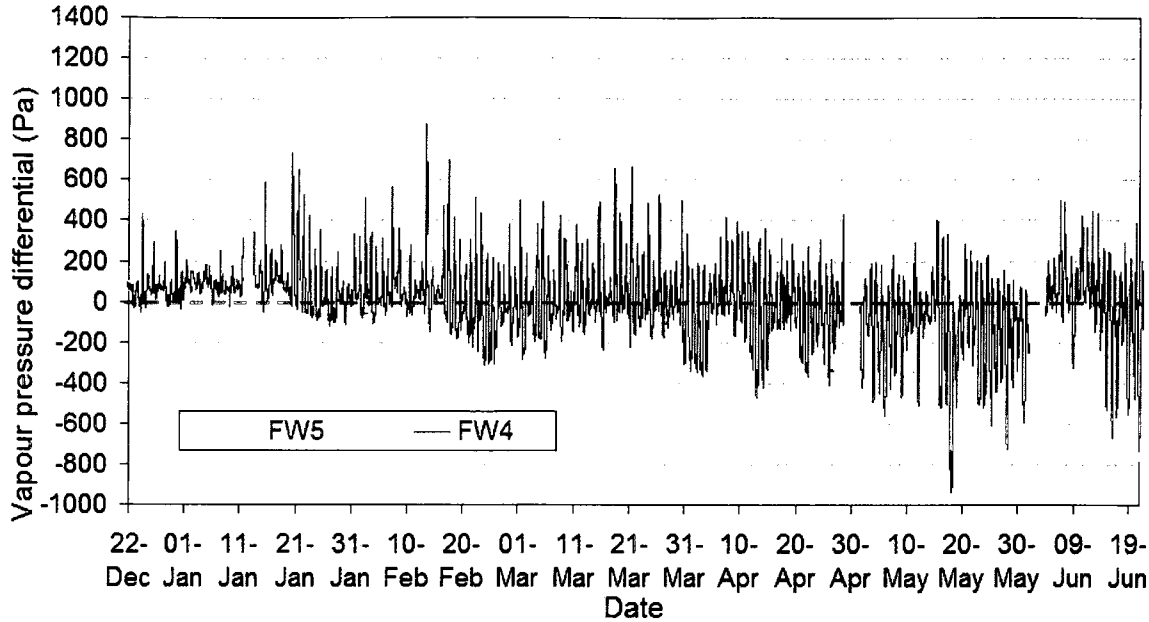

Figure 4-2-27: Vapour pressure differentials between outdoor air and the air cavity in test walls FW5 and FW4 from Dec. 22, 07 to Jun. 21, 08.

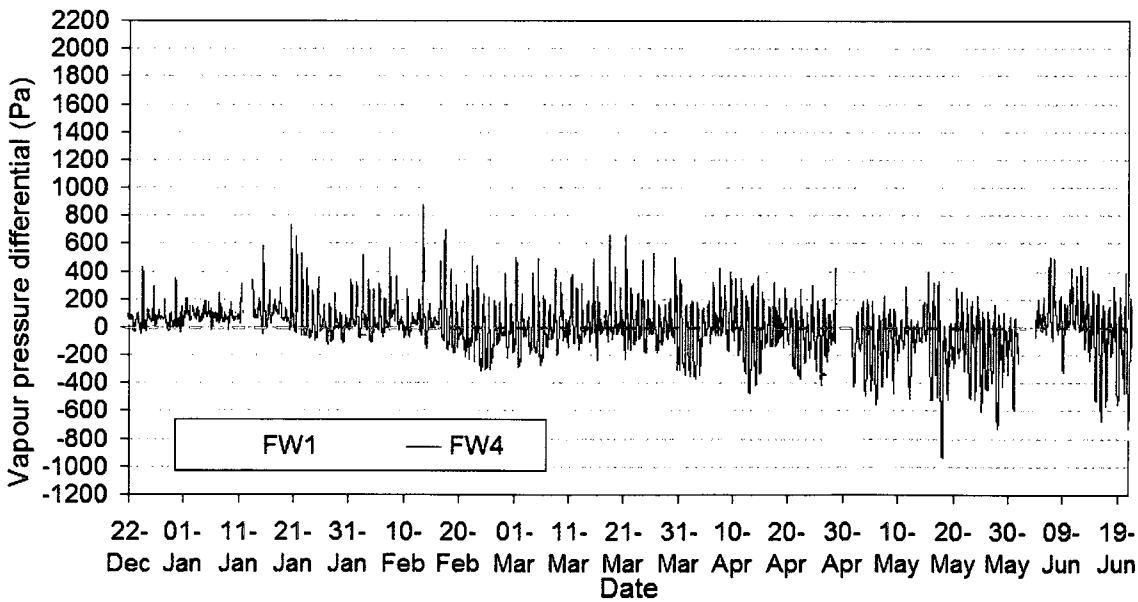

Figure 4-2-28: Vapour pressure differentials between outdoor air and the air cavity in test walls FW1 and FW4 from Dec. 22, 07 to Jun. 21, 08.

The vapour pressure differentials in FW5 and FW4 were similar for the negative values while the positive values of FW5 were slightly higher than those of FW4. FW1 had much larger positive values and slightly larger negative values of vapour pressure

differentials compared to FW4. It indicates again that cavity depth has significant influence on the cavity vapour pressure which is another indicator of drying and wetting affected by ventilation.

The average monthly vapour pressure differentials for both brick walls and fibre cement walls are calculated. For all the brick walls at upper part of cavities, the vapour pressure differentials between air cavity and outdoor air were positive which means that the cavities were still wetter than the outdoor environment except for BDU12 during the entire test period (Figure 4-2-29). BDU12 had negative average vapour pressure differentials from May to June, indicating the cavity was drier than outdoor and may have potential for ventilation wetting.

For the dry fibre cement walls of FD2 and FD3, except in January, the average monthly vapour pressure differential between cavity and outdoor air was negative throughout the entire test period, as shown in Figure 4-2-30. For the wet fibre cement walls of FW1, FW4 and FW5, the average vapour pressure differentials started to be negative from April to the end of spring. In March, the average cavity vapour pressures for all the fibre cement walls were almost equal to the outdoor air cavity vapour pressure. Starting from the beginning of spring, the average vapour pressure differential was negative ranging from -40 to -230 Pa for all the fibre cement walls. It is an indication again that the cavity ventilation can potentially bring in moisture into the cavity and wet cladding and plywood sheathing in the spring season.

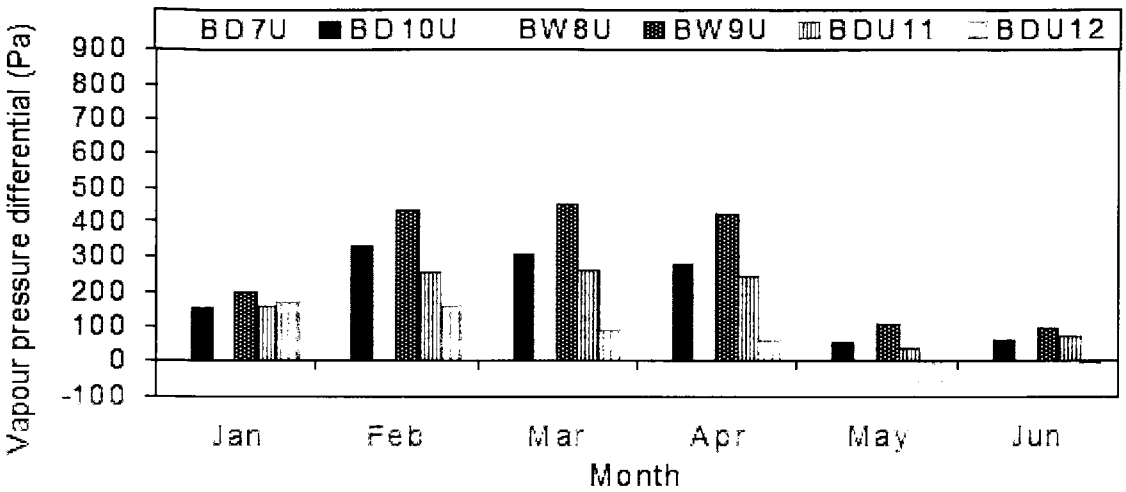

Figure 4-2-29: Average monthly vapour pressure differentials between outdoor air and the air cavity for all six brick walls from Jan. to June, 08.

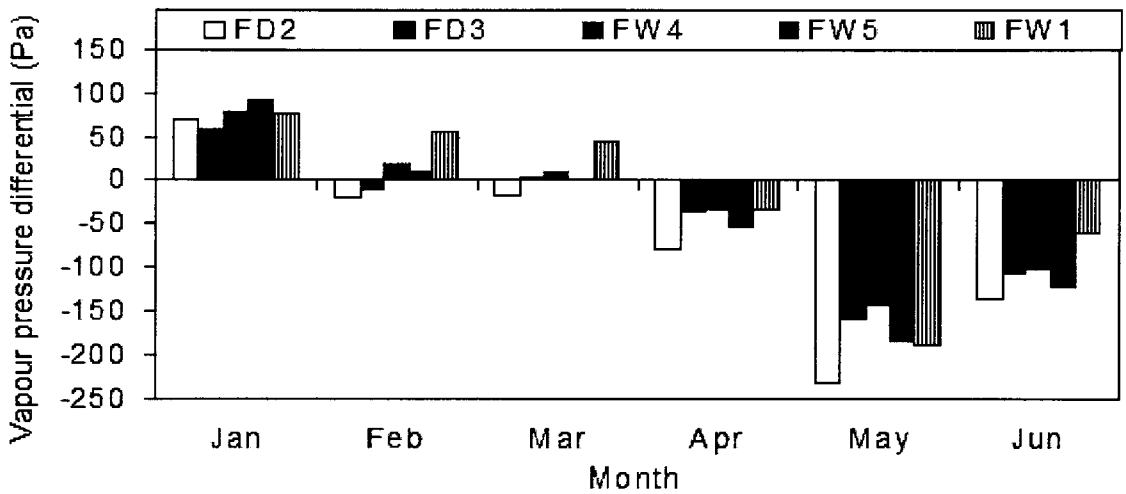

Figure 4-2-30: Average monthly vapour pressure differentials between outdoor air and the air cavity for all five fibre cement walls from Jan. to June, 08.

4.3 Summary

Generally, the average outdoor temperature at BETF' site approximately doubled every two months. In contrast, the average RH slowly reduced from December to April and then stayed at the similar level to June. The prevailing wind direction was from ESE

during in the test period. Wind speed had a wide range from less than 0.5 to 10 m/s. The low wind speed within 2 m/s had the highest frequency of 83 -88% through the entire test period. WDR is strongly influenced by wind direction and wind speed. The SE façade of BETF, where the test walls were installed, received the highest amount of WDR. Solar radiation increased gradually and the hourly maximum value was 3 -5 times higher the average value. During the continuous sunny periods, the peak solar radiation is not only high but also last for a longer time period on the daily basis. The indoor temperature and RH of BETF were kept uniform and constant during the test duration.

The change of MC of plywood sheathing is used as the indicator to evaluate the drying and wetting affected by cavity ventilation. The MC of all the dry test walls was below 19% during the wetting season. All the wet walls managed to dry to below 19% MC in about 70 days for fibre cement walls and 80 days for the brick wall with top vents. The brick wall without top vent took above four months to dry to 19% MC level. The prolonged period of high MC in plywood in brick walls poses risks for mold growth. High solar radiation in the continuous sunny periods had an extremely important influence on the drying of wet walls in the winter.

The significance of cavity ventilation drying depends on the type of vents, cavity depth, moisture loads, and weather conditions. The effect of cavity ventilation drying in brick walls is more significant than fibre cement panel walls. Ventilation helps drying the wet plywood sheathing even with small top vents. For the dry brick walls, the larger vent configuration has the large drying effect. The brick wall without top vents mainly relies on both inward and outward vapour diffusion with aid of evaporations by strong solar radiation during sunny days. Fibre cement panel walls with a 19mm deep cavity dried

slightly faster than the test wall with a 10mm deep cavity; however, the size of top slot vents does not make much difference. After reaching their equilibrium MC levels, the test walls with higher ventilation rates show slightly higher moisture levels in plywood due to potential wetting by ventilation.

In general, the MC at the exterior edge of a stud and at the bottom plate near plywood sheathing is higher than that in the middle thickness of stud and bottom plate in all the brick walls and fibre cement walls.

Cavity vapour pressure is the second indicator for assessing the drying and wetting of rainscreen walls by cavity ventilation. Ventilation reduces vapour pressure in the cavity. For fibre cement walls, once they reached their equilibrium MC in February, the cavity vapour pressures were frequently lower than the outdoor vapour pressure, i.e. cavity was drier than outdoor. Starting from the beginning of spring, the cavity with larger top vents is wetter than the cavity with a smaller top vent. The cavity with wider space is wetter than the cavity with smaller space due to cavity ventilation induced wetting. The monthly average vapour pressure differentials show that the cavity air was still wetter than the outdoor environment for all brick walls except BDU12 during the entire test period. BDU12 had lower average vapour pressure differentials in the cavity than that of the ambient air from May to June, indicating the cavity air is drier than the outdoor air due to a much larger vent area, and the cavity may have potential for ventilation wetting.

Chapter 5: Thermal Performance of Test Wall

Straube and Burnett (1998a) stated from field measurements that natural ventilation does not cool down the wall temperatures since heat capacity of air is so small that little heat can be moved out from air cavity. In this section, the average temperature gradients through the test wall assemblies are compared to verify the ventilation effect for thermal performance of rainscreen walls using field measurement. Under-cooling effects on the temperature of cavity-surfaces, i.e. exterior surface of plywood sheathing and interior surface of brick and fibre cement cladding, are analyzed. The numbers of hours per day when condensation occurs on the cavity-surface of claddings for all test walls are calculated.

5.1 Average temperature gradients through wall assemblies

1. Brick walls

The average temperature gradients in the middle of brick walls are listed in Table 5-1-1 from December 22 2007 to June 21, 2008. The test walls had different temperatures at the surfaces of gypsum and exterior surface of brick. The reasons for the differences on surface temperatures may mainly be caused by the periodic shadow of trees on the walls in the winter. Initial MC in plywood and the cavity ventilation using different vent configurations may have an impact on the temperature gradient, i.e. temperature of the wet sheathing may be lower than that of the dry sheathing and ventilation may reduce

solar radiated heat on the surface of brick veneer. Further study is needed to determine the exact causes for the difference in temperature among test walls.

Table 5-1-1: Average temperature gradient (°C) through wall components for all brick walls from Dec. 21, 07 to June 21, 08

	BD7	BD10	BD8	BD9	BDU11	BDU12
Gypsum-exterior surface	20.5	20.5	21.1	**19.9**	20.8	21.4
Insulation-centre	17.4	16.1	16.9	**16.0**	16.0	17.4
Plywood –cavity-surface	12.3	12.0	13.3	**12.2**	11.8	12.0
Brick-cavity-surface	11.4	11.0	11.8	**10.8**	10.8	11.3
Brick-exterior surface	10.9	10.6	11.2	**10.3**	10.6	11.0

The measurements show that a difference of 0.3 – 0.7°C existed in the temperatures of the same wall components between the dry walls; two-floor high ventilated wall BD10 and vented wall BD7, and between two one-floor high ventilated brick walls, BDU11 and BD12 installed at the upper level of the BETF's façade. The analysis shows that vent configuration does not have much influence on temperature decrease through the wall components in the heating seasons when the plywood sheathing is initially dry. For wall BW9 with an initially high MC in plywood sheathing, the temperature on all components were about 1°C lower than that in BW8 which was also with high initial MC. The combination of ventilation and the shade of a tree periodically on the surface of BW9 may have significantly reduced the temperature through the wall assembly.

During the sunny period in February, the maximum temperature through the ventilated walls BD10 and BW9 were 1 – 5 °C lower than those of BD7 and BW8 with vented cavities during the peak solar hours, as shown in Figure 5-1-1. The potential inward heat flow in the sunny period due to higher exterior surface temperature than the indoor temperature in walls BW8 and BD7 is beneficial in the winter and early spring but may heat up the indoor environment from late spring to early fall.

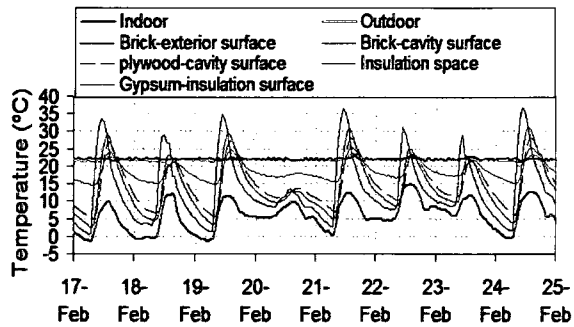

a) BW8: one-floor high brick wall without top vents

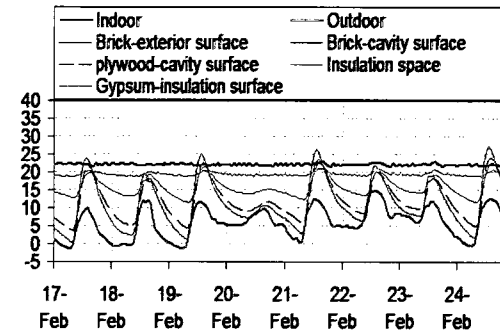

b) BW9: one-floor high brick wall with top vents

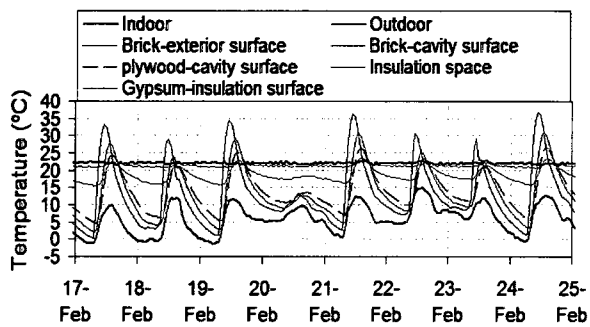

c) BD7: two-floor high brick wall without top vents

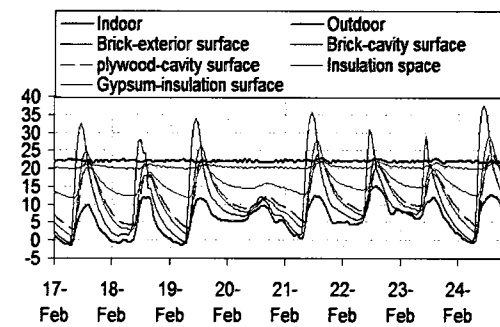

d) BD10: two-floor high brick wall with top vents

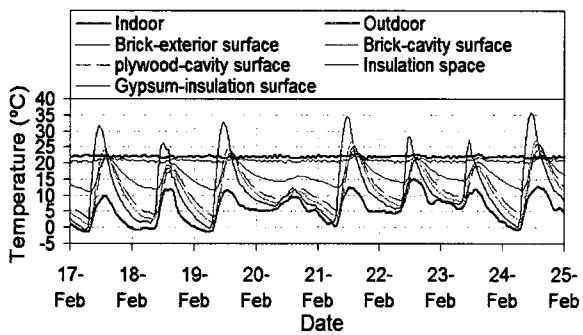

e) BDU11: one-floor high brick wall with 6 discrete vents on top (25mm) and bottom (78mm)

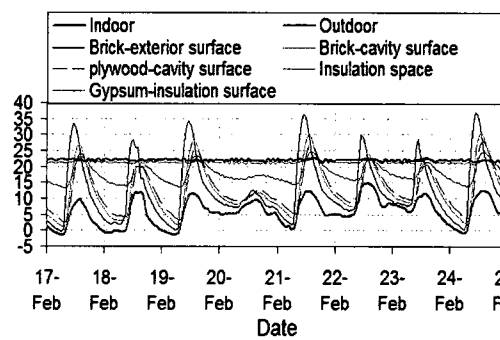

f) BDU12: one-floor high brick wall with 6 discrete vents on top (65mm) and bottom (78mm)

Figure 5-1-1: Temperature profiles of six brick test walls during the sunny period of 17 – 23 in Feb. 08. (temperature on exterior surface of BW9 missing due to disconnection of the thermocouple between walls and terminal strip).

The variation in vent areas does not make much difference on the temperature gradients between BDU11 and BDU12, walls with relatively larger vents at both bottom and top. However, the locations of the test walls may have influence on the temperature profiles

across the wall assemblies. At locations close to the east corner, the temperatures of wall components in BDU12 (with biggest top vent area) were higher than that in BDU11, a similar trend as in BD7 and BD8 compared to B10 and BW9 test walls located at the south corner. Again, the periodic shading from trees located to the south west side of the facility may have contributed to the difference. These trees were removed in May 2008. On cloudy, rainy days and when the weather becomes warmer in the spring, the thermal responses of all the brick walls become very similar. Cavity ventilation provided by discrete vents for brick walls does not seem to have much impact on the cavity temperatures of rainscreen walls, as shown in Figure 5-1-2.

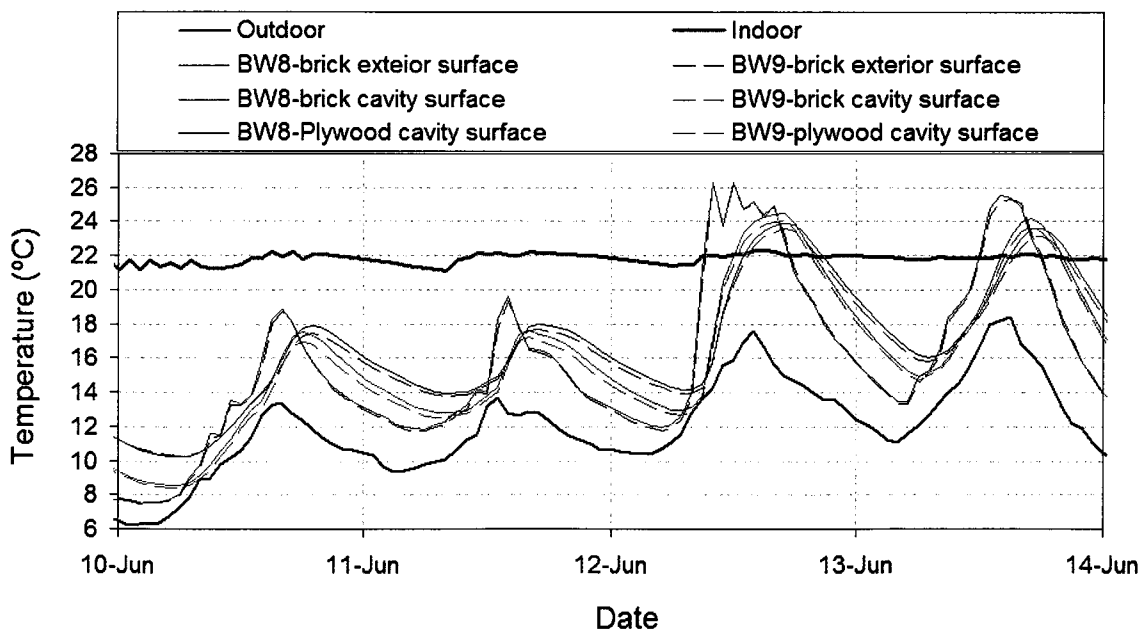

Figure 5-1-2: Cavity-surface temperatures of BW8 and BW9 in June, 08.

2. Fibre cement walls

The average temperature on each component of the six fibre cement walls are listed in Table 5-1-2. Very little difference is shown in the temperature of wall components between ventilated walls with different vent configurations, indicating vent

configurations do not have much impact on the temperatures through the wall assemblies in these periods.

Table 5-1-2: Average temperature gradient (°C) through wall components for all fibre cement walls from Dec. 21, 2007 to Jun. 21, 08

	FD2	FD3	FW1	FW4	FW5	FW6
Gypsum-exterior surface	20.6	20.1	20.2	19.9	20.4	20.0
Insulation-centre	16.1	15.1	14.2	12.8	14.7	14.7
Plywood-cavity-surface	11.5	11.3	10.4	10.3	11.1	9.7
Fibre cement-cavity-surface	9.5	8.9	9.1	8.6	9.2	8.8
Fibre cement-exterior surface	9.7	9.1	9.4	9.1	9.7	8.9

On cloudy and rainy days, the temperatures on the components of all the fibre cement walls were similar and lower than the temperature inside BETF as shown in Figure 5-1-3 and Figure 5-1-4.

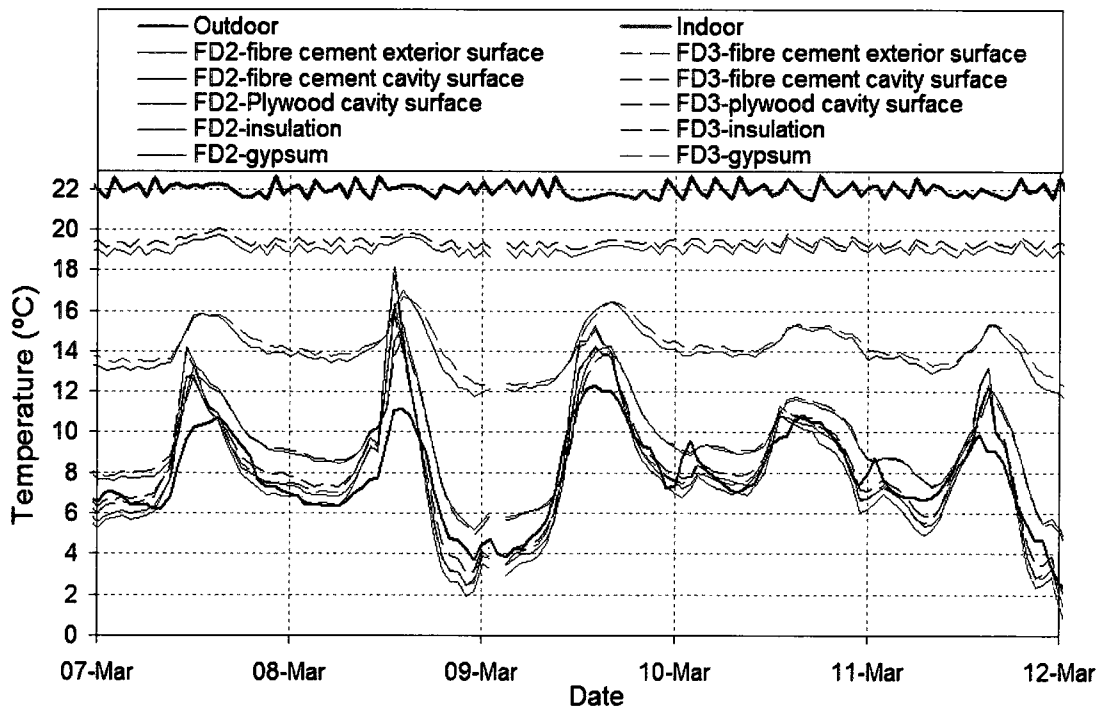

Figure 5-1-3: Comparison of temperature gradients between FD2 and FD3 on cloudy and rainy days in Mar, 08.

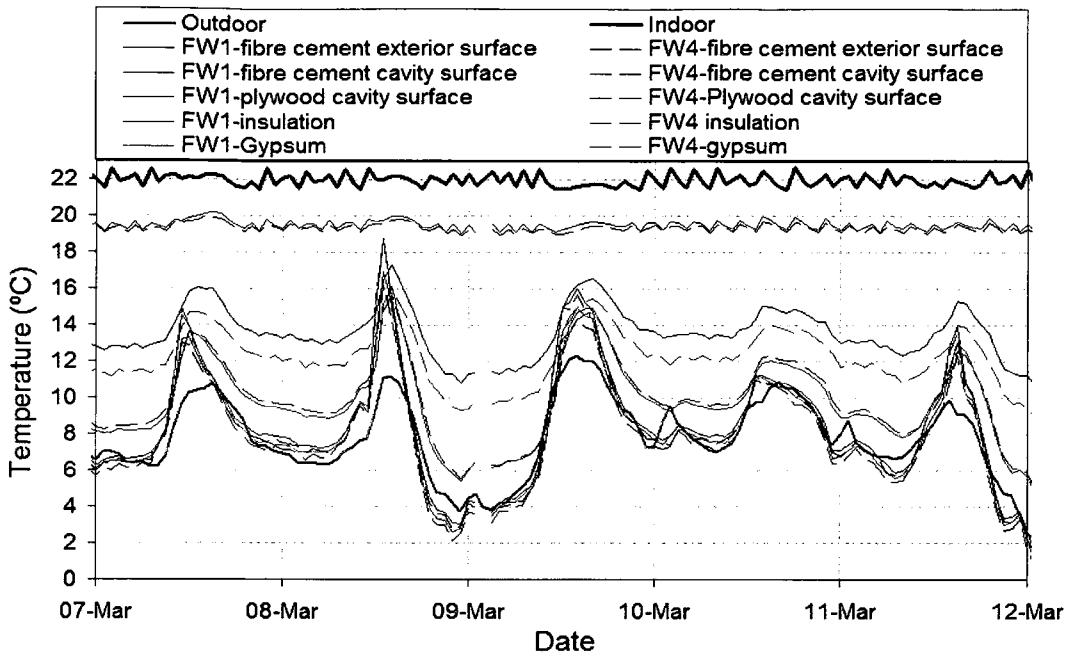

Figure 5-1-4: Comparison of temperature gradients between FW1 (10mm cavity) and FW4 (19mm cavity) on cloudy and rainy days of Mar. 08.

However, during the sunny period in February, an inward heat flow existed during the daytime when the sun came out, as shown in Figure 5-1-5. The maximum temperature of wall assemblies through FD3 and FW4 with larger top vents (12mm) were 2 - 3 °C lower than those of FD2 and FW5 with smaller top vents (1mm) during the peak solar hours. The maximum temperatures of all the components for all the fibre cement walls were higher than indoor temperature at the peak solar hours except for the interior surface temperature of gypsum board. For the walls with the smallest top vents, the surface temperatures of gypsums were very close to the indoor temperature while the walls with larger top vents, the surface temperatures of gypsums were about 2 - 3 °C lower than the indoor temperature, indicating that less venting results in more heat gain. With the 10mm air cavity, the maximum temperature of each wall component is 2 – 3 °C higher than that of FW4 (19mm air cavity) except for the exterior surface temperature of fibre cement

cladding and gypsum board. The temperatures for these components were similar for both walls.

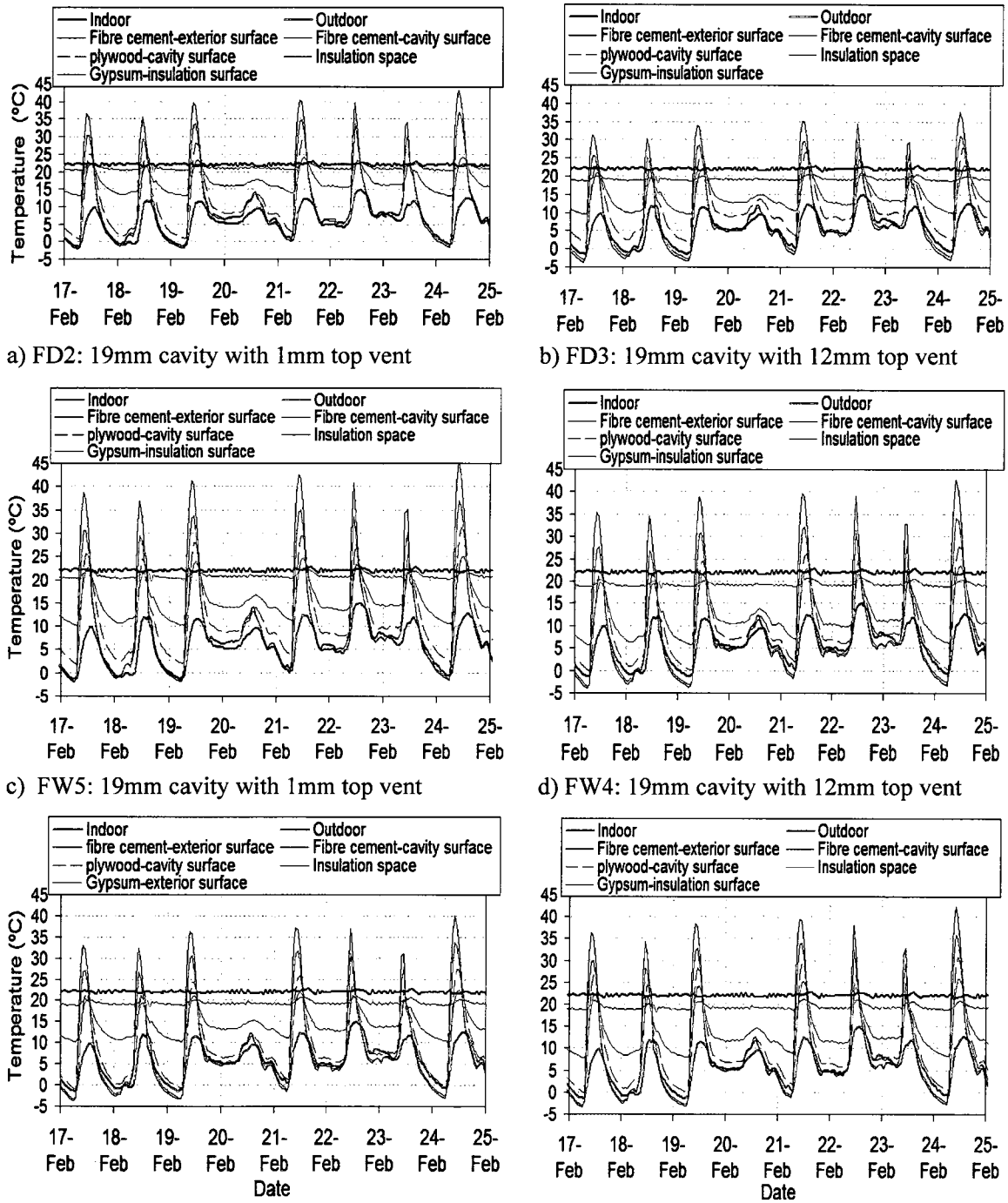

Figure 5-1-5: Temperatures through wall assembly for six fibre cement test walls during the sunny period of 17 – 23 in Feb. 08.

5.2 Temperature difference between air cavity and ambient air

Air temperatures and RH in the air cavities are monitored using RH-T sensors in the cavities of all the test walls as described in the previous section 4.2.2. "Vapour pressure through insulation space and air cavity". The temperature difference between air cavities and ambient air obtained is the difference of air temperature in the air cavities and weather station placed on BETF's roof. Positive values in the figures denote a higher cavity air temperature than the ambient air temperature.

The monthly average and maximum temperature differences at daytime and night-time between cavity and ambient air for the brick walls, using the 10-minute average data, are analyzed and shown in Figure 5-2-1. The average temperature differences between air cavity and outdoor air increased every month until May due to more sunny days and the large thermal mass storage capacity of brick veneer. The ranges of temperature differences between air cavity and ambient air were 2 – 3.5°C in the late December and January, 4 – 5.6°C from February to March, around 6.5 – 7°C in April. The temperature differences decreased in May and June due to the decrease of ambient air temperature difference between daytimes and nights; the range is 5.2 – 6.3°C. With low initial MC in plywood sheathing, the temperature difference in the two-storey high vented wall (BD7) was greater than that in ventilated wall (BD10). The one-storey high walls with small top vents (BDU11) had slightly higher temperature differences than the wall with larger top vents (BDU12) although the differences between the walls are small within 0.2 – 0.6°C. However, temperature differences between the walls with high initial MC in plywood,

BW8 without top vents and BW9 with top vents, were the same in each month through the entire test period.

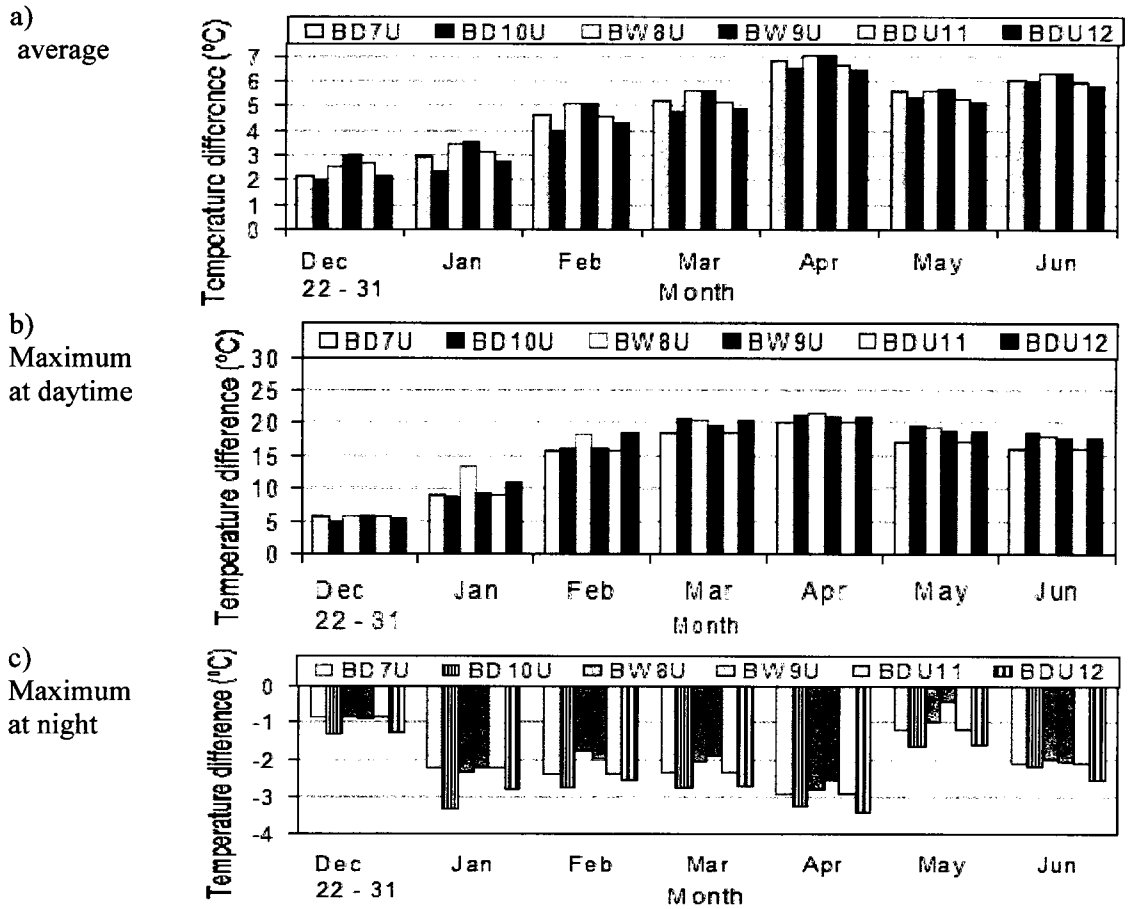

Figure 5-2-1: Monthly average and maximum temperature difference between cavity and ambient air in brick walls from late Dec. 07 to June, 08.

The monthly maximum temperature differences between cavity and ambient air in late December were the lowest and similar for all the brick walls. The ranges were about 4.9 - 5.7 °C at daytime and -0.8 - -1.3°C at night. In the sunny period of February, the maximum temperature differences were higher than January but lower than those in March, within 15.8 – 18.6°C at daytime. The maximum temperature differences between cavity and ambient air at the daytime in March and April were greatest and almost the same, in the range of 18.6 – 21.4°C. The maximum temperature differences at nights

from January to April were similar but became slightly smaller in June. The range was -1.8 - -3.4°C from January to June, except in May. The maximum temperature differences at the nights for all the brick walls in May became very small and similar to those in the late December. The range was -0.4 - -1.7 °C.

Figure 5-2-2 shows the monthly average and maximum temperature differences between air cavity and ambient air at daytime and night for all the fibre cement walls. All the fibre cement walls have lower average temperature differences than those of the brick walls. The difference between fibre cement walls and brick walls were 1.5 – 1.8°C in the winter and 1.7 – 2.5°C in the spring.

a) Average

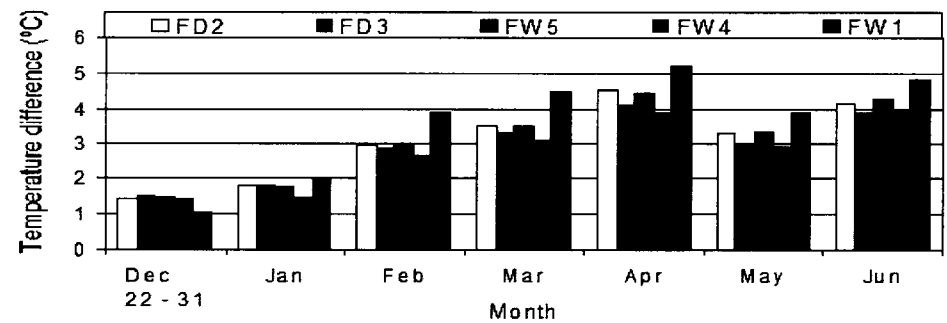

b) Maximum at daytime

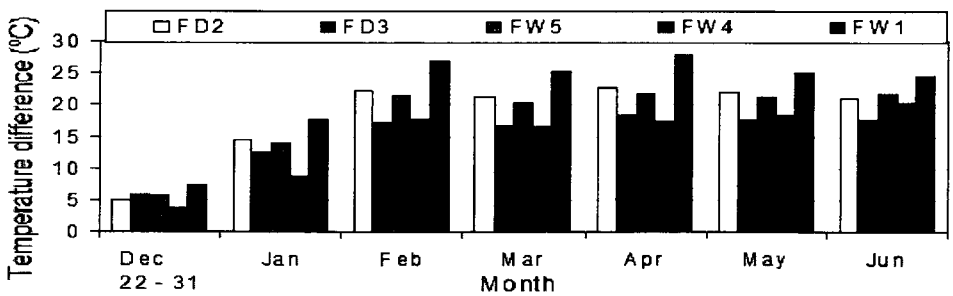

c) Maximum at night

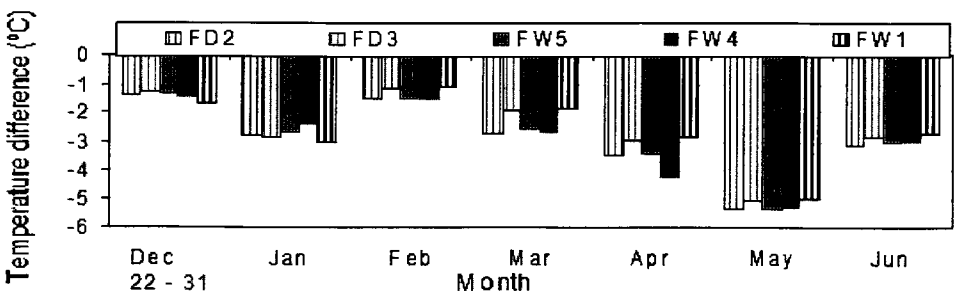

Figure 5-2-2: Monthly average and maximum temperature differences between the cavity and the ambient air in fibre cement walls from late Dec. 07 to June, 08.

For the walls with a 19mm air cavity, the monthly average temperature differences in all the walls were similar. The ranges were 1.2 – 1.8°C in the late December and January, 2.7 – 3.3°C from February to March, around 3.9 – 4.5°C in April and June, 2.9 – 3.3°C in May. The temperature differences in the walls with large top vent were slightly smaller than the walls with smaller top vents. FW1 with a 10mm air cavity had the largest monthly average temperature differences from January to June, approximately 0.5 – 1.2°C greater than that in FW4.

The monthly maximum temperature differences between cavity and ambient air in late December were the lowest, the ranges were about 4 - 7.5 °C at daytime and -1.3 - -1.7°C at night for all the fibre cement walls. In January, the temperature differences between air cavity and outdoor air become larger than those in December, within the range of 7.8 – 8.8°C at the daytime and -2.4 – 3.1°C at the night. In the sunny period in February, the maximum temperature differences between cavity and ambient were the similar to those in late December at night while was similar to those from March to June at daytime, within the range of 16 - 28°C. With large top vents, FD3 and FW4 had smaller temperature differences than FD2 and FW5 with small top vents at the daytime. However, the maximum temperature differences between cavity and ambient air at the night from February to May increased from -1 to -5°C and then became about 2°C smaller in June. The daytime maximum temperature difference in FW4 was over 10°C smaller at daytime but was 0.2 – 1.2°C greater than those in FW1 with a 10mm air cavity.

The monthly average temperature differences are so small that it can not really represent the factor to create enough thermal buoyancy force for ventilation drying. It is the high values in the peak solar hours in the sunny days that play an important role in drying the

evaporated moisture from the plywood sheathings, especially when the plywood sheathing is at the high MC level. The comparison of temperature deference between air cavity and ambient air in detail can be found in Appendix 3: "Thermal Performances of Rainscreen Walls".

5.3 Clear-sky effect

The clear-sky effect on test walls is evaluated to determine whether the cavity ventilation would cause condensation and become an additional moisture source to slow down the drying or to wet the plywood sheathing.

In principle, the net long-wave-emission determines the level of under-cooling of exterior surface of wall components, also called clear-sky effect. The under-cooling or clear-sky effect is determined by the difference between the energy emitted from the surface and the total counter-radiation. There are two kinds of counter-radiation: terrestrial and atmosphere. While an object's surface, for example a wall, emits its long-wave radiation uniformly into the semi-sphere space, it receives the long-wave radiation from the other objects surrounded it and from the sky. The terrestrial counter-radiation is defined as the partial long-wave radiation received from the terrestrial objects such as buildings, trees, and the ground etc. The atmosphere counter-radiation is the amount of radiation received from the sky. The intensity of terrestrial counter-radiation received by the wall is similar to the emission from its surface. However, the intensity of atmosphere counter-radiation is normally less than the emission towards the sky even if the temperature of both atmosphere and emitting surface are the same (WUFI 2007). The emitting surface,

therefore, receives less radiation than the radiation it emits to the surrounding and sky resulting in a continuous heat loss. Consequently, the surface temperature of a building enclosure such as roof and the walls above ground will drop below the surrounding air temperature due to the heat loss at the nights and even during daytimes in the cold and humid winter. The temperature of surface when it is lower than the outdoor air is referred to as the under-cooling temperature in this thesis.

Zeng et al (2004) experimentally studied zinc roof performance in Leuven, Belgium and found that the under-cooling effect on the zinc roof occurs all year round. Two under-cooling peaks happen during March to April and October to November. The risk of condensation at the cavity-surface of the zinc roof sheeting is very high. The daily average condensation potential is more than 2.5 hours and the average frequency is 50.3% of the test time (from 1996 to 1999).

Hens (2006) also theoretically and experimentally evaluated the clear-sky effect on the cavity-surfaces in roof and brick veneer wall systems. He found that the condensation not only occur at nighttimes but also happen during the daytimes in January. Thus he concludes that under-cooling dominates the radiant balance during the entire winter in the cold and humid climate, i.e. -10°C and 85% RH. The ventilation air turns into a major moisture source to wet the cavity-surfaces of the roof. In the brick veneer wall tested, Hens found that the under-cooling effect reduced the drying of brick during the winter significantly.

To evaluate the under-cooling effect on the test walls for the humid winter and spring of coastal BC, the cavity-surface temperature measurements of plywood and rainscreen

claddings, i.e. brick veneer and fibre cement cladding are analyzed and described in Appendix 3. For the brick walls, the range of under-cooling frequency on the cavity-surface of brick veneer is 6 – 32% in the winter time and 5 – 13% in the spring. For the fibre cement walls, under-cooling effects on the cavity-surfaces of fibre cement panels have been observed more frequently in the entire test period, reaching to 25 – 75% of the time in the winter and 7 – 40% in the spring. No condensation was found on cavity-surface of plywood sheathing.

The daily hours of condensation occurring on the cavity-surface of rainscreen cladding for each wall are calculated and discussed below.

1. Brick veneer

Although cavity surfaces experienced certain under-cooling effect for all brick test walls, brick veneers have high thermal and moisture storage capacity, so condensation rarely occurred. Figure 5-3-1 to Figure 5-3-3 show daily hours for condensation occurring on the cavity-surface of brick veneer from December 22, 2007 to June 21, 2008. Condensation occurred occasionally in the winter (December to March) but almost none in the spring (April to June). For two-floor high walls, the lower part of BD7 had a total of 25 condensation hours in the winter, more than that of BD10 (3 hours only) due to its location and facing the strong prevailing wind. No condensation was found at the upper level of two-floor high walls. For one-floor high walls, BW9 had many more condensation hours than BW8 probably due to the wet sheathing with top vent and the shade of trees on the exterior surface of brick veneer. It was a total of 32 hours for BW9

while 6 hours for BW8. No condensation was found at the cavity-surface of brick veneer for BDU12 while BDU11 had 14 hours of condensation in winter and 2 hours in May.

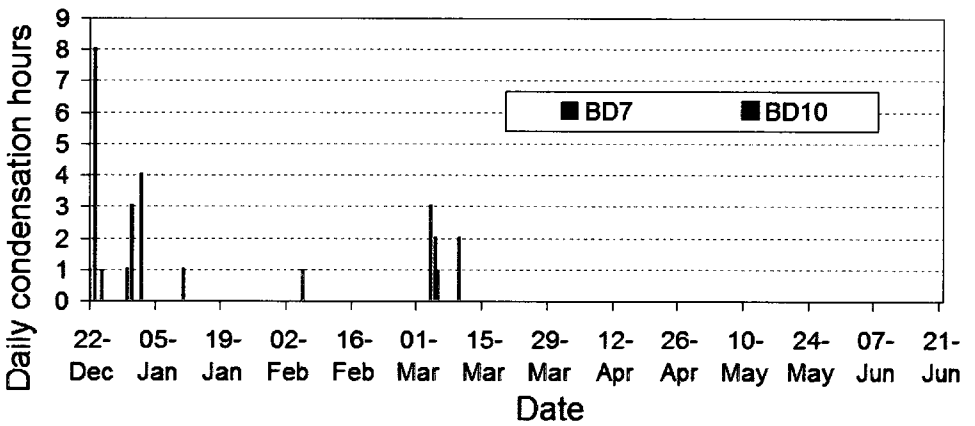

Figure 5-3-1: Daily condensation hours on cavity-surface of brick veneer for brick walls of BD7 and BD10 from Dec 22, 07 to Jun 21, 08.

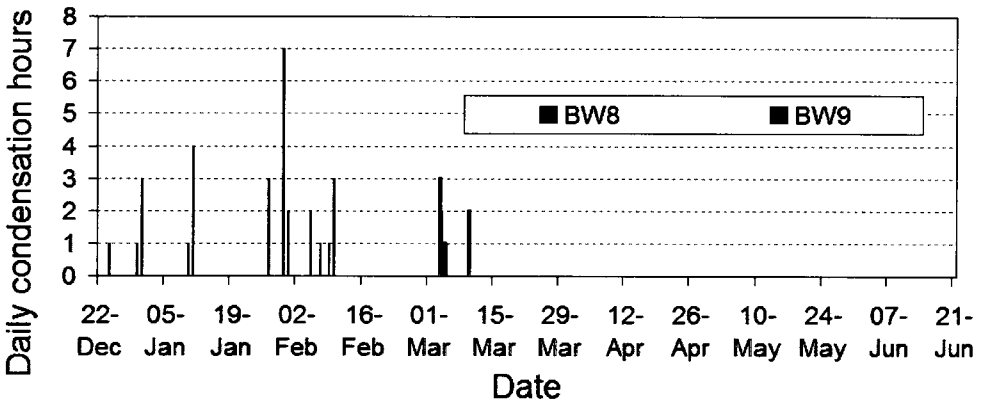

Figure 5-3-2: Daily condensation hours on cavity-surface of brick veneer for brick walls of BW8 and BW9 from Dec 22, 07 to Jun 21, 08.

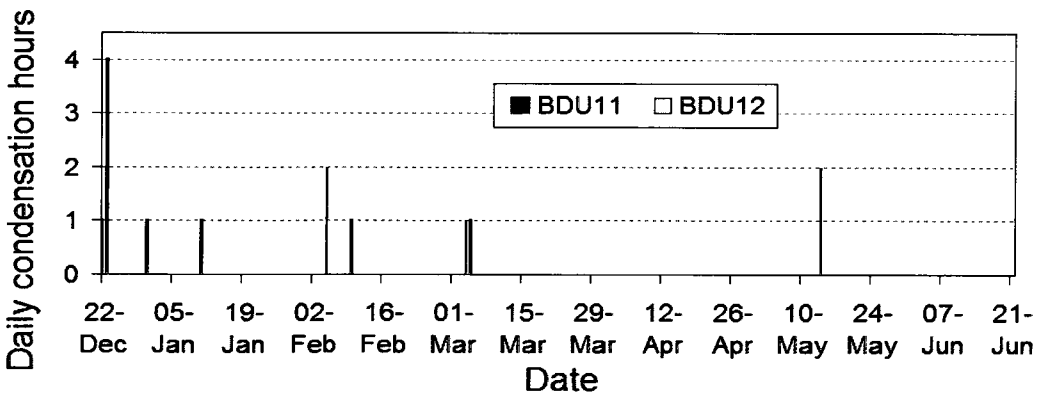

Figure 5-3-3: Daily condensation hours on cavity-surface of brick veneer for brick walls of BDU11 and BDU12 from Dec 22, 07 to June 21, 08.

Table 5-3-1 summarizes the condensation frequency on the cavity-surface of brick veneer for all the brick walls with different vent configurations and initial MC in plywood sheathing. The monthly condensation hours were small (0 – 17 hours) and the condensation frequencies were very low (0 – 5.3%). The thermal and moisture storage capacities of brick veneer seem to protect the brick veneer walls well from the under-cooling induced condensation.

Table 5-3-1: Summary of monthly condensation frequency (%) for brick walls during the test period from Dec. 22, 07 to June 21, 08

Months	BD7	BD10	BW8	BW9	BDU11	BDU12
Dec (22-31)	5.3	0.4	0	2.0	2.4	0
Jan	0.7	0	0	2.3	0.1	0
Feb	0	0.1	0	1.0	0.4	0
Mar	0.9	0.1	0.8	0.4	0.3	0
Apr	0	0	0	0	0	0
May	0	0	0	0	0.3	0
Jun	0	0	0	0	0	0

2. Fibre cement cladding

There are many more condensation events occurred on the cavity-surface of the fibre cement claddings than on the cavity surface of brick veneer walls due to the smaller thermal storage capacity of fibre cement cladding and their higher cavity ventilation rate provided by larger vent areas. Therefore, the moist outdoor air flowing through the air cavity becomes a potential moisture sources that may wet the sheathing and cladding.

In general, condensation occurred more in the winter than in the spring for all the fibre cement walls because the dew-point temperature of outdoor air was very close to the air temperature when the RH of outdoor air was very high (can be 98 – 100%) in the winter.

Figure 5-3-4 shows the daily condensation hours of fibre cement cladding in FD2 and FD3. The total condensation hours of FD3 were 17 hours more than that of FD2. Peak

daily condensation hours in FD2 happened during three periods in the winter: the beginning of the test in late December, January 21 – 30, and from February 29 to March 12. The condensation occurred during the first two periods had a significant impact on the MC of plywood. The water vapour diffused to the sheathing from both directions: inside of BETF and outdoor air flowing through the air cavity. It may be one of the reasons why the MC at the top of plywood sheathing in FD2 increased to 25% and stayed for over a month until the end of January, as shown in Figure 3 in Appendix 2 "Analysis of moisture content of plywood".

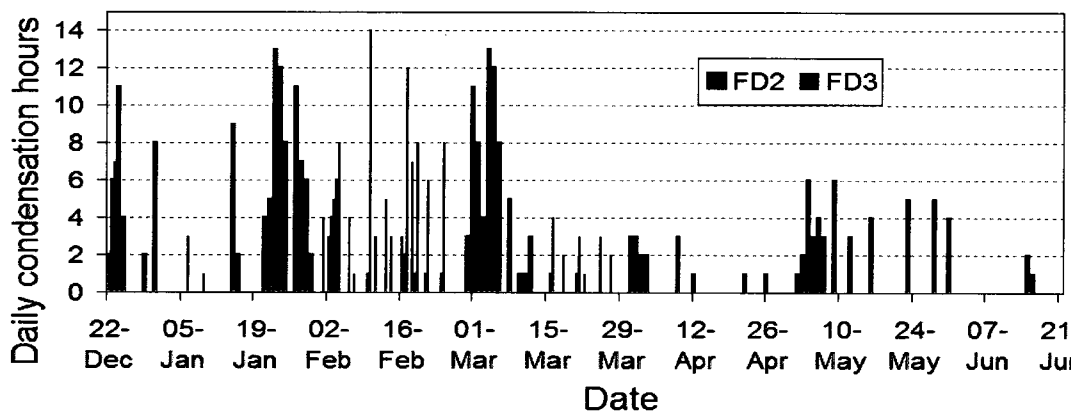

Figure 5-3-4: Daily condensation hours on cavity-surface of the fibre cement cladding for dry fibre cement walls of FD2 and FD3 from Dec 22, 07 to Jun 21, 08.

For FD3, the long daily condensation hours occurred from the end of January through February to the beginning of March. The combined effects of condensation on cladding-cavity surface and high indoor RH contributed to the high MC in plywood. The MC of plywood stayed at the high level from late January until the sunny period in February, as shown in Figure 3 in Appendix 2.

For walls with a high initial MC in plywood sheathing, the vent configurations have a significant influence on the surface condensation of fibre cement cladding, as shown in Figure 5-3-5. Cavity-surface temperatures of the fibre cement cladding in FW4 (with a

12mm top vent) were lower than the dew-point temperature of outdoor air at so much time in the winter. Condensation occurred more frequently in FW4 wall than in FW5 test wall with a smaller top vent and both walls had fewer and similar condensation events in the spring.

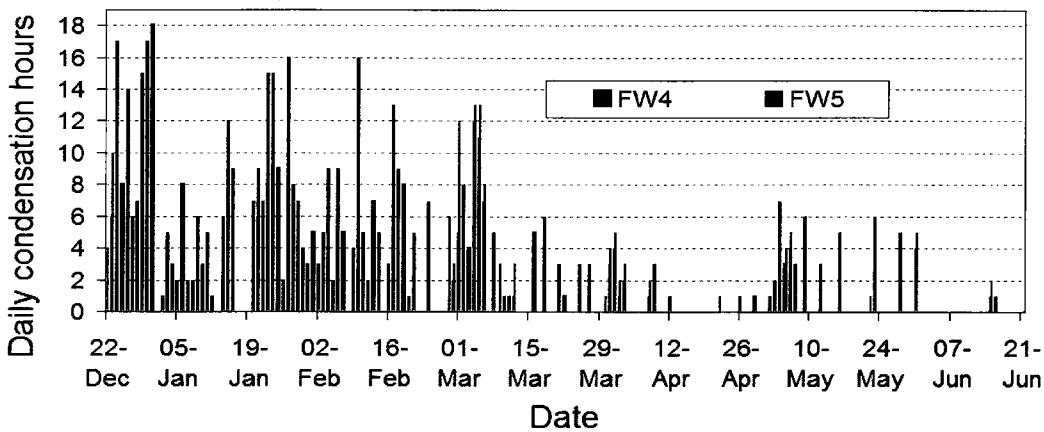

Figure 5-3-5: Daily condensation hours on cavity-surface of fibre cement cladding for wet fibre cement walls of FW4 and FW5 from Dec 22, 07 to Jun. 21, 08.

The daily condensation in FW4 reached a maximum of 18 hours daily at the end of December, 2007 and varies from 3 to 16 hours daily from January to the beginning of March, indicating the condensation not only occurs during the nights but also in the daytime. The frequency of condensation in FW5 from December to March was much less than that in FW4, within 1 – 13 hours due to small ventilation rates and slightly higher cavity-surface temperature. The difference in total condensation hours between FW4 and FW5 is 217 hours.

By comparing the walls with initially dry sheathing to the walls with initially wet sheathing, it indicates that the high initial MC in plywood sheathing has a significant influence on the occurrence of condensation on the cavity-surface of fibre cement for the walls with a 12 mm top vent. As shown in Figure 5-3-6, the daily condensation hours in

FW4 were more than double the condensation hours in FD3 at the beginning of the test until the end of January, 2008 after the first sunny period in the winter.

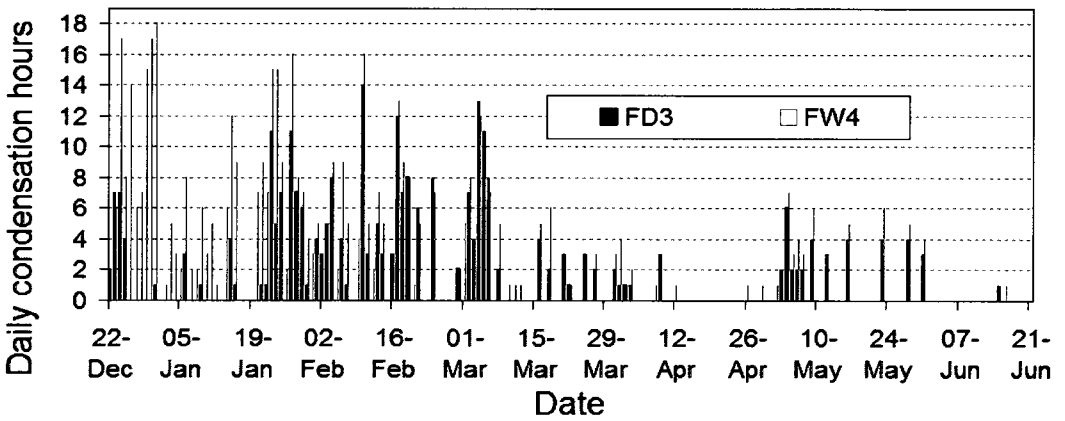

Figure 5-3-6: Daily condensation hours on the cavity-surface of fibre cement cladding of FD3 and FW4, walls with a 12mm top vents and different initial MC in plywood.

However, for the walls with small top vents, FD2 and FW5, the daily condensation hours were similar during the entire test period, as shown in Figure 5-3-7. It indicates that the smaller top vents for fibre cement walls have less condensation on the surfaces of cavity in the winter due to the higher surface temperature although the MC levels of plywood sheathing are different. In total, FW5 had 65 more hours of condensation than FD2 while FW4 had 265 more hours of condensation than FD3.

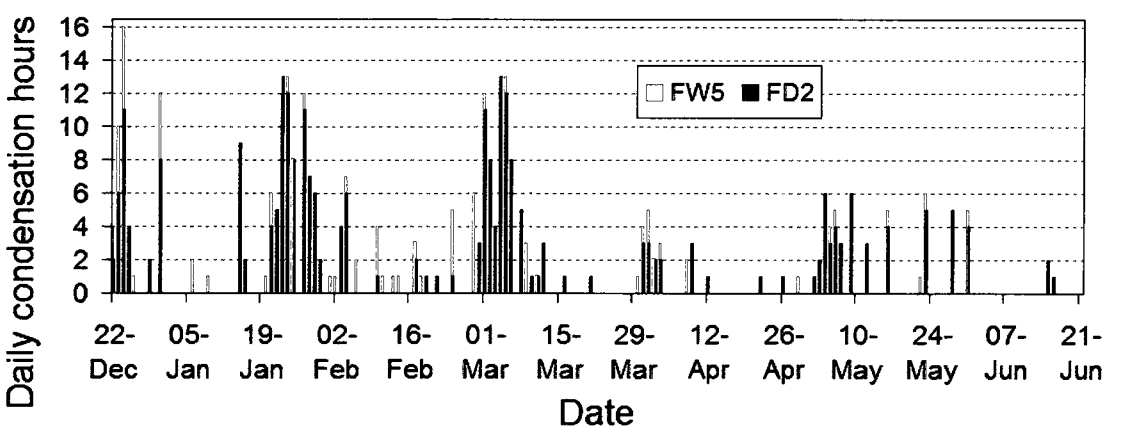

Figure 5-3-7: Daily condensation hours on the cavity-surface of fibre cement cladding of FD2 and FW5, walls with 1mm top vents and different initial MC in plywood.

Compared with FW4, the days of condensation and daily condensation hours on the cavity-surface of fibre cement cladding in FW1 were slightly fewer during the entire test period, as shown in Figure 5-3-8, indicating that FW1 with a 10mm cavity reduced condensation frequency in the humid winter of coastal BC. The difference in condensation hours between FW4 and FW1 is 148 hours during the entire test period.

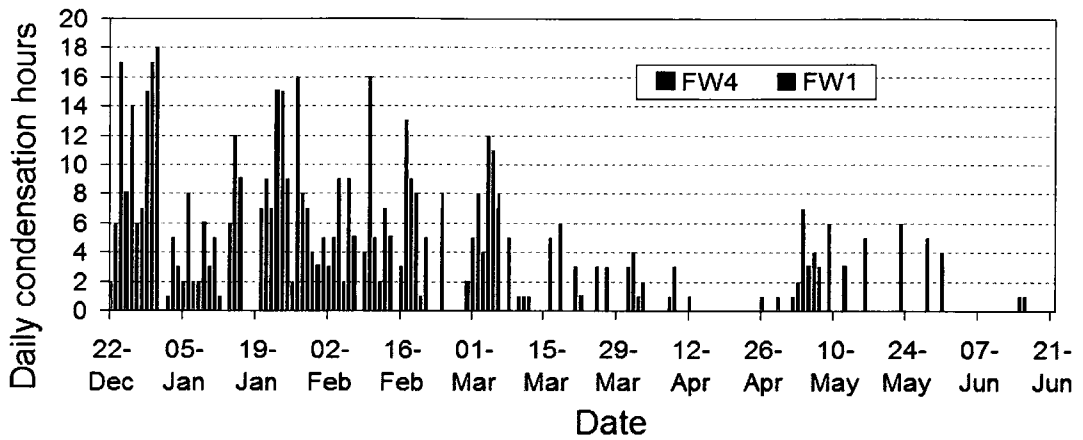

Figure 5-3-8: Daily condensation hours on the cavity-surface of fibre cement cladding of FW1 with a 10mm cavity and FW4 with a 19mm cavity.

Table 5-3-2 summarizes the condensation frequency on the cavity-surface of fibre cement cladding for all the fibre cement walls.

Table 5-3-2: Summary of monthly condensation frequency (%) for fibre cement walls during the entire test period from Dec 22, 07 to Jun. 21, 08.

	FD2	FD3	FW1	FW4	FW5	FW6
Dec (22-31)	13	8	31	44	20	33
Jan	11	8	15	23	12	18
Feb	3	14	13	18	6	15
Mar	10	8	9	11	11	9
Apr	2	1	1	2	3	1
May	6	5	6	7	7	6
Jun	0.4	0.1	0.1	0.3	0.4	0.1

For the dry walls, FD2 had 7- 20 more condensation hours than FD3 every month except for February. The peak month for cavity condensation in FD2 was in January and the number of condensation hours is 79 hours, 11% of the time in January. The peak month

for cavity condensation in FD3 was in February and the number of condensation hours is 96 hours, 14% of the time in February.

For the wet walls, December and January were the peak months for condensation on the cavity-surface of fibre cement claddings. In about ten days of December, the condensation occurred 44% of the time for FW4, over 30% for FW6 and FW1, and 20% only for FW5. In January, FW4 had the highest number of condensation hours, 167 hours and 23% of the time compared with all other wet walls. FW6 and FW1 had 114 - 132 hours of condensation, 15 - 18% of the time. FW5 had the least condensation hours in its peak month, 86 hours and 12% of the time.

In the spring with higher outdoor temperature and lower RH, the frequencies of condensation became lower than those in the winter. All the walls experienced relatively high condensation hours in May compared to April and June. There are 5 – 7% in May while 1 – 3% in April. June has the least condensation frequencies of 0.1- 0.4%. Condensation occurs mostly at night after rain when the outdoor air is in the high RH level. Once the sun comes out during the days, the moisture on the surfaces would evaporate and be carried out by cavity ventilation air. Therefore, the impact of condensation in general in the spring is not critical in terms of the hygrothermal performance of test walls.

5.4 Summary

Overall, during the winter and spring seasons from December 22, 2007 to June 21, 2008, the variation of vent configurations has little impact on the average temperature on each layer of the wall assemblies for both brick veneer and fibre cement walls. However, during the sunny period in February, the temperature on each layer of the brick walls without top vents is a maximum of 1 – 5 °C higher than that of the walls with top vents. For fibre cement walls with a 12mm top vent, the temperature is 2-3 °C lower than the fibre cement walls with 1mm top vents. The narrower air cavity (10mm) restricts the air flow, which resulted in a higher temperature than those with the wider air cavity (19mm). . All the walls have inward heat flow at daytimes during this period.

The measurements show that vent areas, cavity depth, and the amount of solar radiation are the main factors affecting the temperature difference between the cavity and ambient air. On the cloudy and rainy days, the average temperature differences are low, within -2 to 6°C for all the test walls. On the sunny days, the maximum temperature difference can be 6-10 times higher than those on the cloudy and rainy days at daytimes for fibre cement walls and 4 -5 times higher for brick walls but the temperature differences are similar for all test walls at night times.

Under-cooling effect occurs more on the cavity-surface of brick veneer and fibre cement cladding in the winter than in the spring due to the low outdoor temperature and high RH in the winter. Condensation on the cavity-surface of brick veneer occasionally occurred from December to March while no condensation occurred for most of brick veneer walls

in the spring. It indicates that the wood-frame back walls are well protected behind the brick in terms of condensation caused by under-cooling effect.

Condensation occurs on the cavity-surface of fibre cement cladding every month for all fibre cement walls and more condensation occurs in the winter than in the spring. The condensation in the winter significantly increases the MC of plywood sheathing for dry walls and slows down the drying for the wet walls. The impact of condensation in the spring is not critical since the moisture generated by condensations on the surfaces is rare and would be evaporated and carried out by cavity ventilation air.

The walls with dry sheathing have less condensation and the difference of condensation frequencies between the walls with small and large vent configurations are small. For the walls with wet sheathing, the larger vent areas cause more condensation and the ventilation air becomes an extra moisture source to provide potential wetting. For walls with a 19mm air cavity and 1mm high top vent, there are fewer incidents of condensation compared with walls with larger top vents, no matter whether the sheathing is dry or wet initially, probably due to the slightly higher cavity-surface temperature of fibre cement claddings. However, with the largest top vents (12mm high), the wall with wet sheathing has almost two to four times as much condensation hours as the wall with dry sheathing. Therefore, the walls with small top vents perform better in terms of reducing surface condensation and protecting the wood-frame back walls.

Chapter 6: Prediction of Cavity Ventilation Rates

6.1 Pressure differentials for cavity ventilation

The two main driving forces for cavity ventilation are wind pressure differential between the top and bottom vents and buoyancy-induced pressure differential between outdoor and inside of air cavities. In this section, all the positive values of pressure differentials denote that the wind, buoyancy and total pressures at the bottom position of an air cavity are higher than that at the top position; all the negative values mean pressures at the top position are higher than that at the bottom position.

6.1.1 Wind pressure differentials

The wind pressure differential between the top and bottom of walls, which were near vent position, was monitored at five locations of the SE façade of BETF as described in section 3.4 in Chapter 3 "Experiment Design and Setup". The two- floor high brick walls, BD7 and BD10 were located at both corners. The one floor high brick walls BW8 and BW9 were near both corners (beside BD7 and BD10) and the fibre cement wall FD2 was at the centre. The pressure differential measurements are influenced by the locations of the walls, wind speed and direction, and vertical distance between top and bottom measuring points.

The monthly average wind-induced pressure differentials are calculated and shown in Figure 6-1-1, using 10-minute average pressure differential from the range of -10 Pa to 10

Pa of one-second interval measurement, which includes over 80% frequency of the reading during entire test period in spring and winter of 2008. Unfortunately, the wind pressure data in January were not complete and was widely scattered. For comparison, the absolute monthly average wind-induced pressure differentials are also calculated and shown in Figure 6-1-2. The pressure differentials at corners decreased from a maximum of 4.5 Pa at BD7 and 3.5 Pa at BD10 in February to within 1.5 Pa in June. The pressure differentials at BW8 and BW9 were similar from about 2 Pa down to within 0.7 Pa. FD2 in the centre has negative value within 2 Pa in January and February and reduced to 0.6 Pa in June.

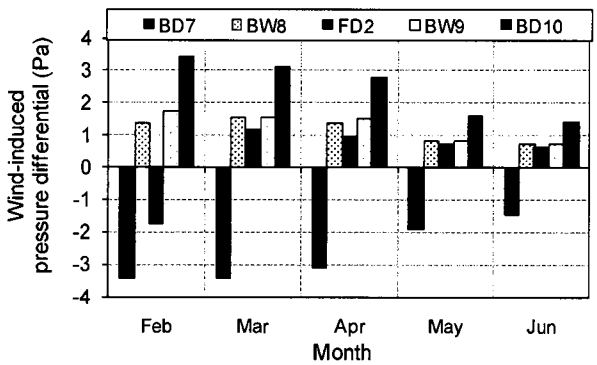

Figure 6-1-1: Monthly average wind-induced pressure differentials at test walls from Feb. to June, 08.

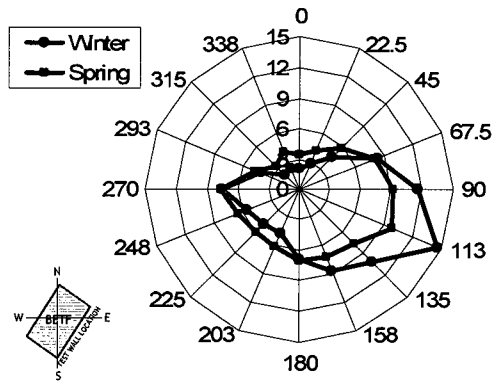

Figure 6-1-3: Comparison of wind direction between the winter and spring of 2008.

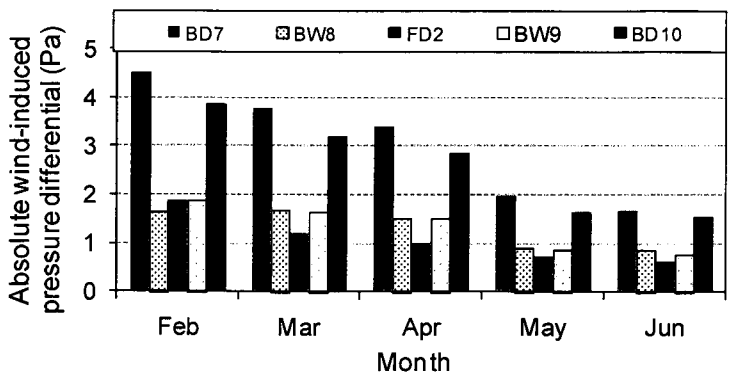

Figure 6-1-2: Monthly average absolute wind-induced pressure differentials at test walls from Feb. to June, 08.

The decrease in wind-induced pressure differential mainly is due to the change of wind direction. The frequency of wind coming from the east-southeast decreased from 14.7% in the winter to 9.8% in the spring, as shown in Figure 6-1-3.

The use of absolute value is to avoid the cancellation of values in reverse direction since the airflow rate in the cavity affects the moisture level but not the airflow direction. The statistical analysis in Table 6-1-1 shows that the reversal of wind pressure differential in direction exists but it occurs only about 1- 4% of the time for brick wall and 15% for FD2.

Table 6-1-1: The statistical analysis of wind pressure differential from Feb. to Jun. 08

	FD2	BW8	BW9	BD10	BD7
Total data points	18132	15250	16470	16211	14754
positive	15446	14975	16282	15889	537
negative	2686	275	188	322	14217
% of negative	14.81	1.80	1.14	1.99	96.36
% of positive	85.19	98.20	98.86	98.01	3.64

6.1.2 Buoyancy induced pressure differentials

The thermal buoyancy pressure differential can be calculated using temperature measurements in the air cavity and ambient air. The combination of thermal and moisture buoyancy pressure differential are calculated using RH and temperature measurements in the air cavity and ambient air.

1. Thermal buoyancy pressure differentials

The pressure differential induced by thermal buoyancy between the bottom and top vents can be calculated from equation (Hutcheon, N.B.1953).

$$\Delta P_s = 0.0342 \cdot H \cdot P_t \left(\frac{1}{T_{outdoor}} - \frac{1}{T_{cavity}}\right) \quad (6\text{-}1)$$

where ΔPs is thermal-induced buoyancy pressure differential, also called stack effect; H is the height of air cavity; P_t is total pressure at standard conditions of atmosphere, 101325 Pa; $T_{outdoor}$ is ambient air temperature, T_{cavity} is cavity airflow temperature.

The thermal-induced buoyancy induced pressure differentials in the cavities of two-floor high brick walls were greater than that in one-story walls, and the maximum was more than twice higher from December 22, 2007 to June 21, 2008. As shown in Figure 6-1-4 to Figure 6-1-6, the thermal pressure differential was -0.2 - 2.2 Pa for BW8 and BW9, -0.2 - 2.1 Pa for BDU11 and BDU12, -0.6 - 4.3 Pa for BD7 and -0.5 - 4 Pa for BD10. The results indicate that most of the thermal-induced buoyancy pressure differentials are positive in cloudy and rainy days for all the brick walls. On sunny days, the buoyancy pressure differentials have great fluctuation from positive to negative values from daytimes to nights. However, the negative values are much smaller and less frequent than the positive value.

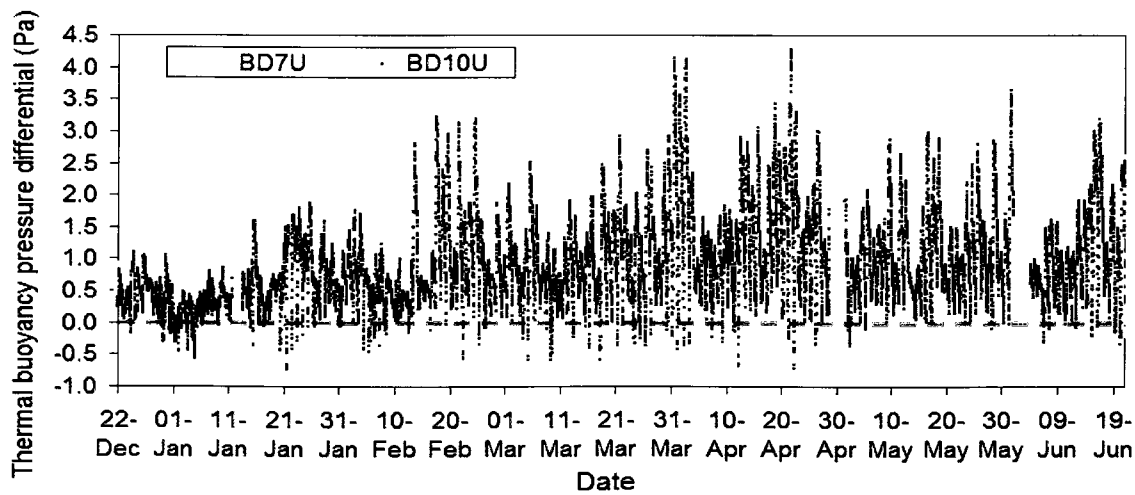

Figure 6-1-4: Comparison of thermal-induced buoyancy induced pressure differentials in the cavities between BD7 and BD10 from Dec 22, 07 to Jun. 21, 08 ("U" refers measurement at the upper part of cavities).

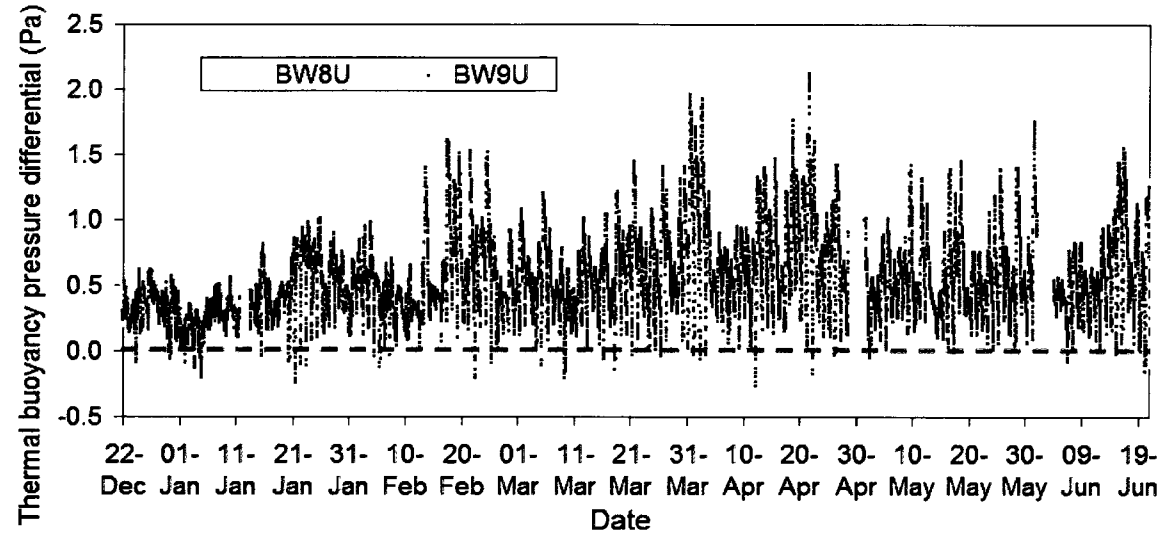

Figure 6-1-5: Comparison of thermal-induced buoyancy induced pressure differentials in cavities between BW8 and BW9 from Dec 22, 07 to Jun. 21, 08 ("U" refers measurement at the upper part of cavities).

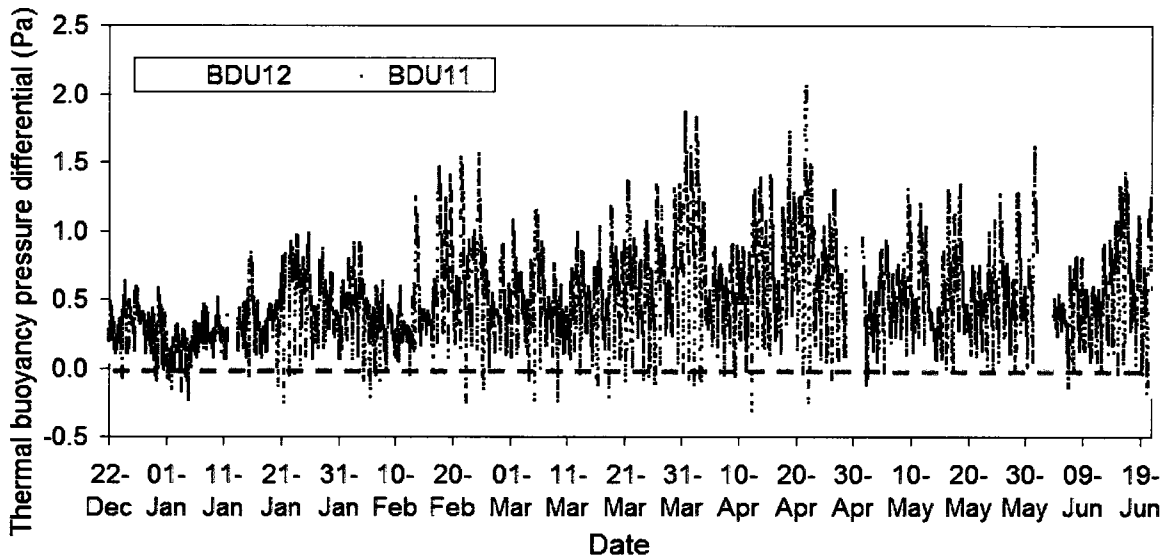

Figure 6-1-6: Comparison of thermal-induced buoyancy induced pressure differentials in the cavities between BDU11 and BDU12 from Dec 22, 07 to Jun. 21, 08.

Figure 6-1-7 and Figure 6-1-8 show the pressure differential induced by the thermal-induced buoyancy effect for the fibre cement walls with a 19mm air cavity. The results indicate that the trends of thermal-induced buoyancy pressure differentials for all the fibre cement walls are similar trend to brick walls.

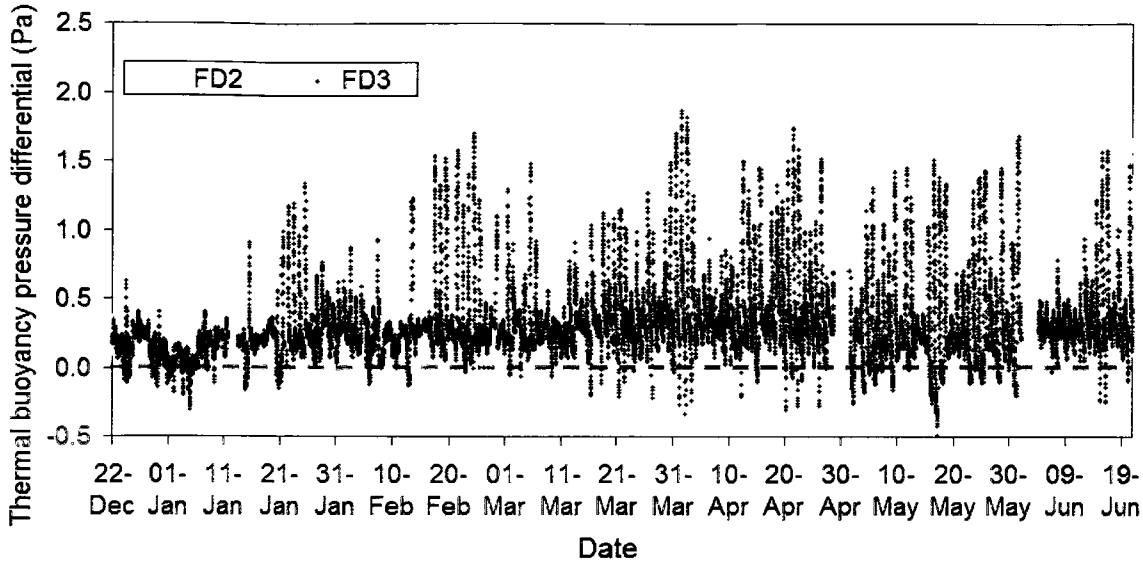

Figure 6-1-7: Comparison of thermal-induced buoyancy induced pressure differentials in the cavities between FD2 and FD3 from Dec. 22, 07 to Jun. 21, 08.

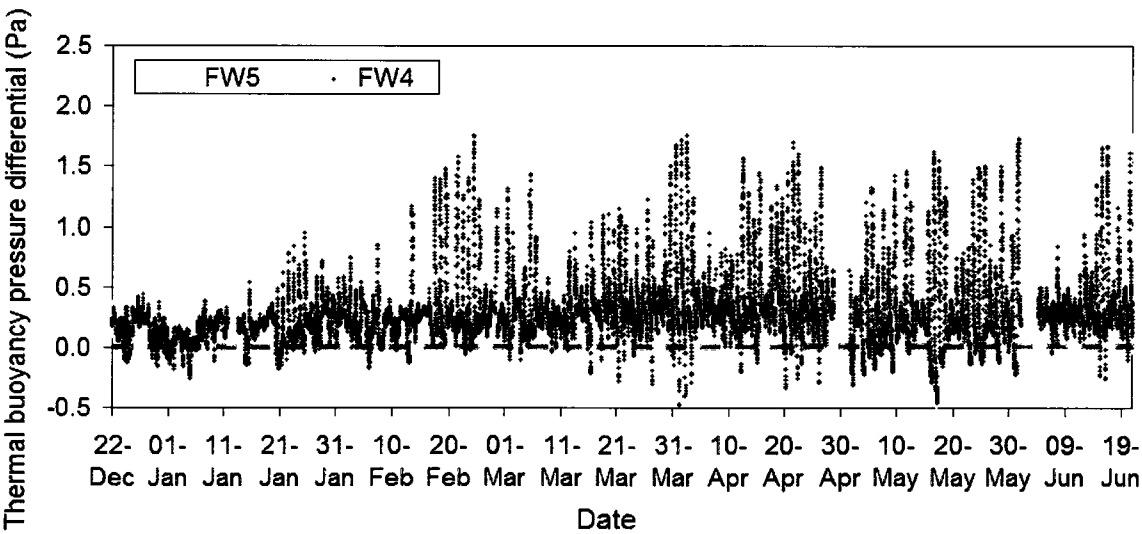

Figure 6-1-8: Comparison of thermal-induced buoyancy induced pressure differentials in the cavities between FW4 and FW5 from Dec. 22, 07 to Jun. 21, 08.

The maximum thermal-induced buoyancy induced pressure differentials in FD3 and FW4, the walls with 12mm high slot top vents, were approximately 0.5 Pa smaller than those in FD2 and FW5, the walls with 1mm high slot top vents, indicating the air cavities with large vent configuration on the sunny days has lower temperatures resulting in lower thermal-induced buoyancy induced pressure differentials than the cavities with small top

vents. The range of thermal-induced buoyancy pressure differential in the entire test period was -0.5 - 1.8 Pa for FD3 and FW4 and -0.5 - 2.3 Pa for FD2 and FW5.

Figure 6-1-9 shows the comparison between FW1 with a 10mm air cavity and FW4 with a 19mm air cavity. Both walls have 12mm continuous slot top vents. The thermal-induced buoyancy induced pressure differentials in FW1 were maximum 1Pa greater than that in FW4 during the daytime, but similar at night for the entire test period. Overall, the range of thermal-induced buoyancy induced pressure differential in the cavity of FW1 is -0.5 to 2.8 Pa.

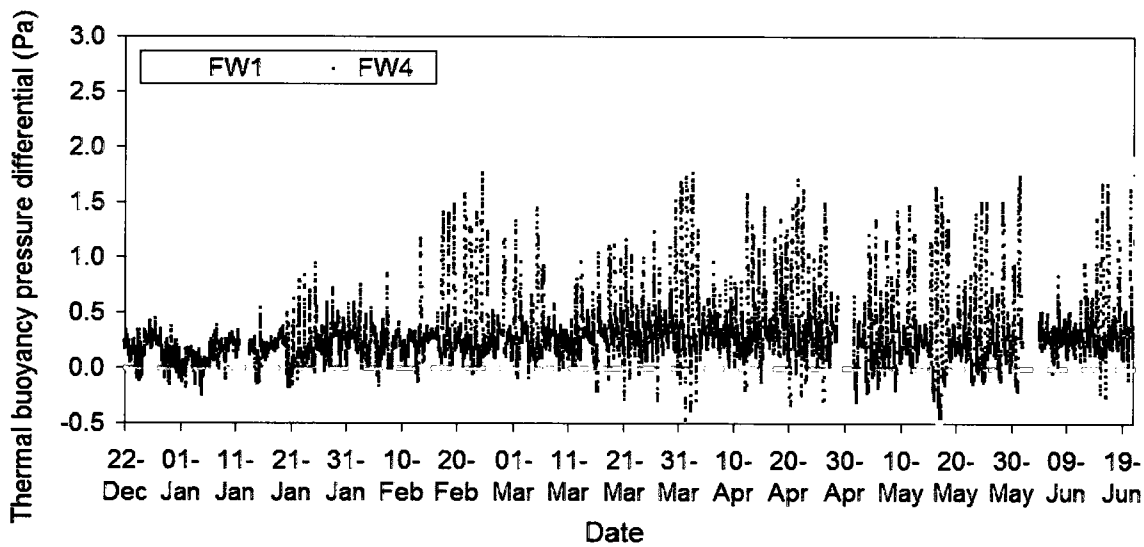

Figure 6-1-9: Comparison of thermal buoyancy induced pressure differentials in the cavities between FW1 and FW4 from Dec. 22, 07 to Jun. 21, 08.

2. Combined thermal and moisture buoyancy pressure differentials

Considering the air density change due to both temperature and moisture, the combined buoyancy pressure differentials between the cavity of test walls and outdoor environment through the full height from the bottom vents to top vents can be calculated as (ASHRAE 2005):

$$\Delta P_b = (\rho_{outdoor} - \rho_{cavity}) \cdot g \cdot H \tag{6-2}$$

The density of cavity and outdoor air can be calculated using the ideal gas law of mixed air including dry air and water vapour. Then, the combined buoyancy pressure differential can be also described as (Straube, et. al. 2004):

$$\Delta P_b = [(\frac{P_{a,outdoor}}{R_a \cdot T_{outdoor}} + \frac{P_{v,outdoor}}{R_v \cdot T_{outdoor}}) - (\frac{P_{a,cavity}}{R_a \cdot T_{cavity}} + \frac{P_{v,cavity}}{R_v \cdot T_{cavity}}) \cdot g \cdot H \tag{6-3}$$

Assume a total pressure at standard conditions of atmosphere is 101325 Pa and the dry air pressure (Pa) can be obtained as:

$$P_a = P_t - P_v \cong 101325 - P_v \tag{6-4}$$

where P_t is total pressure at standard conditions of atmosphere.

Hence, average combined buoyancy pressure differentials are calculated and shown in Figure 6-1-10 and Figure 6-1-11. For all the test walls, the smallest thermal buoyancy pressure differentials were in early winter until the end of January, greatest in early spring through April, similar in the rest of winter and spring. Large vent areas slightly reduced the buoyancy effects due to the smaller resultant temperature differences, but the difference between the large and small vent area is very small.

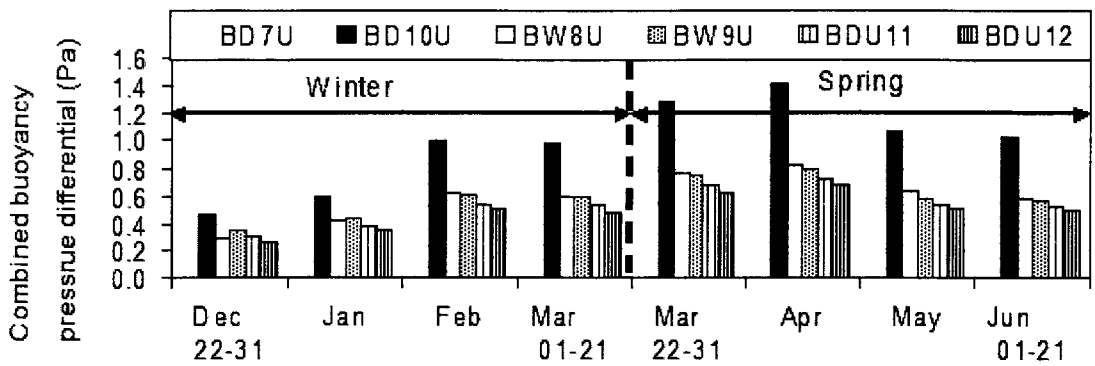

Figure 6-1-10: Average combined buoyancy pressure differentials between cavity and outdoor of brick walls in the winter and spring of 2008 (using temperature data from RH-T sensors at upper part and in middle of cavities).

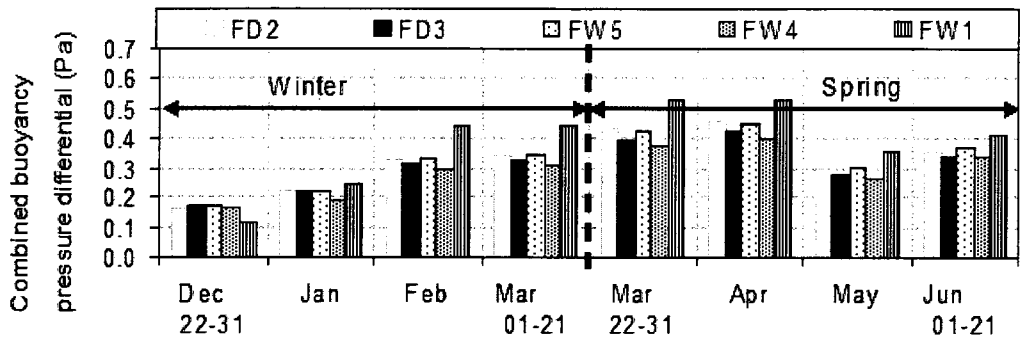

Figure 6-1-11: Average of the combined thermal and moisture buoyancy pressure differentials in fibre cement walls in the winter and spring of 2008.

Two-floor high air cavities in brick walls have higher buoyancy effect than one-floor high air cavities. The difference of buoyancy pressure differentials between the walls with and without top vents for two-floor high brick walls is bigger than that for the one-floor high walls.

Compared to the one-storey brick walls, the buoyancy induced pressure differentials in fiber cement walls are about half of that in brick walls. Between fibre cement walls with the same vent configurations, the walls with High initial MC in plywood show very small difference than walls with low initial MC in terms of combined buoyancy pressure differentials. Cavity depths have larger influence on the buoyancy effect compared to vent configurations. The narrower cavity of FW1 results in the largest buoyancy pressure differential among all the fibre cement walls. The difference between FW1 and FW4 (wide cavity with same vent configurations) is twice to three times greater than the difference between FW4 and FW5 (both with same depth of cavities but different vent configurations) after January.

Figure 6-1-12 shows the combined thermal and moisture buoyancy pressure differentials during the sunny period of February 17 – 25. The results indicate that all the test walls

have the largest average values but the smallest negative values in this sunny period in the winter.

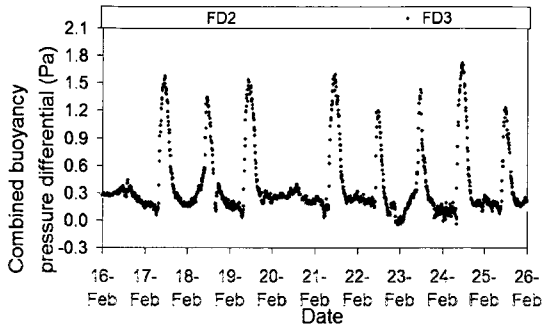

a) Fibre cement walls FD2 and FD3 with low initial MC of sheathing

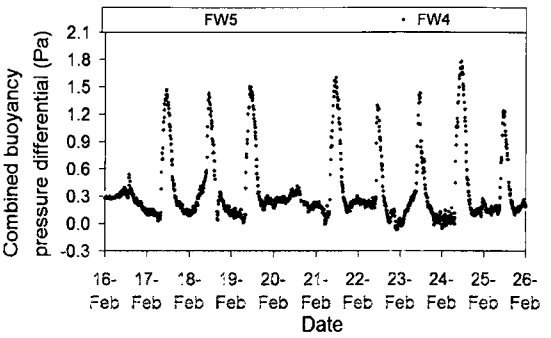

b) Fibre cement walls FW4 and FW5 with high initial MC of sheathing

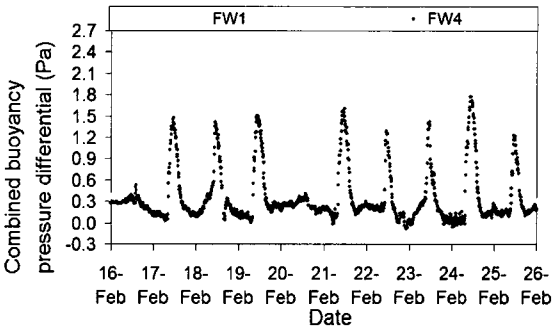

c) Fibre cement walls FW1 with a 10mm cavity and FW4 with a 19mm cavity (high initial MC of both sheathing)

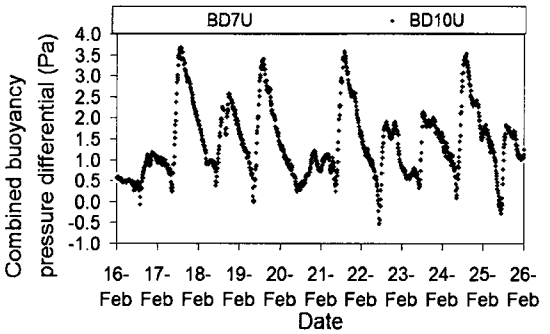

d) Brick walls BD7 without top vents and BD10 with top vents (two-floor high cavity and low initial MC of sheathing)

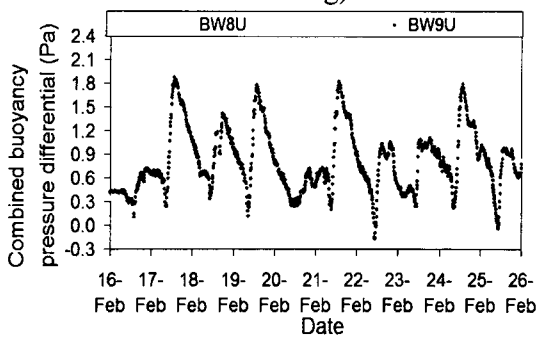

d) Brick walls BW8 without top vents and BW9 with top vents (one-floor high cavity and high initial MC of sheathing)

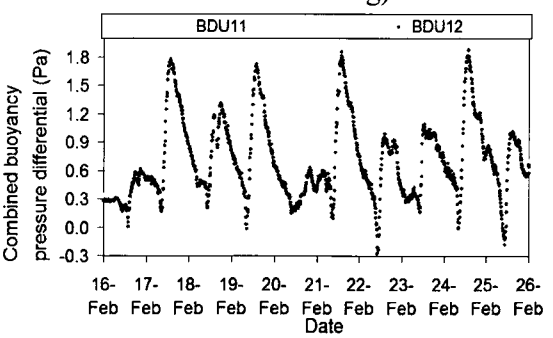

e) Brick walls BDI11with 6-25mm high top vents and BDU12 with 6-65mm high top vents (one-floor high cavity and low initial MC of sheathing)

Figure 6-1-12: Combined buoyancy induced pressure differentials in fibre cement walls and brick walls during the sunny period in Feb. 08.

The strong solar radiation resulted in higher increase in cavity temperatures of FW5 and FD2 which have small top vents; hence, the combined buoyancy pressure differentials in FW5 and FD2 were 0.4 – 0.6 Pa greater than that in FD3 and FW4. The buoyancy induced pressure differentials in FW1, the test wall with a 10mm cavity, were about 1.0 Pa higher than that in FW4 even though both walls have the same vent configurations (12mm) in the sunny period, indicating the depth of air cavities has more influence in terms of combined thermal and moisture pressure differentials than vent areas.

The monthly average moisture and thermal buoyancy induced pressure differentials are compared. The moisture buoyancy induced pressure differentials are generally very small in the winter and spring for all the brick walls and fibre cement walls compared with the thermal buoyancy induced pressure differentials. Thermal buoyancy pressure differential is dominated in the combined buoyancy pressure differential.

6.1.3 Total, wind, and buoyancy pressure differentials

Total pressure differentials obtain from the sum of wind pressure differentials and combined buoyancy pressure differentials. As shown in Figure 6-1-13, the general trend of total pressure differentials follows those of wind pressure differentials. The value of total pressure differentials are higher than both buoyancy and wind pressure differentials since the wind and buoyancy pressure differentials create the same airflow direction from bottom to the top in the air cavity for most of the time during the testing period for all the walls except for BD7, which is located at east corner of the façade. For BD7, the wind induced pressure differentials are against the buoyancy pressure differential during the

entire test period of winter and spring in 2008. Therefore, the total pressure differentials of BD7 are actually reduced. Further research work is required to investigate the cause for the reversed wind-induced pressure differential at BD7.

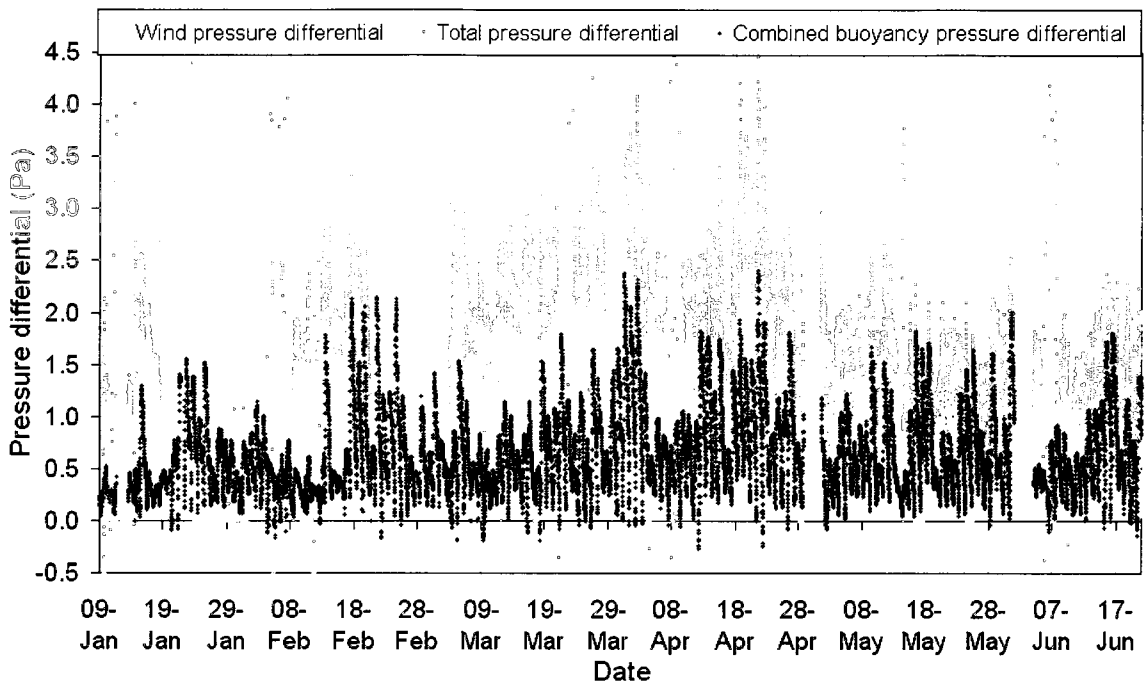

Figure 6-1-13: Comparison among the total, wind, and combined buoyancy pressure differentials at BW8 in the winter and spring of 2008.

The absolute monthly average of the total pressure differentials from February to June are calculated and shown in Figure 6-1-14. The absolute pressure differentials at corners decreased from a maximum of 4.0 Pa from February to 1.2 Pa in June on BD7 and from 5 Pa to 2.8 Pa on BD10. The pressure differentials on BW8 and BW9 were similar, from about 2.4 Pa down to less than 1.4 Pa. The pressure differentials on FD2, located in the centre, were the smallest, from 1.7 Pa in February to 1.0 Pa in June

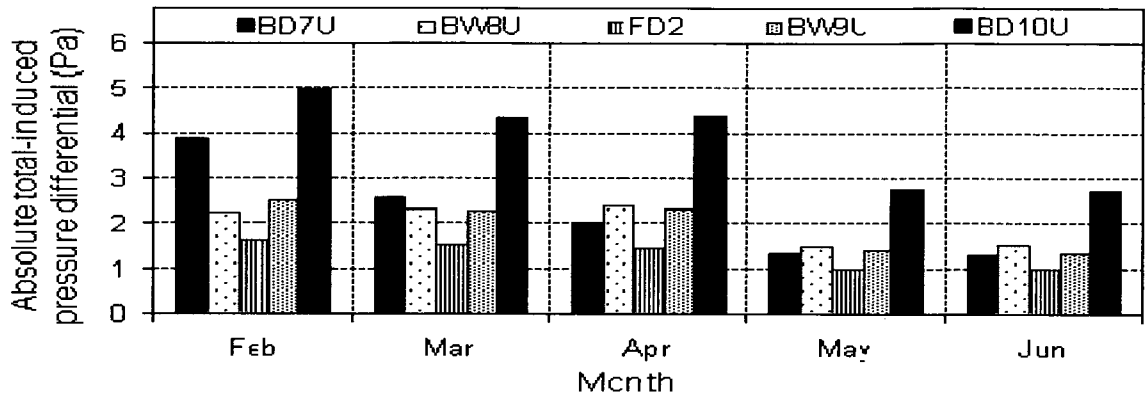

Figure 6-1-14: Monthly average of absolute total pressure differential from Feb. to June, 08.

6.2 Cavity ventilation rates

The airflow rate in the air cavity is determined by the pressure differentials between the top and bottom openings and the resistance along the airflow path. The cavity ventilation rates are calculated using both the total pressure differentials and combined buoyancy pressure differential. The air speed in the air cavity was measured using one hot-sphere anemometer placed in the center of the cavity at the middle height for each test wall. The average air speed measured is used for the evaluation of airflow types and a general comparison between measurements and prediction. However, the detailed data analysis is beyond the scope of this thesis. For the purpose of completeness, the experimental setup of air speed measurements and preliminary analysis is included in Appendix 5: "Cavity Air Speed Measurements".

6.2.1 Equations of cavity ventilation rates

The cavity airflow rate is affected by the resistances of the entrance and exit vents and through the cavity. Hence, the total pressure drop is defined for the cavity of a rainscreen wall as:

$$\Delta P_{total} = \Delta P_{entrance} + \Delta P_{cavity} + \Delta P_{exit} \quad (6\text{-}5)$$

where ΔP_{total} is the total pressure drop including the pressure drops at the exit, at the entrance, and within a cavity; $\Delta P_{entrance}$ and ΔP_{exit} are the pressure losses at the exit and entrance of the cavity through the top and bottom vents, ΔP_{cavity} is the pressure loss as the air flows through the cavity.

1. Pressure loss in air cavity, ΔP_{cavity}

Assuming that the airflow through the air cavity is laminar and its velocity is constant, the steady velocity can be defined as (ASHRAE 2005):

$$V = \frac{Q}{A} = \frac{\Delta P}{h} \cdot (\frac{D_h^{\ 2}}{32 \cdot \mu}) \quad (6\text{-}6)$$

Then the airflow rate in the cavity can be converted from the equation above with the hydraulic diameter for rectangular duct (Straube et. al. 2004) as:

$$\Delta P_{cavity} = \frac{32 \cdot K_f \cdot \mu \cdot Q \cdot h}{\gamma_c \cdot D_h^{\ 2} \cdot A} \quad (6\text{-}7)$$

where, K_f is correction friction factor; 1.5(d/w≈ 0, Re<2000); μ is kinetic viscosity of air, 0.000015 m²/s; μ is the kinetic viscosity of air, γ_c is the blockage factor, 0.8 for a clear cavity behind the brick veneer and 1.0 for a cavity behind the fibre cement wall, h is the

distance between the top and bottom vents, m (meter); Q is the airflow rate, m^3/s; D_h is the hydraulic diameter of the cavity, m; A is the cross area of the air cavity, m^2.

To confirm whether the airflow in the test walls is laminar flow, the average air speed measured is used to calculate the Reynolds number (Hutcheon, 1953):

$$\mathrm{Re} = \frac{D_h \cdot V \cdot \rho}{\mu} \tag{6-8}$$

where D_h is hydraulic diameter, V is airflow velocity, ρ is air density, μ is viscosity.

Laminar flow exists in the air cavity when the Reynolds number is below 2000. The Reynolds number for fully turbulent airflow is above 10000 while transitional flow exists between a Re number of 2000 - 10000 (ASHRAE 2005). The results calculated using the equation (6-5) and hourly average cavity air speed measurements (V) listed in Table 6-2-1 and Table 6-2-2.

Table 6-2-1: Reynolds number (Re) results and hourly average cavity air speed measurements of the test walls (Jan. 24 to Jun. 21, 08)

	Reynolds numbers					Air speed measurement (m/s)				
	BD7	BD10	BW8	BW9	FD2	BD7	BD10	BW8	BW9	FD2
Average	194	207	124	258	187	0.060	0.064	0.038	0.079	0.078
Minimum	81	96	93	108	38	0.025	0.030	0.029	0.033	0.016
Maximum	734	537	295	323	828	0.226	0.165	0.091	0.099	0.328
Standard Deviation	85	58	22	50	128	0.026	0.018	0.007	0.015	0.053

Table 6-2-2: Reynolds number (Re) results and hourly average cavity air speed measurements of the fibre cement test walls (Sep to Dec 19, 2008)

	Reynolds numbers		Air speed measurement (m/s)	
	FD2	FD4	FD2	FD4
Average	183	187	0.076	0.077
Minimum	37	69	0.016	0.028
Maximum	993	733	0.412	0.304
Standard Deviation	162	112	0.067	0.047

Average Reynolds number (Re) for all six brick and fibre cement walls are within the range of laminar airflow type. For the four brick test walls, the average Re's are between

124 – 258 with maximum 295-734 in the winter and spring. For fibre cement walls of FD2 and FW4, average Re is above 180. The maximum Re is much larger and reaches to 993 for FD2 compared with the maximum of 733 for FW4.

2. Local resistance coefficients and factors

To accurately estimate the airflow rate, the assumption of friction loss factors for the exit and entrance are critical. For the rainscreen walls with panel type cladding and continuous slot vents, the pressure loss with friction loss factors for the exit and entrance are taken as:

$$\Delta P_{entrance} = (\xi_{entrace} + \zeta_{elbow}) \cdot \frac{\rho}{2} \cdot (\frac{Q}{A_{entrance}})^2 \tag{6-9}$$

$$\Delta P_{exit} = (\xi_{exit} + \zeta_{elbow}) \cdot \frac{\rho}{2} \cdot (\frac{Q}{A_{exit}})^2 \tag{6-10}$$

where ρ is the air density, Q is the airflow rate, and A is the area of the entrance and exit openings. $\xi_{entrance}$ and ξ_{exit} are friction loss factors for the entrance and the exit, respectively. Straube and Burnett (1995) recommended $\xi_{entrance}$=0.5 for the entrance and ξ_{exit}=0.88 for the exit. These values are valid for turbulent flow. Thus, Straube et al (2004) adopted Idelchik's equation (Idelchik, 1994) to calculate friction loss factors for laminar and transitional flow as:

$$\xi_{entrance} = 6.5\,\mathrm{Re}^{-0.4} + 0.5 \cdot (0.066\,\ln(\mathrm{Re}) + 0.16) \tag{6-11}$$

$$\xi_{exit} = 6.5\,\mathrm{Re}^{-0.4} + 0.066\,\ln(\mathrm{Re}) + 0.16 \tag{6-12}$$

ξ_{elbow} is the friction loss factor for a rectangular elbow, recommended by Hens (1992).

$$\zeta_{elbow} = 0.885 \cdot (\frac{d_c}{d_v})^{-0.86} \tag{6-13}$$

where d_c is the cavity depth and d_v is the entry and exit slot depth.

The calculation results of the friction loss factor, $\xi_{entrance}$ and ξ_{exit} in the winter and spring from January 24 to June 21, 2008 and in the fall from September 22 to December 19, 2008 are listed in Table 6-2-3 for fibre cement walls of FD2 and FW4.

Table 6-2-3: Friction loss factors at entrance and exit for fibre cement walls of FD2 and FW4 in the winter and the fall, 2008

	Winter and spring		Fall			
	Jan 24 - Jun 21		Sep 22 - Dec 19			
	FD2		FD2	FW4	FD2	FW4
	$\xi_{entrance}$	ξ_{exit}	$\xi_{entrance}$	$\xi_{entrance}$	ξ_{exit}	ξ_{exit}
Mean	1.21	1.45	1.17	1.11	1.41	1.36
Minimum	0.79	1.08	0.72	0.76	1.03	1.06
Maximum	1.72	1.92	1.73	1.42	1.93	1.64
Standard Deviation	0.16	0.14	0.21	0.15	0.19	0.13

The average of local resistance factor for the entrance is 1.17 – 1.21 for FD2 while 1.11 for FW4. For the exit, it is 1.41-1.45 for FD2 while 1.36 for FW4, indicating the average resistance for FW4 is lower than FD2 but the difference is very small. Moreover, the ranges between minimum and maximum values of FD2 are larger, approximately 1.0 for the entrance and roughly 0.9 for the exit compared with those of FW4. It is only 0.66 for the entrance and 0.58 for the exit. To accurately predict the fluctuation of ventilation, the hourly average local resistance factors are applied in the calculations of prediction ventilation rates.

The insect screen blockage factor for the vent areas, γ_v is estimated as 0.5 (Finch 2007). However, the blockage factor is not necessary to apply for the 1mm high top vent of FD2 because the insect screen is inserted in the cavity with a depth of 19mm. The net area for air flowing through the blocked cross area on the top of cavity is much larger than that through the 1mm top vent.

For the brick walls with ventilated cavity of BW9 and BD10, the vent areas at top and bottom are not the same due to the insertion of insect screen in the top vents. It is difficult to account the available area for the airflow through an insect screen. Hence, the local discharge coefficient, C_d, of a vent with insect screen are used from the vent screen test results by Straube and Burnett (1998) as listed in Table 6-2-4 (vent screen types show in figure 6-2-1).

Table 6-2-4: Vent screen test results for brick veneer (from Straube and Burnett, 1998)

Masonry Vent Type (10 x 65 mm head joint)	Discharge Coefficient (Cd)	Flow Exponent (n)
Open	0.626	0.56
Cell-Vent	0.089	0.72
Goodco	0.047	0.52
Yeovil	0.056	0.56
Aircraft	0.030	0.50

Note: Linear regression best-fit to flow equation $Q = C_d \cdot A \cdot (\Delta P)^n$. Area based on an open head joint.

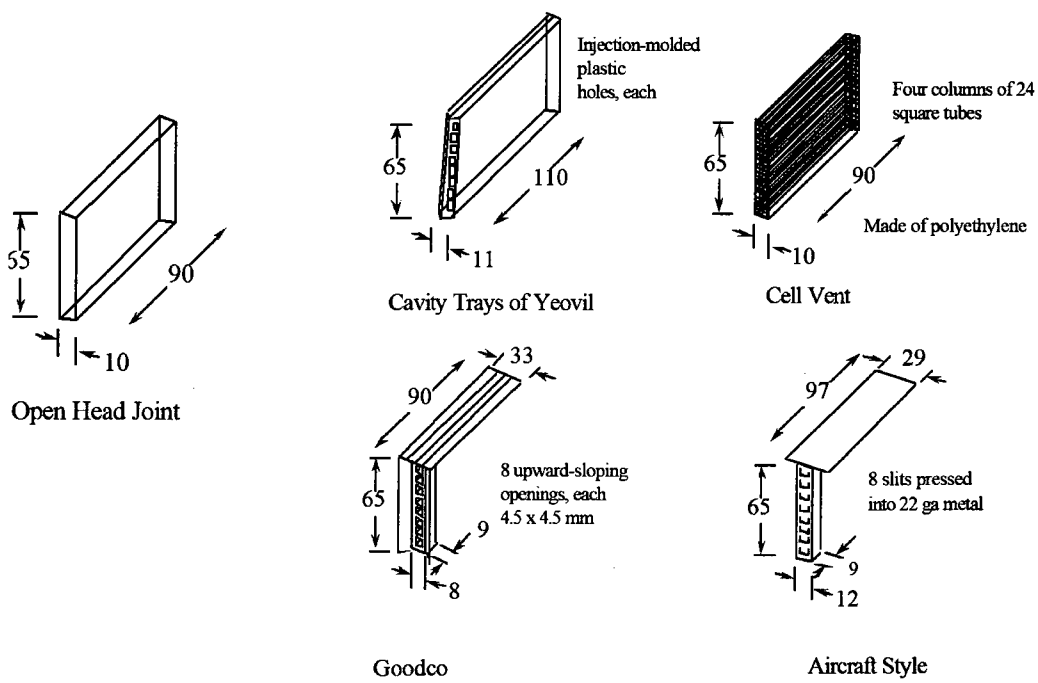

Figure 6-2-1: Vent without screen (open head joint) and types of vent screen tested (from Straube and Burnett, 1998).

For the bottom open vents (without insect screen), a discharge coefficient of $C_{d,top}$=0.626 is employed. For the top vents, a discharge coefficient of $C_{d,bottom}$= 0.047 for vents with Goodco insect screens, as described in Figure 6-2-19, is employed. In this case, the blockage factor at the vent is included in the discharge coefficients.

6.2.2 Results of cavity ventilation rates

To predict the airflow rate in the air cavity of test walls, the following equations are used:

a) Equation (6-14) for fibre cement walls with continuous slot vents

$$\Delta P = (\xi_{entrance} + \xi_{elbow}) \cdot \frac{\rho}{2} \cdot \left(\frac{Q}{A_{v,entrance} \cdot \gamma_v}\right)^2 + \Delta P_{cavity} + (\xi_{exit} + \xi_{elbow}) \cdot \frac{\rho}{2} \cdot \left(\frac{Q}{A_{v,exit} \cdot \gamma_v}\right)^2$$

b) Equation (6-15) for brick walls with discrete vents

$$\Delta P = \frac{\rho}{2} \cdot \left(\frac{Q}{C_{d,bottom} \cdot A_{v,bottom} \cdot \gamma_v}\right)^2 + \Delta P_{cavity} + \frac{\rho}{2} \cdot \left(\frac{Q}{C_{d,top} \cdot A_{v,top} \cdot \gamma_v}\right)^2$$

Predicted ventilation rates of two brick walls BW9, BD10 and two fibre cement walls FD2, FW4 are calculated with hourly average total pressure differentials. As shown in Figure 6-2-2 and 6-2-3, the ventilation rates were low for both ventilated brick walls from February 1 to June 21 BD10 had higher ventilation rates than BW9 due to the two-floor high air cavity. The average cavity airflow rate was 0.13 L/s for BW9 and 0.18 L/s for BD10. The ventilation rates for fibre cement walls FD2 and FW4 are much higher than those of brick walls. It is 0.46 L/s for FD2 and 1.46 L/s for FW4. The ventilation rate of FD2 is 1/3 of the amount in FW4 due to a smaller top vent.

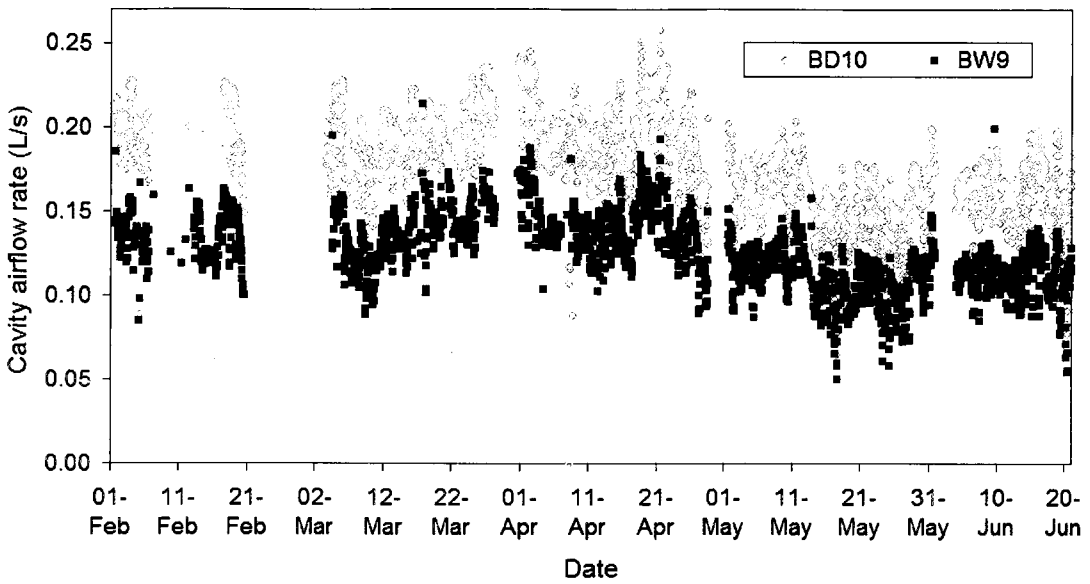

Figure 6-2-2: Predicted average cavity ventilation rates for brick walls BW9 and BD10 from Feb. to June, 08.

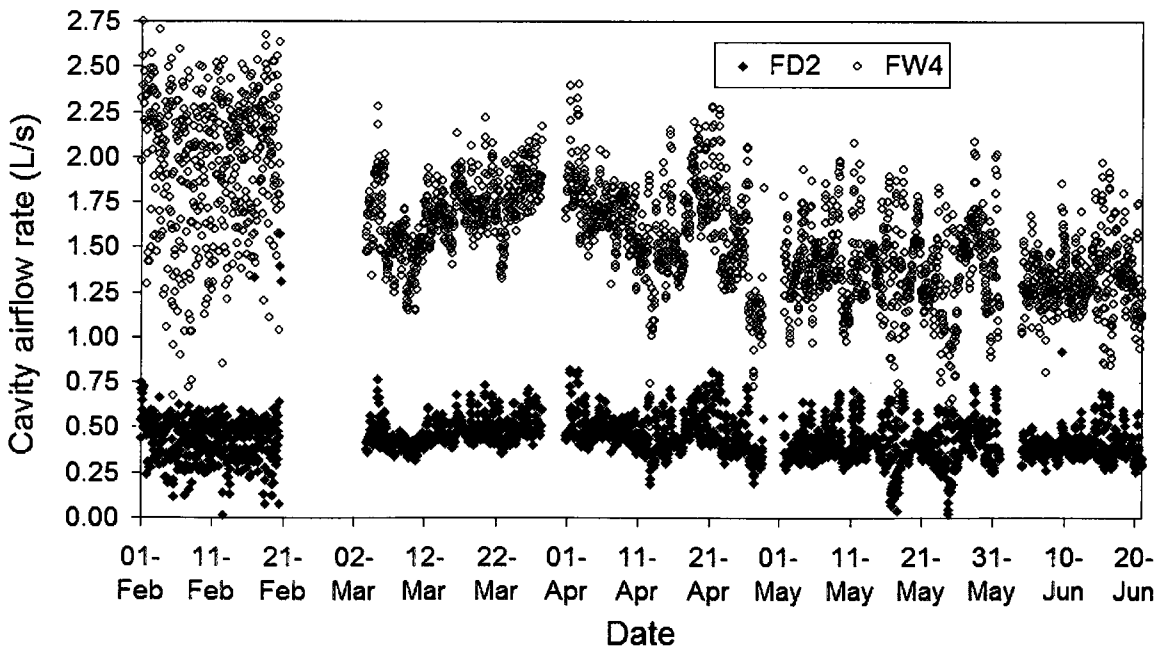

Figure 6-2-3: Predicted average cavity ventilation rates for fibre cement walls FD2 and FW4 from Feb. to June, 08.

The air change per hour (ACH) is more commonly used in referring to ventilation rates; therefore, the cavity airflow rates in L/s are converted to air change rates listed in Table 6-2-5 for the brick walls.

Table 6-2-5: Calculated hourly cavity air changes per hour (ACH) in ventilated brick walls BW9 and BD10 from Feb.1 to June 21, 08

	BW9			BD10		
	Predicted ACH			Predicted ACH		
	Total ACH	Buoyancy ACH	Wind ACH	Total ACH	Buoyancy ACH	Wind ACH
Mean	6	3.	5	4	2.	4
Minimum	1	0.02	0.03	1	0.1	0.02
Maximum	11	7	14	6	5	7
Standard deviation	1	1	2	1	1	1

The average hourly air change rate in one-story brick wall BW9 was about 3 - 6 ACH with a maximum value of 7 -14 ACH. For two-storey brick wall BD10, the average hourly ventilation rate was 2 - 4 ACH with a maximum of 5 -7 ACH. Table 6-2-6 shows that the hourly average predicted air change rate for fibre cement wall FD2 was an average of 40 - 89 ACH with a maximum of 306 - 468 ACH. The ventilation rate was 122 - 318 ACH with a maximum of 354 - 873 ACH for FW4 during this period.

Table 6-2-6: Calculated hourly cavity air changes per hour (ACH) in fibre cement walls FD2 and FW4 from Feb. 1 to June 21, 08

	FD2			FW4		
	Predicted ventilation rate			Predicted ventilation rate		
	Total ACH	Buoyancy ACH	Wind ACH	Total ACH	Buoyancy ACH	Wind ACH
Mean	89	41	80	318	122	271
Minimum	3	1	1	42	0.1	1
Maximum	468	306	459	653	354	874
Standard deviation	36	24	40	87	60	109

6.3 Summary

This section presents the measurements of wind-induced pressure differentials at five locations on the SE façade of the BETF, the calculation of combined buoyancy pressure differentials and prediction of cavity ventilation rates

The wind-induced pressure differential is small at the centre and near corners of one-floor high walls. It is much higher on the two-floor high walls at both corners. Thermal buoyancy effect is the dominant factor in the combined buoyancy pressure differentials for both brick and fibre cement walls with different initial MC in sheathing. The average combined buoyancy pressure differentials are lower in the winter than that in the spring due to the smaller amount of solar radiation, It is similar for all the fibre cement walls with 19mm cavity while slightly higher for the wall with a 10mm cavity. The two-floor high brick walls have higher average buoyancy pressure differentials than that in one-floor high walls. However, the strong solar radiation during the sunny period in February results in much higher temperature increases in the cavities of the fibre cement walls. In contrast, all the brick walls with low initial MC in plywood sheathing have very little difference of combined buoyancy pressure differential. With high initial MC in plywood sheathing, the brick wall without top vents has slightly higher combined buoyancy pressure differential than the wall with top vents. The pattern of total pressure differentials follows more closely to wind induced pressure differentials on the cloudy and rainy days but to buoyancy induced pressure differential on the sunny days.

On average, the predicted ventilation rate is about 6 ACH for one-story wall BW9 and about 4 ACH for the two-storey wall BD10 induced by total pressure differentials while 3 ACH for BW9 and 2 ACH for BD10 induced by buoyancy pressure differentials.. The predicted air change rate for FD2 is 89 ACH while 318 ACH for FW4 induced by total pressure differentials while 41 ACH for FD2 and 122 ACH for FW4 induced by buoyancy pressure differentials. The wind –induced pressures fluctuated very much and are the dominated factor to create large swing and ranges of total pressure differentials.

Chapter 7: Hygrothermal Simulation and Comparison

7.1 Introduction

Field and laboratory experiments are the reliable methods to assess the hygrothermal performance of building envelopes. However, experiments are acknowledged as both expensive and time consuming.

To predict the moisture damages caused by precipitation, indoor conditions, improper building envelope designs and construction deficient details such as air leakage and water penetration, the development of hygrothermal models started over twenty years ago. The advanced non-steady state simulation methods have been validated by experimental results. The reliability of those simulation tools is recognized and accepted by more and more researchers and practitioners (IBP, 2001). A well established and benchmarked model can be a powerful tool for predicting the HAM (heat, air and moisture) transport under field conditions, the selection of a durable performance strategy, and decision-making of building envelope design.

CMHC (2003) initiated a project to review available models for the hygrothermal performance assessment of building envelope retrofits in order to accurately predict and ensure that retrofit strategies do not adversely impact the performance of the retrofitted assemblies and that the intended improvements in system performance are achieved (McGowan, 2003). Of several commercial hygrothermal models evaluated, it is found that WUFI (Warme- und Feuchtetransport Instationar "Transient Heat and Moisture Transport"), a one-dimensional model, is able to predict the performance of building

envelopes under field conditions incorporating the environmental loads such as wind-driven rain, solar radiation, clear-sky radiation and cavity ventilation. The model can also simulate building envelopes with deficiencies such as air and rain leakage. Therefore, WUFI pro. 4.1 is chosen in this thesis to perform hygrothermal simulation of four test walls: two brick walls, BW9 and BD10, and two fibre cement walls, FD2 and FW4 during the period from January 1 to June 30, 2008.

In this chapter, the input data such as indoor and outdoor conditions, surface film coefficient, rain load, material properties, initial MC of wall components and cavity ventilation rates will be described. Results in terms of MC in plywood sheathing and surface temperature of cladding between simulations and experiment measurements will be compared. The main parameters that significantly influence the accuracy of hygrothermal simulation are analyzed and recommendations on choosing proper input data and material property data from WUFI's data base are provided. The limitations of modeling will be also discussed.

7.2 Input parameters

The input parameters required for simulations include:

1. configuration of the wall assembly and the material properties of each layer,
2. Outdoor weather and indoor conditions (climate files),
3. surface transfer coefficients,
4. driving rain load
5. initial MC of each wall components

6. cavity air change rates

7.2.1 Components of wall assembly and their properties

The configurations of the four wall assemblies used for simulation are the same as the assemblies tested, (refer to Chapter 4 "Experiment Design and Setup"). The initial MC of plywood in simulations is the actual MC measurements of plywood at the starting points of simulations, January 1, 2008. The configuration and initial MC in plywood in four walls are briefly described in Table 7-2-1.

Table 7-2-1: Configuration and the initial MC in plywood in the four test walls

Walls	Cladding	Air cavity		Vent configurations		Initial MC of sheathing
		depth	Height	Top	Bottom	
BW9	Brick	25mm	2.44m	2-discrete vent with insect screens	2-discrete vents fully open	High (30%)
BD10			4.88m			Low (16%)
FD2	Fibre cement board	19mm	2.44m	1mm high slot vent	12mm high slot vent	Low (16%)
FW4			2.44m	12mm high slot vent		High (29.6%)

Since the material properties of all the wall components were not measured in this experiment, the data available in "Generic North America Database" and "Generic Materials" databases in WUFI (WUFI, 2007) are used in the simulations except for plywood density. The material database in WUFI is collected from various sources and the properties are compared and validated in the modeling and experiments in:

- ASHRAE RP 1018 project (Kumaran, M.K. et. al. 2002b)
- NRC Task 3 of MEWS project (Kumaran, et. al. 2002a)
- combination of ASHRAE RP 1018, NIST publications, ORNL publications or/and IBP measurements

The properties in the database of WUFI include bulk density, heat capacity, thermal conductivity, and vapour diffusion resistance factors for all materials. For most of the porous materials, moisture-dependent properties such as moisture storage function, liquid transport coefficient (suction / redistribution) and vapour resistance factor are also included.

The density of plywood used in the experiment was measured using a ventilated oven according to ASTM D 4442-92 standard (ASTM, 1992) as described in Chapter 3. It has a density of 432 kg/m^3, which is between the density of "plywood (medium density)" and "plywood low (low density)" listed in WUFI's database. The proper selection of material properties of plywood is essential for the accuracy of simulation results in terms of MC in plywood sheathing. The properties of plywood (medium density) were chosen for the simulations. This selection will be discussed in great detail later in this chapter. The basic properties of claddings and air in cavities under dry condition, i.e. 0%RH, are listed in Table 7-2-2. The properties of wood-frame back wall components (which are identical for all four walls) are listed in Table 7-2-3.

Table 7-2-2: Basic material properties of claddings and air in air cavities used for simulations

Cladding and air cavity	Bulk density	porosity	Specific heat capacity	Thermal conductivity	Vapour diffusion resistance factor
	Kg/m^3	M^3/m^3	J/(kg•K)	W/(m•K)	-
For brick walls					
Red clay brick	1935	0.217	800	0.495	137.8
Air (25mm cavity)	1.3	0.999	1000	0.155	0.51
For fibre cement walls					
Fibre cement board	1380	0.479	840	0.245	990.9
Air (19mm cavity)	1.3	0.999	1000	0.13	0.56

Table 7-2-3: Basic material properties of wood-frame back wall used for simulations

Wood-frame back walls	Bulk density	porosity	Specific heat capacity	Thermal conductivity	Vapour diffusion resistance factor
	Kg/m^3	M^3/m^3	J/(kg•K)	W/(m•K)	-
SBP membrane	448	0.001	1500	2.4	328.4
Plywood	432	0.69	1800	0.084	1078.2
Glass fibre batt insulation	88	0.999	840	0.043	1.21
polyethylene-membrane	130	0.001	2300	2.3	50000
Interior gypsum board	625	0.706	870	0.16	7.03

7.2.2 Outdoor weather and indoor conditions

Beside the climate files stored in its database for outdoor and indoor conditions, WUFI Pro. 4.1 allows the creation of user defined climate files, using a specific format, for exterior and interior environment conditions. User defined climate files were generated for the simulations using weather data recorded from an on-site weather station and indoor conditions inside BETF.

The exterior climate file includes hourly temperature, RH, global solar radiation and diffuse radiation, atmospheric pressure, wind speed, horizontal rainfall and wind direction distribution. All the data is from the on-site weather measurements except for atmospheric pressure. The atmospheric pressure data are from the Environment Canada's YVR airport weather station. The diffuse radiation must be calculated using the global solar radiation by empirical methods (Duffie, W. and Beckman, J., 1991; WUFI, 2007) in order to apply the solar radiation on a vertical surface for given orientations during the simulation using WUFI. The procedure and methodology are given in detail in Finch's thesis (Finch, 2007). The weather data in May were missing due to the malfunction of the data logger for the weather station. The missing data in the outdoor climate file is

replaced using the data collected on a building near the testing site within 1.5 km distance.

The hourly interior conditions including temperature and RH recorded inside BETF are used to create the climate file. It is important to note that the format of climate files needs to be strictly followed; otherwise, simulations won't be run properly.

7.2.3 Surface transfer coefficients

In WUFI, the exterior and interior surface transfer coefficients include:

- exterior and interior surface heat transfer coefficients
- mass transfer coefficient
- rainwater (liquid) absorption on exterior surface
- solar radiation absorptivity and emissivity of exterior surface
- optional explicit radiation balance, i.e. considering clear-sky effect

7.2.3.1 Exterior and interior surface heat transfer coefficients

1. Exterior surface

There are two options of the exterior surface heat transfer coefficients in WUFI for users to choose depending on whether clear-sky effect needs to be accounted for:

- simplified long-wave radiation exchange mode
- full radiation balance mode

A wall surface exchanges heat to surroundings. This heat transfer includes two major transport mechanisms: convection through air movement, and long-wave radiation

emitted from the surface. A simplified heat exchange model, which is recommended for most applications, is the default by WUFI. It contains a constant surface heat transfer coefficient combining the convective and radiation transfer coefficients as:

$$q = (h_c + h_r) \cdot (t_a - t_s) \tag{7-1}$$

where q is heat flux (W/m^2), h_c is convective heat transfer coefficient, W/m^2; h_r is radiation heat transfer coefficient, W/m^2, t_a is outdoor temperature, °C; and t_s is surface temperature, °C.

This simplified mode treats convective heat flow and long-wave exchange as one heat exchange with the ambient air; whereas, the short-wave (solar) radiation is treated as a heat source at the exterior surface. This heat source is obtained by the irradiation incident on the surface multiplied by the short-wave absorptivity.

The constant heat transfer coefficient by default of WUFI is 17 $W/(m^2 \cdot K)$ including a convective transfer coefficient of 10.5 $W/(m^2 \cdot K)$ and a radiative transfer coefficient of 6.5 $W/(m^2 \cdot K)$. WUFI employs surface heat transfer resistance which is simply the reciprocal of the heat transfer coefficient. Hence, the input data will be 0.0588 $m^2 \cdot K/W$ for the heat transfer resistance of an exterior wall.

The full radiation balance mode allows the quantitative computation of clear-sky effect by explicit determination of the long-wave radiation components. The overall radiation balance combines the long-wave radiation and the short-wave radiation components into a collective heat source at the surface and will be described in the next section. The heat source may have a positive (heating) or negative (cooling) value, depending on the overall radiation balance (WUFI 2007).

If the full radiation balance mode is used, the exterior heat transfer coefficient should contain only the convective part. Hence, the surface heat transfer coefficient becomes 10.5 W/(m² •K). The heat transfer resistance is 0.095 m²•K/W.

Which mode should be used depends on how significant the clear-sky effect is. Normally, it is adequate to run with simplified radiation mode for long-term hygrothermal performance of building envelope (WUFI, 2007). However, for a climate zone which has a cold and humid winter, such as the coastal climate of BC, clear-sky effect may dominate the radiation balance in the situation where condensation on surfaces of the wall may occur often when the surface temperature drops below the dew-point temperature of the air (Hens, 2006). In this case, full radiation balance mode i.e. explicit radiation balance, may be required for the simulation. If using the full radiation balance mode by checking the option of "Explicit Radiation Balance" in the dialogue of "Surface Transfer Coefficients", WUFI can calculate temperature and moisture of building envelope components affected by clear-sky effect.

In practice, if clear-sky effect only causes a few hours of condensation, using explicit full radiation mode may overestimate the influence resulting in over-wetting for the plywood sheathing as discussed later in section 7.4. Therefore, in this thesis, whether clear-sky induced condensation would occur on cladding surfaces based on measurements is used to determine which mode should be used in simulations for each wall. The modes chosen for each of the four walls are listed in Table 7-2-4.

Table 7-2-4: Radiation modes used in simulations for four walls

Walls	mode	Note
BW9	Simplified long-wave radiation exchange mode	Large mass of brick veneer
BD10		
FD2		Dry sheathing with small top vent
FW4	Full radiation balance mode	Wet sheathing with large top vent

2. Interior surface

For the simplification, WUFI provides a constant heat transfer resistance based on the mean temperature of interior space. Since the inside of BETF conditions are relatively constant and uniform, a constant heat transfer resistance of 0.125 $m^2 \cdot K/W$, default value by WUFI is used for the simulations.

7.2.3.2 Vapour diffusion resistance of surface coating and rain water absorption

WUFI uses a Sd-value to account for the vapour diffusion resistance of surface coating such as paints, wall papers, or any surface repellents. Sd-value expresses the vapour diffusion resistance of a material in a form of the equivalent thickness of a stagnant air layer that has the same resistance as the coating material. The larger Sd-value, the greater the vapour diffusion resistance.

"No coating" should be selected if there is no such coating on the surfaces of building components, or if the coating has been included in the assembly with a material (WUFI 2007). For example, if acrylic stucco exterior cladding is already included in the wall assembly, the Sd-value of exterior surface should be selected with "no coating"; otherwise, the resistance of exterior surface will be doubled if the "acrylic stucco" is chosen again in the Sd-values offered by the software. In these simulations, "no coating"

is chosen for the Sd-value of exterior / interior surfaces since there is no coating applied on both surfaces of brick and fibre cement walls.

WUFI uses a rain water absorption factor to account for the proportional reduction of capillary absorption caused by rainwater splashing off the wall surface. For common walls, the value of 0.7 is adequate for most cases in the rainy condition while zero for the cases in the snow and hail events. However, if a facade is protected from rain by an overhang, no rain absorption shall be applied (WUFI 2007). The default value of 0.7 is used in the simulations since the BETF's façade has minimum overhang.

7.2.3.3 Short-wave absorptivity and Long-wave emissivity

When solar radiation falls on the opaque exterior surface of walls, it is partially absorbed and partially reflected depending on the material properties (ASHARE 2005). The short-wave absorptivity determines the fraction of total incident solar radiation absorbed by the exterior cladding of walls. In WUFI pro. 4.1, the short-wave absorptivity of common building materials is provided and separately treated as its impact on the surface temperature is significant. It also has a user-defined option to allow users to input data. For the simulation of brick walls in this project, the short–wave absorptivity of red clay brick provided by the program, 0.68, is used. For the fibre cement walls, the absorptivity is set as 0.5, which is the average of the value for "stucco normal bright", 0.4, and the value for "stucco dark (age)", 0.6. The default long-wave emissivity of 0.9 is used for the exterior surface.

7.2.4 Initial moisture content of wall components

The initial MC of wall components specified in the simulations is based on the measurements of RH and MC readings taken in the experiment for each wall. In detail, for the plywood sheathing, the initial MC is set at the value same as the gravimetric reading on January 1, 2008. The initial MC of the interior gypsum board and butt fibreglass insulation is set at the value equal to the RH reading inside BETF and in the insulation space for the dry walls. For the wet walls, the initial MC in insulation space is set at a slightly higher RH value of 60%RH as measured to take into account the influence of the high initial moisture content in plywood.

The brick veneer and fibre cement claddings are the outer layer, therefore, the most exposed in the weather conditions. The initial MC is adjusted slightly from the outdoor RH measurements based on the sensitivity analysis of the cladding initial MC on the accuracy of simulated MC in plywood for each wall. The thinner cladding and larger vent configurations may result in higher moisture load due to condensation caused by clear-sky effect. Thus, the initial MC of fibre cement is set higher than that of brick veneer. The initial MC of fibre cement in the wet wall is set higher than that in the dry wall, as shown in Table 7-2-5

Table 7-2-5: Initial MC of wall components for the simulation of all four walls

Wall components	BW9		BD10		FD2		FW4	
	RH (%)	MC (kg/m^3)	RH (%)	MC (kg/m^3)	RH (%)	MC (kg/m^3)	RH (%)	MC (kg/m^3)
gypsum	50	4.59	50	4.59	50	4.59	50	4.59
insulation	60	0. 17	50	0.014	50	0.014	60	0.17
plywood	90.7	121.96	87	76.59	83	69.12	90.9	129.6
Brick veneer	91.5	2.9	91.5	2.9				
Fibre cement					93	300	95	330
* Poly and SBP membrane are set at initial MC of 0 kg/m^3 as default in WUFI								

7.2.5 Driving rain load

Two different methods to calculate the driving rain load are offered by WUFI:

- Driving rain coefficients R1 and R2
- ASHRAE Standard 160p (ASHRAE , 2009)

The driving rain coefficients R1 and R2 are used in the equation to estimate the driving rain load on a surface as:

$$R_d = R_h \cdot (R1 + R2 \cdot V_{wind}) \tag{7-2}$$

where R_d is hourly driving rain, mm/hr, R_h is hourly horizontal rainfall intensity, mm/hr, V_{wind} is the mean wind velocity, R1 is the coefficient for the inclination of surface, and R2 is driving rain factor for surface of building envelope. For vertical surfaces, R1 is zero. R2 is 0.07 s/m for surfaces at the center of a facade on a low-rise building (WUFI, 2007). It may even be greater at exposed locations such as at the corners or the edges of a building. Thus WUFI allows users to input their own coefficient according to measurement or user's knowledge.

On the other hand, the driving rain load on a vertical wall can be computed using the method described in ASHRAE Standard 160P "Design Criteria for Moisture Control in Buildings" (ASHRAE, 2009). The equation used in this method is as:

$$R_d = R_h \cdot EF_{DR} \cdot DF_{DR} \cdot 0.2 \cdot V_{wind} \tag{7-3}$$

where R_d is driving rain, mm/hr, R_h is hourly horizontal rainfall rate or intensity, mm/hr, V_{wind} is the mean wind velocity, EF_{DR} is a rain exposed factor and DF_{DR} is a rain deposition factor, 0.2 is the empirical constant driving rain factor in an air field, i.e. free standing without disturbing from surroundings such as buildings and trees, s/m.

The driving rain load in the simulation has a significant influence on the results for MC in plywood sheathing. Therefore, the driving rain factor for the walls (DRF) will be calculated using the on-site measurements of horizontal rainfall and driving rain on the SE façade of BETF taken during the same time period as the simulation. The DRF can be computed as expressed in the following equation:

$$DRF = \frac{R_d}{R_h \cdot V} \tag{7-4}$$

The results of monthly average DRFs are calculated to evaluate the difference of DRF every month, as shown in Figure 7-2-1. The locations of rain gages at the surface of SE façade are shown in Figure 7-2-2. The experimental DRFs are found to be different in each month and at different locations. The DRF is approximately 0.2 s/m in January while is 0.05 – 0.07 s/m from February to April. The DRF in June is the least and is only 0.02 s/m.

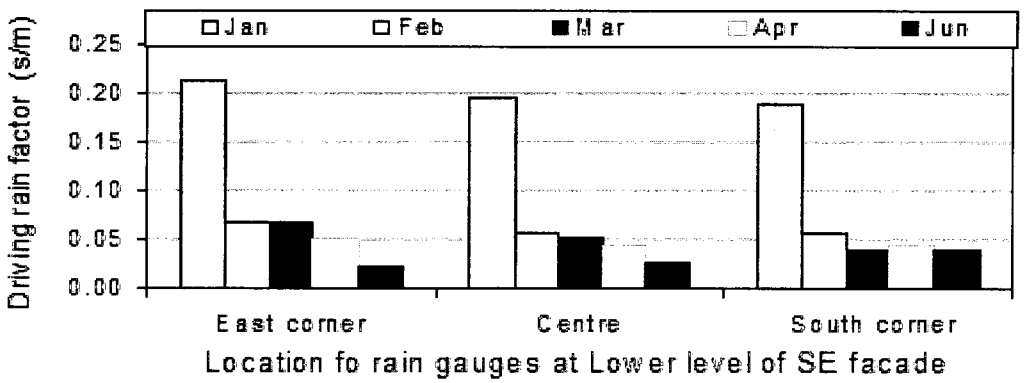

Figure 7-2-1: Monthly average driving rain factor (DRF) calculated using wind-driven rain measurement at the Lower level of SE façade of BETF with horizontal rainfall and on-site wind speed.

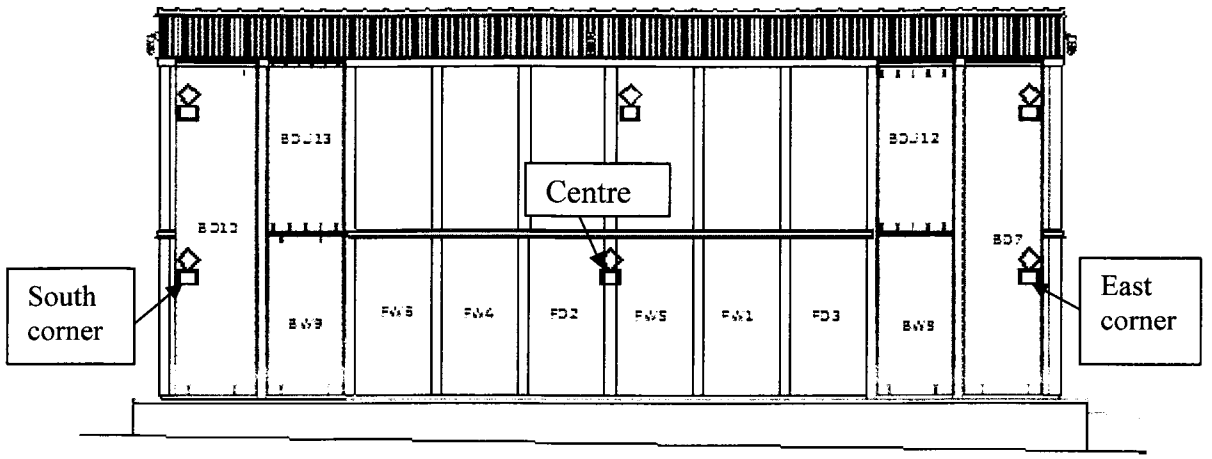

Figure 7-2-2: Locations of rain gauges at the SE façade of BETF.

For the simulations, WUFI only takes a constant DRF for the driving rain coefficient. Thus, the average value of experimental DRF will be used for the input of simulation as shown in Figure 7-2-3. Since the fibre cement walls of FD2 and FW4 are located at the centre and BW9 and BD10 are located near the south corner, the DRF of 0.07 is used for the simulation. However, there is a disadvantage to use average values of DRF. The driving rain load will be under-estimated in January while over-estimated in June.

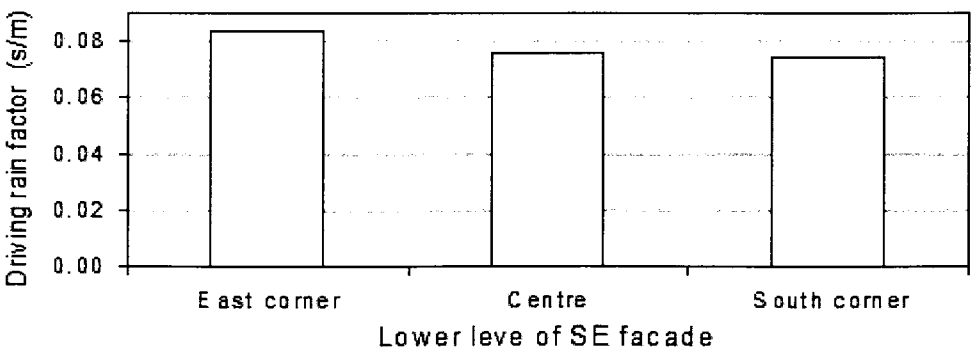

Figure 7-2-3: Average driving rain factor calculated using wind-driven rain measurement at the Lower level of SE façade of BETF from Jan. to June, 08.

7.2.6 Cavity ventilation rates

Ventilation air change rate is one of the important parameters for simulation of MC in sheathing of the ventilated rainscreen walls. The predicted hourly cavity air change rates (ACH) will be used for simulation since the hourly air change rate can not be accurately estimated using a single point air speed measurement. In addition, the comparison of air change rate between predictions and measurements using tracer gas technique show good agreements according to Bassett and McNeil (2005a), as shown in Figure 7-2-4 and 7-2-5. The average predicted ACH used is 6 ACH for BW9 and 4 ACH for BD10. The average predicted ACH is 89 ACH for FD2 and 318 ACH for FW4.

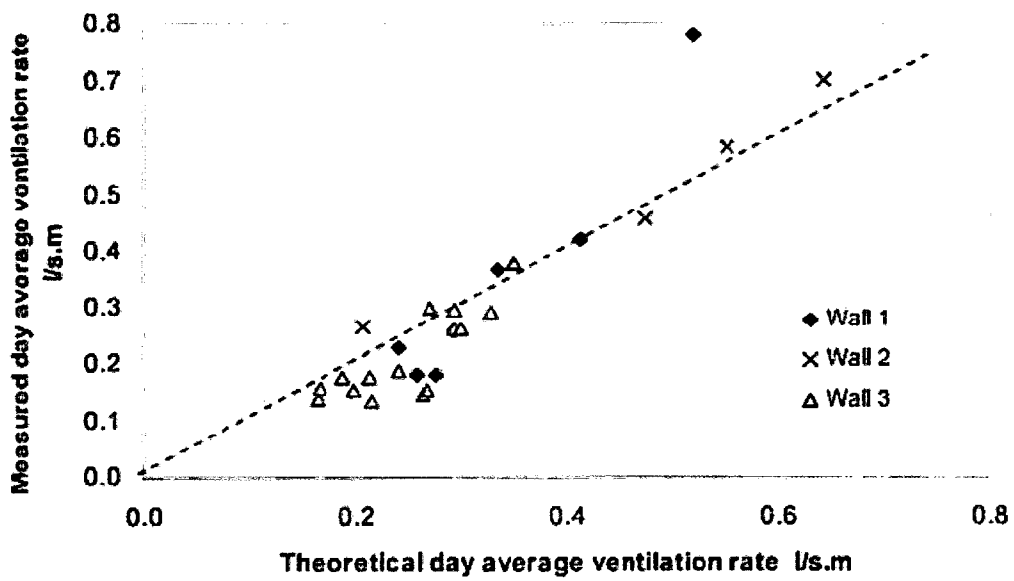

Figure 7-2-4: Day average ventilation rates in open rainscreen wall clad with stucco cladding with non-intentional top vent (adapted from Bassett and McNeil, 2005a).

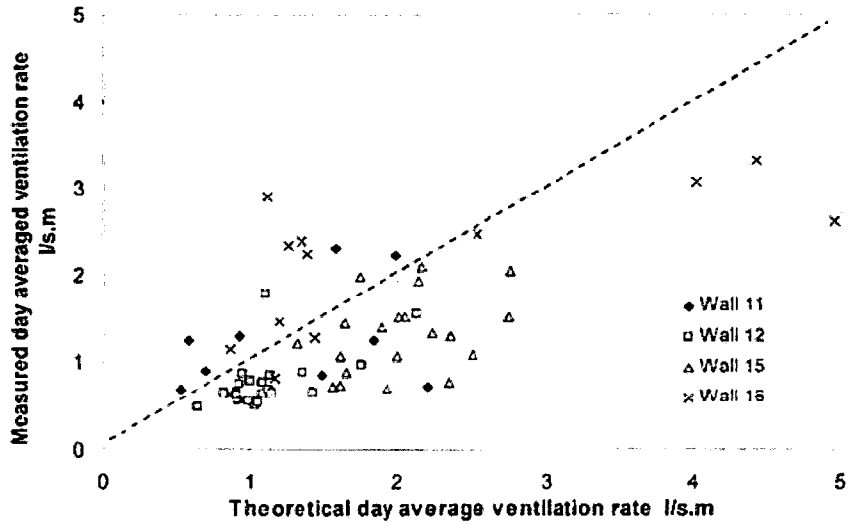

Figure 7-2-5: Day averaged ventilation rates in ventilated rainscreen walls clad with stucco cladding (adapted from Bassett and McNeil, 2005a).

7.3 Comparison of results between simulations and measurements

The results of simulations, generally, have good agreements with experimental measurements of MC in plywood sheathing. The average differences for all four walls are within 1 % with a maximum of 2% for brick walls and 4% for fibre cement walls, indicating that WUFI can simulate the hygrothermal performance of building envelopes with a reasonable accuracy as long as the input data are accurate enough.

7.3.1 Brick walls of BW9 and BD10

The simulations of brick walls BW9 and BD10 were run with the simplified radiation mode, i.e. without clear-sky effect. The results shown in Figure 7-3-1 and 7-3-2 indicate that simulations have quite good agreements with the experimental results except for at

the beginning of the test. The average differences for both walls are within 1% MC with a maximum of 2% MC.

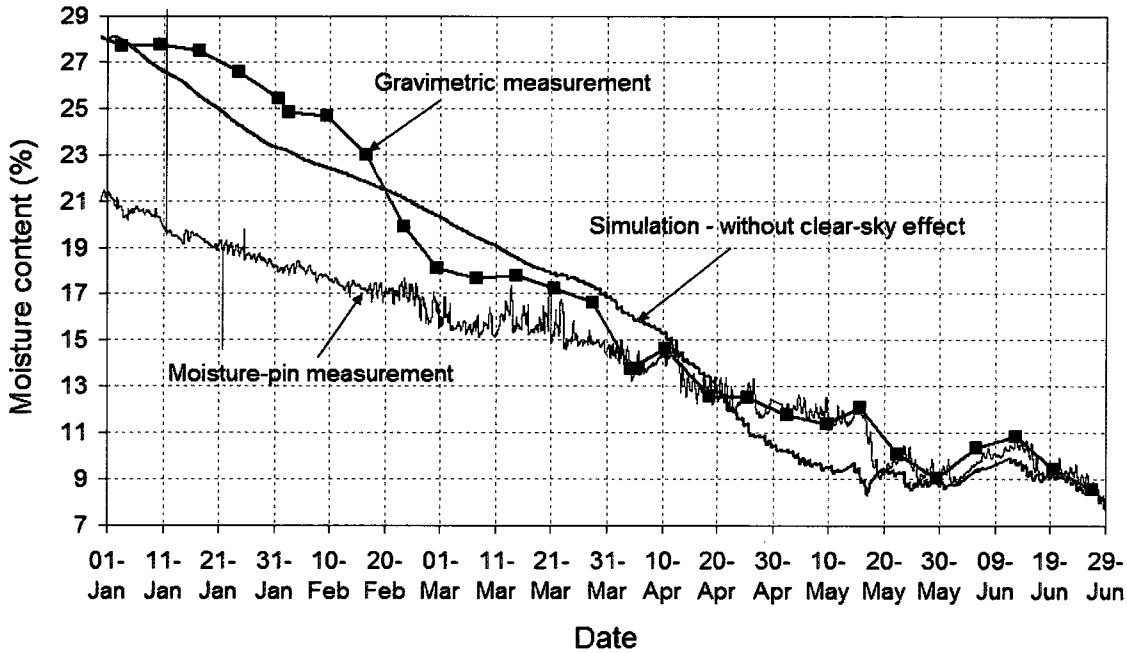

Figure 7-3-1: Comparison of MC in plywood sheathing (medium density) of BW9 between measurements and WUFI simulation (simplified long-wave radiation mode).

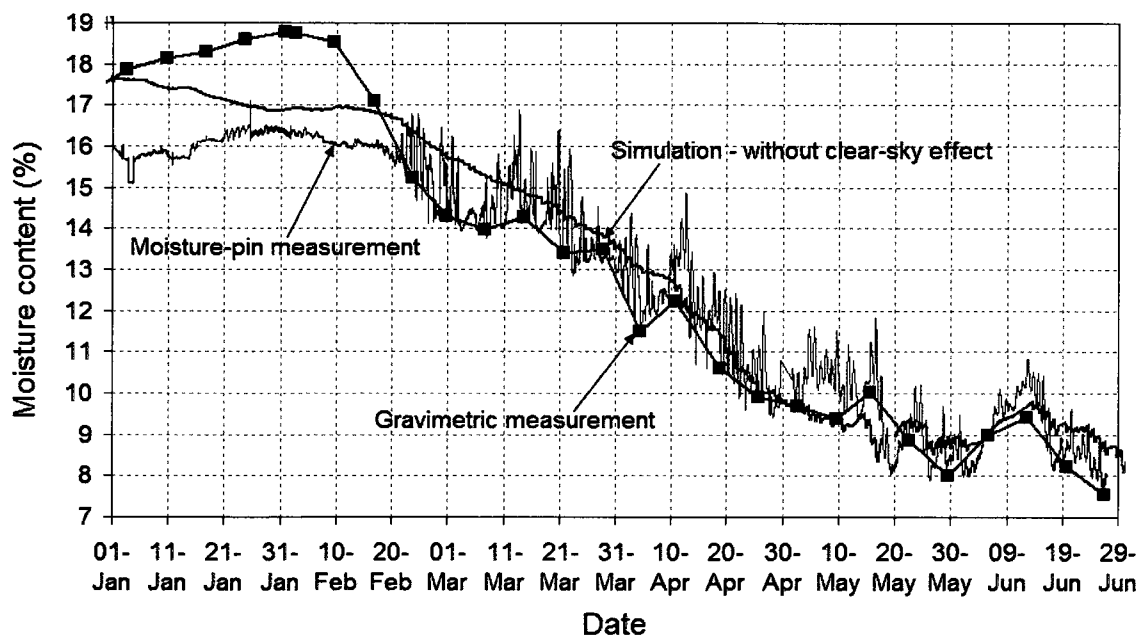

Figure 7-3-2: Comparison of MC in plywood sheathing (medium density) of BD10 between measurements and WUFI simulation (simplified long-wave radiation mode).

However, simulations do not show wetting in BD10 and slow drying in BW9 from January to February. It also does not have a sharp drop of MC during the sunny period in February as the gravimetric measurement does. The reasons affected the simulation results may be the combination effect of underestimating the WDR using average DRF, and using constant and non-moisture-dependent thermal conductivity measured in the drying conditions from WUFI's database; hence it overestimates drying in plywood in January and has no fast drying appeared in the sunny period in February.

7.3.2 Fibre cement walls of FD2 and FW4

Fibre cement walls of FD2 and FW4 are adjacent to each other on the centre of SE façade of BETF. However, FW4 has as much twice condensation hours as FD2 in the winter from the beginning of the experiment, December 2007 to the end of February 2008. It is mainly caused by the larger vent area and higher initial MC of plywood sheathing. The higher cavity ventilation rate induced by the larger vent area in combination with the clear-sky effect resulted in more hours of lower surface temperatures of fibre cement cladding than outdoor air temperature. Even slightly lower surface temperatures on the cladding than those of FD2 can cause many more condensation hours since the ambient air is at a very high RH level in the winter.

The simulations of FD2 were run with the simplified radiation mode while the simulations of FW4 were run with the explicit full radiation balance mode since the condensation levels are much higher. For FD2, the comparison of MC in plywood sheathing between simulation and experimental measurements are shown in Figure 7-3-3.

The simulation results have a good agreement with the experimental results measured by both gravimetric sample and moisture-pin, except in January. The simulation results correlate better with experimental measurement of moisture-pin than the gravimetric measurement. The average difference between simulations and experimental results measured by moisture-pin are within 1% MC with a maximum difference of 2.5% MC. The difference between simulations and experimental results measured with gravimetric sample has an average of 1% MC with a maximum 3.5% MC.

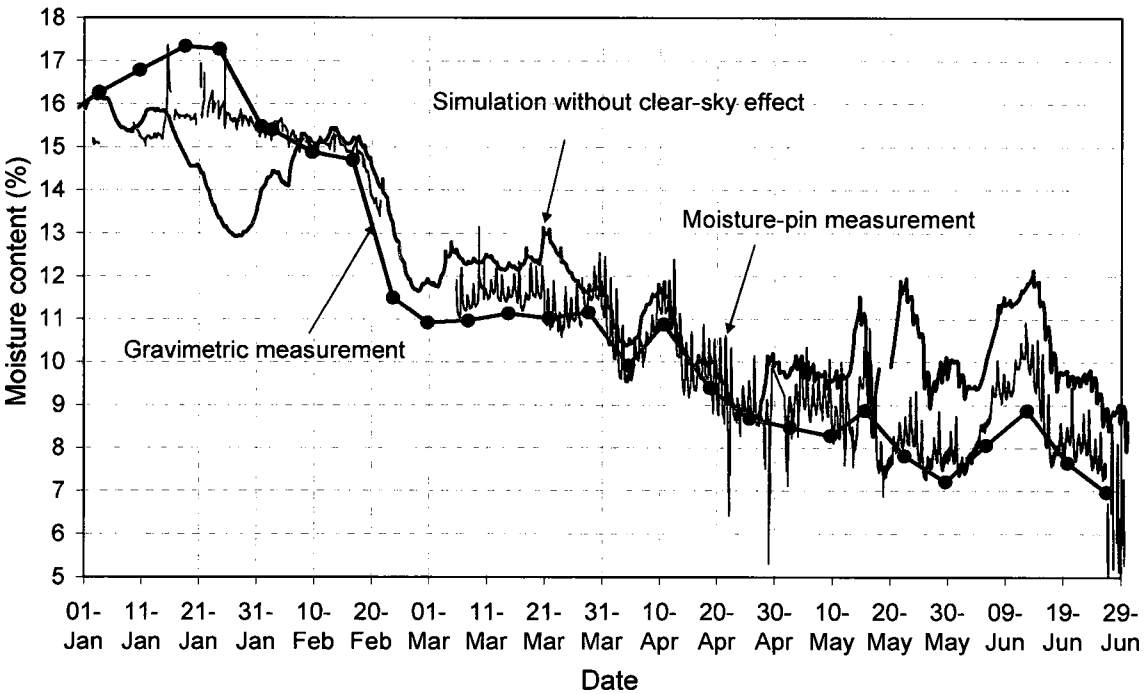

Figure 7-3-3: Comparison of MC in plywood sheathing (medium density) of FD2 between measurements and WUFI simulations (simplified long-wave radiation mode).

The large difference between simulation and experiment results occurs in January. The simulation result without clear-sky effect shows that the solar radiation drying dominantly affects the MC of plywood sheathing, which results in a sudden drop from about 16% to 13% during the sunny period on January 20 - 25. However, the experimental results showed the MC in plywood increased by 1.5% instead. It is

probably because the driving rain load effect in this month is underestimated. The rain load calculated using average experimental DRF of 0.07 for simulation is almost three times less than the actual DRF of 0.2 in January.. On the other hand, the average DRF for simulation is greater than actual DRF of 0.044 -0.027 after March shown in Figure 7-2-4. The simulation results show higher MC in plywood sheathing than those of experimental results especially in June due to the overestimation of driving rain load effect.

Figure 7-3-4 shows the results of MC in plywood sheathing in FW4 by both simulations and experimental measurements. The simulation results agree well with the measurements and the average difference in MC is within 1% with a maximum of 4% MC. The larger discrepancies occur during the sunny period on January 17 – 25 and several rainy periods in May and June. Same as for FD2, the use of average DRF for driving rain loads in simulations is probably the major contributing factor for the lower MC in plywood during the winter but higher MC value in the spring.

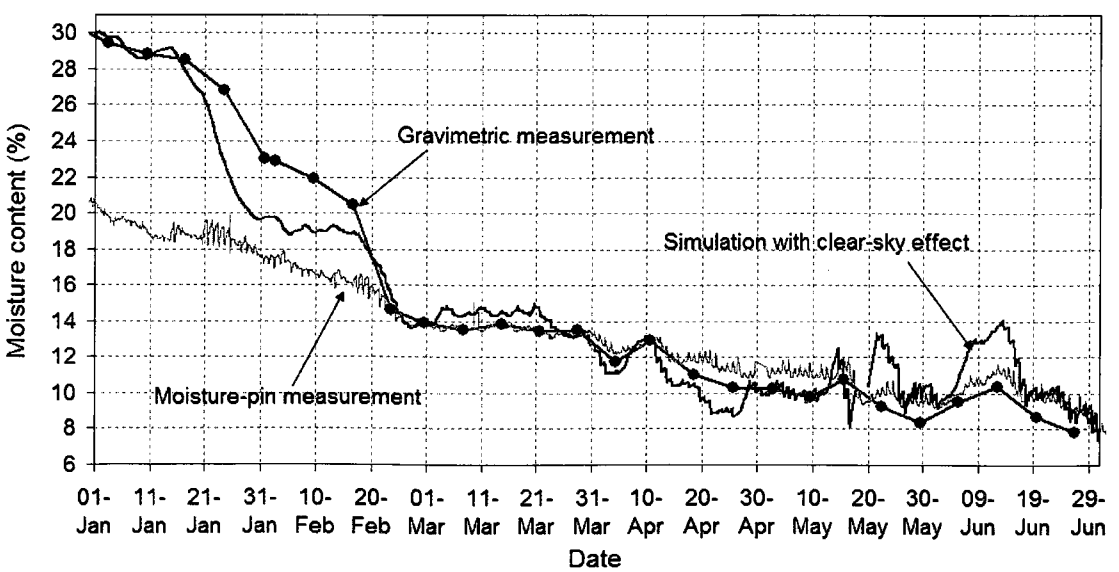

Figure 7-3-4: Comparison of MC in plywood sheathing (medium density) of FW4 between measurements and WUFI simulations (explicit full radiation balance mode).

7.4 Sensitivity of input parameters

WUFI pro. 4.1 is designed for one-dimensional transient heat and moisture transport in components of building envelopes. The model uses numerical and physical equations to solve the heat and moisture transfer and accumulation through the wall assemblies and in each component. Hence, input parameters in building material properties, surface transfer coefficients and environment conditions will affect the accuracy of the simulation results. On the other hand, the software has limitations because the model simplifies the complex phenomenon of heat, air and moisture response for the realistic weather and indoor conditions.

The material properties of building components, MC of brick veneer and fibre cement cladding, and the emissivity of cladding are not measured in the experimental study. Thus, a sensitivity study is conducted to evaluate the impact of input data on the accuracy of MC predication using simulations including different properties of plywood, initial MC of brick veneer and fibre cement cladding, and different radiation modes with and without clear sky effect.

7.4.1 Plywood sheathing properties

Three types of plywood identified by their density and properties are included in the database of WUFI for North American materials. The main difference in the properties between these three types of plywood is the diffusion resistance factor, as listed in Table 7-4-1.

Table 7-4-1: Properties of three types of plywood in WUFI's database

Plywood type	Bulk density	porosity	Specific heat capacity	Thermal conductivity	Vapour diffusion resistance factor
	Kg/m^3	m^3/m^3	J/(kg•K)	W/(m•K)	-
Plywood high	600	0.96	1800	0.101	383.4
Plywood	470	0.69	1800	0.084	**1078.2**
Plywood low	400	0.64	1800	0.068	493.1

The diffusion resistance factor of "Plywood" (medium density) is 2.8 and 2.2 times greater than that of "Plywood high" (high density) and that of "Plywood low" (low density), respectively. Without property measurements of plywood, selecting the proper type of plywood from WUFI's database for the simulations becomes very critical for the moisture performance through wall assembly components. The density of plywood used in the experiment is 432 kg/m^3 and between the densities of "plywood" and "plywood low". The simulations using both types of plywood were performed to determine which type of plywood will give better simulation results in comparison to the experimental measurements.

The results of comparison for two brick walls and two fibre cement walls are shown in Figure 7-4-1 to Figure 7-4-4. Overall, the simulation results using "Plywood" have a better agreement with the experimental measurements. Using "Plywood low", the simulations overestimate the plywood sheathing drying capacity, especially from January to February. The simulated MC in plywood is a maximum of 6% lower than the measurement for brick wall of BW9 and of 4% lower than the measurements for BD10. For the fibre cement walls, the overestimations are more obvious in the winter, a maximum of 6% for FD2 and of 8% for FW4 in the January and February. The comparison indicates that it is more suitable to use the properties of "Plywood" for the

commonly used plywood used in construction. Similar conclusion was drawn by Finch (2009).

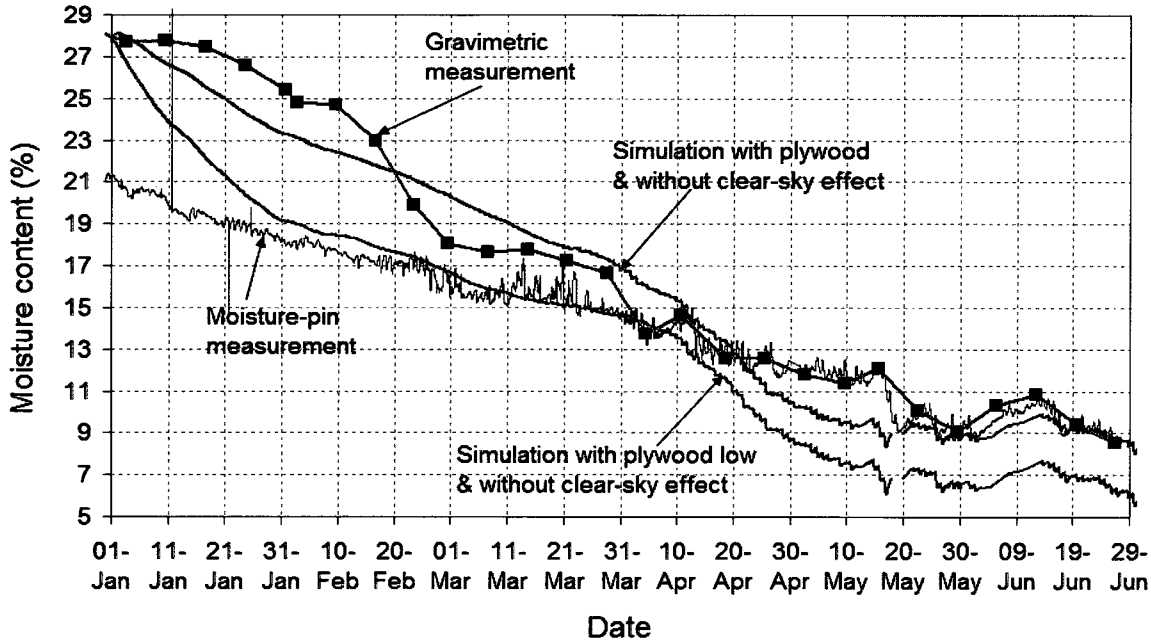

Figure 7-4-1: Comparison of MC in plywood sheathing of BW9 between measurements and WUFI simulations (simplified long-wave radiation mode) using different plywood properties.

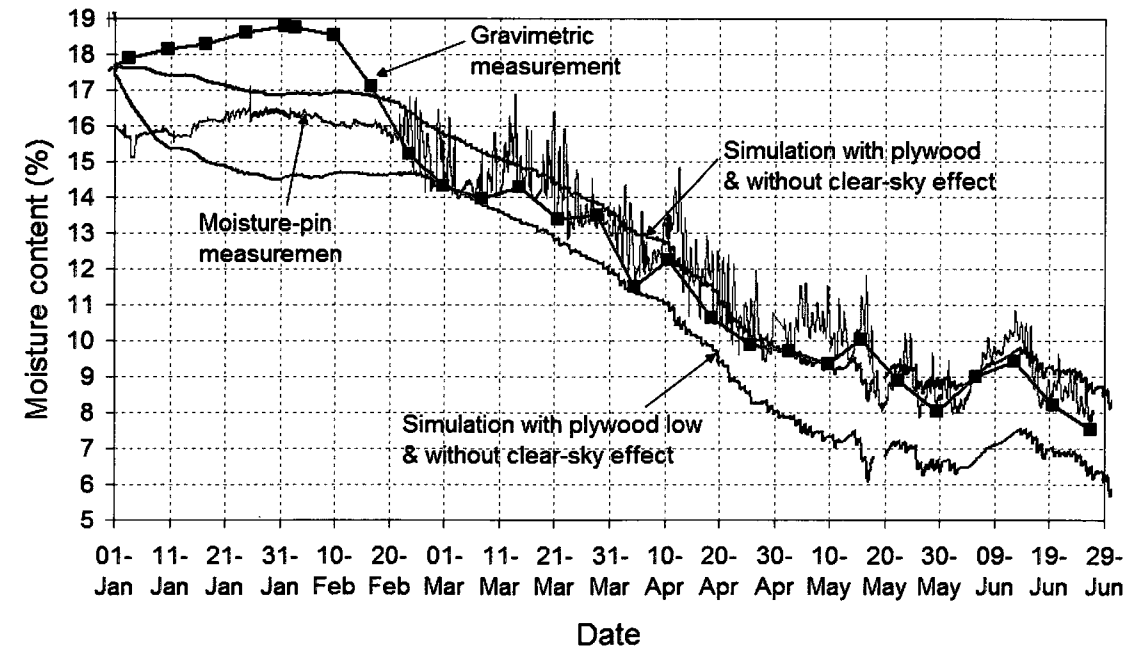

Figure 7-4-2: Comparison of MC in plywood sheathing of BD10 between measurements and WUFI simulations (simplified long-wave radiation mode) using different plywood properties.

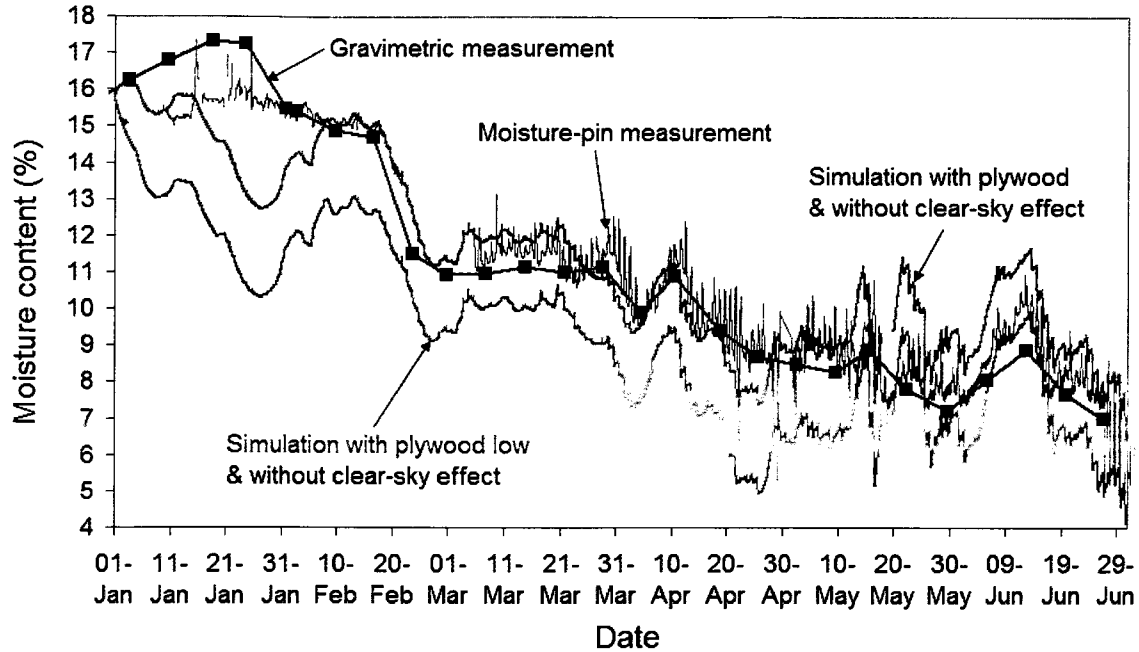

Figure 7-4-3: Comparison of MC in plywood sheathing of FD2 between measurements and WUFI simulations (simplified long-wave radiation mode) using different plywood properties.

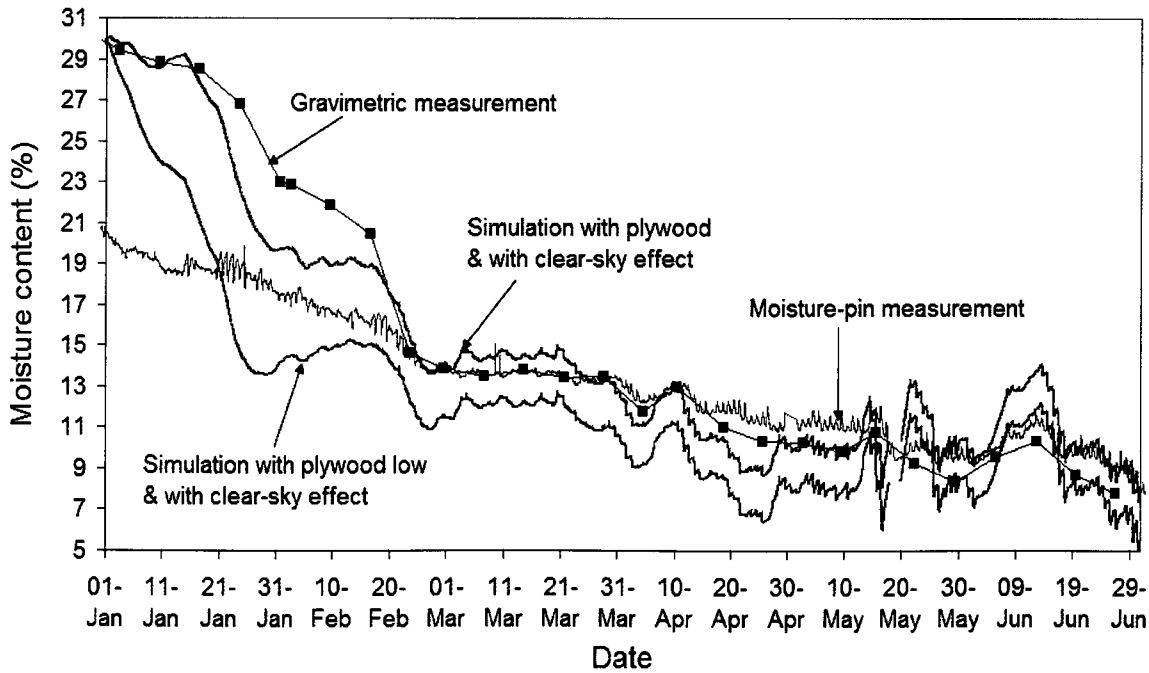

Figure 7-4-4: Comparison of MC in plywood sheathing of FW4 between measurements and WUFI simulations (explicit full radiation balance mode) using different plywood properties.

7.4.2 Clear-sky effect

Figure 7-4-5 and Figure 7-4-6 show the comparison of MC in plywood sheathing of brick walls between measurements and simulations with and without clear-sky effect

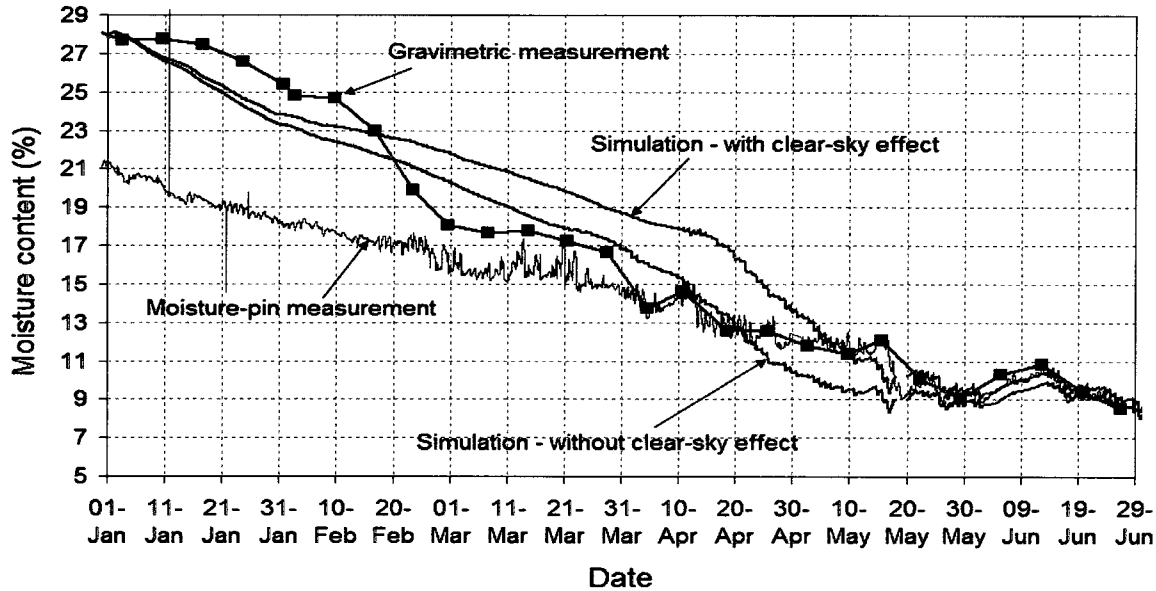

Figure 7-4-5: Comparison of MC in plywood sheathing (medium density) of BW9 between measurements and WUFI simulations with / without clear-sky effect (using simplified long-wave radiation mode / explicit full radiation balance mode).

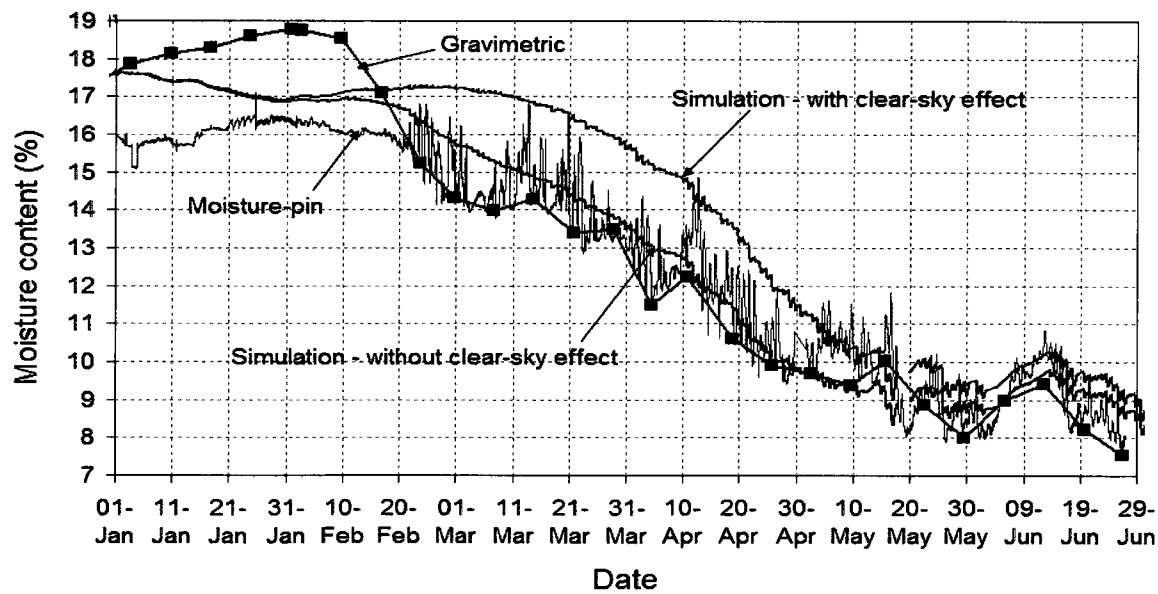

Figure 7-4-6: Comparison of MC in plywood sheathing (medium density) of BD10 between measurements and WUFI simulations with / without clear-sky effect (using simplified long-wave radiation mode / explicit full radiation balance mode).

The explicit full radiation balance mode, i.e. with clear-sky effect, results in an overestimation of MC in plywood from February to April, especially for BD10. The simulated MC in plywood increases in February instead of decreasing as shown by the measurements. On the other hand, the simulated MC in plywood using the simplified radiation mode, without clear-sky radiation, correlates better to the measurements.

As shown in Figure 7-4-7 and Figure 7-4-8, there are a very few condensation hours at the exterior and cavity surfaces of brick veneers in both walls due to the thermal and moisture mass storage capacity of brick. Therefore, the clear-sky effect is not significant.

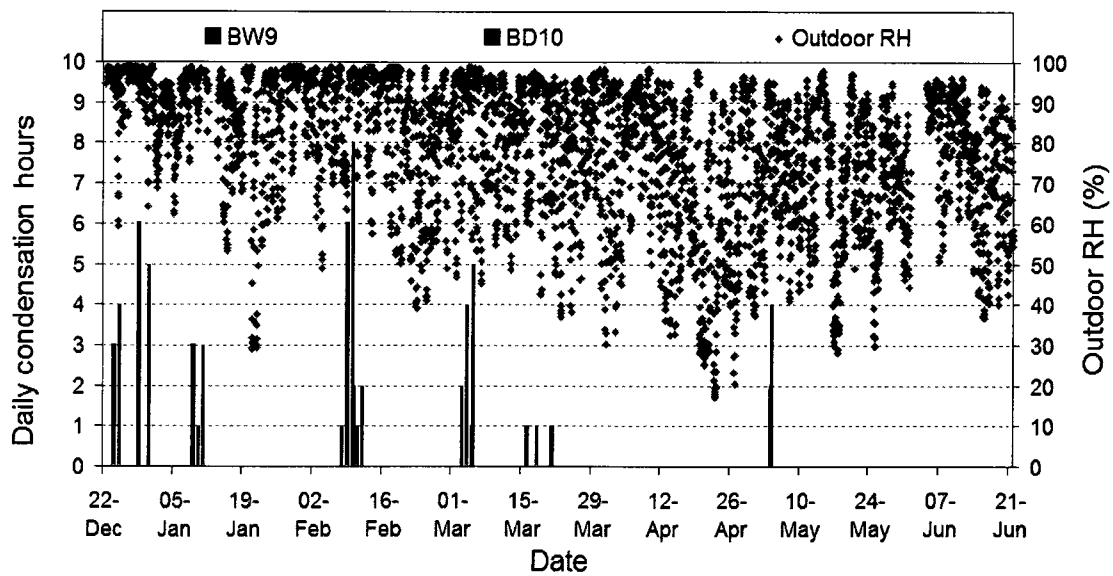

Figure 7-4-7: Comparison of daily condensation hours on exterior surface of brick veneer between BW9 and BD10 during Dec. 22, 07 to Jun. 21, 08.

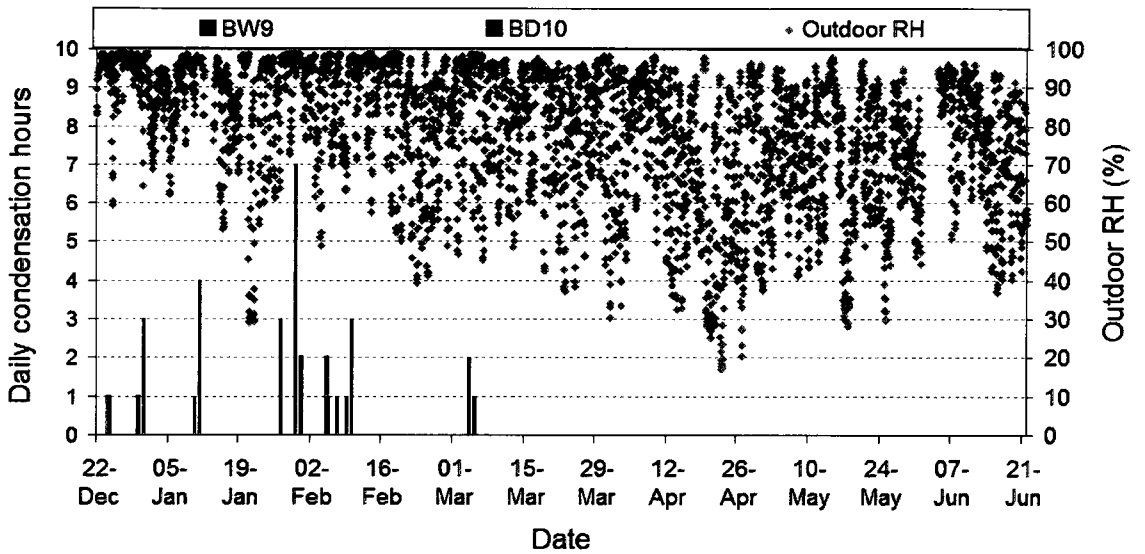

Figure 7-4-8: Comparison of daily condensation hours on cavity-surface of brick veneer between BW9 and BD10 during Dec. 22, 07 to Jun. 21, 08.

Fibre cement cladding has less mass storage capacity due to its thinner thickness; therefore, the radiation balance is more sensitive. The simulation runs without clear-sky effect has a better agreement with the measurements of FD2, as shown in Figure 7-4-9. However, simulated MC in plywood in January with clear-sky effect matched better with the experiment results. Its pattern at the beginning is similar to that of the gravimetric measurements when the outdoor RH is high; then the MC jumped by 2%, the same as the moisture-pin measurement and the MC dropped quickly with lower outdoor RH to the end of January. Starting from the end of January, simulation results with the simplified radiation model agrees well with the measurements. The simulations with the full radiation model seem over-estimate the MC in plywood. Further study is required to investigate the actual causes for discrepancies.

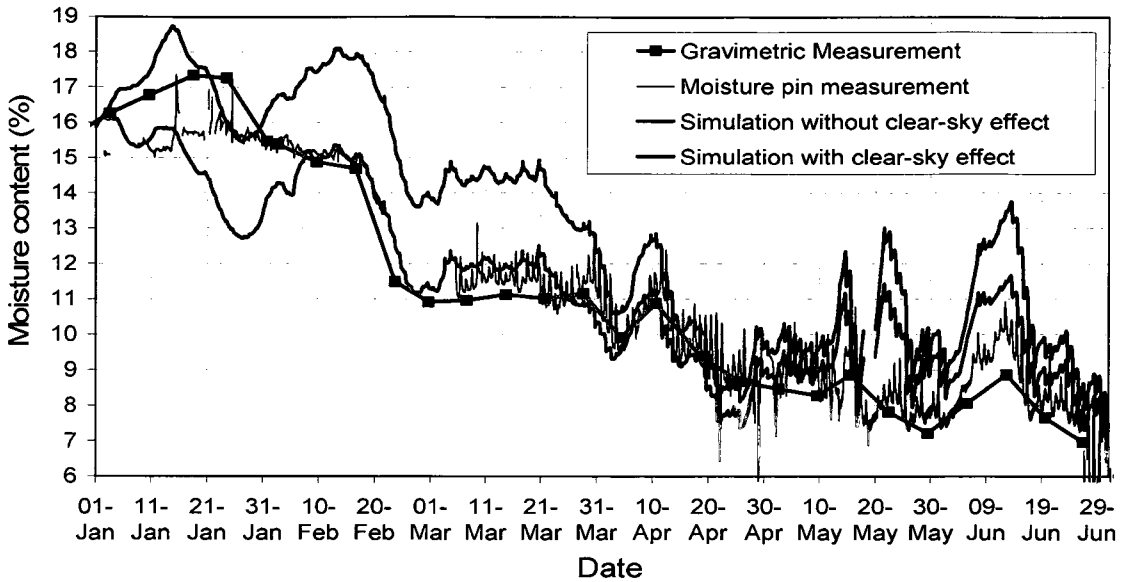

Figure 7-4-9: Comparison of MC in plywood sheathing (medium density) of FD2 between measurements and WUFI simulations with / without clear-sky effect (using simplified long-wave radiation mode / explicit full radiation balance mode).

The simulation result with clear-sky effect agrees better with measurements for FW4 for most of the time, except for some period in May and June, as shown in Figure 7-4-10 due to the use of average DRF.

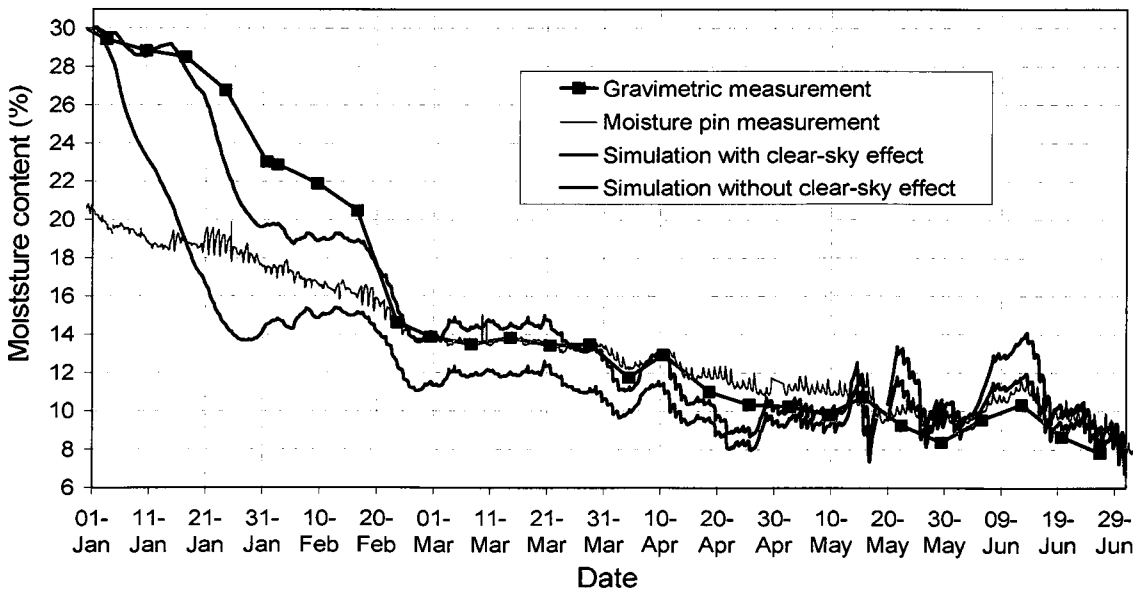

Figure 7-4-10: Comparison of MC in plywood sheathing (medium density) of FW4 between measurements and WUFI simulations with / without clear-sky effect (using simplified long-wave radiation mode /explicit full radiation balance mode).

FW4 and FD2 are located next to each other and the differences between them include top vent size and the initial MC of plywood sheathing. FW4 has a larger top vent size and a higher initial moisture content, which results in more days of condensation on the exterior and cavity-surface of fibre cement cladding than that in FD2 from December to February, as shown in Figure 7-4-11 and Figure 7-4-12.

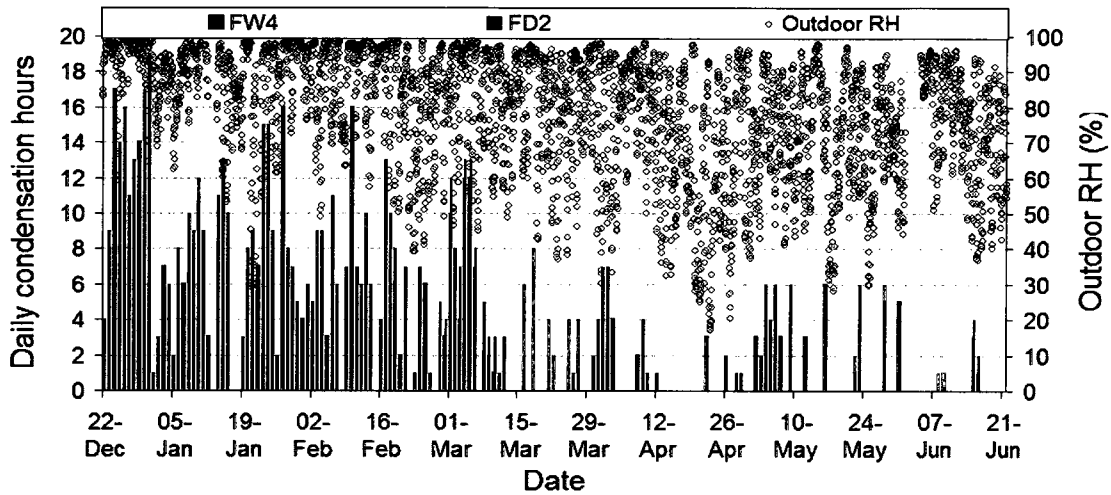

Figure 7-4-11: Comparison of daily condensation hours on exterior surface of fibre cement cladding between FD2 and FW4 during Dec. 22, 07 to Jun. 21, 08.

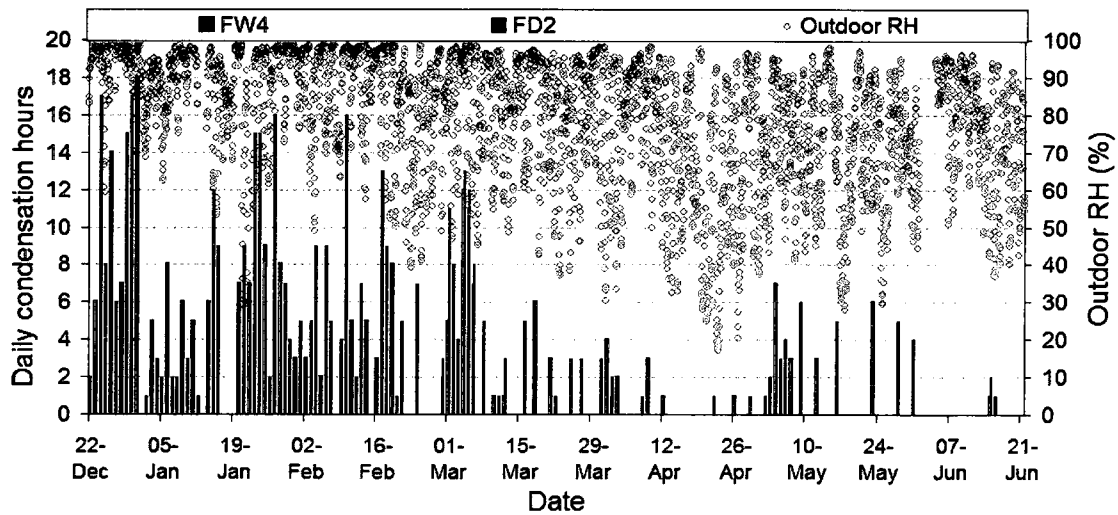

Figure 7-4-12: Comparison of daily condensation hours on cavity-surface of fibre cement cladding between FD2 and FW4 during Dec. 22, 07 to Jun. 21, 08.

Looking into the cavity surface temperatures of fibre cement cladding in the simulation running the same mode between FD2 and FW4, the difference is very little. Conversely, the measurement of cavity surface temperature difference of both walls is much larger than the temperature difference of simulations whether or not running with clear-sky effect. Actually, the difference in measured cladding surface temperatures between FD2 and FW4 is similar to the difference in simulated surface temperatures between FD2 (without clear-sky effect) and FW4 (with clear-sky effect).

For example, Figure 7-4-13 shows the cavity-surface temperature difference between FD2 and FW4 in the simulation with / without clear-sky effect and measurements from January 1 to February 27, 2008.

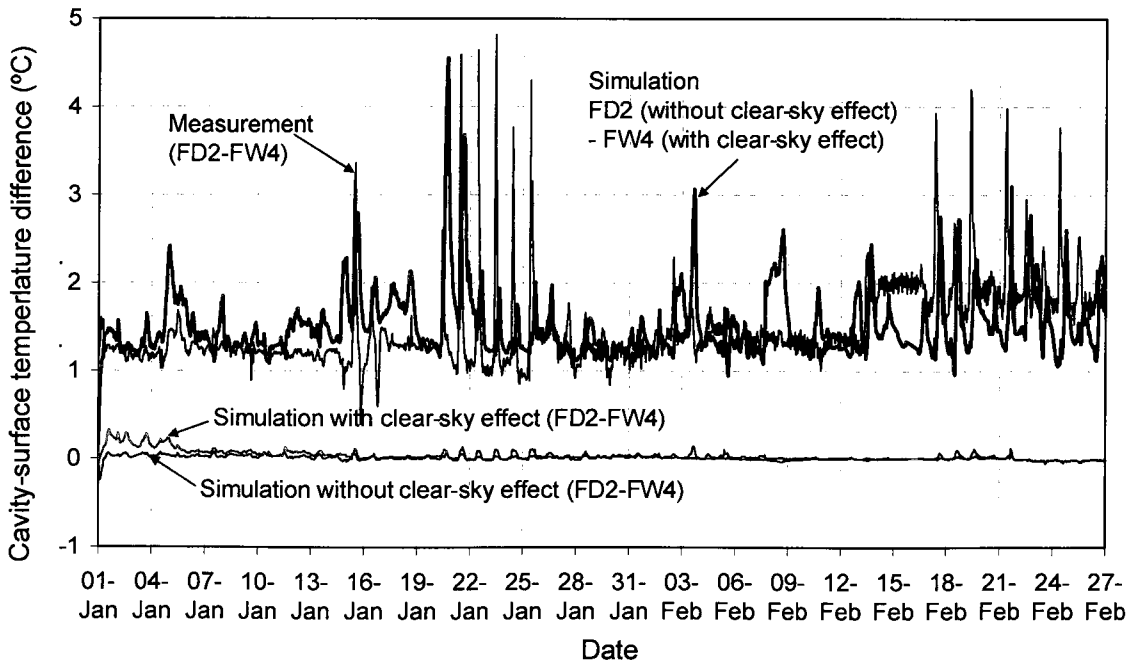

Figure 7-4-13: Cavity-surface temperature differences of fibre cement claddings of FD2 and FW4 in WUFI simulation with / without clear-sky effect and measurements during Jan 1 to Feb 27, 08.

The figure indicates that the temperature difference is almost equal to zero when the simulations of both walls run in the same modes, which mean that the simulated cavity-

surface temperatures of fibre cement cladding for both walls are very similar when running in the same weather conditions.

However, in the reality, the cavity-surface temperatures between FD2 and FW4 are different because the fibre cement cladding of both walls experience different conditions (different vent configurations and initial MC of plywood sheathing). As a result, the cavity-surface temperature difference of fibre cement cladding between FD2 and FW4 are mostly 1 - 2 °C. The temperature in FD2 is always higher than that in FW4. However, further research is required to identify the actual causes for the discrepancy between simulation and measurements.

7.4.3 Initial MC of rainscreen claddings (brick and fibre cement)

The initial default values of brick and fibre cement in WUFI are of 90% and 80%, respectively. The RH of the ambient air measured is in the range of 89 – 94% at the end of December 2007. Due to the lack of MC measurement in claddings, several initial MC in brick veneer and fibre cement cladding are tested and the simulation results are compared to measurements, as listed in Table 7-4-2.

Table 7-4-2: Initial MC in rainscreen (brick veneer and fibre cement cladding) chosen for simulations of four walls

Wall	BW9		BD10		FD2		FW4	
rainscreen	Brick veneer				Fibre cement cladding			
	RH %	MC kg/m³	RH %	MC kg/m³	RH %	MC, kg/m³	RH %	MC kg/m³
WUFI's default	90	2.5	90	2.5	80	190	80	190
Initial MC of rainscreen for simulation	80	2.3	80	2.3	80	190	80	190
	91.5	2.9	91.5	2.9	90	250	90	250
	92	6	92	6	93	300	95	330
	93	12.3	93	12.3	95	360	100	432

The comparisons of MC in plywood between measurements of gravimetric samples, moisture-pins and simulation results with different initial MC in brick veneer for BW9 and BD10 are shown in Figure 7-4-14 and 7-4-15. These simulations are run with the simplified radiation mode, i.e. without clear-sky effect. The simulation results with all the different initial MC of brick veneer from 80 – 93% RH are the same from the middle of May to the end of June and slightly different in January. The simulated MCs in plywood, with initial MC in brick between 80% RH and 91.5% RH, have very little difference and they all matches the gravimetric measurements of both walls with a reasonable accuracy. However, when the assumed initial MC in brick is above 91.5% RH, the difference between measurements and simulations become bigger, especially for BD10. With 0.5 – 1.5% higher initial MC, WUFI overestimates the MC in plywood from February to the end of April by a maximum of 3-4% compared to measurements. The MC profile for BD10 even changes and the MC level stays high until the end of April when the initial MC of brick is 93%.

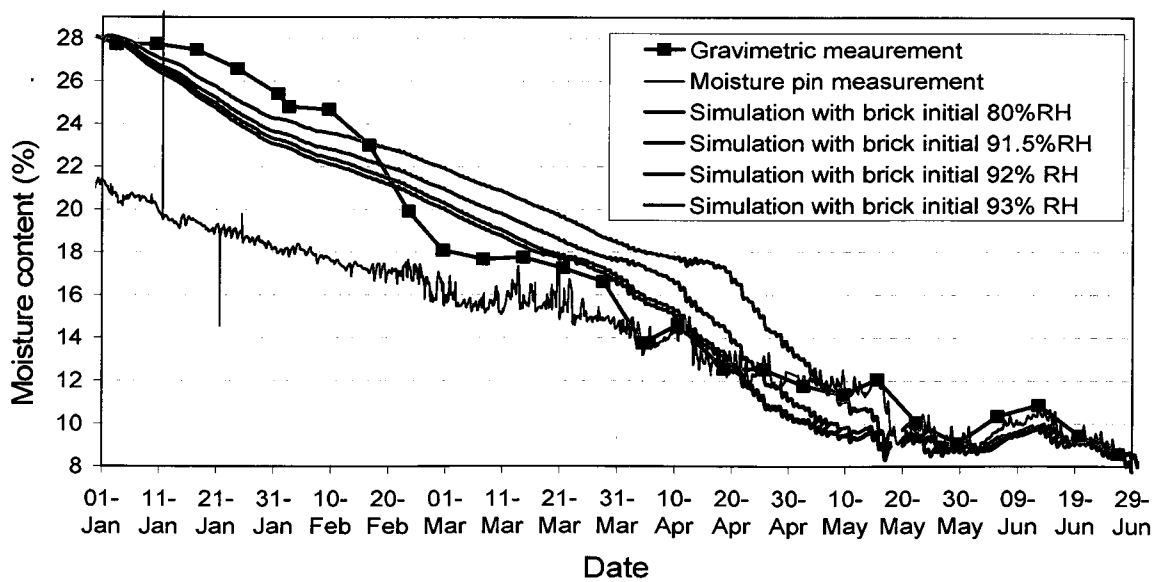

Figure 7-4-14: Comparison of MC in plywood sheathing (medium density) of BW9 between measurements and WUFI simulations (simplified long-wave radiation mode) with different initial MC of brick veneer.

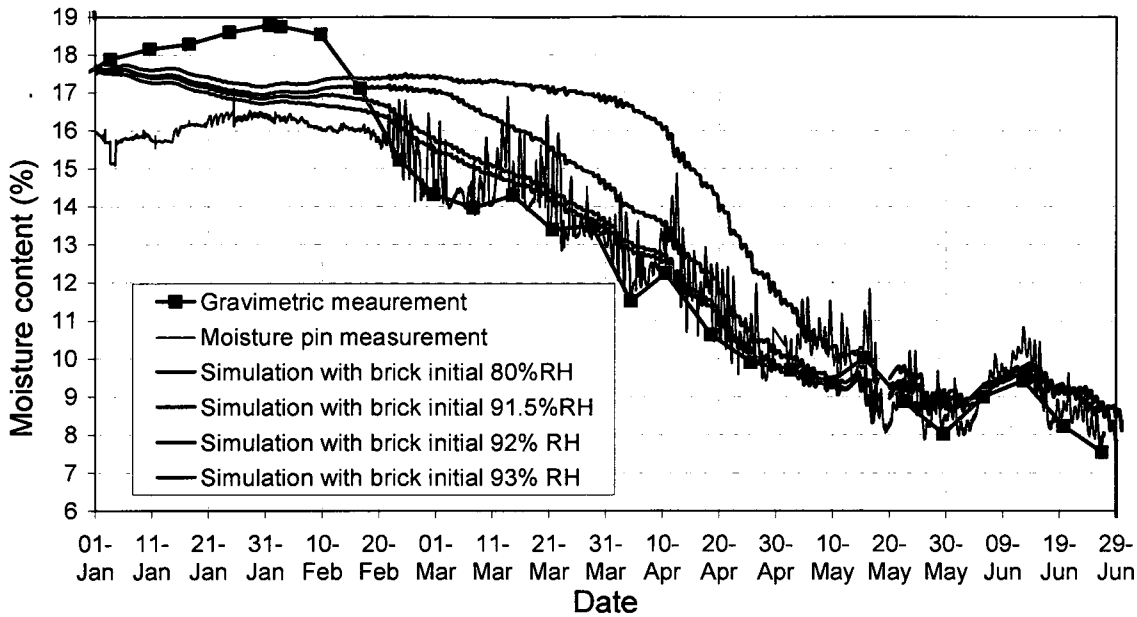

Figure 7-4-15: Comparison of MC in plywood sheathing (medium density) of BD10 between measurements and WUFI simulations (simplified long-wave radiation mode) with different initial MC of brick veneer.

Looking into the properties of brick, it is found that its moisture storage capacity profile is much different when its RH reaches to above 91.5% (WUFI, 2007), as shown in Figure 7-4-16. The moisture storage function is low between 0 – 91.5% RH and the moisture gradually increase to 2.9 kg/m³.

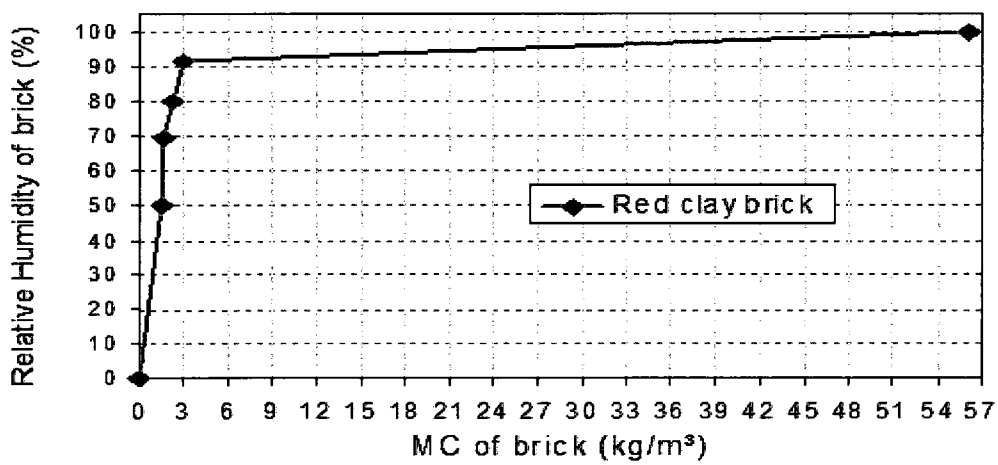

Figure 7-4-16: Moisture storage capacity profile of RH with MC of red clay brick in WUFI's database.

However, it can store 53 kg/m³ moisture from 91.5 – 100%RH. Hence, the increase of MC by 1% means the increase of moisture storage capacity by about 6 kg/m³. It helps to explain why the MC in plywood increases dramatically with higher initial MC of brick above 91.5% in the simulations.

For fibre cement wall of FD2 with small top vent, simulations are run with the simplified radiation mode with different initial MCs in fibre cement cladding. The initial MC of fibre cement affects the simulation results of MC in plywood for the first 20 days as shown in Figure 7-4-17. The MC in plywood rapidly decreases and the influence of the initial MC in cladding diminishes.

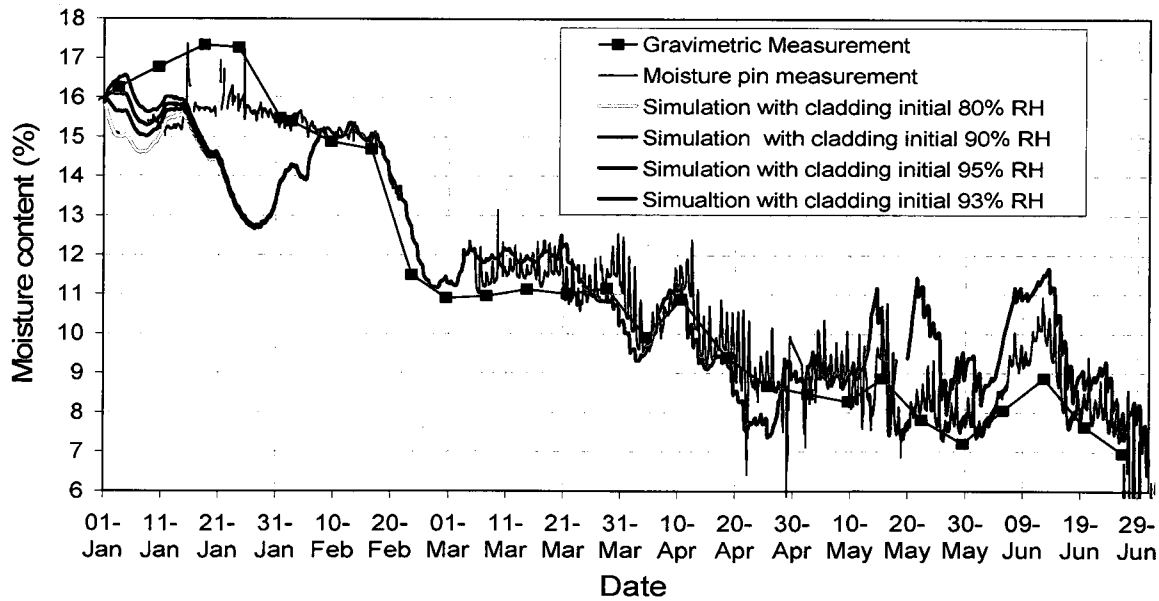

Figure 7-4-17: Comparison of MC in plywood sheathing (medium density) of FD2 between measurements and WUFI simulations (simplified long-wave radiation mode) with different initial MC of fibre cement cladding.

With the explicit full radiation balance mode, i.e. with clear-sky effect, the simulation results of MC in plywood of FW4, with different initial MC in fibre cement cladding, are different in the first two months in winter and then they are the same after sunny period in February, as shown in Figure 7-4-18.

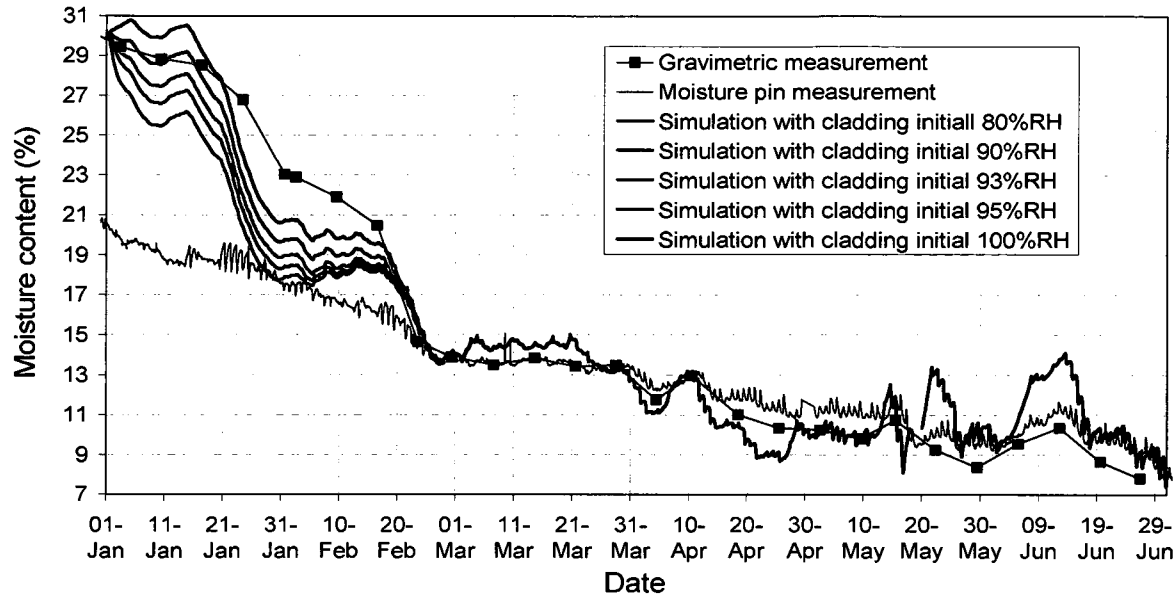

Figure 7-4-18: Comparison of MC in plywood sheathing (medium density) of FW4 between measurements and WUFI simulations (explicit full radiation balance mode) with different initial MC of fibre cement cladding.

The higher the initial MC in fibre cement cladding, the higher the simulated MC in plywood. The condensation at the surfaces of fibre cement affected by clear-sky effect with high RH of ambient air play a significant role to bring in moisture into the air cavity and slow down the drying of plywood sheathing.

7.5 Summary

In this chapter, the MC in plywood sheathing of two brick walls with the same vent configurations, BW9 and BD10, and two fibre cement walls with different vent configurations, FD2 and FW4, were simulated using WUFI pro. 4.1 and the simulation results are compared to experimental measurements.

The comparison shows that simulation results have a good agreement with gravimetric measurements for all four test walls. The average difference in MC of plywood for all the walls are within 1%; and a maximum of 2% MC for brick walls and 4% MC for fibre cement walls. It indicates that WUFI modeling software can be used to predict and evaluate the hygrothermal performance of rainscreen walls with brick (large moisture storage capacity) and fibre cement panel (relatively small moisture storage capacity).

Whether the simplified long-wave radiation mode or explicit full radiation balance mode should be used in simulations using WUFI depends on the rainscreen cladding material and its thickness and the balance between short-wave absorption and long-wave radiation exchange. Based on the comparison of measurement and simulation results, the simulations of rainscreen wall systems with high thermal mass and moisture storage capacity can be run with simplified long-wave radiation mode since the condensation at surface of rainscreen claddings such as brick veneer and concrete rarely occur even in the winter with moderate temperature and high RH.

The simulation of rainscreen wall system with thin panel type non-metal cladding such as fibre cement and stucco can be run with simplified long-wave radiation mode if the top vent is small (1mm) with dry sheathing initially. The surface temperatures of cladding are higher than the dew-point temperature of outdoor air most of the time due to small ventilation rates. However, if the sheathing is initially wet and the vent area is large, i.e. 12mm vent at both top and bottom of cavity, the simulation should be run with explicit full radiation balance mode. The surface temperatures of cladding are lower than the dew-point temperature of moist air frequently in the winter due to large ventilation

Within three types of plywood sheathing in WUFI's database, the properties of "plywood" with medium density are suitable for common plywood used for simulation if users do not have their own material property measurements.

The default initial moisture in brick veneer of 90% RH from WUFI for brick walls is suitable for most situations. For the thin non-metal panel materials with low moisture storage capacity, initial moisture of cladding may need to be set at 93 - 100% RH depending on its surface condensation and RH of outdoor air.

Through the simulations, limitations of WUFI model are found such as clear-sky effect can not be accurately simulated even when the explicit full radiation balance mode is used. Additionally, using average DRF can not accurately simulate the rain load on the exterior surface with time and different rain load, causing over or under-estimation of MC in sheathing.

Chapter 8: Conclusions

8.1 Summary of findings

A full-scale field experiment was conducted to evaluate ventilation drying and wetting of rainscreen wall systems for the coastal climate of British Columbia. The main test variables include vent types and sizes, cavity depths, types of cladding and two levels of moisture loads. Both gravimetric and moisture pins measurements for MC are used to analyze the effect of cavity ventilation on the drying and wetting of plywood sheathing over six months from December 10, 2007 to June 21, 2008. Measurements of temperature and relative humidity are used to evaluate the under-cooling effect on the cavity-surfaces of rainscreen walls. The hygrothermal performance of two brick walls and two fibre cement walls with different vent configurations and initial moisture loads is evaluated using WUFI Pro4.1. The average MC of plywood sheathing obtained from simulations is compared to measurements for each one of the four test walls.

The main conclusions include:

1. Impact of vent configurations on moisture performance of test walls

Measurements show that the provision of top vents for all the test walls helps drying. The significance of cavity ventilation drying and wetting mainly depends on the moisture loads and weather conditions. For the initially wet plywood, fibre cement walls with a 19mm cavity dried slightly faster than the test panel with a 10mm cavity. The sizes of

top slot vent themselves do not make much difference. All test walls managed to dry from an initial of about 28% to below 19% MC in 70 days. The effects of cavity ventilation between brick walls with different vent configurations are more significant than those between in fibre cement panels. However, brick panels took more time than the fibre cement panels to dry below 19% MC; 80 days for the brick wall with top vents while 120 days for the brick wall without top vents.

For initially dry plywood, the cavity depth and vent size has an insignificant effect for the fibre cement panels. For brick walls, the larger ventilation has the greater drying effect. The maximum difference between the dry brick walls can be 5% MC.

2. Impact of vent configurations on the thermal performance of test walls

Over the entire test period, the differences of average temperature gradients through the wall components of all the brick and fibre cement walls are small, indicating cavity ventilation does not increase heat loss in the heating seasons. The average air temperature difference between the cavity and outdoor on the cloudy and rainy days is also small within -2 to 6 °C for all the test walls. However, on the sunny days, the temperature differences at daytime can reach a maximum of 17 - 23°C for the fibre cement walls with a 19mm air cavity, 27 °C for the wall with a 10mm cavity and 15 – 18 °C for brick walls, indicating that high solar radiation in the sunny periods has a significant influence on the drying for wet walls with different vent configurations in the winter.

3. Under-cooling effect

Under-cooling effect is a major factor that provides a moisture source for potential wetting of the plywood sheathing. It also slows and even stops the drying of wet sheathing in the winter. In general, the under-cooling events are more frequent in the winter than the spring for all the test walls during the test period. The condensation only occurs occasionally on the cavity-surface of brick veneers in the winter. The monthly accumulated condensation hours are few (0 – 17 hours) and the condensation frequencies of test time are very low (0 – 5.3%). It indicates that the wood-frame back walls are well protected behind the brick veneer with large mass thermal and moisture storage capacity. The contributing factors for condensation on the surfaces of brick veneer are the locations of test walls, shade by trees nearby the test facility, and initial MC in plywood sheathing rather than the area of the top vent.

Condensation occurs on the cavity-surface of fibre cement cladding every month for all fibre cement walls due to the high out RH and low moisture and thermal storey capacity of fibre cement cladding. The condensation hours and frequencies are over ten times more than those in the brick walls in the winter. The impact of condensation in the spring is not critical since the moisture generated by condensation on the surfaces would be evaporated and carried out by cavity ventilated air with higher temperature and lower RH.

The difference of condensation frequencies of test time between the dry fibre cement walls with small and large vent configurations are insignificantly small. Comparing the walls with wet sheathing, the larger top vent cause more condensation, indicating the ventilation air, in these cases, becomes a major extra moisture source to provide potential wetting. With the small top vent, both walls with wet and dry sheathing have similar

condensation frequencies. The initial high MC in plywood does not increase the total condensation hours significantly in the winter. With the largest top vents, the wall with wet sheathing has almost two to four times of the daily condensation hours as the wall with dry sheathing.

Therefore, based on the drying / wetting by solar radiation / under-cooling effect and moisture and thermal storage functions of rainscreen claddings, the conclusion can be made that cavity ventilation assists both rainscreen wall system to dry in cold and humid winter of coastal BC. For brick walls, the larger cavity ventilation has the larger drying effect. However, for fibre cement walls, the wall with small top vent and 19mm cavity perform better in terms of reducing cladding surface condensation and protecting the wood-frame back walls and claddings. There is very little difference for the drying and wetting rates in the plywood sheathing for all the fibre cement walls, i.e. walls with small and big top vents and wide and narrow air cavities.

4. Wind and buoyancy induced pressure differential and predicted cavity ventilation rates

The wind-induced pressure differential between top and bottom vents is influenced by the on-site wind speed, wind direction, and the location of a test wall on the façade. The monthly average wind-induced pressure differentials for the test walls are small, within 1 Pa for one-storey test walls and within 3-5 Pa for two-storey walls located at the corners. The average combined thermal and moisture buoyancy-induced pressure differentials are 0.4 – 0.8 Pa for one-story walls and 0.7 – 1.6 Pa for two-story test walls. However, the buoyancy induced pressure difference can reach about 4 Pa for the two-storey walls and 2

Pa for the one-storey walls during sunny period which has a significant influence on the drying of sheathing.

On average, the predicted ventilation rates induced by total pressure differentials are about 6 ACH for one-story wall BW9 and about 4 ACH for the two-storey wall BD10 while 89 ACH for FD2 and 318 ACH for FW4.

5. Hygrothermal simulations by WUFI

Hygrothermal simulations were carried out for two brick walls of BW9 and BD10 and two fibre cement walls of FD2 and FW4 and the results are compared to gravimetric MC measurements in plywood. The accuracy of simulation results depend on the quality of input data including properties of materials, treatment of boundary conditions including wind-driven rain and the long-wave radiation. The results show that simulations and measurements for all four test walls have similar trends and good agreements. The average differences for all the walls are within 1% MC with a maximum of 2% MC for brick walls and 4% MC for fibre cement walls. It indicates that WUFI simulation software can be used to predict and evaluate the hygrothermal performance of rainscreen walls with brick (large moisture storage function) and fibre cement panel (small moisture storage function) with a reasonable accuracy.

The limitations of WUFI program found include: clear-sky effect on the MC of plywood sheathing can not be precisely simulated even using explicit full radiation balance mode. The full radiation mode tends to over-estimate the under-cooling effect. Using an average DRF can not accurately simulate the rain load on the exterior surface and causes over or under-estimation of MC in sheathing.

8.2 Contributions

The main contributions of this research project include:

1. This is the first field experiment carried out on evaluating the impact of vent configurations on the hygrothermal performance of rainscreen walls clad with brick veneer and fibre cement board in western Canada, especially in coastal climate of BC using BCIT's building envelope test facility (BETF).
2. The development and implementation of the test protocol helps to validate the newly developed test facility and to provide insights in the uniformity of on-site environmental conditions, improving further test set-up and the control of indoor environment.
3. A large set of field data including temperature, relative humidity, and moisture content in plywood of rainscreen walls is collected, which can be used for validation of a number of computer programs.
4. The insights gained from the full-scale field testing provide guidance for local building industry in term of design the rainscreen walls for the coastal climate of British Columbia.
5. The field measurements were compared with simulations using hygrothermal simulation program WUFI pro. 4.1 to verify the capacity and accuracy of the computer model. Recommendations are provided in term of setting up the appropriate boundary conditions, material properties and long-wave radiation modes in order to run the program successfully, which will be useful for other professionals using this program.

8.3 Recommendations for future work

1. The field test for hygrothermal performance of rainscreen walls should be further studied in the coastal climate of BC:
   - With different cladding such as stucco, fibre cement and vinyl siding. The balance between ventilation drying by solar radiation and wetting by under-cooling may be different when different cladding materials are used.
   - Test walls to be installed on different orientation of façade. The walls on the different façades experience different loading i.e. wind-driven rain, solar radiation, which governs the balance of wetting and drying. The impact of cavity ventilation may be different for walls facing other orientations.
   - Further investigation of moisture content gradient along the vertical surface of sheathing. Higher moisture content was found at the top of plywood, which may be due to thermal bridge of double top plate, convection within the insulation space and air cavity. Further study should identify the actual cause for the vertical distribution of MC and provide solutions for a better design to achieve the uniformity and durability of hygrothermal performance of rainscreen walls.
2. Further investigation is required to identify the actual causes for the discrepancy between simulation and measurements, especially the effect of clear-sky effect. It seems that the explicit full radiation balance mode can not estimate the clear-sky effect accurately. Also, detailed simulations using monthly wind-driven rain factor for the wall surface instead of using an average wind-driven rain factor should be carried out to evaluate the effect of wind-driven rain loads on the accuracy of simulations

when the wind-driven rain measurements cannot be used or are not available. Moreover, material properties of all components used in the test walls should be tested and input into simulations.

References

ASHRAE (2005). *Fundamental Handbook.* American Society of Heating. Refrigerating and Air-conditioning Engineers, Inc. Atlanta, GA. USA.

ASHRAE (2004). A thermal and moisture transport property database for common building and insulating materials. Research Project 1018-TRP Final Report. American Society of Heating and Air-conditioning Engineers, Inc. Atlanta, GA. USA.

ASTM. (1992). ASTM D 4442-92, Standard Test Method for Direct Measurement of Wood and Wood-base Materials. *Annual Book of Standards,* Vol. 04-10. pp. 493-497.

McGowan, A. (2003). Review of hygrothermal models for building envelope retrofit analysis, Research Highlights. Project for Canadian Mortgage and Housing Corporation (CMHC), Ottawa. Canada.

BAKOR. (2009). Blueskin®SA self-adhesive air/vapour barrier membrane. Technical Data Sheet. Henry Company. www.bakor.com.

Bassett, M.R. & McNeil, S. (2005). Drained and vented cavity walls – measured ventilation rates. *IRHACE Conference" Institution of Refrigeration, Heating and Air Conditioning Engineers",* Nelson, New Zealand.

Bassett, M.R. & McNeil, S. (2005). The theory of ventilation drying applied to New Zealand cavity walls. *IRHACE Conference" Institution of Refrigeration, Heating and Air Conditioning Engineers",* Nelson, New Zealand.

BCBC. (2006). British Columbia Building Code. Ministry of Forests and Range and Minister Responsible for Housing, Canada.

BC Housing. (2006). Construction detail drawings for Several Project in Mainland of BC, Canada.

BCdex. (2006). Leaky Condo Statistics. BC Construction and Landscaping Network.

Best, A.C. (1950). The size distribution of raindrops. *Quarterly Journal of the Royal Meteorological Society,* (76), pp. 16-36.

Bomberg, M.T. and Brown, W.C. (1993). Building Envelope and Environmental Control: Part 1 – Heat, Air and Moisture Interactions. National Research Council Canada (NRC-IRC), Ottawa, Canada.

Brown, W.C. et. al. (1999). Designing exterior walls according to the rainscreen principle. *Construction Technology Updates.* No. 34. National Research Council Canada (NRC-IRC).

Burnett, E. and Reynolds, A. (1991). The Ontario wall drying project. Research Report. Canada Mortgage and House Cooperation (CMHC), Ottawa, Canada.

Burnett, E. (2001). The Ontario wall drying project – phase 2. Research Report. Canada Mortgage and House Cooperation (CMHC), Ottawa, Canada.

Burnett, E. & Straube, J. (1995). Vents, ventilation drying, and pressure moderation. Research Report. Canada Mortgage and House Cooperation (CMHC), Ottawa, Canada.

Burnett, E. Straube, J. And Karagiozis, A. (2004). Synthesis report and guidelines – report#12 final report. ASHRAE 1091-Development of Design Strategies for Rainscreen and Sheathing Membrane Performance in Wood Frame Walls.

Campbell. (2007). WXT510 Weather Transmitter Instruction Manual. Campbell Scientific, Inc.

Chown, G.A. et. al. (1997). Evolution of wall design for controlling rain penetration. *Construction Technology Update,* No. 9. Nation Research Council Canada (NRC-IRC).

City of Vancouver. (1999). City of Vancouver Building By-law No. 8057. Community Services Group, Office of the Chief Building Official. Vancouver, BC, Canada.

CMHC. (1989). Report on Atlantic Canada Wood Framing Moisture Survey. Ottawa, Canada.

CMHC. (2001). Wood-Frame Envelopes in the Coastal Climate of British-Best practice guide, Building technology., Ottawa, Canada.

Cornick, S. & Rousseau, M.Z. (2003). Understanding the severity of climate loads for moisture-related design of walls. *Building Science Insight 2003 Seminar Series-15 Cities across Canada.* National Research Council Canada (NRC-IRC).

Davidovic, D. (2004) Convective drying potential of ventilated wall cavity systems in building enclosures. Master's Thesis, The Pennsylvania State University, Pennsylvania, USA.

Dingle, A.N., and Lee, Y. (1972). Terminal fall speeds of raindrops. *Journal of Applied Meteorology*, 11(6), pp. 877 - 879.

Dufie, W. and Beckman, J. (1991). Solar Energy of Thermal Processes – Second Edition. John Wiley and Sons Inc. New York, NY, USA.

Environment Canada. (2009). Canadian climate normals or average 1971 – 2000. *National Climate Data and Information Archive.* From the Website: www.climate.weateroffice.ec.gc.ca

Finch, G. (2007). The Performance of Rainscreen Walls in Coastal British Columbia. Master's Thesis. University of Waterloo, Waterloo, Ontario, Canada.

Finch, G. (2007a). Hygrothermal modeling –Appendix B "The performance of Rainscreen Walls in Coastal British Columbia". Master's Thesis. University of Waterloo, Waterloo, Ontario, Canada.

Finch, G. (2007b). Solar radiation measurements and calculations –Appendix H "The performance of Rainscreen Walls in Coastal British Columbia" Master's Thesis. University of Waterloo, Waterloo, Ontario, Canada.

Finch, G. (2009). Personal conversation on the simulation using WUFI.

Forest, T. and Walker, I. (1993). Attic Ventilation and Moisture. Research Report. Department of Mechanical Engineering, University of Alberta. Project for Canadian Mortgage and Housing Corporation (CMHC), Ottawa, Canada.

Garrahan, P. (1989). Moisture meter Correction factors, *In-Grade Testing of structural Lumber*, pp36-43. Forest Products Society, Madison, WI, USA.

Garden, G.K. (1963). Rain penetration and its control. Canadian Building Digest (CBD-40). National Research Council Canada (NRC-IRC), Ottawa, Canada.

Ge, H., Ye, Y. and Fazio, P. (2009). Field investigation of the impact of cavity ventilation on the wetting and drying of brick veneer wall systems in the costal climate of British Columbia. The 12th Canadian Building Science and Technology Conference. Montreal, May 2009.

Ge, H. (2009). Wind-driven Rain Study in the Coastal Climate of British Columbia – Final Report. Project for CMHC, HPO and BC housing.

Ge, H., Ye, Y. and Fazio, P. (2008). A two-storey field station for investigation of building envelope performance in the coastal climate of British Columbia. *Proceedings of the symposium in Building Physics*. Leuven, Belgium.

Ge, H. and Ye. Y, (2007). Investigation of Ventilation Drying of Rainscreen Walls in the Coastal Climate of British Columbia. The Buildings X Conference - Performance of Exterior Envelopes of Whole Buildings, Clearwater Beach, Florida.

Ge, H. (2002). *Study on Overall Thermal Performance of Metal Curtain Walls.* PhD thesis, Concordia University, Montreal, Quebec, Canada.

Gudum, C. (2003). *Moisture Transport and Convection in Building Envelopes Ventilation in Light Weight Outer Walls.* PhD thesis, The technical University of Denmark, Finland edition, pp. 1-124

Gudum, C. and Rode, C. (2004). Moisture transport by convection in lightweight exterior facades. *Performance of Exterior Envelopes of Whole Buildings IX,* Clearwater Beach, FL, USA

HAL Industries Inc. (2006). Breather membranes for wood framed walls. *HAL Industries Inc. website; http://www.halind.com/content/products/BU0400.html*

Handegord, G.O. (1982). The performance of exterior walls*Building Science Forum '82 "Exterior Walls: Understanding the Problems"* and a series of seminars presented in major cities across Canada in 1982. National Research Council Canada (NRC-IRC).

Hansen, M.H. et. al. (2002). On the influence of cavity ventilation on moisture content in timber frame walls. *Building Physics 2002 – 6th Nordic Symposium.*

Hazleden, D. (1999). Designing for durable wood construction: the 4 Ds. *8th International Conferences on Durability of Building Materials and Components.* Vancouver, BC, Canada.

Hazleden, D. (2001). Envelope drying rates experiment final report. *Research Highlights,* Canada Mortgage and House Cooperation (CMHC), Ottawa, Canada.

Hazleden, & Morris, (2003). Evaluation of vapour diffusion ports on drying of wood-frame walls under controlled conditions. *Research Highlights,* Canada Mortgage and House Cooperation (CMHC), Technical Series 02-130, Ottawa, Canada.

Hens, H. (1992). Bouwfysica 1: Warme - En Massatransport, Leuven, Belgium.

Hens, H. (2003). Building Physics: Heat and Mass Transfer. 6th edition in English. Katholieke Universitei Leuven, Belgium.

Hens, H. (2006). Undercooling: theory and consequences. *IEA-EXCO Energy Conservation in Buildings and Community Systems-Annex 41"Whole Building Heat, Air and Moisture Response MOIST-ENG",* Kyoto, Japan.

Hens, H. and Fatin, A. (1995). Heat-Air-Moisture Design of Masonry Cavity Walls: Theoretical and Experimental Results and Practice. *ASHRAE Transactions, CH-95-3-2,* pp. 607-626.

Hens, H. & Janssens, A. (2004). Cathedral ceilings: a test building evaluation in a cool, humid climate. *Performance of Exterior Envelopes of Whole Buildings IX,* Clearwater Beach, FL, USA.

Holm, A. et. al. (2004). Exterior surface temperature and humidity of walls – comparison of experiment and numerical simulation. *Performance of Exterior Envelopes of Whole Buildings IX,* Clearwater Beach, FL, USA.

Horn, D. (2007a). Gravimetric, electrical resistance & moisture meter moisture content measurement comparison for OSB, Plywood, and SPF samples. *Internal Report.* Building Science Centre for Excellent at BCIT, Burnaby, BC, Canada.

Horn, D. (2007b). Humidity and temperature sensor test report. *Internal Report.* Building Science Centre for Excellent at BCIT, Burnaby, BC, Canada.

Houvenaghel, G. et. al. (2004). The impact of airflow on the hygrothermal behavior of highly insulated pitched roof systems. *Performance of Exterior Envelopes of Whole Buildings IX,* Clearwater Beach, FL, USA.

Huang, S. (2005). *Solar-driven Vapour Flow in Wood-frame Walls with Wetted Cladding.* Concordia University. Montreal, Quebec, Canada.

Hubbs, B. & Finch, G (2006). Monitor of rainscreen wall assembly: exploring findings of condensation. BC Building Envelope Council *(BCBEC)" From Research to Reality",* Vancouver, BC, Canada.

Hutcheon, N.B. (1953). Fundamental Considerations in the Design of Exterior Walls for Buildings. Division of Building Research of NRC (NRC No. 3057). Presented to Annual Meeting of the Engineering Institute of Canada, Halifax, Canada.

IBP. (2001). Software / WUFI / Basics / Overview of WUFI. Website of Fraunhofer Institute for Building Physics (IBP) http://www.hoki.ibp.fhg.de/ . Germany.

IBP. (2007). Material property in WUFI data base. *WUFI-PC program for calculating the coupled heat and moisture transfer in building components.* Pro. 4.1. Fraunhofer Institute for Building Physics (IBP). Germany.

Idelchik, I.E. (1994). Handbook of Hydraulic Resistance, third edition. CRC Press: Boca Raton, FL, FL, USA.

Inculet, D.R. and Davenport, A.G. (1994). Pressure-equalized rainscreens: A study in the frequency domain. *Journal of Wind Engineering and Industrial Aerodynamics*, vol.53, pp. 63-87.

Jung, E. (1985) dauerstandverhalten von verblendziegelmauerwerk unter witterunsbeansphruchung und asuwirkungen von kerndämm-Maβnahmen. *Baustoffindustrie,* No. 6, pp. 185-188.

Karagiozis, A. (2001). *Advanced Hygrothermal Models and Design Models.* Report of Oak Ridge National Laboratory Building Technology Centre, Oak Ridge, TN. USA.

Karagiozis, A. (2002). *Building Enclosure Hygrothermal Performance Study Phase 1.* Report of Oak Ridge National Laboratory Building Technology Centre, Oak Ridge, TN. USA.

Karagiozis, A. (2004). Parametric evaluation of ventilation drying & sheathing membrane performance – report#11 final report. ASHRAE 1091-Development of Design Strategies for Rainscreen and Sheathing Membrane Performance in Wood Frame Walls.

Karagiozis, A. et. al. (2005). The hygrothermal performance of ventilated, vented and non-vented brick and vinyl wall claddings for two North American climates. *10th Canadian Conference on Building Science and Technology,* Ottawa, May.

Kerr, D. (2004). Keeping Walls Dry (part 1 and part 2). Canadian Mortgage and Housing Corporation (CMHC), Ottawa, Canada.

Kerr Associates. (2001). The Rainscreen Wall System. *Technology Transfer.* Canada Mortgage and Housing Corporation (CMHC), Ottawa, Canada.

Kontopidis, T.D., (1992) "Control of rain penetration through pressurized cavity walls", Ph.D. thesis, Center for Building Studies, Concordia University, Montreal, QC. Canada.

Kontopidis, T., Reddy, M.S. and Fazio, P. (1993) "Potential of rain screen walls to prevent rain penetration: pressurized cavity principle", *Building Research and Information*, Vol. 21, No. 3.

Kumar, K.S., Stathopoulos, T., & wisse, J.A. (2003). Field measurement data of wind loads on rainscreen walls. *Journal of Wind Engineering and Industrial Aerodynamics,* vol. 91, pp. 1401-1417.

Kumar, K.S.& wisse, J.A. (2001). Pressure equalization of rainscreen facades: Analysis of the field data in the frequency domain. *Wind and structures*, 4(2), pp.101-118.

Kumaran, M.K. et. al. (2002). A thermal and moisture transport property database for common building and insulating materials. Final Report. ASHRAE Research Project 1018-RP. National Research Council Canada.

Kumaran, M.K. et.al. (2002). Hygrothermal properties of several building materials. Summary Report from Task 3 of MEWS Project. National Research Council Canada.

Künzel, H. M. (1995). One- and two-dimensional calculation using simple parameters. PhD thesis. Faraunhofer Institute for Building Physics in Holzkirchen, Germany.

Larose, A. (2008). Test-hut interior thermocouple test results. *Internal Report.* Building Science Centre of Excellence at BCIT, Burnaby, BC, Canada

Larrsson, L.E. (2001). Moisture content in a wooden sheathing above an attic with high-insulated ceiling construction. *CIB W40 Heat and Moisture Transfer in Buildings. PP. 282-289.* Wellington, New Zealand.

Latta, J.K. (1962). Water and Buiding Materials (CBD-30). National research Council Canada (NRC_IRC), Ottawa. Canada.

Laviolette, S.P. and Keller, H. (2000). Performance of a brick veneer/steel stud wall system – Phase 4. Research report of CMHC, Ottawa, Canada.

Lawton, M.D. (1999). Reacting to durability problems with Vancouver buildings. *Durability of Building Materials and Components 8. edited by M.A. Lacasse and D.J. Vanier.* National Research Council Canada (NRC-IRC), Ottawa, Canada.

Lazaruk, S. (2006). Search still on for leak-proof wall. Website of The Province, British Columbia.
http://www.canada.com/theprovince/news/money/story.html?id=014b609d-8c19-4d07-9a40-d7bb11954819&p=1

Li, Y. (2002). Analysis of Natural Ventilation – a Summary of Existing Analytical Solutions. *Technical Report.* Annex 35 Hybvent. Denmark.
Mao, Q. et. al. (2004). A Literature Survey on The Air Space behind the Exterior Cladding. *Research Report.* Building Envelope Performance Laboratory, Centre for Building Studies, Department of Building, Civil and Environmental Engineering, Concordia University, Montreal, QC. Canada.

MATCH (2003). Moisture and temperature calculations for constructions of hygroscopic materials. *PC program for transient calculation of the transport of heat and moisture through composite building constructions.* http://www.match-box.dk.

Marshall, (1983). Moisture Induced Problems in NHA Housing: Part 1, 2 and 3. *Technical Report.* Marshall, Macklin, Monaghan Ltd. Project for Canadian Mortgage and Housing Corporation (CMHC), Ottawa, Canada.

Marshall, R. (2001). 2001 Building Failures Study. *Technical Report.* R.J. Burnside % asociates Ltd. Project for Canadian Mortgage and Housing Corporation (CMHC), Ottawa, Canada.

Mayer, E. and Künzel, H. (1983). "Untersuchungen über die notwendige Hinterlütung an Auβenwandbekeidung aus groβformatigen Bauteilen". Fraunhofer Institut für Bauphysik, Forschungsbericht B Ho 1/83.

MOIST (1997). *Pc Program for Predicting Heat and Moisture transfer in Building Envelopes. Version 3.0.* National Institute of Standards and Technology. Gaithersburg, MD USA.

Morrison Hershfield Limited, (1990) "A study of the rainscreen concept applied to cladding systems on wood frame walls". *Technical Series.* 90-214. Canadian Mortgage and Housing Corporation (CMHC), Ottawa, Canada.

Morrison Hershfield Limited (MH). (1998). Survey of Building Envelope Failures in the Coastal Climate of British Columbia. *Technical Report.* Survey for Canadian Mortgage and Housing Corporation (CMHC), Ottawa, Canada.

Mukhopadhyaya, P. et. al. (2004). Vapour barrier and moisture response of wood frame stucco wall – results from hygrothermal simulation. *CIB World Building Congress.* Toronto, ON, Canada.

NBC, (1995). National Building Code of Canada. National Research Council Canada (NRC-IRC).

Nehdi, M. (2001). Parametric study of moisture and heat transfer in a new rain-screen stucco wall. *Journal of Thermal Envelope & Building Science, 24(4),* 335-347.

Ojanen, T. & Ahonen, J. (2005). Moisture performance properties of exterior sheathing products made of spruce plywood or OSB. *VTT Working Paper. VTT Information Service. VTT Building and Transport,* Betonimiehenkuja, Finland.

Onysko, M. D. et. al. (2000). Drying of Walls with ventilated a parametric analysis. Research report. Canada Mortgage and Housing Corporation (CMHC), Ottawa, Canada.

Piñion, J. et. al. (2004). Characterization of ventilation Airflow in screen-type wall systems volume 1 – report#5 final report. ASHRAE 1091-Development of Design Strategies for Rainscreen and Sheathing Membrane Performance in Wood Frame Walls. American Society of Heating and Air-conditioning Engineers, Inc. Atlanta, GA. USA.

Pfaff, F. and Garrahan, P. (1985). Temperature Correction Factors and Combined Temperature-Species Correction Factors for the Resistance Type Moisture Metre. Forintek Canada Corporation, city, Canada.

RDH Building Engineering Ltd. (2005). Performance monitoring of rainscreen wall assemblies in Vancouver British Columbia. Draft.

Roodvoets, D.L. (2001). Practical implication of the elimination of natural attic ventilation in mixed climates. *Thermal Performance of the Exterior Envelopes of Buildings VIII: From the Basement to the Roof-Practices,* Clearwater Beach, FL. USA.

Rose, W.B. (2001). Measured summer values of sheathing and shingle temperature for residential attics and cathedral ceilings. *Thermal Performance of the Exterior Envelopes of Buildings VIII: From the Basement to the Roof-Practices,* Clearwater Beach, FL. USA.

Rose, W.B. & TenWolde, A. (2002). Venting of attics & cathedral ceilings. *ASHRAE Journal,* October, 2002. pp. 26-33.

Rousseau, J. (1983). Rain penetration and moisture damage in residential construction - Technical documentation produced for *Building Science Insight'83*, "humidity,

Condensation and Ventilation in Houses" and a series of seminars presented in major cities across Canada.

Rousseau, M.Z. et. al. (1998). Pressure equalization in rainscreen wall systems. *Construction Technology Update,* No. 17, National Research Council Canada (NRC-IRC).

Rousseau, J. et. al. (1999). Performance Monitoring of a Brick Veneer / Steel Stud Wall System-Phase 4 Results (Revision 1), Canada Mortgage and House Cooperation (CMHC), Ottawa, Canada.

Rousseau, M.Z. (1990). Facts and fictions of rain-screen walls. *Construction Canada*, 32 (2).

Rousseau, M.Z. & Dalgliesh, W.A. (2004). Selected findings of an IRC study of the wetting and drying potentials of wood-frame walls exposed to different climates. CIB 2004 World Building Congress, Toronto, Ontario, Canada.

Rowley, F.B. et. al. (1939). Condensation of moisture and its relation to building construction and operation. *ASHVE Transaction, No. 1115.*

Salonvaara, M.H. et.al. (1998). Drying capabilities of wood frame walls with wood siding. *Thermal Performance of the Exterior Envelopes of Buildings VII: Moisture Assessments-Principles*, Clearwater Beach, FL, USA. pp. 165-177.

Salonvaara, M.H. et.al. (2003). Indoor air humidity variations and its effects on the moisture performance of building envelope. *Eighth International IBPSA Conference*, Eindhoven, Netherlands. pp. 163-169.

Sandin, K. (1991). Skalmurskonstruktionens fukt- och temperaturbetingelser. Rapport R43:1991. Byggforskniningstådet, Stockholm, Sweden.
Sedlbauer, K. (2001). Vorhersage von Schimmelpilzbildung auf und in Bauteilen. Fakultät von Bauingenieur- und Vermessungswesen. Universität Stuttgart. Deutschland.

Schumacher, C. et. al. (2004).Ventilation drying in screen-type wall systems: physical demonstration – report #3, final report. ASHRAE 1091-Development of Design Strategies for Rainscreen and Sheathing Membrane Performance in Wood Frame Walls. American Society of Heating. Refrigerating and Air-conditioning Engineers, Inc. Atlanta, GA. USA.

Shi, X. et. al. (2004). Ventilation drying under simulated climate conditions – report#7 final report. ASHRAE 1091-Development of Design Strategies for Rainscreen and Sheathing Membrane Performance in Wood Frame Walls. American Society of Heating. Refrigerating and Air-conditioning Engineers, Inc. Atlanta, GA. USA.

Shi, X. and Burnett, E. (2006). Ventilation drying in walls with vapor impermeable claddings. *Proceedings of the 3rd international conference in Building Physics and Building Engineering*. pp. 395-402. Montreal, Canada.

Simonson, C.J. et.al. (2005). Moisture performance of an airtight, vapor-permeable building envelope in a cold climate. *Journal of Thermal Envelope & Building Science,* 28(3), pp. 205-226.

Stovall, T.K. & Karagiozis, A. (2004). Airflow in the ventilation space behind a rain screen wall. *Performance of Exterior Envelopes of Whole Buildings IX, Clearwater Beach*, FL, USA, pp. 1-11.

Stovall, T. and Karagiozis, A.N. (2004). CFD simulation of airflow in ventilated wall system – report#9 final report. ASHRAE 1091-Development of Design Strategies for Rainscreen and Sheathing Membrane Performance in Wood Frame Walls. American Society of Heating. Refrigerating and Air-conditioning Engineers, Inc. Atlanta, GA. USA.

Straube, J. and Burnett, E. (1995). Vents, Ventilation Drying, and Pressure Moderation. Research Report for Canada Mortgage and Housing Corporation, Ottawa, Canada.

Straube, J. and Burnett, E. (1997). Field testing of filled-cavity walls. *ICBEST proceedings*. Bath, U.K. April 1997. pp. 429 – 435.

Straube, J. and Burnett, E. (1998a). Vents, ventilation and masonry veneer wall systems. *Proceeding of the 8th Canadian Masonry Symposium*, Jasper, Alberta, pp. 194-207.

Straube, J. & Burnett, E. (1998b). Drainage, ventilation drying, and enclosure performance. *Conference Proceedings, Thermal Performance of the Exterior Envelopes of Buildings VII.* Clearwater Beach, FL, USA, pp. 189-198.

Straube, J. et. al. (2002). Methodology and Design of Field Experiments for Monitoring the Hygrothermal Performances of Wood Frame Enclosures. Department. of Civil Engineering, University of Waterloo, Waterloo, ON. Canada.

Straube, J. et. al. (2004). Review of literature and theory – report#1 final report. ASHRAE 1091-Development of Design Strategies for Rainscreen and Sheathing Membrane Performance in Wood Frame Walls. American Society of Heating. Refrigerating and Air-conditioning Engineers, Inc. Atlanta, GA. USA.

Straube, J. and VanStraaten, R. (2004). Field drying study of wood frame walls – report#8 final report. ASHRAE 1091-Development of Design Strategies for Rainscreen and Sheathing Membrane Performance in Wood Frame Walls. American Society of Heating. Refrigerating and Air-conditioning Engineers, Inc. Atlanta, GA. USA.

Straube, J. & Burnett, E. (2005). Building Science and Building Enclosures. Building Science Press Inc. Westford, Massachusetts. USA.

Straube, J and Schumacher, C. (2006). Driving Rain Loads for Canadian Building Design. Report for CMHC. University of Waterloo, Building Engineering Group, Waterloo, ON, Canada.

Straube, J. (2006). Walls for Vancouver: past, present & future. The presentation in the Independent Contractor's and Businesses Association (ICBA). Coquitlam, BC, Canada.

TenWolde, A. et. al. (1995). Airflow and moisture conditions in walls of manufactured homes. *Airflow Performance of Building Envelopes, Components, and Systems*, M. P. Modera and A. K. Persily, Editors. ASTM STP 125, American Society for Testing and Material, Philadelphia, PA, USA, pp. 137-155.

TenWolde, A. (2001). Chapter 7: Manual analysis tools. Manual on Moisture Analysis in Buildings.

TenWolde, A. & Walker, I.S. (2001). Interior moisture design loads for residences. *Proceedings for Performance of Exterior Envelopes of Whole Buildings VII: Intergation of Building Envelopes.* Clearwater Beach, FL, USA.

TenWolde, A. et.al. (1998). Air pressures in wood frame walls. *Proceedings for Performance of Exterior Envelopes of Whole Buildings VII.* Clearwater Beach, FL USA.

TenWolde, A.& Rose, W. (1999). Issues related to venting of attics and cathedral ceilings. *ASHRAE Transactions, (105).*

TenWolde, A. et. al. (1995). Airflow and moisture conditions in walls of manufactured homes. *Airflow Performance of Building Envelopes, Components, and Systems*, M. P. Modera and A. K. Persily, Editors. ASTM STP 125, American Society for Testing and Material, Philadelphia, PA, USA, pp. 137-155.

VanStraaten, R. (2003). Measurement of Ventilation and Drying of Vinyl Siding and Brick Clad Wall Assemblies. Master's thesis. University of Waterloo, ON, Canada.

VanStraaten, R. & Straube, J. (2004). Field study of airflows behind brick veneers–report#6 final report. ASHRAE 1091-Development of Design Strategies for Rainscreen and Sheathing Membrane Performance in Wood Frame Walls. American Society of Heating. Refrigerating and Air-conditioning Engineers, Inc. Atlanta, GA. USA.

VanStraaten, R. & Straube, J. (2004). Laboratory study of airflows behind vinyl siding–report#4 final report. ASHRAE 1091-Development of Design Strategies for Rainscreen and Sheathing Membrane Performance in Wood Frame Walls. American Society of Heating. Refrigerating and Air-conditioning Engineers, Inc. Atlanta, GA. USA.

Viitanen, H.A. (1997). Modelling the time factor in the development of mould fungi-The effect of critical humidity and temperature conditions on pine and spruces sapwood. *Holzforschung*, 51 pp. 6-14.

Wolkes, K.E. et. al. (2004). Effect drying protocols on measurement of sorption isotherms of gypsum building materials. *Performance of Exterior Envelopes of Whole Buildings IX,* Clearwater Beach, FL, USA.

Wilson, A.G. and Tamura, G.T. (1968). Stack effect in buildings. *CBD -104.* National Research Council Canada (NRC-IRC). Ottawa, Canada.

WUFI (2007). Details / Long-wave Radiation Exchange. *WUFI pro. 4.1.* Online-Help.

Ye, Y. et. al. (2009). Influence of cavity ventilation on the drying and wetting of plywood sheathing in rainscreen walls in the coastal climate of British Columbia. *4th International Building Physics Conference.* Istanbul, Turkey.

Zheng, R. et. al. (2004). An evaluation of highly insulated cold zinc roofs in a moderate humid region – part I: hygrothermal performance. *Construction and Building Materials*, (18), pp. 49-59.

Appendix

Appendix 1: Monthly Weather Data Analysis

Monthly wind directions in all hours and rain hours

Figure 1 shows that during the rain hours, wind direction prevailed from the east in December, March and June.

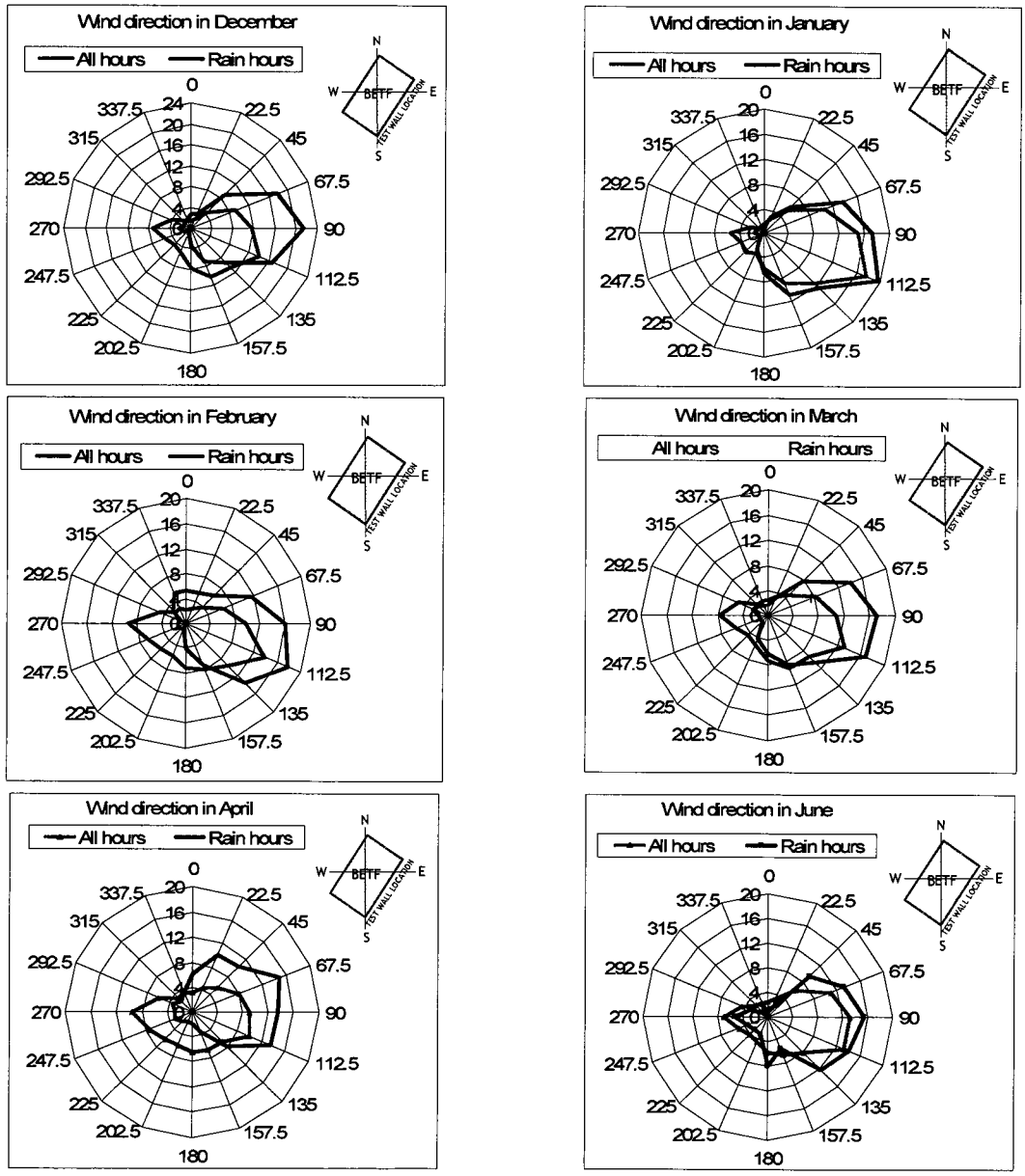

Figure 1: Monthly wind direction rosettes from Dec. 07 to June 08 on BETF site.

The differences are that the frequency of prevailing wind in December is highest while it is the lowest in June. The wind direction prevailed in the ESE direction in January and February while the prevailing wind was from east-north-east (ENE) in April. The prevailing wind direction from east to ESE in the rainy winter (December to March) may significantly influence the amount of wind-driven rain on the SE façade of BETF.

The frequency of prevailing wind direction (ESE) during all hours in the test period in each month is similar, about 13%, except for in January and April. The frequency of prevailing wind direction in January is the highest of 17.5% while it is the lowest in April, 10%. The frequencies of prevailing wind direction during rain hours decreased from 21.3% in December to 19.8% in January while they were similar in February and March, about 17%. Then the frequencies became smaller after March, around 15%.

Monthly wind speed in all hours and rain hours

Frequency distribution of wind speeds for each month was analyzed. The frequencies for all the months have the similar trends as those during all hours, rain hours and in the specific wind direction of ENE to SE (67.5° to 135°) during the rain hours for the whole test period except in February, as shown in Figure 2. The range of "0" means that the wind speed is either still or too low to be recorded by the wind anemometer.

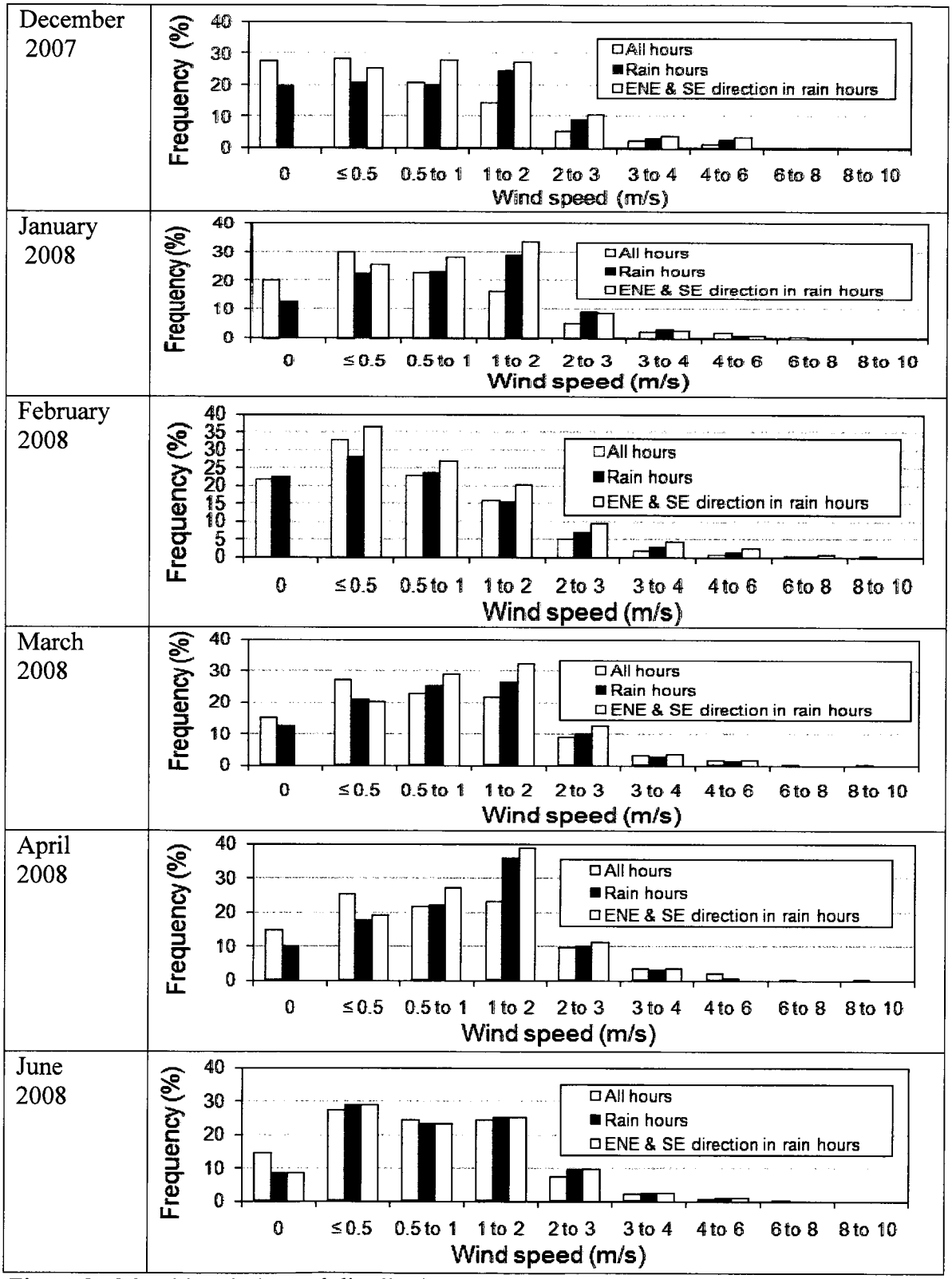

Figure 2: Monthly wind speed distributions during all hours, rain hours, and on NE to SE direction in rain hours.

In February, the frequency of wind speeds below 0.5m/s was the highest and decreased with the increase of wind speeds. The low frequencies in the high wind speed ranges for February, when it had relatively high rainfall, has significant influence on the reduction of wind-driven rain. Other months had the highest frequencies of wind speed in the range of less than 0.5 m/s during all hours of the test period. Whereas, the highest frequencies of wind speed in the rain hours were in the range of 1 – 2 m/s, which may increase potential wind-driven rain on the SE façade of BETF.

Monthly Wind-driven rain on site of BETF

The monthly WDR from January to June, 2008 is analyzed and is shown in Figure 4-1-11. The SE façade of BETF received the most rain in March because March had large amounts of rainfall with high frequency of strong winds from the ENE to ESE direction. All the building façades received the least amount of WDR in April since the horizontal rainfall in this month is only about half of the amount of rain in March. It is interesting to note that in February, the WDR is at least 50% less than that in January and March although there is a similar amount of horizontal rainfall and prevailing wind direction. The main reason is due to a high frequency of low wind speed in February from the ENE to ESE, the frequency of wind speed less than 1.0 m/s is 63% and 10% higher than those in January and March. In contrast, the frequency of wind speed within 1-2m/s in February is 20% and 13% lower than those in January and March. That means that with the same amount of rainfall and same wind direction, WDR is strongly influenced by wind speed.

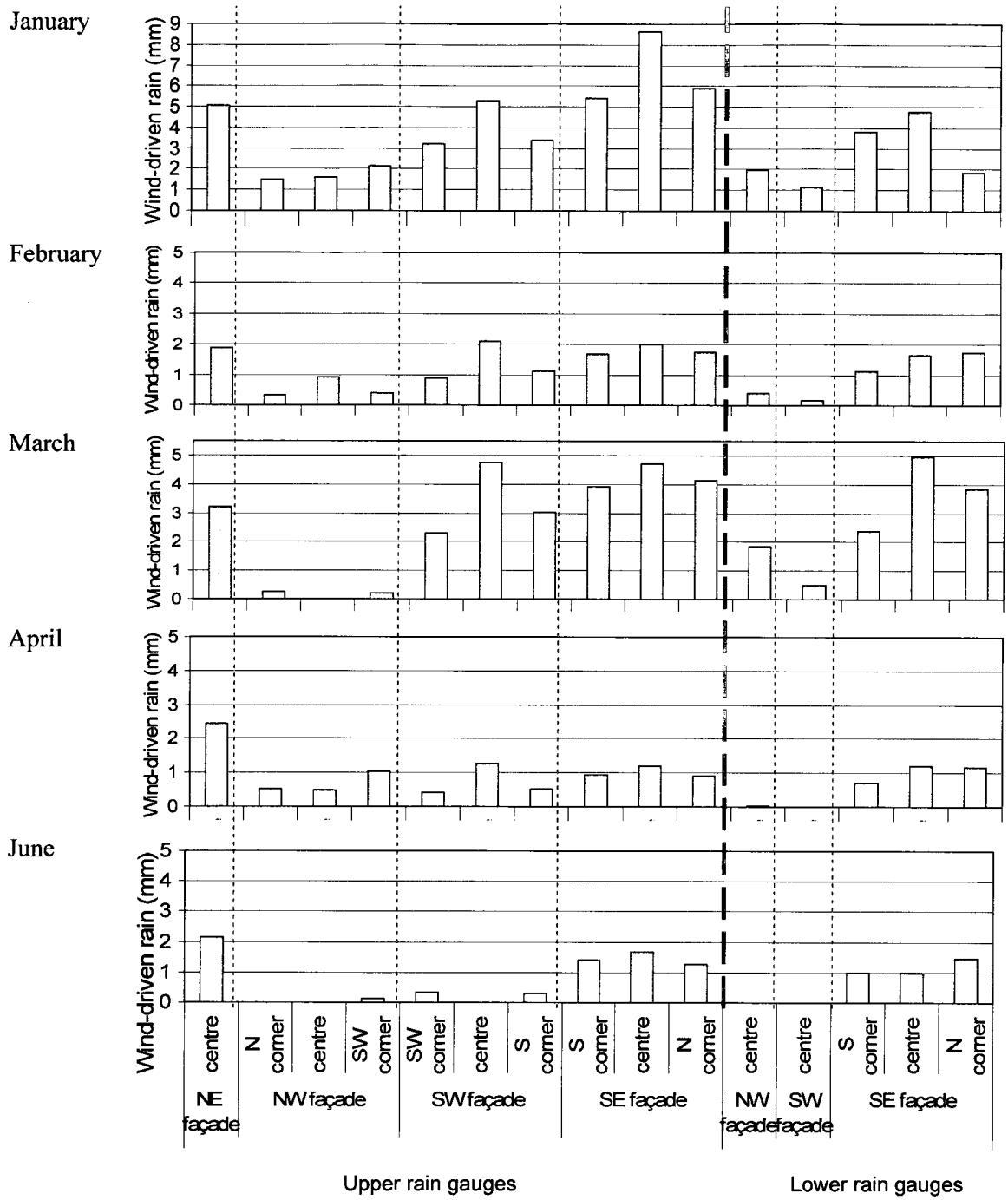

Figure 4-1-11: Total amount of wind-driven rain received by each façade of the BETF for each individual month from Jan. to June 08 (except for May).

Appendix 2: Moisture Content Measurement of Plywood

Moisture content near the vent locations and behind airtight membrane

Moisture content on the top of plywood sheathing experience more impact of un-controllable variable such as thermal bridge from top plate of wood frame and indoor HVAC system operations and vapour accumulated from the MC evaporated from the lower part of plywood while near the bottom vent location (sample #5) is influenced by the weather. MC in plywood behind the airtight membrane (sample #7) is influenced by general outdoor temperature and solar radiation increase with humidity decrease, resulting in slowly drying. MC near bottom vents (sample #5) corresponds more with weather change especially for solar radiation.

Brick walls

Figure 1 shows the comparison of the MC in sample #1, #5 and #7 between BD7 and BD10. BD7 and BD10 are the brick walls with two-floor high cavity and two 1.22m wide and 2.44m completely air sealed wood-frame back walls, one is at the lower level and the other is at the upper level of the façade. Sample #1 in BD7 and BD10 is on the top of plywood sheathing at lower portion of the whole two-floor high walls as the same locations as in one-floor high walls. The two top wood plates and bottom plate of upper potion create thermal bridge since their thermal conductivity is only a half of fibreglass batt insulation (IBP-WUFI, 2007). Therefore, MC in sample#1 in both walls increase faster during the preparation period and the beginning of test. Without top vents, MC in sample #1 of BD7 is 2% lower than that in BD10 due to higher temperature in its air

cavity lower airflow movement at the beginning. However, MC in BD7 increases sharply at the end of January and becomes 1.5% higher than that in BD10. It is because MC from the lower part of plywood evaporated and accumulated on the upper potion during the first sunny period. Before the sunny period in February, MC of sample #1 reaches 20% for BD10 while 21.5% for BD7. During the sunny period, MC drop 2% in BD10 but only 1% in BD7 due to without top vents with larger moisture storage mass of brick veneer. staying above 19% through the entire March until the beginning of April while the MC drops to below 19% during the sunny period with the ventilation providing with the top vents. In the spring, sample #1 in BD7 dries much faster than that in BD10 until the end of May because of higher thermal buoyancy effect as mentioned as section 5.2 and less wetting caused by ventilation will be described next. As a results, the MC in sample #1 of BD7 is close that of BD10 to about 10% at the end of spring.

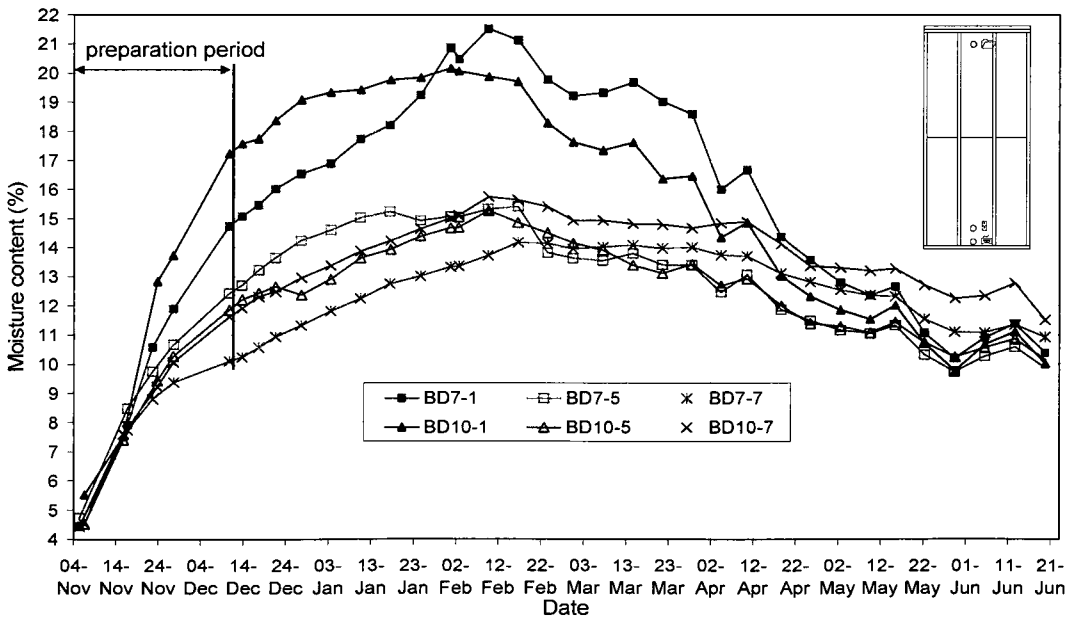

Figure 1: Comparison of MC profiles in plywood samples on the bottom and top at lower potion between BD7 and BD10

Sample #5 and #7 in both walls have slow wetting / drying in the entire test period, the maximum MC is 14 – 16% before the sunny period in February. The difference is MC between sample #5 and #7of BD7 is larger, about 3%, and MC in sample #7 which behind the airtight membrane is lower than that in sample #5 is right above the bottom vents. Instead, difference of MC in these two samples at the very lower part of plywood in BD10 is much closed and MC of sample #5 is higher. Moreover, MC of sample #5 drops 2% during the sunny period in February and then stay in the similar level in rainy month. MC in the same location of BD10 decreased constantly through the sunny period and March without sharp drop in the sunny period. As a results MC in sample #5 become very similar after March.

Furthermore, After, MC in sample #7 in both walls stops increase during the sunny period and stay the same level through the March, MC in BD10 decreases slower and varies more with the weather change than that in BD7.For the wet walls, sample #1 in BW9 had very high MC of 41 to 44% due to the air leakage in preparation and the thermal bridge of top wood plates until the end of December, 2007 as shown in Figure 2. Then It start decrease in January and speeds drying in the entire February due to less WDR and more solar radiation. Then it dries slowly during rainy March and have a sharp drop of 2% in the sunny period at the end of March, reaching below 19% of MC. Instead, sample #1 in BW8 dries fast in the preparation stage but only decrease about 3% without much change of its MC level till the April 10. Then it speeds it drying and reaches to below 19% in the middle of May. At the end of spring, MC in sample #1 of BW9 becomes the lowest of 10% while that of BW8 is still the highest of 13.3%.

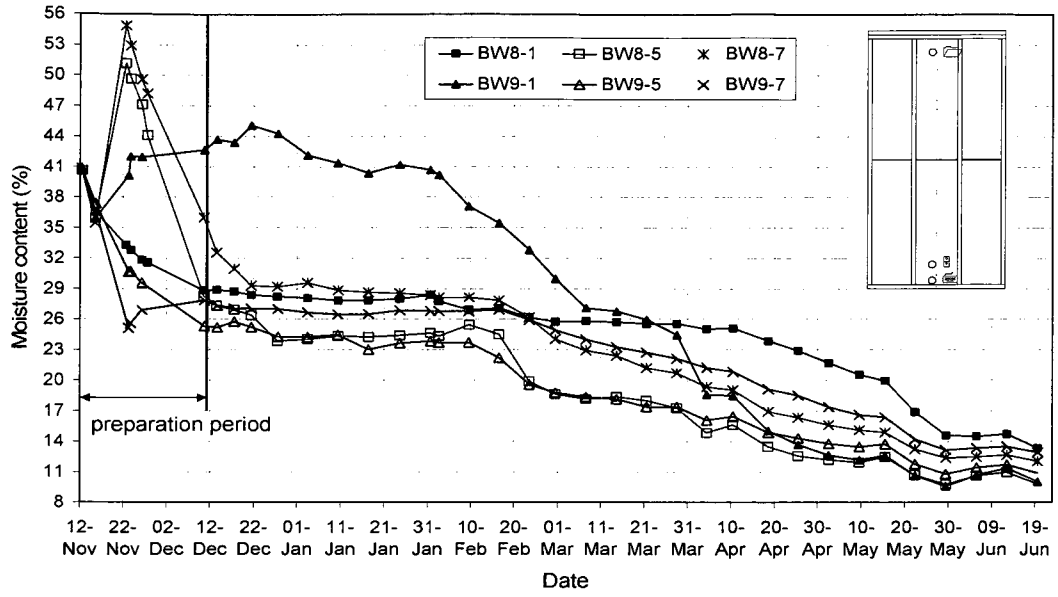

Figure 2: Comparison of MC profiles in plywood on the bottom and top between BW8 and BW9

Sample #7 in Both BW8 and BW9 had similar trend in the entire test period. The samples #7 in both walls stay in the same level of 28 -29% from the December 10 to before the sunny period in February. Then the MC dries constantly to the end of May, reaching to about 13%. Solar radiation in the several sunny periods had little influence for them. Instead,. In addition, The MC level in sample #7 in BW8 is 1% higher in the beginning of test period until the sunny period in February and then the MC drops more during the sunny week, becoming in lower MC level compared with that in BW9. At the end of spring the MC in sample #7 of BW8 is 12% while that of BW9 is 12.9%.

sample #5 in both wet walls have similar behaviour; having the lowest MC level with little change in MC level from the beginning of test stage until the sunny week of February, dropping the MC sharply during the sunny period to below 19%, and gradually drying till the end of spring to about 10%.

Fibre cement walls

For the dry walls shown in Figure 3, MC in Sample #1 on the top of plywood sheathing of FD2 increased extremely high, up to 23 – 25% compared with FD3 during the preparation stage. The location of FD2 is at the centre of the SE elevation. The high MC probably is influence the combination of high outdoor WDR, high indoor RH, plus the relationship of location between the wall and hot steam flow path from a humidifier. It is found that receiving MC was more from inside instead of from outside according to the observation of the stain on the surfaces of the sample. The high level of MC stayed in 2 and a half of months until the sunny period in February. MC in sample #1 of FD3 has constantly increased at the preparation period and the beginning of test. Then jumped to 23% from 19% in 10 days from middle of January. The stain on the inside surface is also observed. That may indicate the high jump of MC is mainly influenced by the high indoor RH.

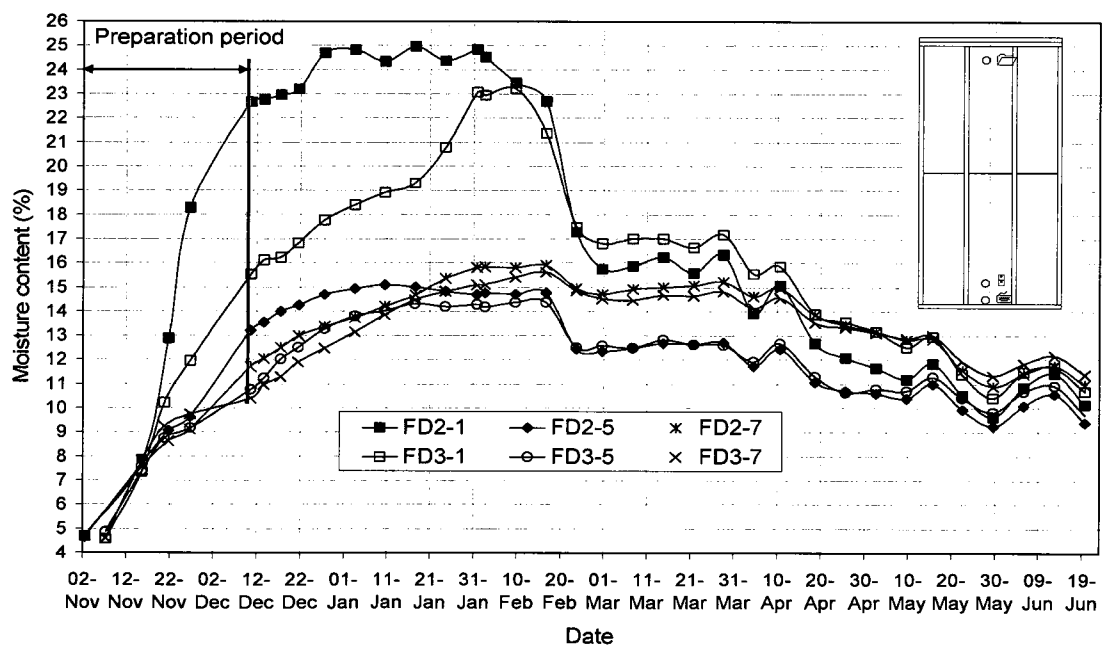

Figure 3: Comparison of moisture content profiles in plywood samples #1, #5 and #7 of FD2 and FD3.

During the sunny period in February, MC in Sample #1 of both walls drops about 6% sharply, reaching 17.5% for FD3 and 14.8% for FD2, indicating MC of FD2 dries faster in the sunny period due to the higher thermal buoyancy pressure differential in the air cavity. Sample #7s in both walls have the least impact by outdoor conditions and have the slowest wetting / drying in the entire test period. Sample #5s in both walls have slower wetting in the beginning of test period and stops wetting earlier than all the other samples. As a result, the MC in these samples is the lowest in March. However, they also have slower drying in the spring. At the end of spring MC range of FD2 is 9.5 – 11% while 9.8 – 11.5 for FD3.

For the wet walls with 19mm air cavity, Figure 4 shows all three samples in FW5 which is with small top vent have lowest MC level except in the beginning of test period. Sample #7s in three walls had similar trend and are in the high MC level and then become the highest from the first sunny period on 20 – 25 in January due the lowest drying speeds. The sample #1s at the top of plywood sheathing in three walls has the highest MC in the beginning of test period but have fastest drying from the first sunny period through to the sunny period in February in general. As a result, sample #1 for all three walls becomes the lowest through March and spring after the sharp drop in the sunny period in February. MC in sample #1 and #7 of FW5 has faster drying speed during the sunny periods compared with the same samples in other two wet walls. Then sample #7 of FD2 has similar MC as sample #5 while the sample #7 in both FW4 and FW6 is higher 2% to the end of May and reaches the equilibrium level with Sample #5s in all the wet walls at the end of spring, reaching 8% of MC level for sample #1s, 10 – 11% for sample #5 and 11 – 12% for samples #7 of three wet walls.

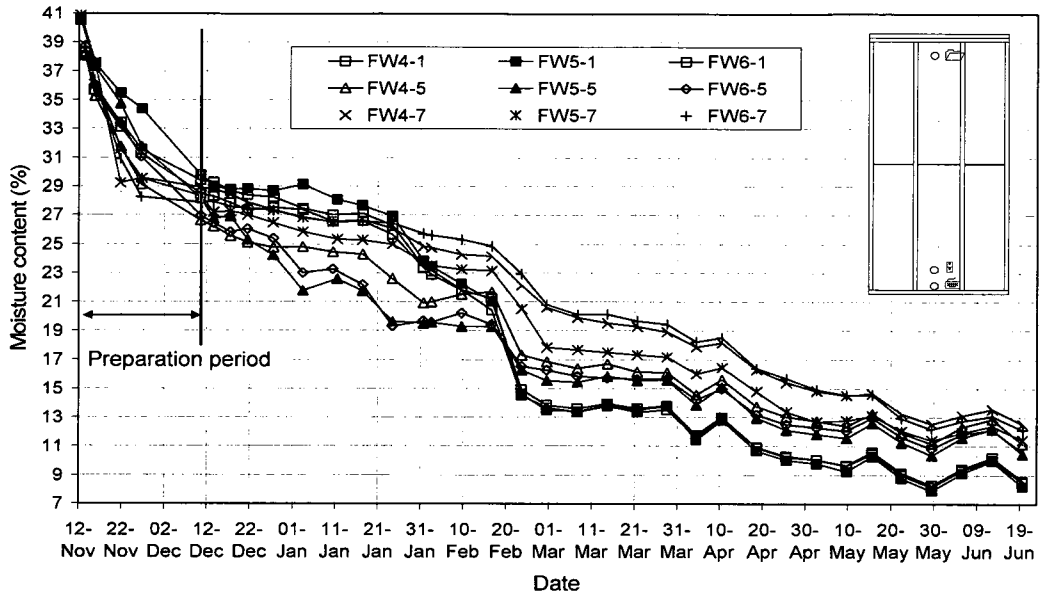

Figure 4: Comparison of moisture content profiles in plywood samples of #1, #5 and #7 of FW4, FW5 and FW6

Compared with the MC in the three samples on the top and bottom of plywood sheathing in FW4, Figure 5 shows that MC in all the three samples of #1, #5 and #7 in FW1is lower.

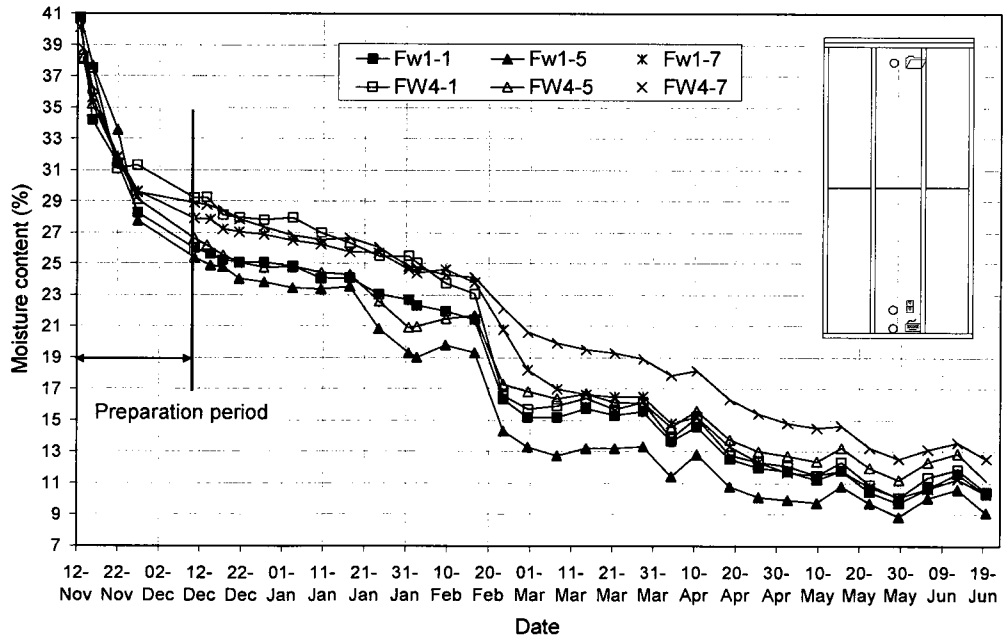

Figure 5: Comparison of moisture content profiles in plywood on the top and bottom between FW1 and FW4

The MC in sample #5 is the lowest since it decreases faster than that in FW4 during the first sunny period starting from January 20. During the second sunny period in February, all the samples have sharp drops in different degree. Sample #7s in both walls decreases their MC in slower speeds but constant compared to other two samples. Between these two walls, sample #7 in FW1 has faster drying during the sunny period and in the entire spring than in FW4.

Comparison of average MC at upper and lower part of plywood sheathing

Brick walls

Looking into the moisture content distribution in lower and upper parts of plywood sheathing, it is found that the MC in the upper plywood of BD7 is 1 – 2% higher than that in the lower part of plywood from January to May as shown as in Figure 6.

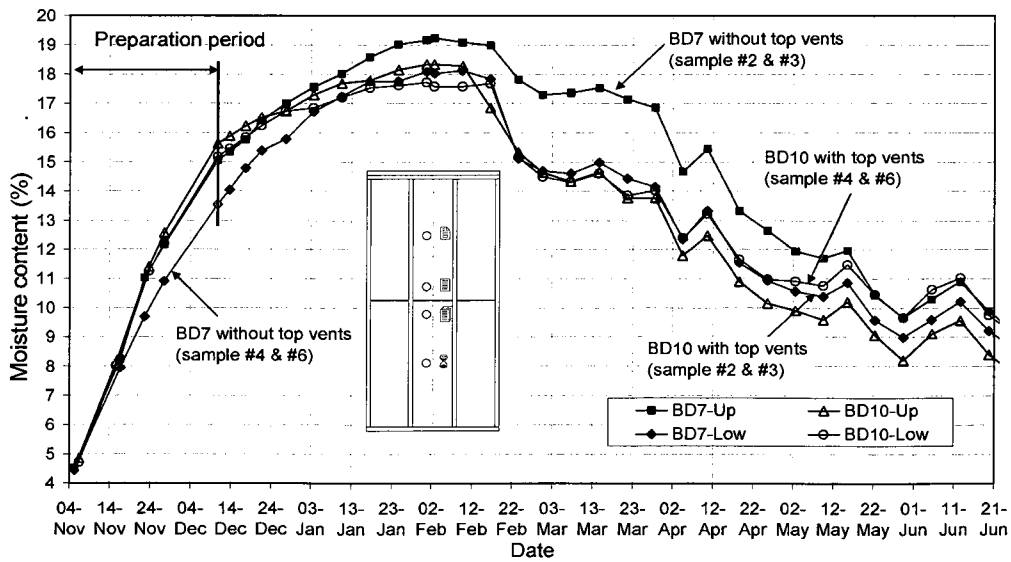

Figure 6: Comparison of average MC in upper and lower parts of plywood between BD7 and BD10 at the first floor of SE façade on BETF from Nov. 07 to Jun. 08.

It indicates that moisture accumulates at the upper part of air cavity causing faster wetting and slower drying of plywood sheathing during rainy winter and early spring, the

maximum difference of MC between lower and upper part of plywood occurs after the sunny period of February to entire rainy March. The MC at the upper part is getting close to the MC value in the lower part probably due to the warmer and drier outdoor conditions from May. The MC in upper part of the plywood is similar to that in the lower part for the brick wall BD10 (with top vents and insect screens) during the winter through to the end of March, indicating that cavity ventilation allows moisture carried up by cavity airflow to escape out of the wall from the top vents during this period. However, MC in the lower part of BD10 is higher than that in the upper part starting from the end of April. This is probably due to the wetting by cavity ventilation, which brings in moist outdoor air and the moisture is absorbed by plywood at the lower part first when most of the time the air flows upward. At the end of spring, the difference of MC between upper and lower parts is about 1.3%.

The MC in plywood at the upper part is similar to that at the lower part for both BW8 and BW9 during the winter until the sunny period in February, as shown in Figure 7.

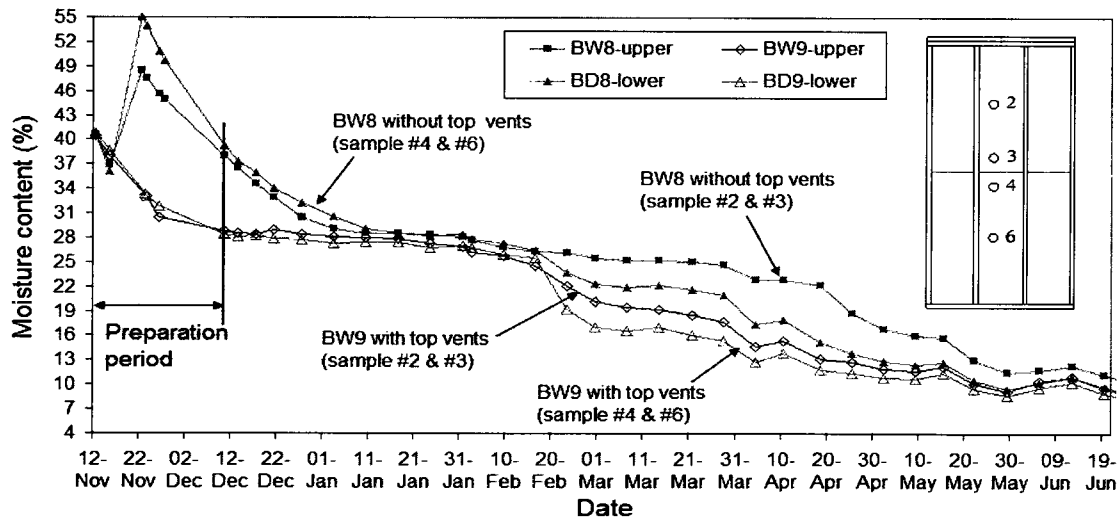

Figure 7: Comparison of average MC in upper and lower parts of plywood between BW8 and BW9 from Nov. 07 to Jun. 08.

The long sunny period in February accelerates the drying of bottom part of BW8 but has a very little impact on the upper part. The difference in MC between the upper and lower part of plywood in BW8 is 3%. The MC at the upper part dries faster starting from the mid-April with less rain and more solar radiation but is still 1.5% higher than that at the lower part.

The MC in the lower part of plywood in BW9 has a sharp drop of 8.5% during the sunny period in February but the MC in upper part drops less for 4.4%. Compared to BW8, the provision of top vents allows the moisture accumulated at the top of cavity to move out but the effect is not that significant due to the small top vent area. By the end of the sunny period, the difference in MC between the upper and lower parts of plywood in BW9 is 3% as the same as BW8. The MC is accumulated at the upper part and slows down the MC diffusion from plywood in this area. Unlike the moisture behavior in BD10 that the MC at upper part is lower than that at its lower part after sunny period in February, the MC at upper part of BW9 is still higher than that at the lower part. The MC at both lower and upper plywood sheathing become very close within 0.5% from the middle of April to the end of spring. It may be explained that the shorter air cavity (one-floor high) provides more even thermal and moisture conditions through the whole cavity compared with the two-floor high cavity. Hence, the MC of plywood becomes similar after the plywood sheathing achieves its equilibrium level.

Fibre cement walls

The average MC in upper and lower parts of plywood sheathing for the dry walls of FD2 and FD3 are shown in Figure 8a. The moisture levels at the upper part for both walls are

higher than those at the lower parts in the winter before the sunny period of February. A big rain event on January 14 with following sunny day (Figure 8b and 8c) has larger impact on the upper plywood panels of both dry walls due to high RH in outdoor air with clear-sky effect and possible shade of trees on the upper part of exterior surfaces of the walls. MC of upper plywood increases 2% but does not affect the lower parts.

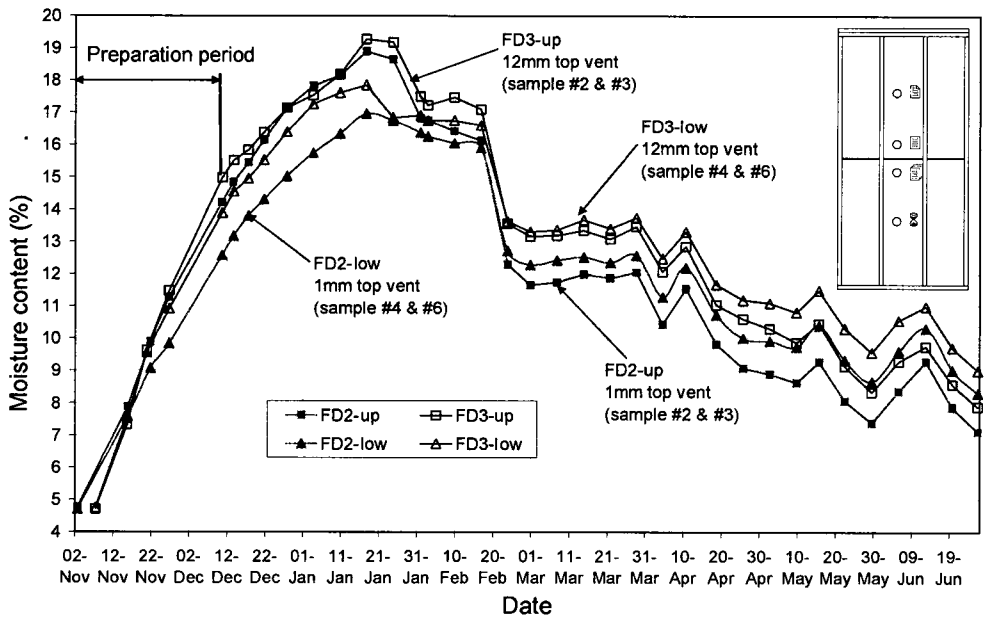

Figure 8a: Comparison of average MC in upper and lower parts of plywood between FD2 and FD3 from Nov. 07 to Jun. 08.

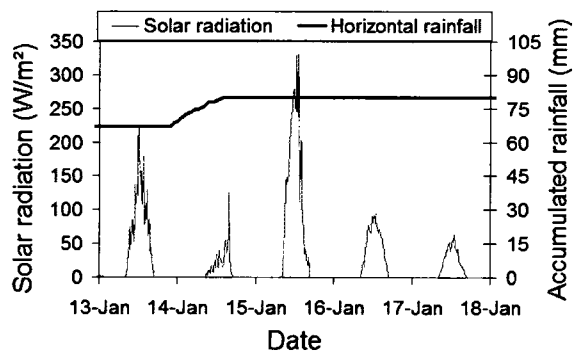

b)

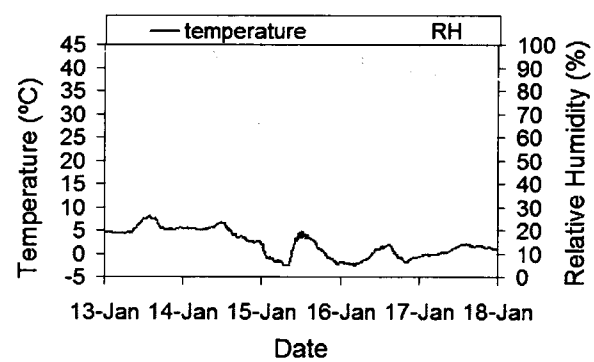

c)

Figure 8b & c: On-site weather conditions of BETF on January 13 – 18, 2008; b) solar radiation / accumulated rainfall, c) temperature / RH.

The difference in MC between the upper and lower parts of plywood sheathing of FD2 is 1% greater than that of FD3 at the beginning of experiment. However, once achieving the equilibrium after the sunny period of February, the difference in FD3 becomes similar to that of FD2 in the late spring after May. In addition, the order of MC at the upper and lower parts of plywood for both walls is reversed. The lower panels have higher MC than that in the upper panels, indicating cavity ventilation wetting occurs since the cavity, at least at the lower part, is drier than the outdoor air.

The same trends exist for the wet walls of FW4, FW5 and FW6, as shown in Figure 9. The difference is that the rain event on January 14 with following clear-sky effect had little influence at the upper parts of plywood sheathing for these wet walls. It is probably because the MC in plywood of the wet walls is still very high and the vapour pressure in plywood is higher than the outdoor saturated air. Hence, the plywood continued to dry out instead of receiving extra moisture from their surrounding environment. The comparisons of MC at the lower and upper parts of the plywood among the wet walls with different sizes of top vent show that the MC at lower parts of all the walls decreases faster slightly than that at upper parts during the preparation period. It is probably because the cavity ventilation directions are upward and carry the moisture from the lower part to upper part in cavity when the wall panels covered up by the fibre cement claddings on the façade of BETF. As a result, MC at the upper parts is higher than that in the lower panels at the beginning of the test period from December 10, 2007 to January, 2008. The difference in MC between lower and upper panels of FW4 and FW5 are similar, within 2%, while the difference in MC between the lower and upper part of FW6 is smaller, only about 1%.

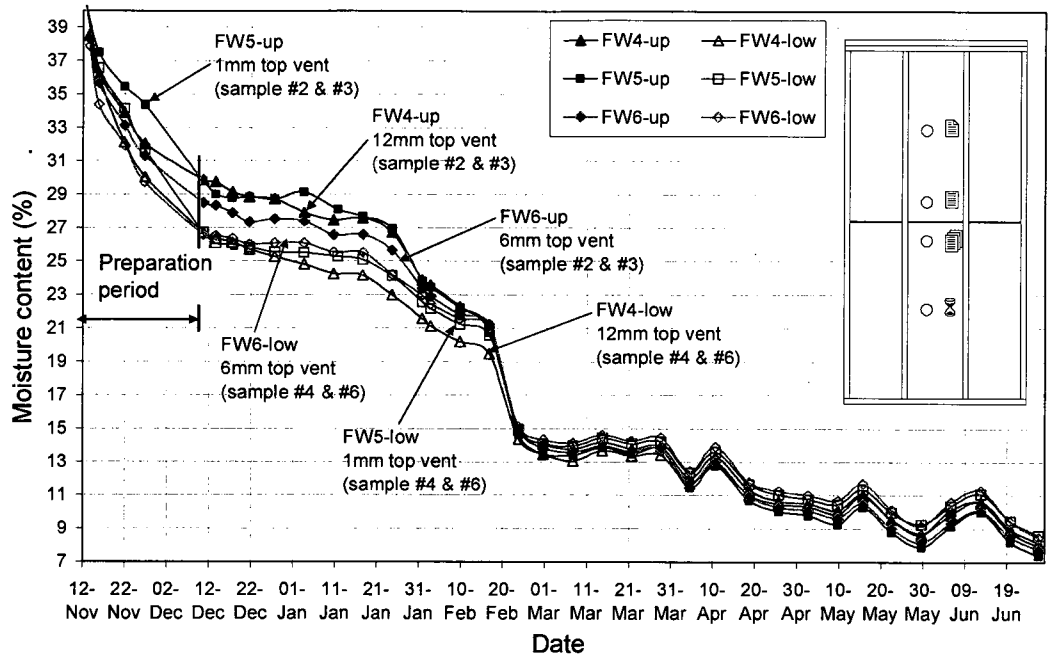

Figure 9: Comparison of the average MC in upper and lower parts of plywood among FW4, FW5 and FW6 from Nov. 07 to Jun. 08.

After the first sunny period on January 20 - 25, the MC in upper parts of FW4 and FW5 drops to the similar level as that of FW6. MC in both upper and lower panels for all three wet walls reaches to the similar levels below 15% after sharp drops during the sunny period of February. From March to the end of spring, the lower parts of plywood experience cavity ventilation wetting and their MC is higher than those at the upper parts. The MC levels in three walls are very similar and the difference is negligible.

Compared to FW4 with a 12mm top vent and a 19mm air cavity, overall FW1 which has the same size of top vent with a 10mm air cavity has a similar MC in plywood as shown in Figure 10. From the beginning of test to after the first sunny period in January, MC at the upper part of plywood sheathing stayed at the same level of 27% without change while the MC of FW4 and the MC at the lower part of plywood in FW1 constantly decease, indicating that a narrow air cavity generates less ventilation resulting in higher

MC accumulating at the top. MC of plywood reaches the equilibrium level after the second sunny period in February and fluctuates with the weather change from March to end of April. From May to the end of spring MC at upper panel drops to the lowest level while the plywood lower panel experiences wetting by ventilation, the same as that for FW4.

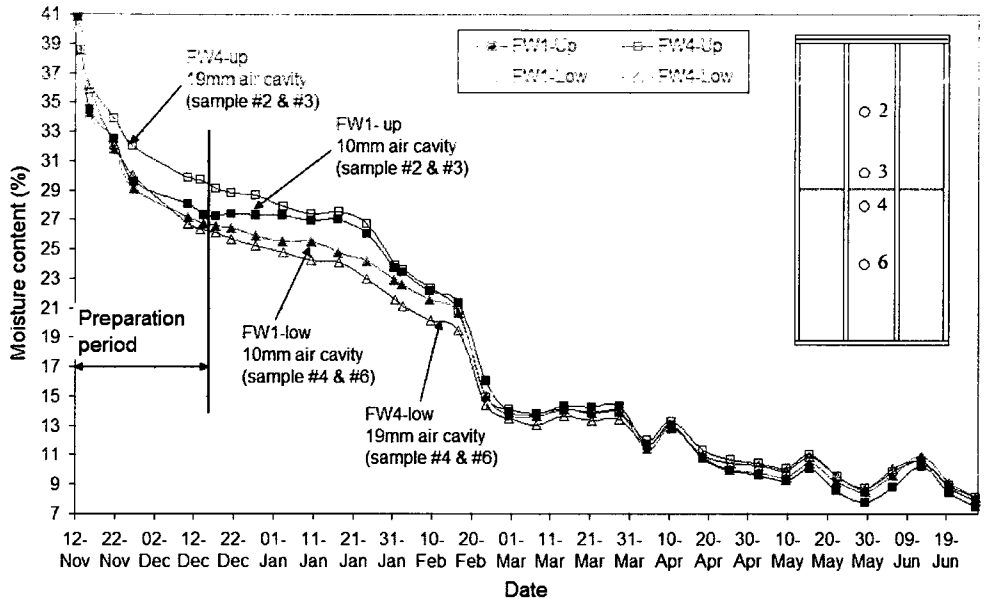

Figure 10: Comparison of the average MC in upper and lower panels of plywood between FW1 and FW4 from Nov. 07 to Jun. 08.

3. Comparison of MC at different depth of plywood

To measure the MC distribution across the plywood, three pairs of MC sensors were installed at three different depths of plywood sheathing at the symmetrical locations to gravimetric samples #2 and #6 along the center line of the test bays in all wet walls. The layout is shown in Figure 11. The moisture-pins installed at 6mm (centre) and 10mm (near exterior surface) from the interior surface are insulated pins, which measure MC at the specified depth. The third pair of moisture-pins used is stainless screws that were inserted about 3mm into the plywood from the interior surface. The moisture-pin

readings are available from December 28, 2007 due to the sensor installation delay and calibrations.

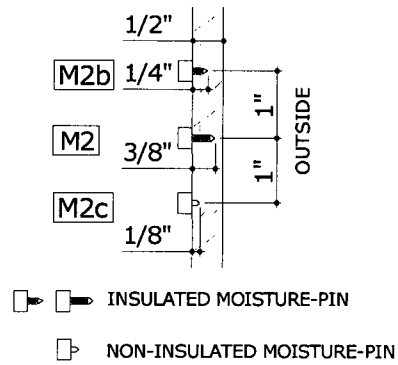

Figure 11: Moisture-pins at three depths of plywood sheathing in all the wet walls. Label "2" denotes at the symmetrical position to samples #2.

In general, MC at the centre depth of plywood is the highest at the beginning compared to MC at the other two different depths of plywood for most walls, indicating that the plywood was completely wet all the way through the whole depth. However, the MC profiles at different depths of the plywood are different for test walls depending on the vent configurations, type of claddings, and air cavity depths.

Brick walls

The MC at the centre depth of the upper part of plywood (symmetric position to sample #2) in BW8 was the highest throughout the entire test period and the interior surface was drier than the exterior surface until early April, as shown in Figure 12. The maximum differences between centre and interior of MC were 1% and 2% between centre and exterior surfaces from December 28, 2007 to the end of February. Then the MC at the exterior and interior surfaces became close. Three depths of the plywood reach similar MC levels when the MC of plywood reached its equilibrium value at the end of May.

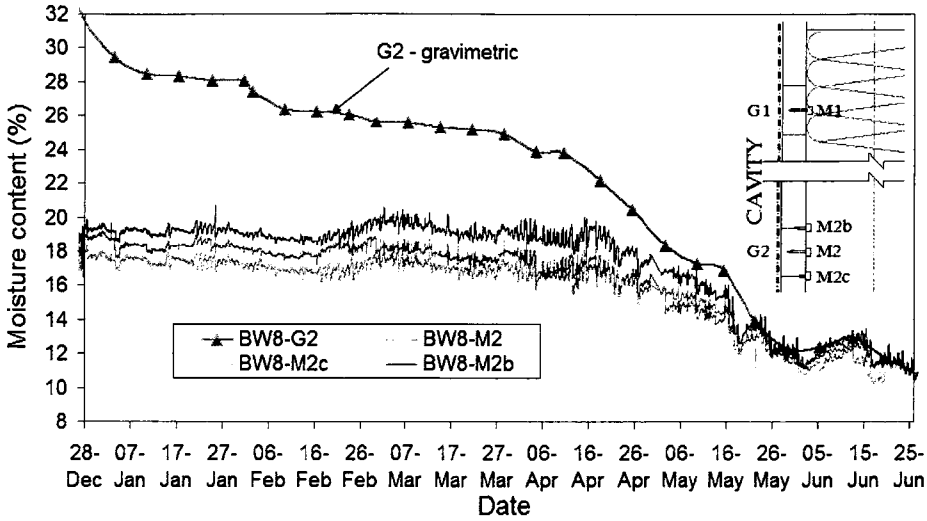

Figure 12: Comparison of MC at different depths of plywood at symmetric position to sample #2 in brick wall BW8 without top vents.

However, for BW9, the wall with top vent, the MC level of the upper part of plywood was higher on the exterior and lower on interior, and the MC at the center depth falls in between, as shown in Figure 24. The drying of plywood was from interior to exterior at the beginning of the test until the sunny week of February. In April after reaching the equilibrium MC level, MC on interior surface slightly increased and became the highest. The vapour diffusion probably reversed to inward.

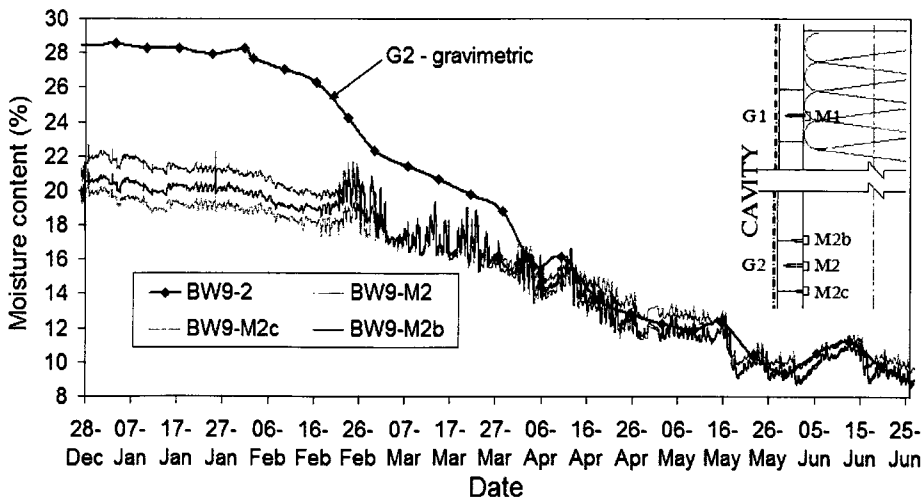

Figure 13: Comparison of MC at different depths of the upper part of plywood in brick wall BW9 with top vents.

At the lower part of plywood (symmetric position to sample #6), MC at the centre depth and exterior surface of plywood for both walls was similar and higher than the interior surface before the sunny period in February, as shown in Figure 14 and Figure 15.

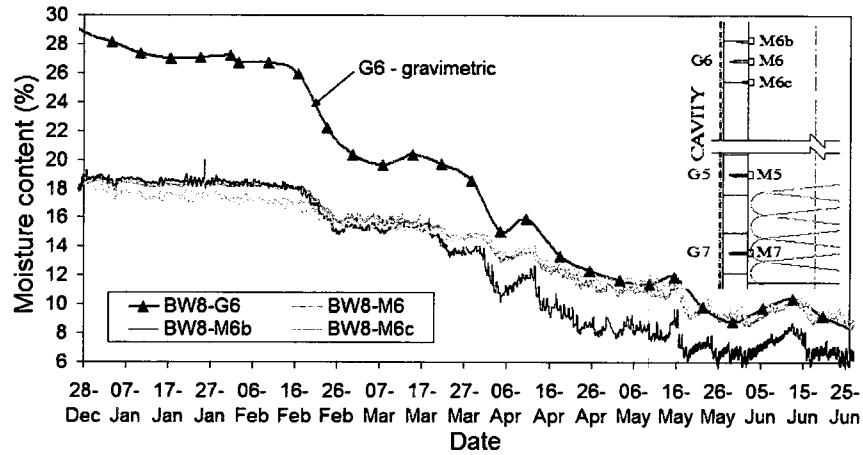

Figure 14: Comparison of MC at different depths of the lower part of plywood (symmetrical position to sample #6) in brick wall BW8 without top vents.

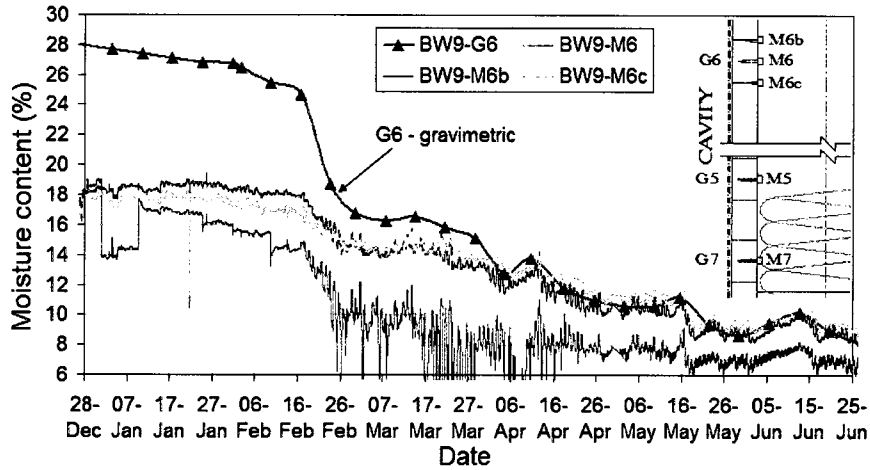

Figure 15: Comparison of MC at different depths of the lower part of plywood (symmetrical position to sample #6) in brick wall BW9 with top vents.

The difference of MC at three depths was larger in BW9 than that in BW8. The exterior surface of plywood for BW9 dried much faster than at the other two depths due to the ventilation through the air cavity and the vapour diffusion mainly from indoor to outdoor. The plywood at the centre depth of BW8 dried faster than the other two depths after the sunny period in February due to lack of ventilation, indicating that the drying of plywood

mainly depends on the vapour diffusion inward and outward from the centre to the both surfaces.

Fibre cement walls

The MC change at different depths of plywood for all the wet walls with a 19mm air cavity (FW4, FW5 and FW6) has similar trends. For example, the MC at the centre depth of plywood in FW4 is the highest at the beginning of the experiment and then MC at interior surface became the highest after the MC at the centre depth had a sharp drop during the sunny period in February, as shown in Figure 16 and Figure 17. After reaching the equilibrium MC level after the sunny period, the MC at the exterior surface and centre depth of plywood fluctuates in response to the change in outdoor weather conditions. The difference in MC at different depths between upper and lower part of plywood is that the MC at the centre depth at lower part is closer to the MC at interior depth with small fluctuations while the MC at the centre depth of the upper part is close to the MC near the exterior surface with large fluctuations.

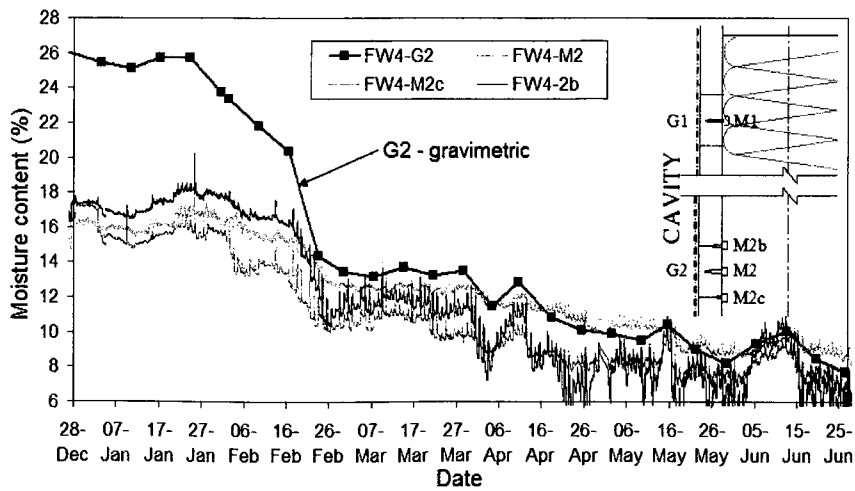

Figure 16: Comparison of MC at different depths of the upper part of plywood (symmetrical position to sample #2) in fibre cement wall of FW4 with a 19mm air cavity.

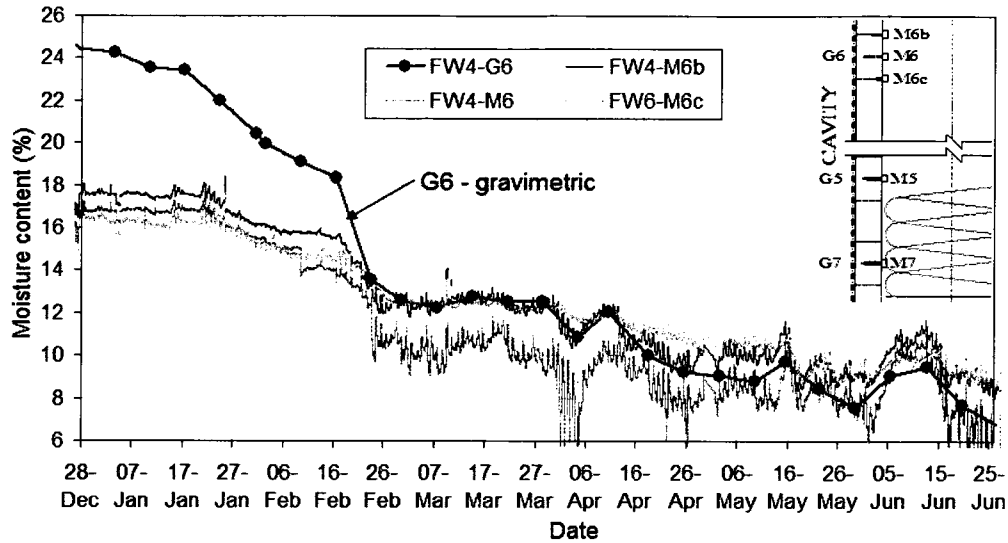

Figure 17: Comparison of MC at different depths of the lower part of plywood (symmetrical position to sample #6) in fibre cement wall of FW4.

However, FW1 with a 10mm air cavity had different patterns of MC at different depths of the upper part of plywood, as shown in Figure 18. MC near exterior surface was the highest throughout the entire test period, which may indicate a slower drying rate at the exterior surface due to restricted airflow resulting from a narrower air cavity.

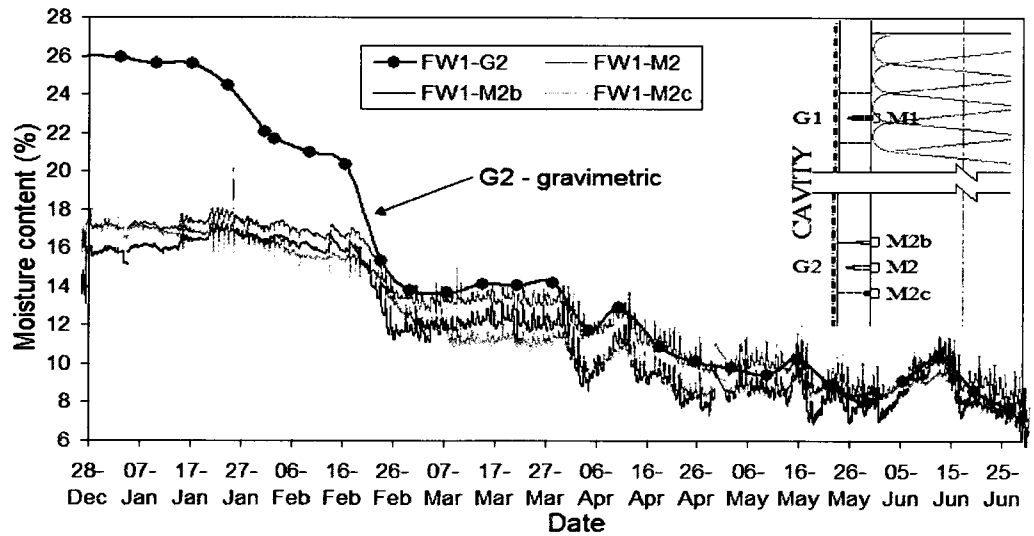

Figure 18: Comparison of MC at different depths of the lower part of plywood (symmetrical position to sample #2) in fibre cement wall of FW1 with a 10mm air cavity.

4. Vapour pressures inside air cavity

Vapour pressures inside the cavities for brick walls vary significantly depending on the vent configuration, especially at the upper part of the cavity. For fibre cement walls, the differences of vapour pressure at the lower part inside the cavities are affected more by cavity depths than the sizes of top slot vents.

Brick walls

Figure 19 shows the vapour pressures in two-storey test walls BD7 and BD10 for a test period from February 16 to March 5, 2008. The vapour pressure in the air cavity was higher than outdoor vapour pressure.

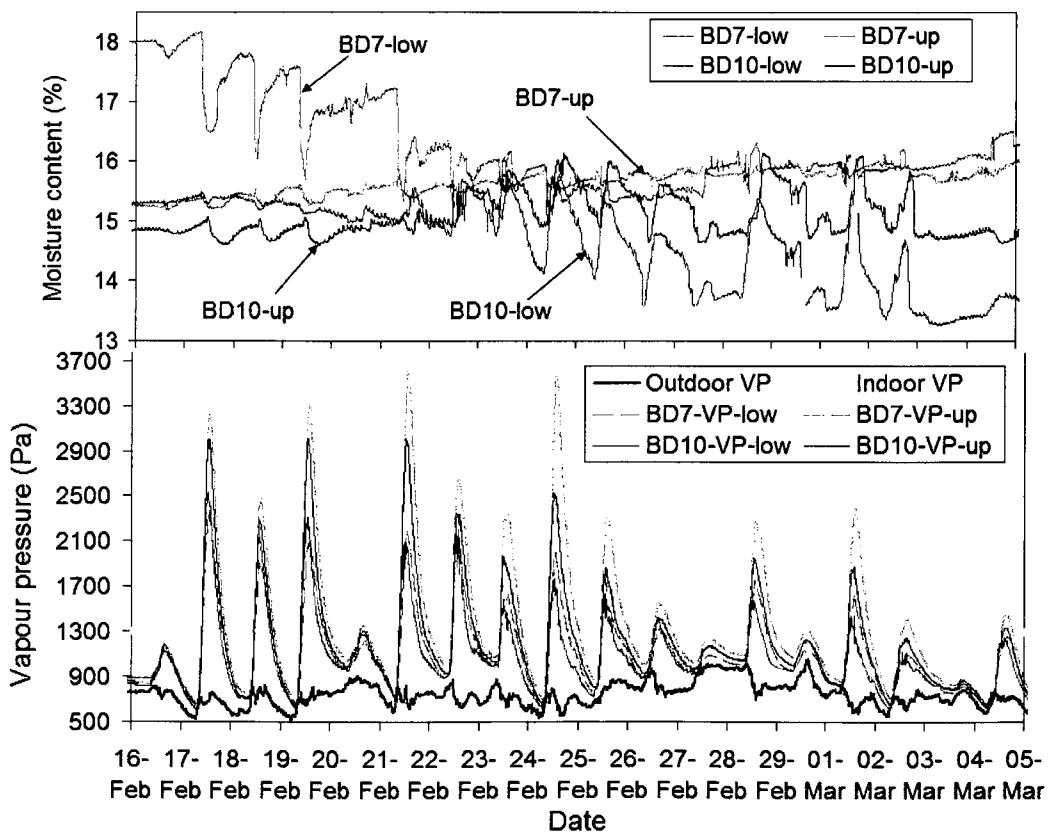

Figure 19: Moisture contents in plywood and vapour pressures in air cavity of test walls BD7 and BD10 from Feb. to Mar. 08 ("up" refers to the upper level in the cavity, and "low" refers to the lower level in the cavity).

In addition, the vapour pressure at the upper level was higher than that at the lower level. This trend indicates that ventilation will help to move moisture up to the top of the cavity. The lack of top vents in BD7 resulted in a much higher vapour pressure at the upper level than that at the lower level, especially during the sunny period. The vapour pressure difference between the upper and lower level can reach as high as 1600 Pa in BD7. The difference in vapour pressure between the upper level and lower level in BD10 was much smaller, about 860 Pa lower, than that in BD7. The provision of top vents in BD10 allows moisture to move out of the cavity.

Responding to the vapour pressure in the cavities during the sunny period in February, the MC of plywood at the lower level decreased for both walls while the MC of plywood at the upper level of BD7 increased continuously. As a general trend, he MC in both lower and upper level of plywood for BD10 fluctuated largely within a day, 2% MC difference at the lower part and 1% MC at upper part. The decrease of MC at the lower part of BD10 is faster than that at upper part. The distribution of vapour pressure in the air cavity with MC change of plywood indicates that cavity ventilation is effective in removing moisture under sunny conditions for the brick walls. However, the moisture removal depends on the vent size and the cavity height. With the small top vent, ventilation is not sufficient to move moisture out of the air cavity and as a result the MC at upper wall is higher than that at the lower wall.

A similar trend of vapour pressure in the cavity is observed for brick walls BW8 and BW9, as shown in Figure 20. In general, the vapour pressures in BW8 and BW9 are higher than those in BD7 and BD10 due to the initially high moisture load in the plywood. The maximum vapour pressure reached 4200 Pa for BW8 and 3400 Pa for

BW9. The MC in plywood during and after the sunny period decreased 7% for BW9 and only 2% for BW8. The short air cavity results in a higher ventilation air change rate and BW9 dried faster than BD10. The difference in MC decrease between BW8 and BW9 is more obvious than that between BD7 and BD10.

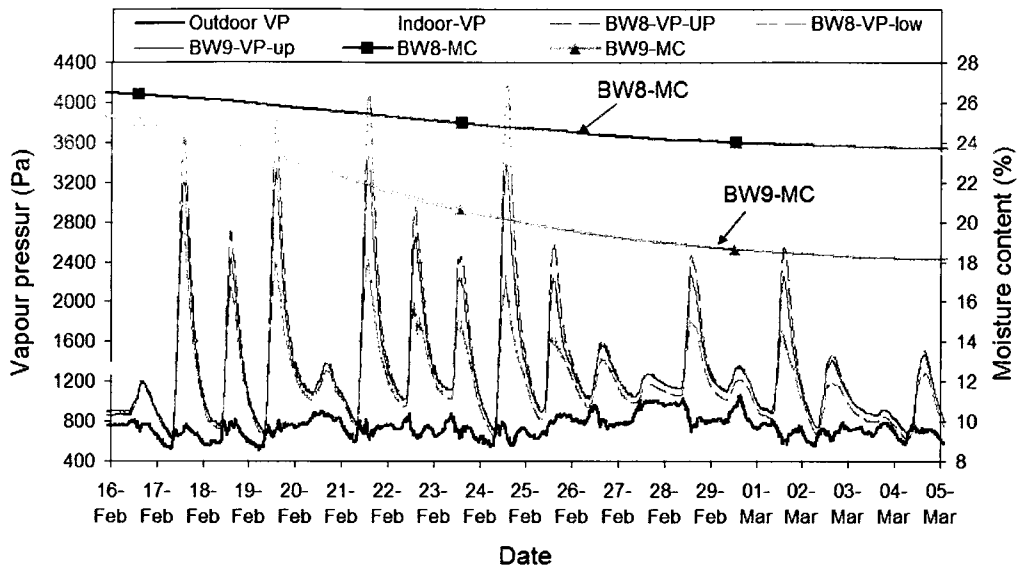

Figure 20: Moisture contents in plywood and vapour pressures in air cavity of brick walls BW8 and BW9 from Feb. to Mar. 08. ("up" refers to the upper level in the cavity, and "low" refers to the lower level in the cavity).

Two brick walls BDU11 and BDU12, installed at the upper level of the façade, have one RH sensor installed in the middle of each cavity. Figure 21 shows that the vapour pressures in the air cavities were mostly higher than outdoor vapour pressure for both walls from February 16 to March 5, 2008. The larger top vents in BDU12 results in a much lower vapour pressure in the cavity than that in BDU11 with smaller top vents. The maximum vapour pressure for BDU12 during the sunny period in February was only 1700 Pa and was about 1200 Pa lower than that in BDU11. The responses of MC in plywood to the different vapour pressure in the cavities show that BDU12 dried much faster than BDU11. The MC in BDU12 decreased about 4% while BDU11 only

decreased by less than 2%. Again, the difference of vapour pressure in the cavities and response of MC in plywood for both walls indicates cavity ventilation is most effective in removing moisture under sunny conditions.

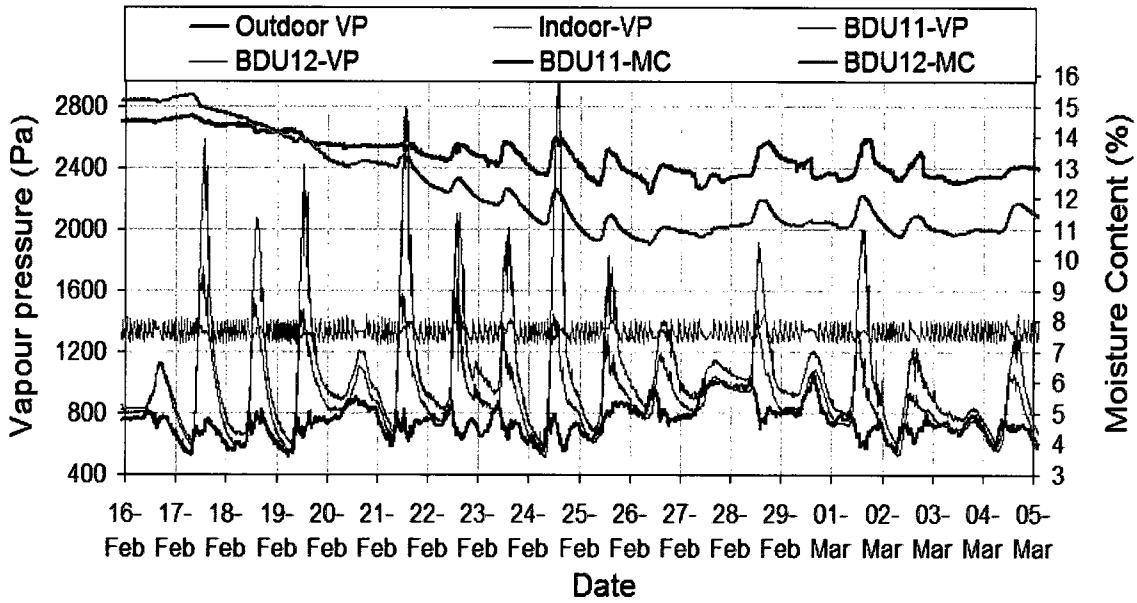

Figure 21: Moisture contents in plywood and vapour pressures in air cavity of brick walls BDU11 and BDU12 from Feb. to Mar. 08.

Fibre cement walls

The outdoor vapour pressures in all fibre cement walls are constantly higher than the cavity vapour pressures during night-time even on the rainy days. The cavities experienced both drying and wetting on a daily basis. Figure 22 shows that the maximum vapour pressure in the cavity of FD2 (with 1mm top vent) was 500 Pa higher at daytime during the sunny days but about 100 – 200 Pa lower at night during cloudy and rainy days than those in FD3 (with a 12mm top vent). It indicates that the walls with larger top vent resulted in lower vapour pressure in the cavity than the walls with smaller top vents under solar radiation. The ranges of cavity vapour pressure were 300 – 1600 Pa for FD2 and 350 – 1300 Pa for FD3 during this period. The responses of MC in plywood to such

small difference of vapour pressure in the cavities show that both walls dried in the similar speed, MC at upper levels decreased slightly more than at the lower levels.

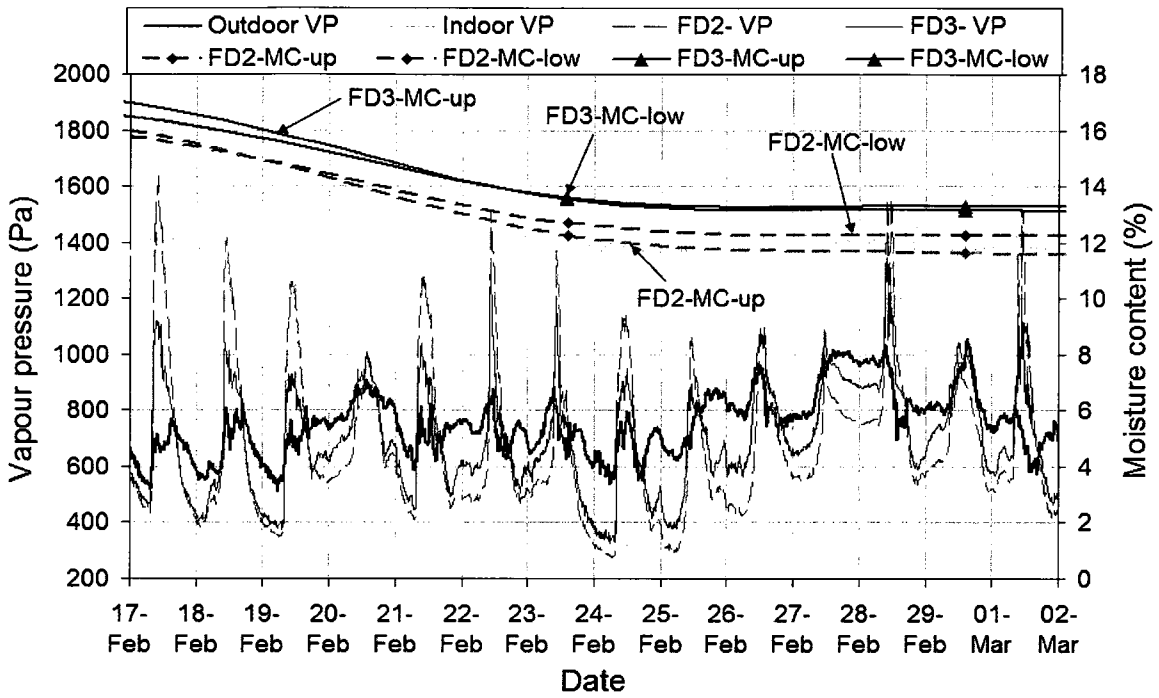

Figure 22: Moisture contents in plywood and vapour pressures in air cavity of fibre cement walls FD2 and FD3 from Feb. to Mar. 08.

A similar trend of vapour pressures in the cavities is observed for FW5 and FW4, as shown in Figure 23. In general the vapour pressures in FW5 and FW4 with an initial high MC in plywood are similar to those in FD2 and FD3. The vapour pressure in the cavity of FW5 was slightly higher than that in FW4 during this short period. The maximum vapour pressure reached to 1500 Pa for FW5 and 1400 Pa for FW4. The plywood at the upper level of FW5 had the fastest drying while the plywood at the lower level of FW4 had lowest drying during the sunny week in February. It can be explained that with smaller ventilation due to smaller top vent, cavity ventilation wetting is less in FW5 than that in FW4, however, the difference of drying in both wall are small and insignificant.

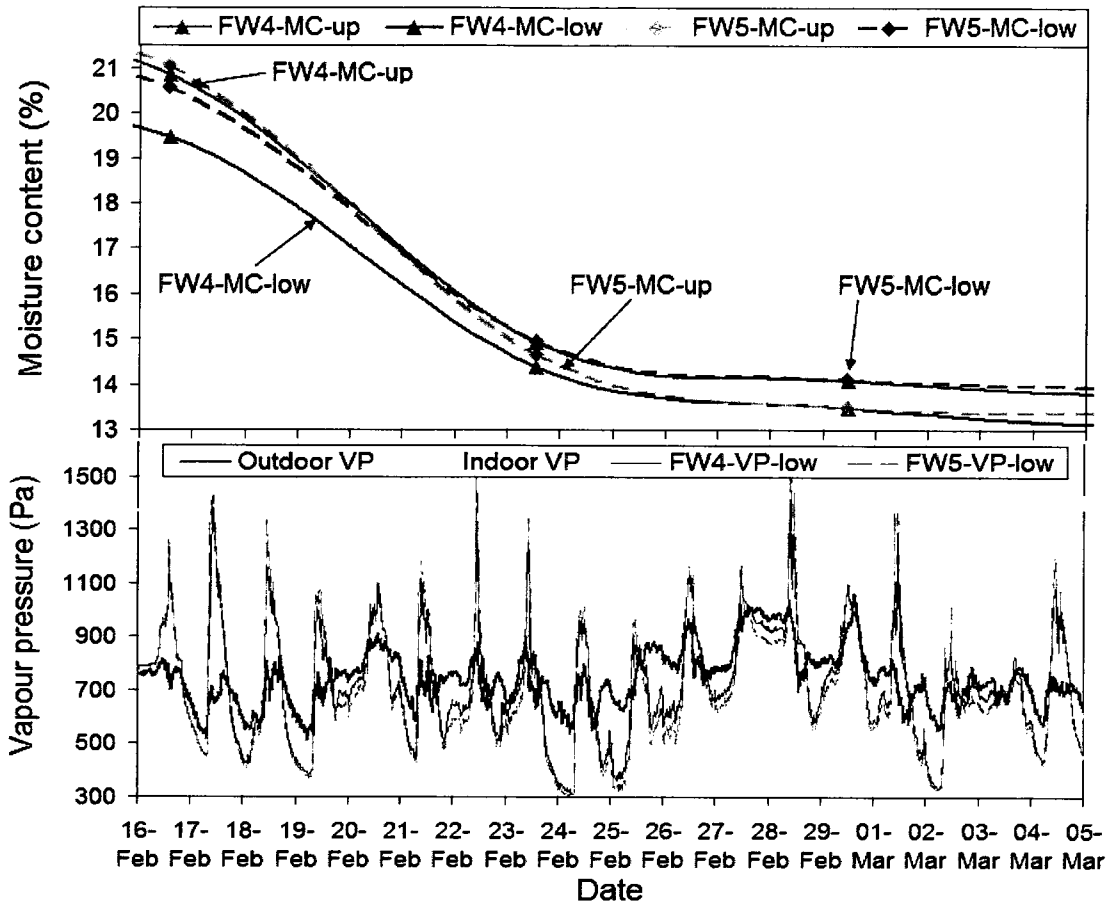

Figure 23: Moisture contents in plywood and vapour pressures in air cavity of fibre cement walls FW4 and FW5 from Feb. to Mar. 08.

Figure 24 shows the vapour pressures in the cavity of FW1 and FW4. The maximum vapour pressure at lower part of FW1 with a 10mm cavity is 1350 Pa higher than that in FW4, reaching 2700 Pa. It indicates that a wider cavity removes more water vapour resulting from the greater cavity ventilation. With a narrower cavity, the moisture evaporated from the plywood and fibre cement cladding is accumulated inside the cavity. As a result, the plywood at the lower part of the cavity in FW1 dried faster than the upper part although the difference of the MC decrease between lower and upper part was quite small.

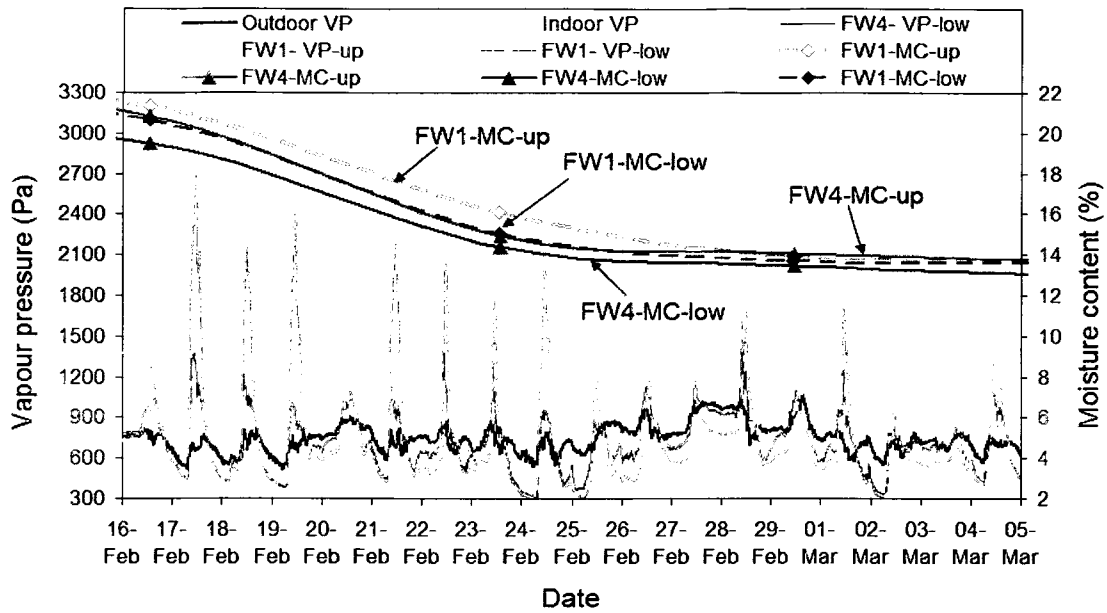

Figure 24: Moisture contents in plywood and vapour pressures in air cavity of fibre cement walls FW1 and FW4 from Feb. to Mar. 08.

Appendix 3: Thermal Performances of Rainscreen Walls

Temperature difference between air cavity and ambient air

Temperatures and RH in the air cavities are monitored using RH-T sensors in the cavities of all the test walls as described in the previous section 5.2.2. "Vapour pressure through insulation space and air cavity". The temperature difference between air cavities and ambient air obtained is the difference of temperature measurements from the RH-T sensors in the air cavities and from weather station placed on BETF's roof, using the 10-minute average data. Positive values in the figures denote a higher cavity temperature than the ambient air temperature.

1. Brick walls

Figure 1 to Figure 3 show the temperature differences between the cavities and ambient air in brick walls from December 22, 2007 to June 21, 2008. Positive values in the figures denote a higher cavity temperature than the ambient air temperature. The comparison of temperature differential between the walls will use temperature measurements of RH-T sensors at upper levels for BD7, BD10, BW8 and BW9 since BW9 only has one top RH-T sensor. The temperature differences in walls located at the south corner of BETF's SE facade are quite small on January 15 and Jan. 21 – 25 as marked in the Figures due to the shade casted on the surface by trees located about 30m to the southeast direction. The temperature differences in BD7 and BD8 at the east corner had a maximum of 5 °C greater than those in BD10 and BW9 at the south corner in this period. The differences between the upper walls of BDU11 and BDU12 were small.

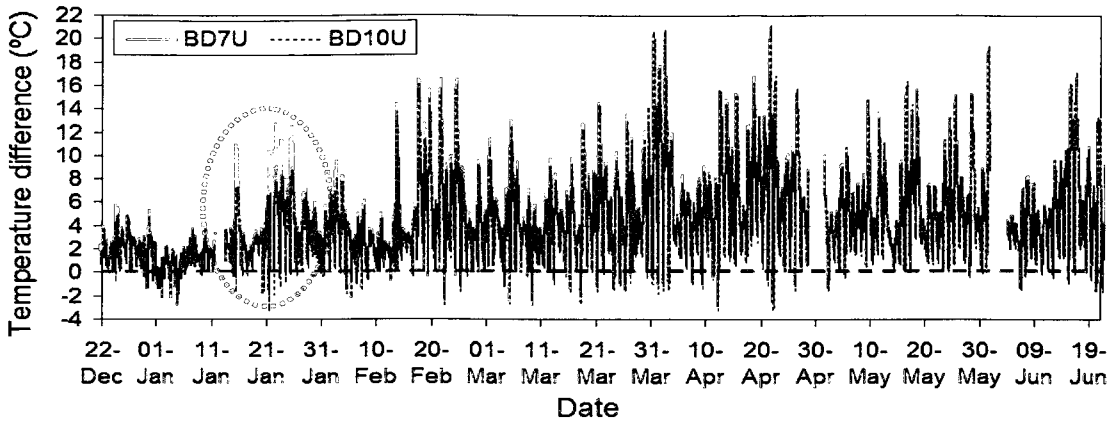

Figure 1: Comparison of temperature difference between cavity and outdoor air in BD7 and BD10 from Dec, 07 to Jun, 08 ("U" refers the RH-T sensors located at the upper part of air cavity).

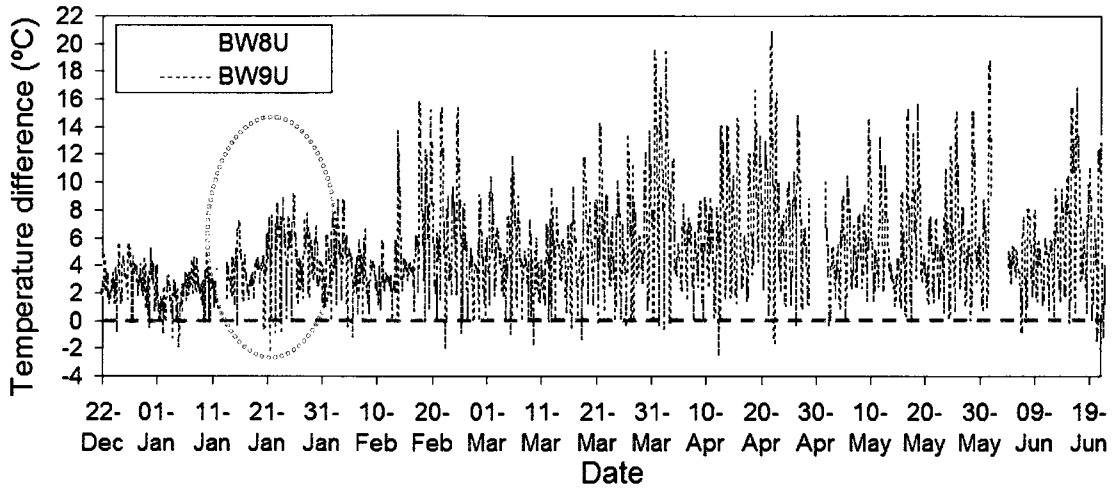

Figure 2: Comparison of temperature difference between cavity and outdoor air in BW8 and BW9 from Dec, 07 to Jun, 08 ("U" refers the RH-T sensors located at the upper part of air cavity).

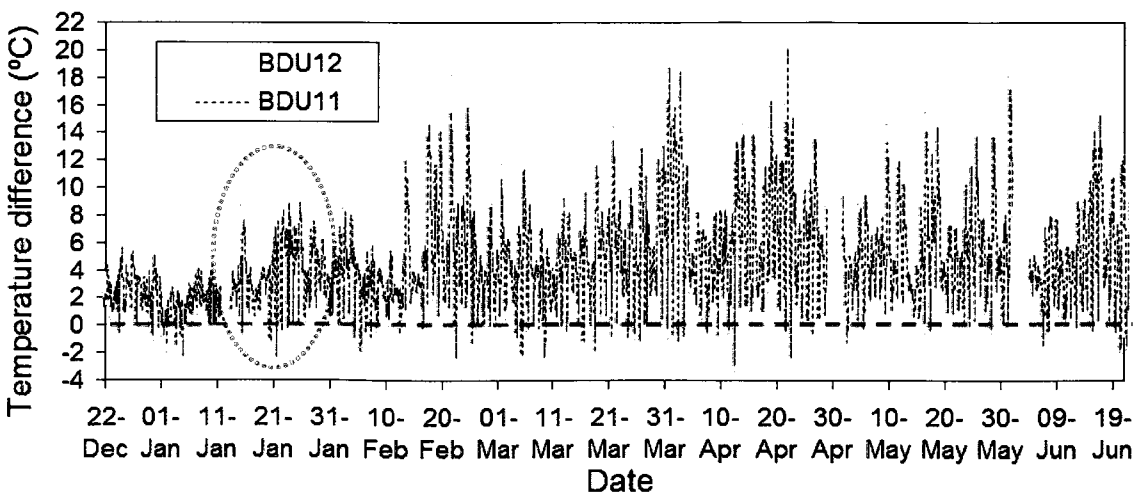

Figure 3: Temperature difference between cavity and outdoor air in BDU11 and BDU12 from Dec, 07 to Jun, 08 (the RH-T sensors located in the middle of air cavity).

The temperature differences between cavity and ambient air are positive at most time and have large fluctuations on sunny days but small fluctuations on cloudy and rainy days. In the winter, the range of temperature difference was within -2 – 6 °C on the cloudy and rainy days for all the brick walls. The maximum temperature differences on the sunny days were 4-5 times larger than those on the cloudy and rainy days at daytimes but it is similar at night.

In general, the walls with top vents have slightly lower temperature differences than the walls without top vent. In the sunny period of February 17 – 25 between the two-floor high walls BD7 and BD10, the difference was small. Temperature differences in BD7 were less than 1 °C higher than those in BD10, indicating that ventilation in the long air cavity with small top vent area has very little influence on the temperature difference. It is interesting to note that in the one-floor high walls of BW8 and BW9 at the lower level of the facade, the temperature differences in BW8 (without top vents) were about 0.5-1.2°C smaller than those in BW9 (with 2-descrite vents and insect screens) at night and on cloudy, rainy days. With solar radiation on sunny days for both walls, the maximum temperature difference in BW8 was 3°C higher than that in BW9 at daytime.

BDU11 is located near south corner and have six-25mm high discrete vents on the top row of the brick veneer covered by the roof flashing. BDU12 is located near east corner with six-65mm high discrete vents on the second top row of the brick veneer below roof flashing. That means BDU12 has bigger top vent area than BDU11 and the top vents are exposed to the weather conditions. The temperature difference in BDU11 is found to be about 3°C lower than those in BDU12 during the daytimes on the sunny days due to the shade of the tree at the exterior surface of BDU11.

In the spring, the temperature differences in all the brick walls fluctuate in response to the weather conditions, i.e. by solar radiation. The temperature differences in all the walls located at the lower level of the facility were very similar due to the thermal mass provided by the brick veneer. The cavity temperatures were mostly higher than the ambient air during both daytime and night time. The temperature differences between cavity and ambient air in BDU11 and BDU12 at upper level were similar to those in brick walls located at the lower level of façade in the daytime on sunny days. However, on the rainy and cloudy days and at nights, the cavity temperatures was approximately 0.5 - 1.5 °C lower than those in the walls at lower level. It is probably because of the clear sky effect together with higher cavity ventilation rate induced by larger vent areas.

2. Fibre cement walls

Similar to the brick walls, the temperature differences between cavity and ambient air for the all the fibre cement walls are positive at most time and have large fluctuation on sunny days but small fluctuations on cloudy and rainy days. A few and small negative values occur at nights, i.e. the outdoor air temperature is higher than the cavity temperature.

Figure 4 to Figure 6 show the results of fibre cement walls from December 22, 2007 to June 21, 2008. In the winter, all the walls with a 19mm air cavity had similar temperature differences at the nights and at daytimes of cloudy and rainy days. The range of temperature differences were 0 – 4°C mostly and it occasionally went down to -2 °C.

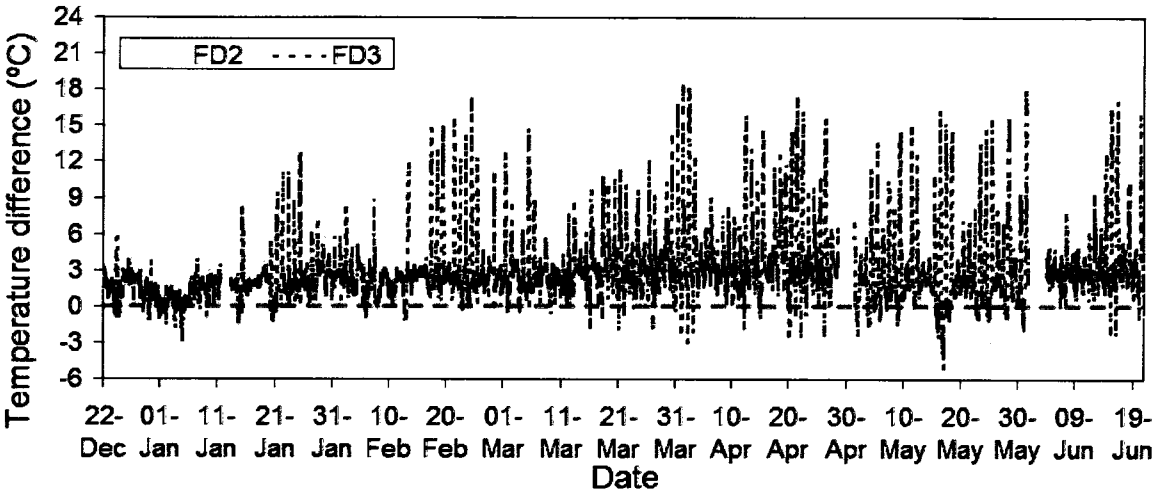

Figure 4: Temperature differences between cavity and outdoor air in FD2 and FD3 from Dec. 07 to June 08 (RH-T sensors located in the middle of air cavity).

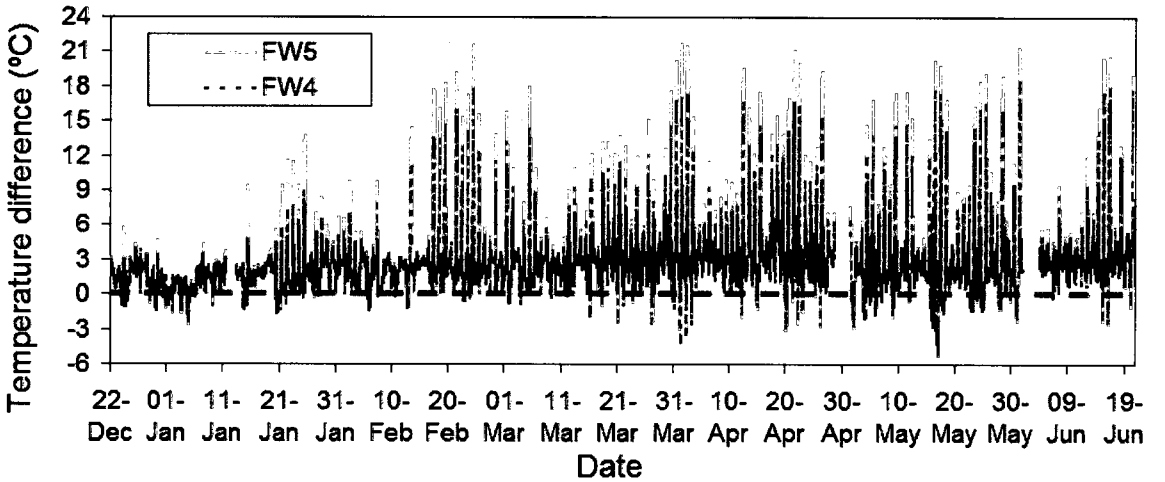

Figure 5: Temperature difference between cavity and outdoor air in FW4 and FW5 from Dec. 07 to June 08 (RH-T sensors located in the lower part of air cavity).

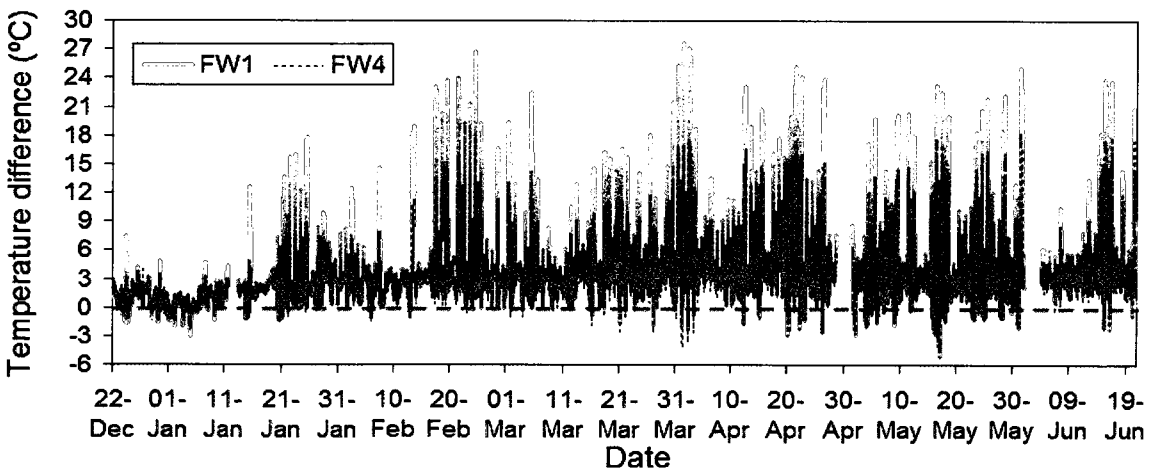

Figure 6: Temperature difference between cavity and outdoor air in FW1 and FW4 from Dec. 07 to June 08 (RH-T sensors located in the lower part of air cavity).

On the sunny days, the maximum temperature difference is 6 - 10 times larger than that on the cloudy and rainy days at daytimes but it is similar at night times. It is 2 – 3 times higher than that in brick walls due to the smaller thermal storage capacity of the thin fibre cement cladding (8mm thick).

The temperature differences at daytime reached a maximum of 17 - 23°C for the walls with a 19mm air cavity during the continuous sunny period of February 17 – 25. During this short period, the large temperature difference between the cavities and outdoor air creates a big enough thermal buoyancy force to induce air flow into the air cavity and carry the moisture evaporated from sheathing and cladding out of the cavities. It is especially beneficial for the walls with a high initial moisture level in the sheathing at the beginning of the experiment. The maximum temperature differences in FD2 and FW5 (with 1mm high continuous slot vent) are 5°C higher than that in FD3 and FW4 (with 12mm high continuous slot vent), i.e. 22°C for FD2 and FW5 and 17°C for FD3 and 18°C for FW4, as shown in the Figures above.

For the wall with a 10mm air cavity and a 12mm top slot vent, the temperature differences between the air cavity and outdoor in FW1 were always greater than that in FW4 with a 19mm air cavity and the same vent configuration. The maximum temperature difference in FW1 was over 9°C higher than that in FW4 at daytime. At the nights, the temperature differences in FW1 were similar to that of FW4. The range of temperature differences between air cavity and ambient air for FW1 was -2 - 27°C in the winter.

In the spring, the temperature differences between cavity and ambient air in all the fibre cement walls have more fluctuations due to more sunny days than in the winter. April and

May have more fluctuation than June due to more sunny days. The negative values at nights occur more often than in the winter due to the under-cooling effect caused by clear sky radiation. The lower temperature in cavity than the outdoor air occurs almost at every night of the sunny days. The maximum temperature difference at night is down to -6°C in May.

On the cloudy and rainy days, the range of temperature differences between air cavity and ambient air is within 2 - 6°C and 2 °C higher than that in the winter for all the fibre cement walls. On the sunny days, the maximum temperature differences at daytimes reach to 18 - 23°C for the walls with a 19mm air cavity and 28°C for the wall with a 10mm cavity in April. The maximum temperature difference at daytime is over 10°C higher in FW1 than that in FW4 in April.

Comparison of temperature difference of test walls in the winter and spring

Overall, the average temperature differences in all the fibre cement walls and brick walls are small during the winter and spring test period in 2008, approximately 2°C in the winter and 4°C in the spring for fibre cement walls. The average difference in brick walls are 2°C higher than those in fibre cement walls in both seasons, around 4°C in the winter and 6°C in the spring, as shown in Figure 7. In this thesis, the winter is defined as from December 22, 2007 to March 21, 2008 and the spring is defined as from March 22 to June 21, 2008. For the fibre cement walls with a thin fibre cement cladding, the maximum temperature differences at daytime are only 1°C higher in the spring than in the winter. However, the maximum negative temperature difference at night is almost 3°C

higher in the spring than that in the winter probably due to the under-cooling effect by the clear-sky radiation.

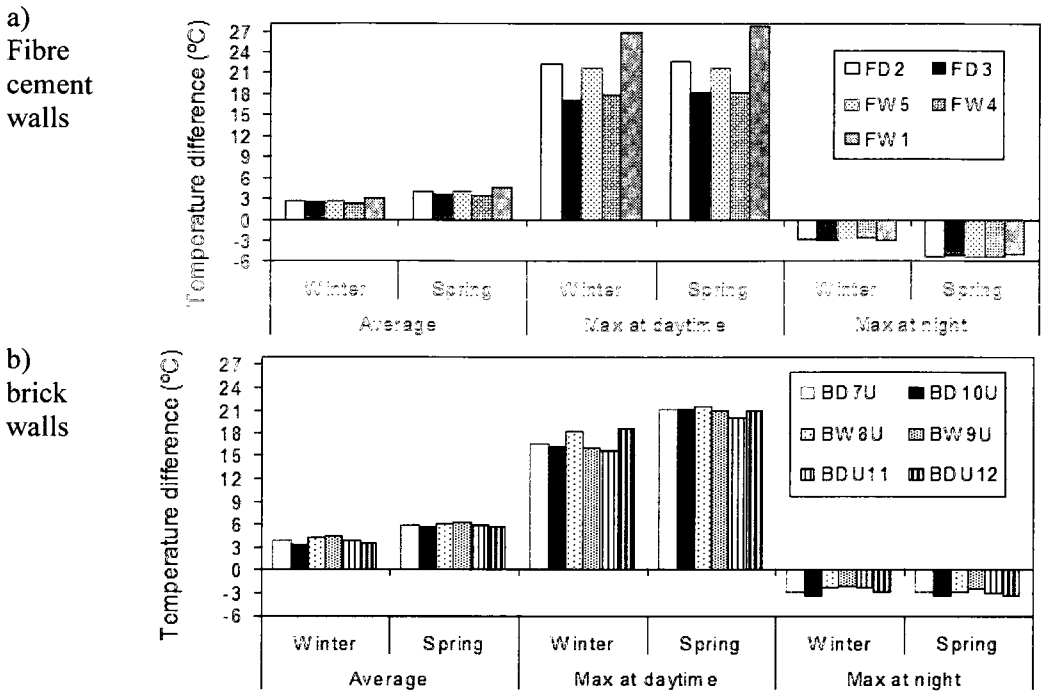

Figure 7: Average and maximum temperature differences between air cavity and ambient air in all test walls between the winter and spring of 2008.

For the brick walls with thick brick veneers, the maximum temperature differences at daytime are 4 to 5°C higher in the spring than that in the winter. However, the maximum negative temperature differences at night are very similar to those in the winter. It is probably due to both the small vent areas and reduced under cooling effect by the thermal mass provided by the brick veneer.

Under-cooling effect on the temperature of cavity-surfaces

Brick veneer and fibre cement cladding are the outer layers of wall components that provide protection against the wind-driven rain and varying outdoor conditions. The plywood sheathing of a wood frame back wall is the most vulnerable component to

surface moisture problems since it is located near the air cavity and has the lowest temperature of a wood-frame back wall. The cavity-surfaces of rainscreen claddings and plywood sheathing may experience the clear-sky effect. It may result in a lower surface temperature than that of outdoor air and even lower than the outdoor dew-point temperature which causes condensation. Potential wetting of the rainscreen claddings and sheathing may occur.

1. Brick veneer

Brick veneer and fibre cement cladding are the outer layers of wall components that provide protection against the wind-driven rain and varying outdoor conditions. The plywood sheathing of a wood frame back wall is the most vulnerable component to surface moisture problems since it is located near the air cavity and has the lowest temperature of a wood-frame back wall. The cavity-surfaces of rainscreen claddings and plywood sheathing may experience the clear-sky effect. It may result in a lower surface temperature than that of outdoor air and even lower than the outdoor dew-point temperature which causes condensation. Potential wetting of the rainscreen claddings and sheathing may occur.

For the brick walls, under-cooling temperatures on the cavity-surfaces of brick walls only occur occasionally. The monthly under-cooling temperature frequency during the test period from December 22, 2007 to June, 2008 is shown in Figure 8. In general, the under-cooling temperature frequencies for all the brick walls decreased from December, 2007 to June, 2008. The peak under-cooling temperature frequency occur in December and January for all brick walls, indicating winter has more risk of condensation caused by

clear-sky effect than spring due to high humidity of outdoor air resulting in high dew-point temperatures.

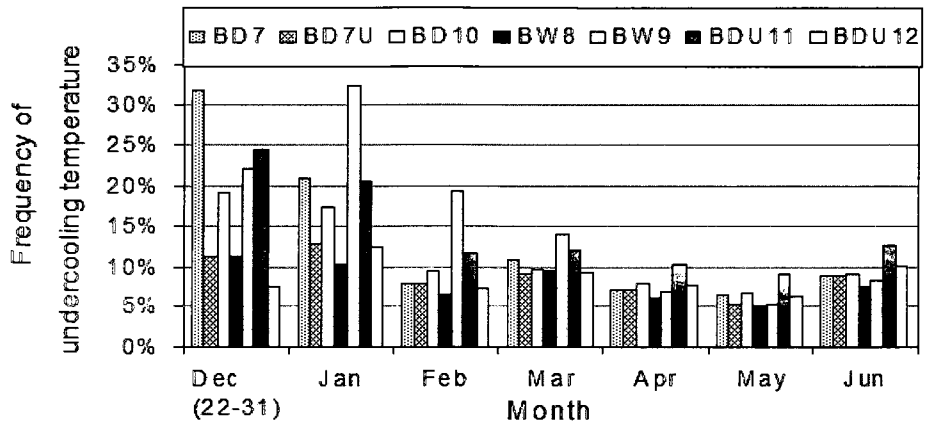

Figure 8: Frequency of under-cooling temperature of cavity-surfaces of brick veneer for all the brick test walls from Dec. 07 to June 08.

The solar radiation has a significant effect to increase the surface temperature of brick and to reduce the impact of under-cooling. The positions of the test walls influenced the amount of solar radiation received, which significantly influenced the under-cooling effect of cavity-surfaces. BW9 (two top vents with insect screen and initial high MC in plywood sheathing) has the highest under-cooling frequency in January to March, from 14% to 32%. BDU11 (six-25mm high top vents covered by roof flashing and low initial low MC in plywood) has the second highest under-cooling frequency during the same period. The range of under-cooling frequency is 21 – 25%. However, BW8 (without top vents with initially high MC of plywood) and BWU12 (six-65mm high top vent full open below roof flashing with initially low MC in plywood) has the lowest frequency in the entire test period, within the range of 5% - 12%.

It is found that there is shadow of trees on the exterior surfaces of BW9, and BDU11 in winter from December 2007 to March 2008, as shown in Figure 9. BW8 and BDU12 are near east corner without any shade of the trees.

Figure 9: Shadow of trees on the test walls in Jan. 08.

As a result, the brick veneer surface temperature for these four walls are different. BW9 and BDU11 have lower temperatures than those of BW8 and BDU12, indicating that different surrounding conditions and orientations of the façade have different under-cooling effect due to receiving different amounts of solar radiation in the winter. Cavity ventilation does not seem influencing the frequency of under-cooling temperature of brick cavity for the brick walls with discrete vents.

2. Fibre cement cladding

For all the fibre cement walls, the cavity-surface temperatures of fibre cement panels are often lower than the outdoor air temperature due to the clear-sky effect combined with their smaller thermal storage capacity. The peak frequency of under-cooling temperature of cavity-surface in fibre cement panels happened in December to February and in May, as shown in Figure 10.

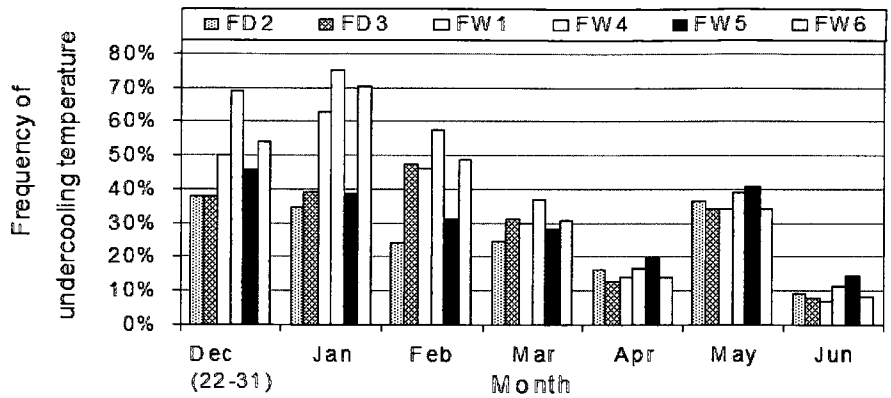

Figure 10: Frequency of under-cooling temperature of cavity-surface of fibre cement cladding for all the fibre cement test walls from Dec. 07 to June 08.

The vent configuration seems having influence on the under-cooling frequency of test walls. For the dry walls, the under-cooling frequency of fibre cement panels FD3 (12mm high top vent) is twice that of FD2 in February while is similar or lower than that of FD2 in January and the spring. The range of under-cooling frequency during the entire test period of 2008 is 8% - 47% for FD3 and 9% - 36% for FD2.

With a high initial MC in plywood sheathing, FW4, which has a 12mm high top vent, has the highest under-cooling frequency of 75% in January while FW5 with a 1mm high top vent has an under-cooling frequency of 39% only, and FW6 with a 6mm high top vent has the second highest under-cooling frequency of 70%. FW1, the wall with a 10mm air cavity and 12mm high top vent has the third highest under-cooling frequency of 63%. In the spring, similar to the walls with low initial MC in plywood sheathing, the difference in under-cooling frequency became quite small among all test walls. Overall, the range of under-cooling frequency is 12% - 75% for FW4, 8% - 70% for FW6, and 15% - 46% for FW5. FW1 has less under-cooling temperatures compared with FW4. The range of frequency is 7% - 63%.

It can be concluded that lower cavity ventilation with smaller continuous top vent reduces under-cooling effect. In addition, the under-cooling effect on the surface with a narrower air cavity is lower due to slightly higher cavity-surface temperature than those with wider air cavity. Observably, the shadow of trees may also have influence on the under-cooling effect at the surface of fibre cement panels, as shown in Figure 5-3-16. However, due to their location the frequency of shadow casted on fibre cement walls is quite low. Therefore, the cavity ventilation flow is the dominant factor to affect the under-cooling temperature of cavity-surface of fibre cement cladding.

The histograms of under-cooling temperature on cladding cavity-surfaces are analyzed. The high frequency of under-cooling effect occurred at different times of a day for brick and fibre cement walls due to the difference in cladding thickness and their thermal storage capacities. For example, as shown in Figure 11, the peak frequency of under-cooling temperatures on the cavity-surface of brick veneer in BW9 and BW8 is at 10:00am in the morning. Whereas, the peak frequencies of under-cooling temperatures on the cavity-surface of fibre cement claddings in FW4, FW6 and FW5 are from midnight to 5:00am in the morning, as shown in Figure 12. The 90mm thick brick veneer provided enough thermal mass to store the solar energy received during the day and released the heat during the night, which kept the brick cavity surface higher than the ambient air during the night and thus reduced the under-cooling effect and delayed the peak under-cooling frequency to 10:00am in the morning. In contrast, the 8mm thick fibre cement cladding provided less thermal storage and as a result the under-cooling effect started from mid-night until early morning.

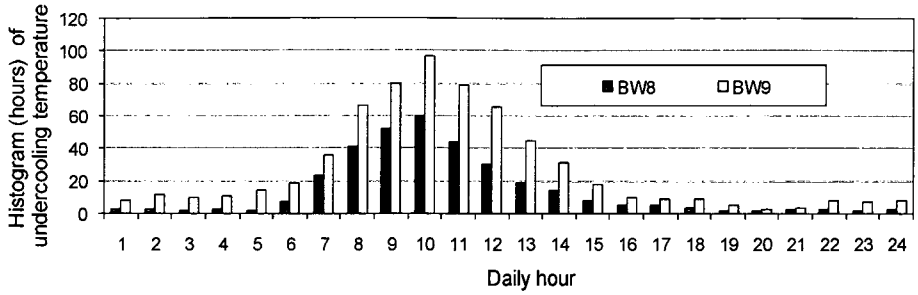

Figure 11: Histograms of undercooling temperature on cavity-surfaces of brick veneers in BW8 and BW9 on a daily base from Dec. 07 to Jun. 08.

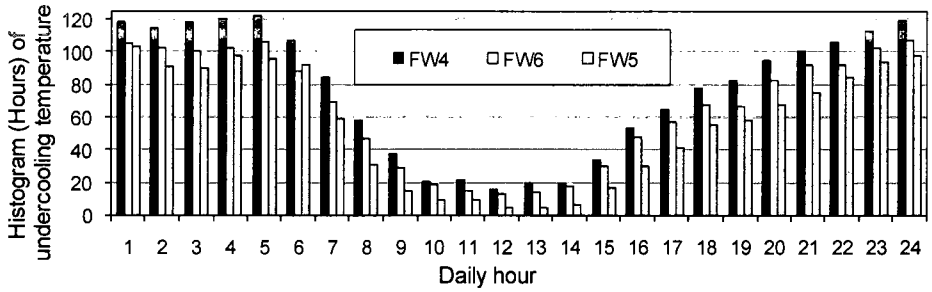

Figure 12: Histograms of under-cooling temperature on cavity-surfaces of fibre cement claddings of FW4, FW6 and FW5 on a daily base from Dec. 07 to June08.

3.Cavity-surface of plywood sheathing

According to the temperature measurements of plywood sheathing (which the thermocouples are inserted into the 3/4 thickness of plywood from inside surface, i.e. 3mm from cavity-surface), the frequencies of under-cooling were low for all the brick and fibre cement test walls. The range of frequencies was 2 – 11% for brick walls while 0.1 – 3% for fibre cement walls. No condensation has been found on the cavity-surface of plywood sheathing for all brick and fibre cement walls caused by under-cooling effect.

Appendix 4: Cavity air speed measurement

To measure the cavity air speed, one omni-directional hot-sphere anemometer was installed in each cavity of six test walls: four brick walls and two fibre cement walls, as shown in Figure 1. Each hot-sphere anemometer was located at the centre of the air cavity and 305mm (12") above the middle height of the wall specimen in order to minimize the interference with the pre-installed tracer gas distribution tube for the future tracer gas testing. The air speed was sampled at 20Hz and averaged at one-minute intervals. The anemometer readings were collected and analyzed from January 2 to June 21, 2008. The readings below 0.05m/s are disregarded since they are outside the anemometer's measurement range. The data for all the walls were missing periodically from the beginning of January to the beginning of March due to a power failure affecting the data acquisition system.

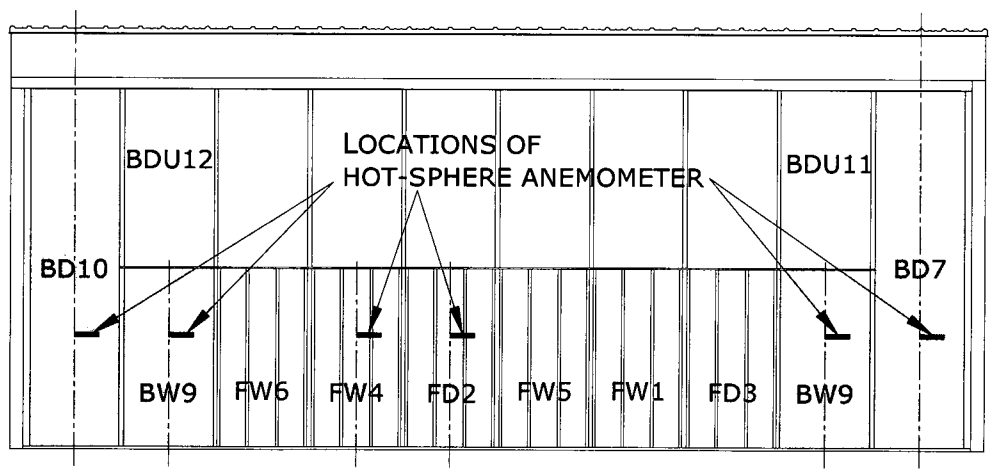

Figure 1: Locations of hot-sphere anemometers in the air cavity of test walls.

In addition, the air speed recorded in the cavity of FW4 (which has 12mm top vent) was constantly and extremely low over the entire test period. It was found later that the shielding tube of the anemometer fell over and covered the velocity probe due to the

failure of clamping during the construction. Hence, the data in the fall from September 22 and Dec 19, 2008 is used to compare the air speed measurement between FD2 and FW4 to examine the influence of vent configuration.

Results of cavity air speed measurements

The air speeds recorded in the cavities of brick walls on typical sunny days and cloudy and rainy days are compared and discussed as follows:

Case 1: comparison of the cavity air speed measurements between BD7 and BW8, as shown in Figure 4. Both BD7 and BW8 have restricted bottom vents with insect screens and have no top vents.

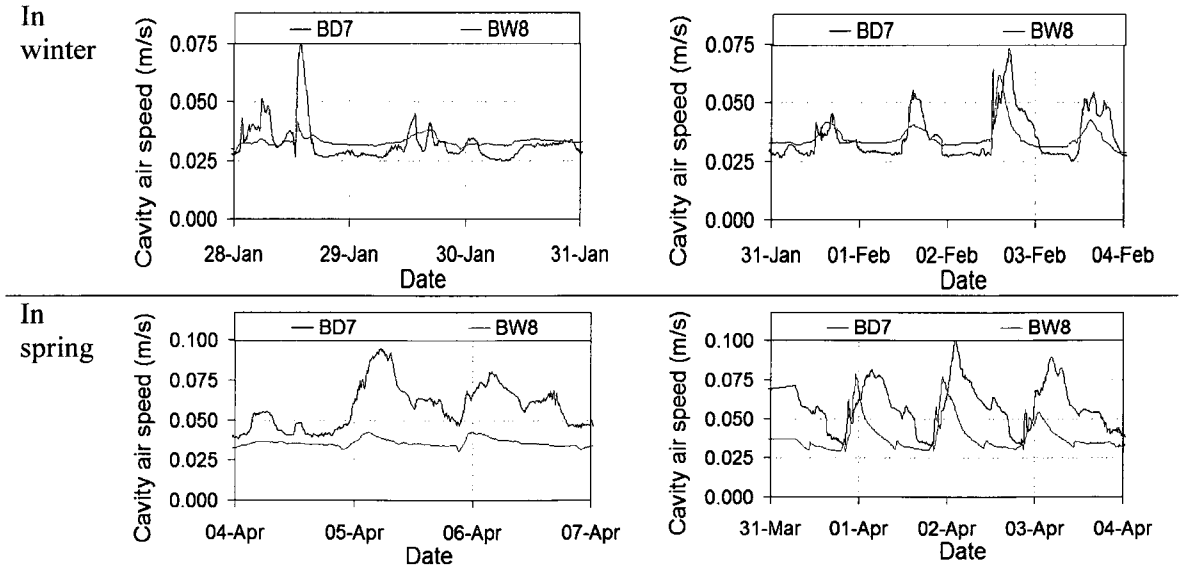

a) on cloudy and rainy days b) on sunny days

Figure 4: Comparison of the air speed measurements in vented cavity of brick walls between BD7 (two floor high) and BW8 (one floor high).

The cavity air speeds in both walls were similar in the winter most of the time but have difference in the spring. The difference became larger when the solar radiation increased. The maximum air speeds in the cavity of BD7 were about 0.03-0.05 m/s higher than that

recorded in the cavity of BW8 in the spring. In addition, the air speed in the cavity of BD7 reached its maximum value about three hours later than that in BW8, probably because it took longer for the internal air circulation induced by thermal stratification to form within the two-story high cavity.

Case 2: comparison of the cavity air speed measurements between BW9 and BD10, both have ventilated air cavities with un-equal areas of top and bottom vents (2-top vents with insect screens but 2-bottom vents are fully open), as shown in Figure 5.

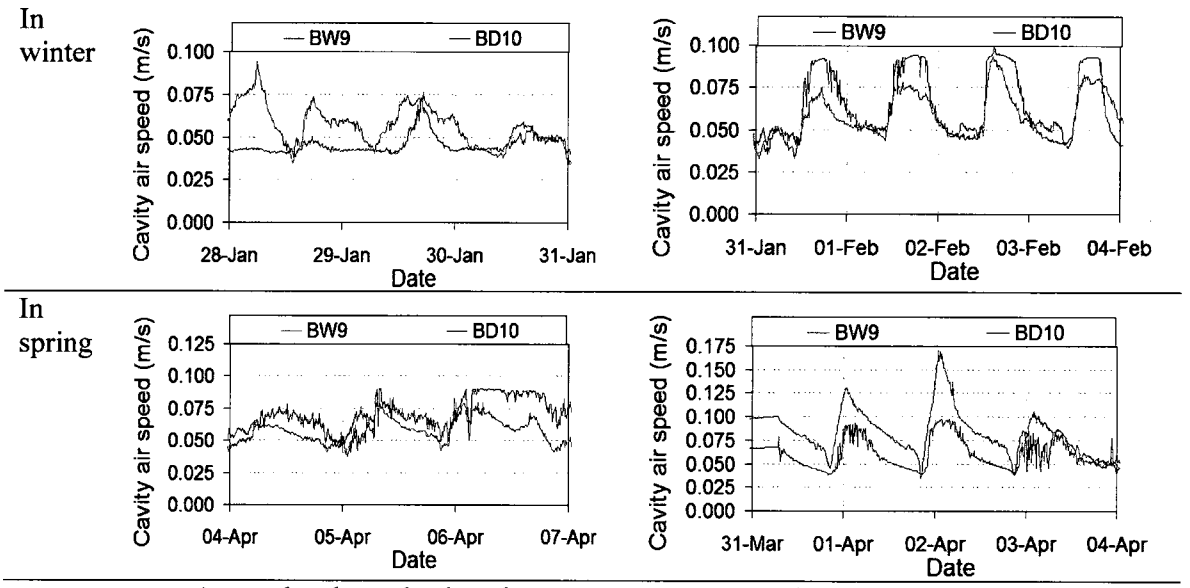

a) on cloudy and rainy days b) on sunny days

Figure 5: Comparison of the air speed in ventilated cavity of brick walls between BW9 (one floor high) and BD10 (two floor high).

The cavity air speeds recorded in BW9 (one-floor high) on the sunny days at the beginning of February were a maximum 0.02 m/s higher than that in BD10 while at the beginning of April the air speeds in BW9 had a peak value of 0.08 m/s lower than that in BD10 (two-floor high). It is because the thermal buoyancy is much higher in BD10 (1.5 – 2 Pa) than that in BW9 in April. On the rainy and cloudy days in January and April, the cavity air speeds in both walls were relatively flat when the exterior temperature and solar radiation are relatively low, i.e.

buoyancy pressure differentials were small. The air speeds in BW9 became lower and flatter in January while similar to those in BD10 in April.

Case 3: comparison of the cavity air speeds measured in the cavity of BD7 and BD10, as shown in Figure 6.

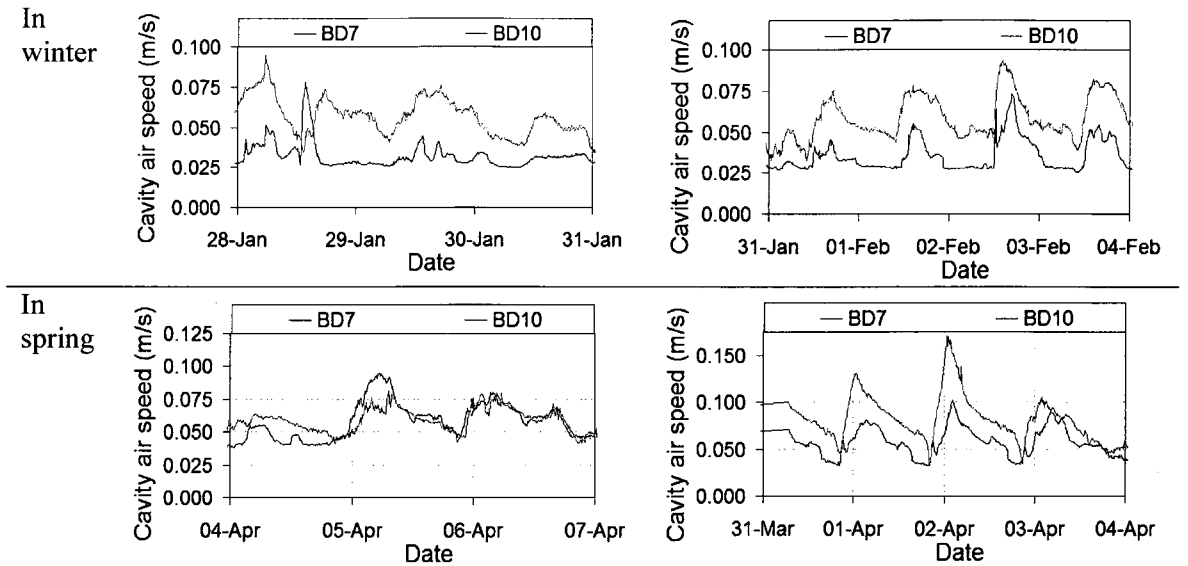

a) on cloudy and rainy days b) on sunny days

Figure 6: Comparison of the air speeds in air cavities of the two-floor high brick walls between BD7 (without top vents) and BD10 (with top vents).

The provision of top vents in BD10 provides an advantage in terms of air speeds especially in the winter. The cavity air speeds in BD10 were 0.04 – 0.07 m/s higher than those in BD7 except on cloudy and rainy days on April 4 – 5. In this period, the cavity air speeds in both walls are similar.

Case 4: comparison of cavity air speed between BW8 and BW9, both are one-floor high walls, shown in Figure 7. Similar to the two-floor walls, even a small top vent area shows a great ventilation effect especially on sunny days in the winter and spring. The air speeds in ventilated cavity of BW9 were about twice to three times as high as those in BW8 depending on the weather conditions in term of solar radiation, indicating that the

airflow is restricted by lack of the vent openings although the air speed in BW8 could rise up to 0.075 m/s in very short time on some sunny days. BW8 reached its peak values three hours earlier than those in BW9 on sunny days. Vent configuration is the dominant factor influencing the air movement through the cavities.

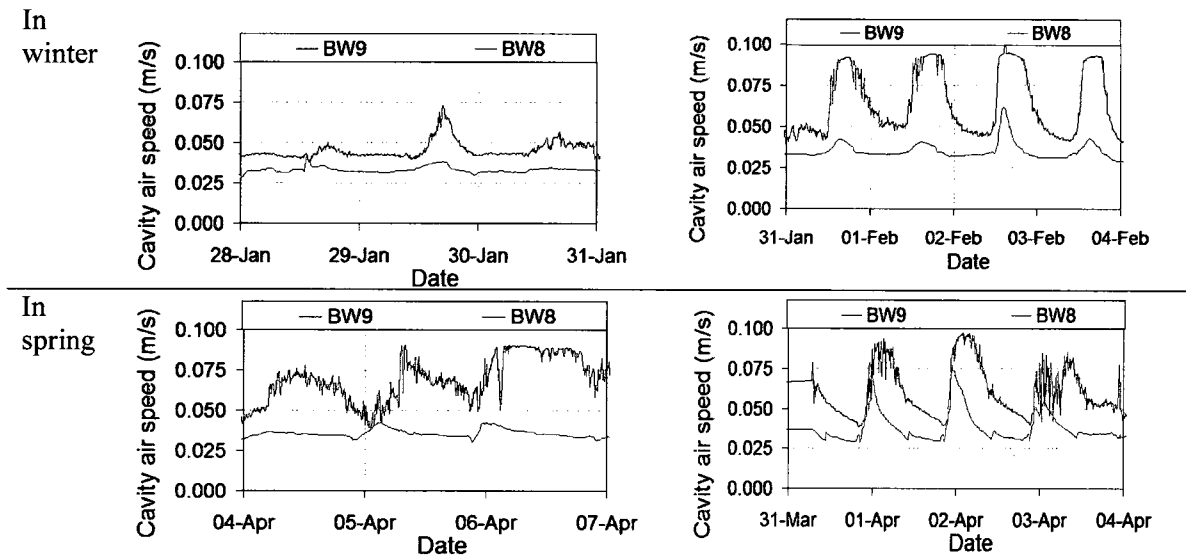

a) on cloudy and rainy days on sunny days

Figure 7: Comparison of the air speed in one-floor high cavities of brick walls between BW8 and BDW9.

For the purpose of simulating cavity ventilation effect on the MC of sheathing, hourly average cavity air speeds are also calculated. The results from January 24 to June 21 listed in Table 1 show that the hourly average and standard deviations of air speeds are the same as the 10-minunte average air speeds for all the brick walls.

Table 5-5-1: Statistical analysis of 10-minute and hourly average cavity air speed from Jan. 24 to Jun. 21, 08

	10-minute				hourly			
	BD7	BD10	BW8	BW9	BD7	BD10	BW8	BW9
	m/s	m/s	m/s	m/s	m/s	m/s	m/s	m/s
Mean	0.060	0.064	0.038	0.079	0.060	0.064	0.038	0.079
Minimum	0.025	0.026	0.028	0.031	0.025	0.030	0.029	0.033
Maximum	0.235	0.178	0.092	0.100	0.226	0.165	0.091	0.099
Standard Deviation	0.026	0.018	0.007	0.016	0.026	0.018	0.007	0.015

The ranges of the hourly average air speed become smaller and the standard errors increase slightly over those of 10-minute average air speeds but differences are small and insignificant.

Figure 8 shows the 10-minute average air speed measured in the cavity of FD2 from January to June in 2008. In general, the air speed recorded in winter was lower than that in spring. The maximum air speed occurred in April when strong solar radiation presented. Compared to the brick walls, the fluctuation and magnitude of FD2 are much larger, from 0.02 to 0.33 m/s. However, the average value of the air speed is only 0.078 m/s, and it is slightly lower than that of BW9 (0.079 m/s) and higher than that of BD10 (0.06 m/s).

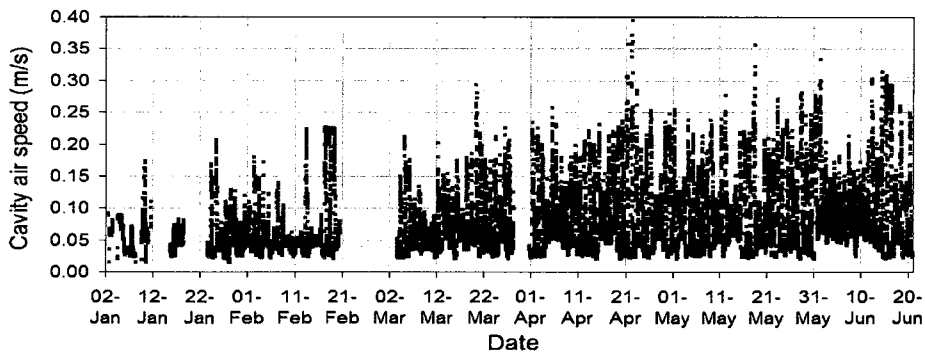

Figure 8: 10-minute average air speeds measured in the cavity of FD2 from Jan. to Jun. 08.

For the comparison of air speeds measured in the cavities of fibre cement walls, FD2 vs. FW4, the 10-minute average of air speed measured from September 22 to December 19 are analyzed. Figure 9 shows that cavity air speeds recorded in FD2 were approximately 0.15 m/s higher than those in FW4 on sunny days with a maximum value recorded as 0.42 m/s in middle of October. The maximum air speed recorded at the same time was 0.29m/s in the cavity of FW4. The fluctuations of cavity air speeds in FW4 were smaller than those in FD2. The temperature differential between cavity and outdoor air was

higher in the cavity of FD2 than that of FW4 on the sunny days, approximately 17 °C for FW4 and 22°C for FD2, as shown in Figure 10, indicating that larger vent area in FW4 promoted lower cavity ventilation due to lower thermal buoyancy pressure differential. On the cloudy and rainy days and at the night of the sunny days, FD2 has lower cavity air speed when the temperature difference between air cavity and outdoor air is smaller.

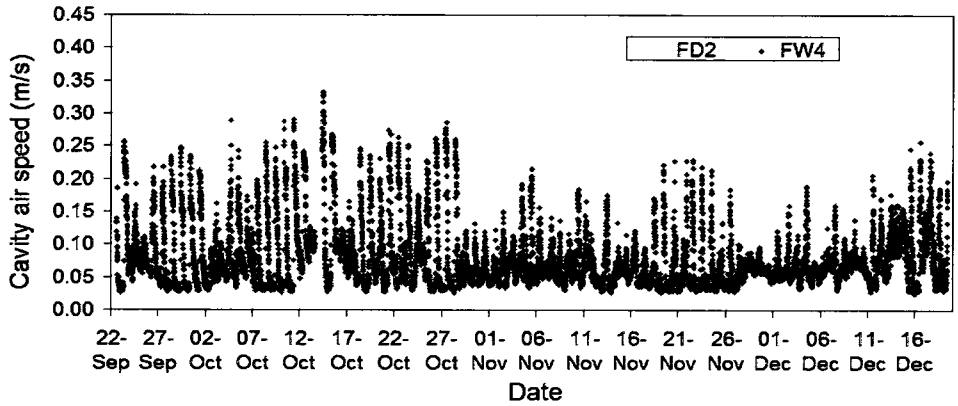

Figure 9: 10-minute average air speeds measured in the cavity of FD2 and FW4 from Sept. 22 to Dec. 19, 08.

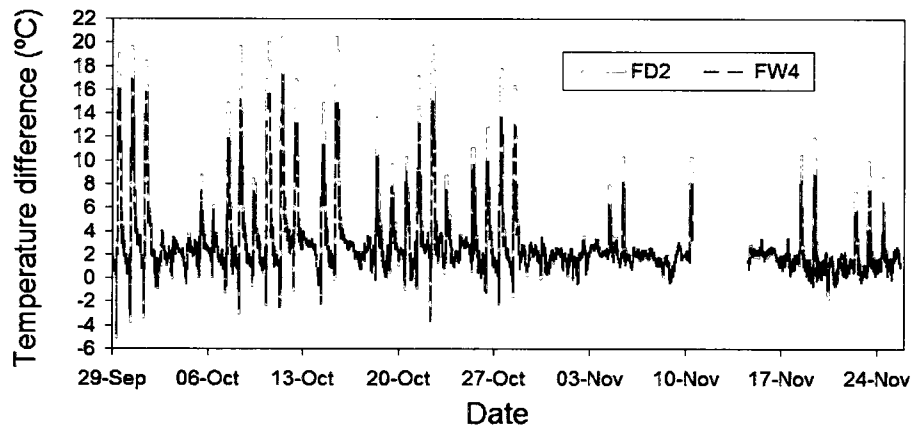

Figure 10: Comparison of temperature difference between outdoor air and the air cavities of FD2 and FW4 from Sep 29 to Nov. 25, 08.

The statistical analysis for the 10-minute and hourly average cavity air speed in FD2 and FW4 are listed in Table 2. The results show that average air speed in the cavity of FD2 is 0.01m/s lower than that FW4, which is 0.076 m/s for FD2 and 0.077 m/s for FW4. The

range of the air speeds in FD2 is larger than that in FW4, 0.016 – 0.407 m/s for FD2 while 0.026 – 0.306 m/s for FW4 from the 10-minute average data.

The hourly average air speeds for both walls are the same as the 10-minunte average air speeds. Similar to the brick walls, the ranges and standard deviations of the hourly average air speeds is smaller and the standard error is slightly larger than those of 10-minutes average air speeds but differences are small and insignificant.

Table 2: Statistical analysis of 10-minute and hourly average cavity air speeds in FD2 and FW4 from Sep 22 to Dec 19, 08

	10-minute		Hourly	
	FD2	FW4	FD2	FW4
	m/s	m/s	m/s	m/s
Mean	0.076	0.077	0.076	0.077
Minimum	0.016	0.026	0.016	0.028
Maximum	0.422	0.332	0.412	0.304
Standard Deviation	0.068	0.048	0.067	0.047

Figure 11shows that the air speeds recorded in the cavity of FD2 on the sunny days in February had bigger fluctuations from 0.02 m/s to 0.22 m/s compared with the cavity air speeds on the cloudy and rainy days in March. The cavity air speeds on the cloudy and rainy days in March were only around 0.03 – 0.15 m/s, which is 0.07 m/s less. In the spring, the fluctuations on both sunny and cloudy days are large. The difference is that the spikes on the sunny days are wide and higher while the spikes on the cloudy days are narrower. Comparison of cavity air speeds between FD2 and FW4 shows that there are almost double air speeds in the cavity with small top vent in FD2 than those in FW4 in the daytime on the sunny days in September. On the contrary, the cavity air speed in FW4 is a maximum of 0.05 m/s higher on the cloudy and rainy days in November 6 - 10. The daily pattern of the cavity air speeds in both walls is different on the sunny days but similar on the cloudy and rainy conditions.

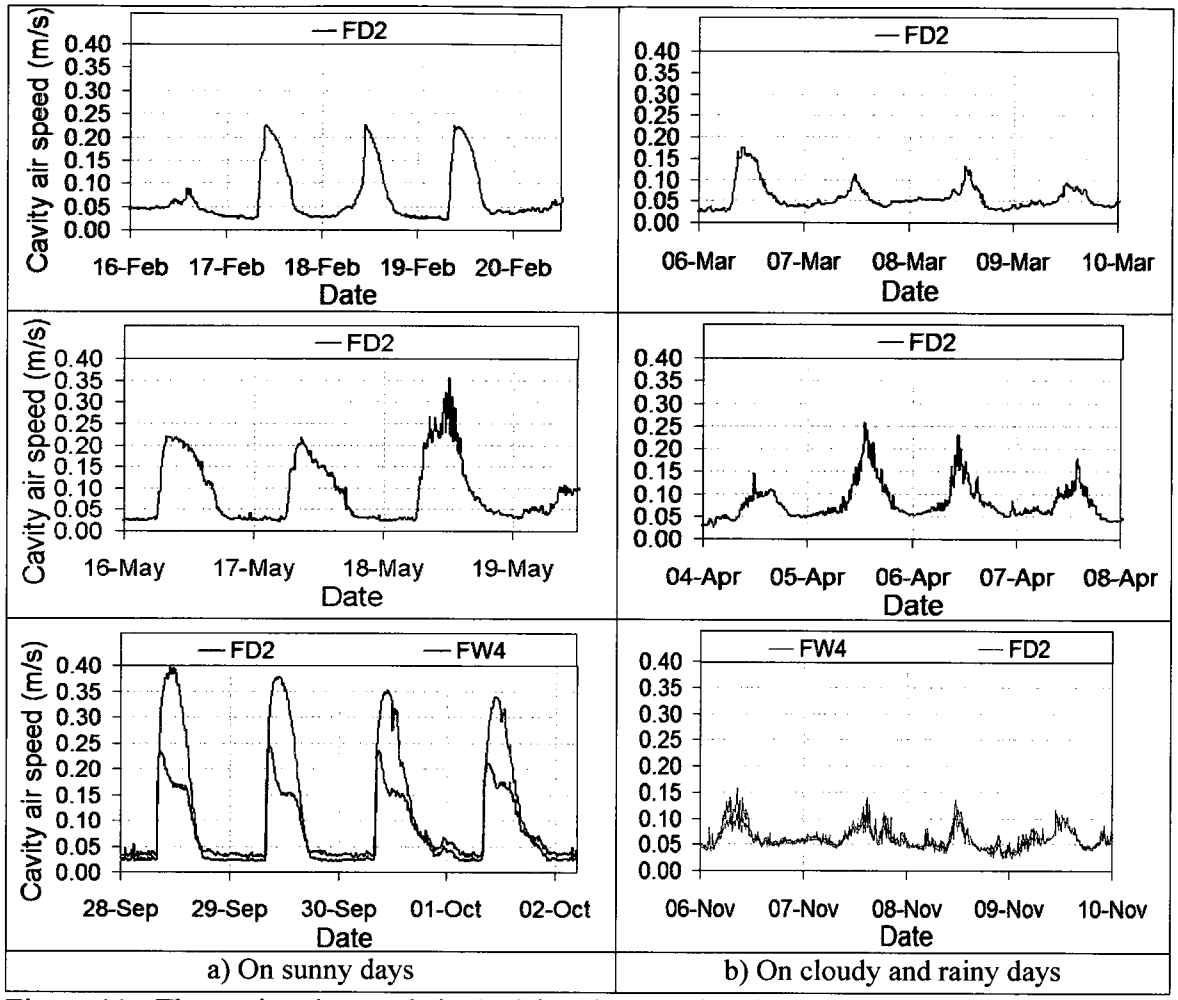

a) On sunny days b) On cloudy and rainy days

Figure 11. The cavity air speeds in FD2 in winter and spring and comparison of air speed between FD2 and FW4 in the fall of 2008.

Monthly average cavity air speed

To monitor the seasonal change in cavity air speed, the monthly average air speeds for the test walls are analyzed. The results shown in Figure 12 reveal that the cavity air speeds in all the brick walls increased from January to June in general in response to outdoor weather change. The warmer the weather is, the higher the average speeds are. The average air speeds in the ventilated cavities in the winter, i.e. from January to March, were higher than those in the vented cavities.

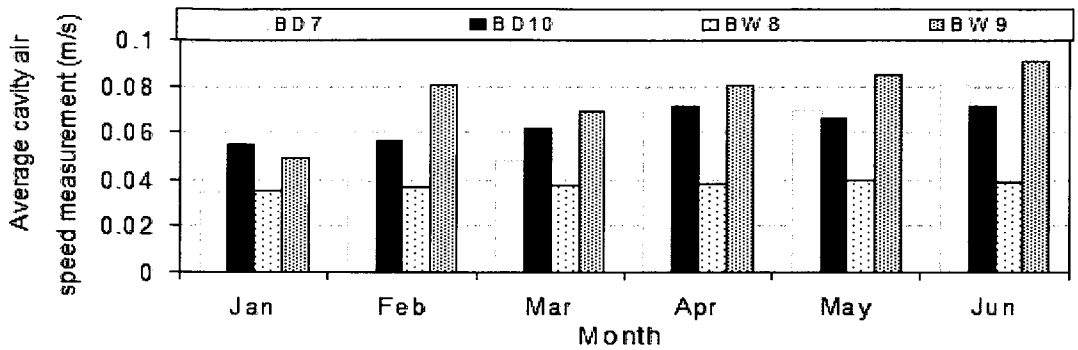

Figure 12: Monthly average cavity air speeds for brick walls from Jan. to Jun. 08.

However, in the spring from April to June, the monthly average air speed in vented cavity of BD7 without top vents was close to that in the ventilated air cavity of BD10 in April and was even higher in May and June. For the one-floor high brick walls, the average cavity air speeds in spring had the same trends as those in the winter.

For the purpose of simulating cavity ventilation effect on the MC of sheathing, hourly average cavity air speeds are also calculated. The results from January 24 to June 21 listed in Table 3 show that the hourly average and standard deviations of air speeds are the same as the 10-minunte average air speeds for all the brick walls. The ranges of the hourly average air speed become smaller and the standard errors increase slightly over those of 10-minute average air speeds but differences are small and insignificant.

Table 3: Statistical analysis of 10-minute and hourly average cavity air speed from Jan. 24 to Jun. 21, 08

	10-minute				hourly			
	BD7	BD10	BW8	BW9	BD7	BD10	BW8	BW9
	m/s	m/s	m/s	m/s	m/s	m/s	m/s	m/s
Mean	0.060	0.064	0.038	0.079	0.060	0.064	0.038	0.079
Minimum	0.025	0.026	0.028	0.031	0.025	0.030	0.029	0.033
Maximum	0.235	0.178	0.092	0.100	0.226	0.165	0.091	0.099
Standard Deviation	0.026	0.018	0.007	0.016	0.026	0.018	0.007	0.015

Overall the average cavity air speeds in all four walls are low within 0.08 m/s. It shows that average air speeds in the brick walls with two-floor high air cavities are similar but

the maximum air speed is lower in the ventilated cavities compare with that in the vented cavities. However, for one-floor high brick walls, the average cavity air speed in ventilated cavity is twice as much as that in vented cavity with similar maximum values. The ranges of air speed in the ventilated air cavity recorded are 0.031 – 0.10 m/s with average 0.08 for BW9 and 0.026 - 0.18m/s with average 0.06 m/s for BD10. The air speeds in the vented air cavity recorded are in the range of 0.028 – 0.092 m/s with average 0.038 m/s for BW8 and 0.025 – 0.24 m/s with average 0.06m/s for BD7.

For the fibre cement wall FD2, the monthly average cavity air speed increases from January to June in the same trend as those of the brick walls, as shown in Figure 13, The range of the average air speed in FD2 is 0.05 m/s in January to 0.097 m/s in June.

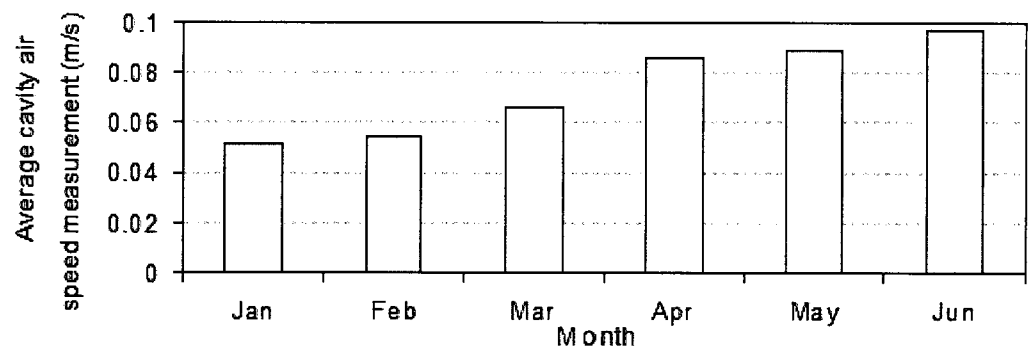

Figure 13: Monthly average cavity air speeds in FD2 from Jan. to Jun. 08.

Figure 14 shows the comparison of monthly average cavity air speeds between FD2 and FW4 from September to December, 2008. The air speeds in FD2 were higher in September due to strong solar radiation influence compared with FW4. However, the larger vent openings induce higher ventilation in the air cavity when the temperature difference between cavity and outdoor air became low due to less solar radiation in late fall.

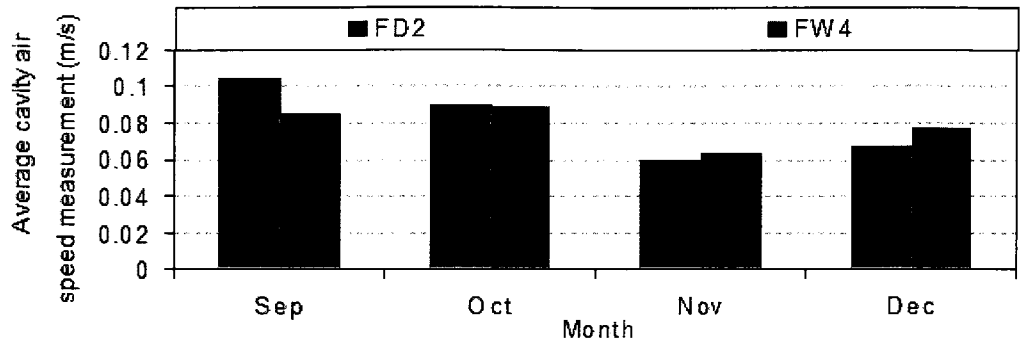

Figure 14: Comparison of monthly average cavity air speeds between FD2 and FW4 from Sep. to Dec. 08.

Appendix 5: Specifications and Calibrations of Instrumentations

1. Calibrations of moisture-pins

To measure MC in wood components, a pair of metal pins which are 25.4mm (1") apart are needed so that the voltage of cross these two pins can be measured by a meter or an acquisition system. Present formulas to determine MC of wood measurement by resistive moisture-pins is based on the results for Douglas-fir measurement at 21 °C, and then converts the resistance reading to the MC for Douglas-fir at 21 °C. Furthermore, the temperature and species correction factor are used to convert the MC of Douglas-fir to the equivalent MC in the specific wood species (Pfaff and Garrahan, 1985; Horn, 2007a).

Several equations must be used before resulting in the corrected MC of plywood with the correlation factors. At first, convert the voltage reading to resistance of wood:

$$R_{wood} = V_{wood} \cdot \frac{R_{sen\,sin\,gresistor}}{(V_{battery} - V_{wood})} \tag{1-1}$$

where, R_{wood} is the resistance of wood, V_{wood} is the voltage measured from a pain of MC pins or screws, $R_{sensingresister}$ is sensing resistance, $V_{battery}$ is voltage of battery.

On the second, calculate MC of Douglas-fir ($MC_{douglas}$) at 21 °C with electrical resistive of wood (R_{wood}) in kohm;

$$MC_{douglas} = 67.579 - 0.1224 \cdot (\log R_{wood})^3 + 2.6038 \cdot (\log R_{wood})^2 - 20.752 \cdot \log R_{wood} \tag{1-2}$$

On the third, the equivalent moisture meter reading for Douglas fir at 21 °C on Delmhors RC-IC meter (two-pin meter)(MCmeter) is derived from MCdouglas is calculated as;

$$MC_{meter} = 0.850 \cdot MC_{douglas} + 0.779 \quad (1\text{-}3)$$

Finally, the MC of wood is calculated using Garrahan's formula (Pfaff an Garrahan, 1985):

$$MC = \frac{MC_{meter} + 0.567 - 0.0260 \cdot T + 0.000051 \cdot T^2}{0.881 \cdot 1.0056^T} - b) / a \quad (1\text{-}4)$$

where MC is the corrected moisture content in wood, MCmeter is reading for Douglas fir at 21 °C on Delmhors TRC-IC meter (two-pin meter), T is the temperature in wood, a and b is species correction coefficients. In this program the species correction coefficients in plywood, stud, and bottom plate used are listed in Table 1.

Table 1: Species correction coefficients of plywood, stud, and bottom plate

Wood component	a	b	Sources
Plywood	1.2	0.3666	a-value corrected in the lab of building science centre at BCIT b- value adapted the OSB value from Straube, et al (2002)
Stud and bottom plate (Spruce)	0.853	0.398	Garrahan. (1989)

In addition, the resistance measurements are the least resistance on the path between the two screws in the sample if the non-insulated screws are being used in these measurements. The measurement results in the maximum moisture point which on the path of moisture-pins within a wood component. However, the resistance measurement can be measure wherever are intent to monitor if the insulated pins are used.

The calibration method was used in comparing gravimetric readings and resistive moisture-pin reading of plywood samples at the same time. Two calibrations of resistive moisture-pins for MC measurement in wood members have been taken:

- Calibrations of species correction factors and accuracy range of plywood and – taken in the summer of 2007 for the experimental need in Building Science Centre for Excellent at BCIT (Horn, 2007a-internal report).
- Calibrations of resistive moisture-pin measurement to verify the accuracy of MC measurement and drying rates between plywood panel and gravimetric sample in plywood (Douglas Fir) and pressure-treated plywood strapping specifically used in the experiment on May of 2008.

The results of the first calibration show that the accuracy range of resistive MC pins is within 6% - 23% for plywood while 7% - 30% for Spruce-pine-Fir (SPF) stud and plate. The accuracy range of resistive moisture-pins here is defined that MC value calculated from moisture-pin reading to within a 2% difference of the gravimetric measurements (Horn 2007a).

For the second calibrations, A total of fifteen 12.7mm (1/2") thick Douglas Fir plywood samples which is the same as the plywood used in the experiment and a total of five 19mm (3/4") thick pressure-treated (PT) plywood samples which is as the same as the PT plywood strapping used in the air cavities of fibre cement walls are used. The sample dimensions are 51mm (2") by 51mm (2").

After reaching around a equilibrium MC level of 7-8% in laboratory conditions (21°C and 47% RH) from their oven-dry weighs, fifteen Douglas Fir plywood Samples and five PT plywood samples were immersed into water to reach a designed initial MC of 40% . Then the Douglas Fir plywood samples were divided into two sets: one set of ten samples retained their edges exposed while another set of 5 samples were sealed the edges with

tuck tape to monitor their MC decrease and compare their drying rates every 24 hours. The results of calibration concluded:

For the samples with un-sealed edges: moisture-pin and gravimetric measurement are similar in the range of 22% - 8% with a maximum difference of 2%. For the comparison of gravimetric MC reading in the samples between un-sealed edge and sealed edge, the MC in un-sealed samples has fast drying in the high MC level. The difference of drying rates in the MC range of 42 – 34% is large, reaching to 4% and then become smaller to 0.49% in the MC range of 34% - 20%, indicating at the high MC level, the MC transfer is two-dimensional since the vapour pressures in the samples are much higher than the surrounding environment.

After reaching to 20% MC, the un-sealed samples slow down the drying speed and the MC becomes similar to that of sealed samples at the end of calibration test, reaching to around 8%. That means at the lower MC level, vapour transfer in the samples is one-dimensional since the vapour travel path is shorter from centre layer of samples which MC is higher than the outer layer to the surface than to the edge.

2. Specifications and calibrations of thermocouples and RH-T sensors

Specifications

The thermocouples used for measuring temperature in the wall specimens are type T with copper vs. constantan (copper-nickel). The accuracies and tolerance of type T thermocouples are listed in Table 2 according American Limits of Error ASTM E230-ANSI MC 96.1.

Table 2: The accuracies of type T thermocouple

Standard limits		Special limits	
Temperature Range	Tolerance Value	Temperature Range	Tolerance Value
>0 to 350 °C	1.0 °C or 0.75% reading	0 to 350 °C	0.5 °C or 0.4% reading

The RH-T sensors performing in the insulation spaces and air cavities provide a DC voltage output for both RH and temperature readings. Each sensor is wired up to a single battery power source of 12 VDC. The manufacture specifications for the sensors are listed in Table 3.

Table 3: Manufacture specifications of RH-T sensors

RH-T sensors: Vaisala HMP50, models YBB1B1A and YBC1A1X			
RH		Temperature	
measurement range	Accuracy at +20 °C	measurement range	Accuracy range at +20°C
0 to 98%	±3% in 0 – 90% ±5% in 90 – 98%	-10 °C to 60 °C	±0.6 °C
Output voltage	0 - 2.5 V	0 - 2.5 V	
Convert range	0 – 100%	-40 - +60	

Calibration

Thermocouples

The possible thermocouples reading errors can occur in many ways, such as the connections, acquisition station operation, running program and thermocouples themselves. The most common errors may be caused by the connections from the wall specimen to the acquisition and the thermocouple itself. Therefore, the calibrations of thermocouple connections and thermocouples had be done in Building Science Centre of excellence at BCIT during the experiment.

The method to calibrate the thermocouples is to physically put the soldered end into an ice bath, forcing their temperature to be 0 °C and establishing them as the reference junction. This is a quite accurate method since the ice point temperature can be very

precisely managed (Omega Engineering, Inc., 2007). A total thirty two type T thermocouples were inserted into an ice bath in the laboratory conditions. An acquisition system scans them for over two and a half hours. The results of the calibration show that the accuracy range of these thermocouples is 0.03 to 0.2 °C (Larose. 2008), within the special limit range (0.5 °C or 0.4% of reading) of American Limits of Error ASTM E230-ANSI MC 96.1.

Connection of thermocouple and terminal strip

The thermocouple wires from wall specimens to the acquisition station are separated into two parts by terminal strips in order to facilitate installations of walls and wires at the same time. Both ends of thermocouple wires from walls and the acquisition station connect to the terminal strips.

The method to calibrate the possible error caused by connection of terminal strip is directly to connect the thermocouple wires from the walls to wires of the acquisition station. Compare the readings between with and without terminal strip connections of three walls which are located at the north and south corner and middle of east side of BETF. The results of calibration show that the connections of terminal strip does not affect the readings of thermocouples (Ye, 2007 - internal report).

RH-T sensors

The purposes to calibrate all the RH sensors are to verify the accuracy of RH and temperature of each sensor, and to verify the discrepancies between sensor readings in the same environments.

The methods of calibration are to create three different RH environments in the containers; 100% RH by 2/3 volume of water, 75% RH by 50mm slurry of sodium

chloride (NaCl), and 33% RH by 50mm slurry of magnesium chloride (H12O6Cl2Mg), according to ASTM designation E 104 – 85 "Standard Practice for Maintaining Constant Relative Humidity by Means of Aqueous Solutions" (Horn, 2007b).

Each of a total 30 sensors was to be calibrated in above three environment conditions. They had been installed in the sealed containers above the liquids for one hour to stabilize before the acquisition system started to scan them. Each container included a thermocouple to compare the reading of temperature through RH-T sensors. The results of calibrations are listed in Table 4.

Table 4: RH-T sensor calibration results in three environment conditions

Environmental conditions	RH difference between sensors	RH difference from published solution	Temperature difference between RH-T sensors	Temperature difference between RH-T sensors and thermocouples
sodium chloride (NaCl) (75%RH)	Average: 2.32% Max.: 2.39%	Average: 3.56% Max.: 3.81%	Average: 0.36 °C Max.: 0.41 °C	Average: 0.09 °C Max.: 0.41 °C
magnesium chloride ($H_{12}O_6Cl_2Mg$) (33% RH)	Average: 1.38% Max.: 1.41%	Average: 2.56% Max.: 2.72%	Average: 0.44 °C Max.: 0.62 °C	Average: 0.17 °C Max.: 0.27 °C
2/3 volume of water (100% RH)	Average: 0.26% Max.: 0.54%	Average: 3.38% Max.: 3.81%	Average: 0.56 °C Max.: 0.59 °C	Average: 0.32 °C Max.: 0.45 °C